Circadian light-input pathways in Drosophila melanogaster

Ajay Sunilkumar

université PARIS-SACLAY

Circadian light-input pathways in *Drosophila melanogaster*

Voies d'entrée des informations lumineuses pour l'horloge circadienne chez Drosophila melanogaster

Thèse de doctorat de l'Université Paris-Saclay

École doctorale n° 568, Signalisations et réseaux intégratifs en biologie (BIOSIGNE)
Spécialité de doctorat : Sciences de la vie et de la santé
Graduate School : Sciences de la vie et santé. Référent : Faculté de médecine

Thèse préparée dans l'unité de recherche Institut des Neurosciences Paris-Saclay (NeuroPSI), Université Paris-Saclay / CNRS,
sous la direction de **François ROUYER**, Directeur de recherche Inserm

Thèse soutenue à Paris-Saclay, le 12 octobre 2023, par

Ajay SUNILKUMAR

Composition du Jury

membres du jury avec voix délibérative

Jean-René MARTIN DR, CNRS, Université Paris-Saclay	Président
Charlotte HELFRICH-FOERSTER Professeure, Université Wuerzburg	Rapporteur & Examinatrice
Xavier BONNEFONT Chargé de recherche, HDR, CNRS, Université de Montpellier	Rapporteur & Examinateur
Daniel VASILIAUSKAS Chargé de recherche, Inserm, Université Paris-Saclay	Examinateur

THESE DE DOCTORAT

NNT : 2023UPASL087

université PARIS-SACLAY

ÉCOLE DOCTORALE
Signalisations et réseaux intégratifs en biologie (BIOSIGNE)

Title: Voies d'entrée des informations lumineuses pour l'horloge circadienne chez *Drosophila melanogaster*

Key words: horloge circadienne - rythmes repos-activité - drosophile - photoréception - cryptochrome - système visuel

Summary: L'horloge circadienne endogène est un système fondamental présent dans la majorité des organismes vivants, qui fonctionne pour réguler et synchroniser les rythmes quotidiens des processus physiologiques et comportementaux. Cette régulation temporelle complexe des processus biologiques est pilotée par un mécanisme moléculaire impliquant des boucles de rétroaction transcriptionnelles-translationnelles, générant des oscillations de l'expression des gènes de l'horloge. Chez *Drosophila melanogaster*, ce mécanisme auto-entretenu fonctionne au sein d'un sous-ensemble d'environ 150 neurones cérébraux appelés neurones d'horloge. Ces neurones synchronisent leurs horloges moléculaires par le biais d'une communication inter-neuronale, ce qui fait de l'horloge cérébrale un réseau neuronal unifié qui génère des rythmes circadiens robustes. Une caractéristique essentielle de l'horloge circadienne est sa capacité à se synchroniser avec des signaux environnementaux externes, ce qui permet aux organismes de s'adapter de manière proactive aux changements environnementaux en alignant leur comportement et leur physiologie sur des moments précis de la journée. Les horloges circadiennes sont entraînées par des facteurs de synchronisation externes connus sous le nom de zeitgebers, la lumière étant le plus puissant et le plus fiable de ces signaux. Outre la lumière, d'autres facteurs tels que la température, ou les interactions sociales jouent également un rôle dans la facilitation de l'entraînement circadien. Chez la drosophile, la photoréception circadienne englobe de nombreuses voies qui utilisent divers photorécepteurs pour ajuster finement la synchronisation de l'horloge. Cette entrée sensorielle peut être largement catégorisée en deux voies : l'une impliquant le photorécepteur sensible à la lumière bleue CRYPTOCHROME (CRY), exprimé dans la majorité des cellules de l'horloge, et l'autre utilisant les voies d'entrée visuelles médiées par différentes rhodopsines. Cette thèse porte sur les différentes voies d'entrée de la lumière qui synchronisent les horloges neuronales avec les cycles lumière-obscurité externes. Trois études ont été menées dans le cadre de ce travail, explorant des aspects distincts de la photoréception. Le premier projet met en évidence la contribution de l'entrée de lumière médiée par les ocelles, révélant le rôle des photorécepteurs des ocelles exprimant Rh2 dans le photo-entraînement du comportement locomoteur des mouches et le circuit neuronal sous-jacent. Le deuxième projet étudie l'entrée de lumière non cellulaire autonome médiée par CRY, mettant en lumière les fonctions collaboratives des neurones de l'horloge et les mécanismes neuronaux distribuant les signaux CRY dans le réseau de l'horloge cérébrale. La troisième étude se concentre sur le circuit neuronal encore inconnu qui relie la rétine aux neurones de l'horloge, et plus particulièrement sur le rôle des photorécepteurs R8 dans la transmission des signaux aux neurones de l'horloge. Les résultats de ce travail permettent de mieux comprendre comment les rythmes biologiques se synchronisent avec les conditions lumineuses ambiantes en révélant certains mécanismes neuronaux et processus moléculaires par lesquels les neurones de l'horloge perçoivent les diverses entrées lumineuses.

université PARIS-SACLAY

ÉCOLE DOCTORALE
Signalisations et réseaux intégratifs en biologie (BIOSIGNE)

Title: Circadian light-input pathways in *Drosophila melanogaster*

Keywords: circadian clock – rest-activity rhythms – *Drosophila* - photoreception – cryptochrome – visual system

Summary: The endogenous circadian clock is a fundamental system present in the majority of living organisms, functioning to regulate and synchronize daily rhythms across physiological and behavioral processes. This intricate temporal regulation of the biological processes is driven by a molecular mechanism involving transcriptional-translational feedback loops, generating oscillations of clock gene expression. In *Drosophila melanogaster*, this self-sustaining mechanism operates within a subset of approximately 150 brain neurons termed clock neurons. These neurons synchronize their molecular clocks through inter-neuronal communication, enabling the brain clock as a unified neuronal network that generates robust circadian rhythms. A pivotal feature of the circadian clock is its ability to synchronize with external environmental cues, enabling organisms to proactively adapt to environmental changes by aligning behavior and physiology with specific times of the day. Circadian clocks are entrained by external synchronizing factors known as zeitgebers, with light being the most potent and reliable of these cues. Beyond light, other cues, such as temperature and social interactions, also play a role in facilitating circadian entrainment. In *Drosophila*, circadian photoreception encompasses numerous pathways that utilize diverse photoreceptors to adjust clock synchronization finely. This sensory input can be broadly categorized into two pathways: one involving the blue-light-sensitive photoreceptor CRYPTOCHROME (CRY), expressed in the majority of clock cells, and the other utilizing the Rhodopsin-mediated visual input pathways. This thesis delves into the multifaceted nature of circadian entrainment, emphasizing the various light input pathways that synchronize the neuronal clocks to external light-dark cycles. Three studies were conducted as part of this thesis, exploring distinct aspects of this sensory system. The first project unravels the contribution of ocelli-mediated light input, revealing Rh2-expressing ocelli's role in the photoentrainment of fly locomotor behavior and the underlying neural circuit. The second project investigates non-cell autonomous CRY-mediated light input, shedding light on collaborative clock neuron functions and the neural mechanisms distributing CRY signals in the brain clock network. The third study focuses on the still unknown neural circuit that connects the retina to clock neurons, particularly focusing on the role of R8 photoreceptors in transmitting signals to clock neurons. Collectively, these data advance our understanding of how biological rhythms synchronize with ambient light conditions by uncovering the neural mechanisms and molecular processes through which clock neurons perceive diverse light inputs.

ACKNOWLEDGMENTS

To be honest, crafting this acknowledgment section has been the most challenging aspect of completing this entire dissertation, as I always feel myself at the loss of words to express my gratitude to all those who enriched my life. Here I am, trying my best, and this thesis would unquestionably lose its significance without appreciating and acknowledging those who believed in me and contributed to my sense of worth. The last five years have been challenging in many ways, but I am fortunate to have a support system of people who believe in me, even on days when it is hard to believe in oneself. Living abroad, far from home and in a completely unfamiliar world, was quite overwhelming, yet it exposed me to a wealth of cultural and academic experiences, and I am deeply indebted to the people here and back home who made this transition not only manageable but also enjoyable. I wholeheartedly believe that my five-year journey as a Ph.D. student, along with the remarkable individuals I encountered during this period, has played a substantial role in shaping my character and defining the person I have become today. For the life I've built here and the countless opportunities and experiences this place has afforded me, I'm profoundly grateful, recognizing the sincere effort and emotional support contributed by many.

First and foremost, I thank my Ph.D. supervisor, Dr. François Rouyer, for choosing me for this doctoral work and granting me the opportunity to work in his incredible laboratory here at NeuroPSI. Fundamental neuroscience has always been my profound passion, and I am immensely thankful to him for entrusting me with the exciting projects I had the privilege of participating in. Your friendly support and unwavering belief in me significantly complemented my productivity. I will forever be grateful for the invaluable suggestions and insights you provided that were instrumental in completing this work.

Next, I would like to seize this opportunity to express my gratitude to Abhishek Chatterjee, who has served as my mentor, motivator, and colleague. You have been my true mentor in this field, imparting a wealth of knowledge, and our discussions have been a source of invaluable lessons that have greatly contributed to my academic growth. I thank you once again for consistently making yourself available to address all my doubts, even after you left the lab. Your presence undoubtedly eased and enriched this journey. I can still vividly recall that one of the three projects I undertook for this thesis was conceived during one of our initial discussions. Collaborating with you on that project was a privilege, and your enthusiasm,

dedication, and intelligence will continue to inspire me. I also want to thank both you and Payel for your warm hospitality, inviting me to your home on numerous occasions and sharing delicious Indian cuisines, which obviously eased my homesickness during the initial days of my arrival.

I consider myself extremely fortunate and privileged to have had the opportunity to work alongside such exceptional colleagues during my time at NeuroPSI. I extend my heartfelt gratitude to all the current and former lab members of Rouyer's team. I express my special acknowledgment to Béatrice, who consistently extended her helping hand whenever I was in need. I would also like to extend my thanks to Elisabeth, Christian, Brigitte, Nicolas and Julie for their invaluable technical support. Your expertise was a huge relief to me and immensely helped me conduct experiments and carry out my work in the lab. I also thank Christine for her guidance and for generously sharing her wealth of knowledge in this field with me during the initial stage. I must emphasize that the delightful presence, generous friendliness, and efficient management of laboratory matters put forward by all these incredible people substantially created a perfect working atmosphere in the lab.

Last but certainly not least, I thank all my fellow Ph.D. students and master’s students who worked alongside me. I want to thank Thierry for his untiring support and the invaluable contributions he made to the lab. Your dedication and management skills are truly commendable, and I wish you all the best in your future endeavors. To George and Theja, I express my appreciation for the assistance you offered, and I wish you both the best in your future careers. To the new Ph.D. students, Chiara, Ping, and Zéphyr, I apologize for not having had more time to spend with you as I neared the end of my work in the lab. However, I want to express my sincere gratitude for your support during those demanding times, and I have no doubt that all of you will have a fantastic journey ahead in your research pursuits. I genuinely appreciate all the master's students who worked under my guidance, including Eva, Abdel, and Elza. Your contributions were outstanding, and I'm immensely thankful for your assistance in advancing my Ph.D. journey. I also want to extend my appreciation to all the other Ph.D. students at NeuroPSI, the team behind 'Happy NeuroPSI,' and all the staff members working in the administration section, IT department, and kitchen team. Your collective contributions have played an integral role in making NeuroPSI a vibrant and supportive research environment. I want to give special recognition to all the members of the other fly labs, including Tihana and her team, Jean-René and his team, and Daniel and his team. I am grateful

for the supportive nature displayed by all these teams and for the productive fly meetings we held together. I'd like to make a special mention of Daniel, who also served on my thesis committee. He provided considerable assistance, and I often felt guilty about troubling him for various reasons. Thank you for your patience and feedback and for genuinely helping me during challenging times.

Next, I take this opportunity to thank all my friends who supported me during these times. While the list is extensive, it's essential to acknowledge that their presence made everything memorable and achievable. I'd like to begin by expressing my gratitude to my favorite people, Jithu and Arya, who also happened to be my flatmates here. They genuinely turned this place into a second home, and I find myself at a loss for words to convey just how thankful I am to them for bringing all the peace and joy to my life. Thank you, Arya, for being who you are and for being in my life. Special thanks to Asma for her constant care and boundless love. To Athullya, for all the memorable moments we've had together and for the love. Thanks to Swedha for all the wildly sarcastic conversations and genuine care. To Bhagya, for always being there for me. Thank you, Sara, for being so supportive and loving. Thanks to Thampi for the good times. A big thanks to my friends in France, including Akbar, Maneesha, Aleena, Shenoy, and Bilal. Another special shoutout to all my friends here in Paris, including Sreelekshmi, Allipra, Ghanim, and Aswathi Chechi. Thanks for all the celebrations and fun times we shared together. Thanks to the CS team for making the Covid period less stressful. Special mention to my CINCHRON friends. I feel lucky and privileged to meet you guys. I also thank all my friends back in IISER-TVM, my B13 batchmates, dear seniors and juniors, and my boys. Those days will always be the best days of my life, and as I reach this epic milestone of my life, I fondly remember everyone for the good times we had in Thiruvananthapuram. Thanks to STHSS, IISER, Chelsea, Insta and W-S-F.

Finally, I thank my mother, father, sister, and all other family members. This thesis is dedicated to Amma, Achan, and Chechi. I am the person I am today because of your support and love. My dreams have come true because of all of you. Thank you for nurturing me and allowing me to soar to greater heights. I will forever be grateful to you.

Here's to one life, science, and the fantastic people who make both of them better. Cheers!

TABLE OF CONTENTS

ABBREVIATIONS

5^{th} s-LNv	5^{th} small – ventral Lateral Neuron
aMe	accessory Medulla
AOT	Anterior optic tract
AOTU	Anterior optic tubercle
AstA	Allatostatin A
AstC	Allatostatin C
bHLH	basic Helix-Loop-Helix
Bmal1/BMAL1	Brain And Muscle Arnt-Like protein 1
bZip	basic leucine Zipper
cAMP	cyclic adenosine monophosphate
CGRP	Calcitonin gene-related peptide
ChAT	Choline acetyltransferase
CK2	Casein Kinase 2
clk/CLK	Clock
CLOCK	Clock Locomotor Output Kaput
CNG	Cyclic-nucleotide-gated
cry/CRY	Cryptochrome
CTT	Carboxyl-terminal tail
CWO	CLOCKWORK ORANGE
cyc/CYC	Cycle
DAG	Diacylglycerol
DBT	Doubletime
DD	Constant darkness (Dark: Dark)
DNs	Dorsal Neurons
DN1s	Dorsal Neurons type 1

DN1a	Anterior type1 Dorsal Neurons
DH31	Diuretic Hormone 31
DN1p	Posterior type 1 Dorsal Neurons
DN2	Dorsal Neurons type 2
DN3	Dorsal Neurons type 3
DRA	Dorsal rim area
E	Evening
EM	Electron microscope
ER	Endoplasmic reticulum
FAD	Flavin adenine dinucleotide
GDP	Guanosine diphosphate
GTP	Guanosine triphosphate
GFP	Green fluorescent protein
GPCR	G-protein coupled receptor
GRASP	GFP Reconstitution Across Synaptic Partners
GSK-3β	GLYCOGEN SYNTHASE KINASE-3β
H-B eyelet	Hofbauer-Buchner eyelet
hdc/HDC	Histidine decarboxylase
Hid	Head involution defective
HisCl1/HISCL1	Histamine-gated chloride channel subunit 1
h/hrs	Hours
IP_3	Inositol 1,4,5-triphosphate
ipRGCs	Intrinsically photosensitive Retinal Ganglion Cells
ITP	Ion Transport Peptide
jet/JET	Jetlag
LD	Light: Dark
LED	Light-Emitting Diode

LH	Lateral Horn
LL	Constant light
l-LNvs	large ventral Lateral Neurons
LNds	dorsal Lateral Neurons
LNs	Lateral Neurons
LPN	Lateral Posterior Neurons
M	Morning
MDC	Middle dorsal commissure
mRNA	messenger RNA
na	narrow abdomen
NALCN	Na^+ leak channel
NLS	Nuclear localization sequence
ninaE	neither inactivation nor afterpotential E
norpA/NORPA	no receptor potential A
NPF	Neuropeptide F
NPY	Neuropeptide Y
ort/ORT	Ora transientless
PAR	Proline and acidic amino acid rich
PAS	Per-Arnt-Sim
pdf/PDF	Pigment Dispersing Factor
pdfr/PDFR	Pigment Dispersing Factor Receptor
Pdp1ϵ/PDP1ϵ	PAR domain protein 1ϵ
per/PER	Period
PI	Pars Intercerebalis
PIP_2	Phosphatidylinositol 4,5-bisphosphate
PKA	Protein kinase A
PLC-β	Phospholipase C - β

PLP	Posterior lateral protocerebrum
POC	Posterior optic commissure
PP1	Protein phosphatase 1
PP2a	Protein phosphatase 2a
PRC	Phase responsive curve
R1-8	Photoreceptor cell 1 to 8 of the compound eye
RFP	Red fluorescent protein
Rh	Rhodopsin
RORα, β, γ	Retinoic acid-related orphan receptors α, β, γ
rpr	Reaper
SCF	Skp1/Cullin/F-box protein
SCN	Suprachiasmatic nucleus
SEM	Scanning electron microscope
SGG	Shaggy
SLIMB	Supernumerary limb
SLP	Superior lateral protocerebrum
s-LNvs	small – ventral Lateral Neurons
sNPF	short Neuropeptide F
tim/TIM	Timeless
TRP	Transient receptor potential
TTFL	Transcription-translation feedback loop
UAS	Upstream Activation Sequence
UV	Ultraviolet
WT	Wild type
V/P	VRI/PDP1
vri/VRI	Vrille
ZT	Zeitgeber Time

Introduction

1.1 Biological timekeeping: Underlying concept

Life began on Earth approximately 3.5 billion years ago, and since then, it has evolved and diversified through the process of evolution into the complex organisms that exist today. Charles Darwin and Alfred Russel Wallace proposed that natural selection is the dominant force driving evolution, which is often summarized as "survival of the fittest." The central concept of natural selection is an organism's evolutionary fitness, which refers to its capacity to survive and reproduce in its natural habitat. To confer this fitness, organisms are known to utilize various advantageous traits, and adaptation is one such biological mechanism by which organisms improve their chances of survival.

Biological rhythms are one among the many adaptive traits that have been evolutionarily conserved across a broad spectrum of organisms, ranging from unicellular organisms to the most complex life forms (Sharma, 2005). These biorhythms refer to recurring patterns in physiological and behavioral processes and are considered to be a ubiquitous feature of nearly all living organisms (Kumar, 2017). Biological rhythms evolved as a time-keeping mechanism to create an internal representation of rhythmic changes occurring in the external environment (DeCoursey, 2004; Hut & Beersma, 2011). By means of this internal representation, the organism can track local time and anticipate the frequent rhythmic changes in the environment. Thus, these rhythms are not a mere response to environmental fluctuations but allow an organism to predict and prepare for such changes, providing a fitness advantage (Ouyang et al., 1998; Pittendrigh & Minis, 1972; Sharma, 2003; Vaze & Sharma, 2013). Biological rhythms are also self-sustaining, meaning they can persist without external support. This characteristic feature can also be considered advantageous to an organism as certain external abiotic factors could sometimes be unreliable and insufficient to provide ambient time information.

The internal temporal organization of these biological rhythms is regulated by an endogenous molecular oscillatory mechanism known as the biological clocks (Pittendrigh, 1993). These clocks can detect reliable temporal cues from external abiotic factors and fine-tune the organism's physiology and behavior accordingly (Daan & Pittendrigh, 1976; Pittendrigh, 1960, 1993). Numerous studies across various organisms indicate that biological clocks regulate and control many vital biological processes at the cellular, organ, and organismal levels (Bell-Pedersen et al., 2005; Dunlap et al., 2004; Kumar, 2017). In

humans, for example, their biological clock systems govern the temporal coordination of various biological events, such as sleep, feeding, body temperature, blood pressure, and immune responses (Dunlap et al., 2004; Kumar, 2017). At the biochemical level, biological clocks are based on specific transcription-translational feedback loops that establish a rhythmic expression of some critical genes known as clock genes (Allada, 2003; Andreani et al., 2015; Hardin, 2005; Reppert & Weaver, 2001). The clock genes regulate their own transcription and translation through these interlocked negative feedback loops to induce their cyclic expression. This self-sustaining oscillatory mechanism then allows certain clock genes to serve as a transcription factor and thereby coordinate the timing of expression for a range of other genes (clock-controlled genes) to facilitate biological rhythms (Hardin & Panda, 2013; Patke et al., 2020; Reppert & Weaver, 2001). Multicellular organisms, including insects and animals, possess a hierarchically organized clock network consisting of a central master clock and numerous peripheral clocks (Dibner et al., 2010; Mohawk et al., 2012; Patke et al., 2020). The central pacemaker clock is located in the brain, while the peripheral clock is situated in various other tissues and organs of the body. In humans, clock machinery is found in nearly all cells and tissues, but their central clock resides in the suprachiasmatic nucleus (SCN), a group of 20,000 neurons in a region at the base of the brain called the hypothalamus (Moore & Eichler, 1972; Ralph et al., 1990; Stephan & Zucker, 1972).

Biological rhythms	Environmental cycles	Cycle length
Circadian	Daily	1 day
Circannual/Seasonal	Annual	365.256 days
Circalunar	Lunar	29.53 days
Circasemilunar	Semilunar	14.8 days
Circatidal	Tidal	0.517 day

Table 1.1 Different types of biological rhythms

The study of biological rhythms and their underlying clocks, known as chronobiology, has gained significant momentum in recent decades, leading to a deeper understanding of

various timing processes in living systems. Organisms exhibit a diverse range of biological rhythms that are usually classified according to their period length, which is primarily determined by the timescales at which rhythmicity in the environment occurs (Table 1.1) (Dunlap et al., 2004; Kumar, 2017). The timescales at which these environmental cycles occur evidently include the daily, tidal, lunar, and annual cycles. Despite the identification of various biological cycles, the bulk of chronobiology research has mainly focused on daily and annual or seasonal rhythms.

1.2 Circadian rhythms

The recurring pattern of day and night is a significant natural cycle that has affected almost all organisms since the beginning of life. This 24-hour cycle, which is caused by the Earth's rotation about its axis, defines one of the prominent temporal domains of our environment. Consequently, the ecological niche of most living systems is characterized by rhythmic fluctuations in light intensity, temperature, and humidity over a 24-hour period. To cope with the daily changes in their surroundings, virtually all living organisms evolved a biological clock that measures the time of the day and controls the daily biological process accordingly (DeCoursey, 2004; Sharma, 2005). Such daily rhythms in behavior and physiology are called circadian rhythms, and the biological clock that regulates them is named the circadian clock. The underlying molecular clock generates a self-sustained rhythmic expression of clock genes with an endogenous period near 24 hours but not precisely 24 hours (Chaix et al., 2016; Patke et al., 2020; Reppert & Weaver, 2001). In humans, this period is roughly 24.2 hours, while for fruit flies, it has been documented to be approximately 23.8 hours (Czeisler et al., 1999; Dubowy & Sehgal, 2017). The term 'circadian' used to describe these rhythms is derived from the Latin words 'circa' and 'diem,' which means 'about' and 'a day,' respectively.

1.2.1 A brief history of circadian biology

The systematic investigation of biological rhythms commenced around 70 years ago, and while there were many postulations and studies on biological rhythms before that, the research conducted by Colin Pittendrigh on circadian rhythmicity in fruit flies and Jürgen Aschoff on humans during the 1950s can be deemed the basis of modern chronobiology

(Chandrashekaran, 1998). The first scientific observation of circadian rhythm was made in 1729 by the French astronomer Jean Jacques d'Ortous de Mairan. He published a study describing the daily leaf movements of a plant and noted that these movements persisted even when the plant was placed in an enclosed space without exposure to sunlight (Fig 1.1). But in his conclusion, he asserted that the plant sensed light signals without seeing them and proposed an external factor for the leaf movement in the darkness (de Mairan, 1729). Around a century later, Swiss botanist Augustin Pyramus de Candolle first proposed the concept of an endogenous timing system. After studying the leaf movements of *Mimosa pudica*, he discovered that the periodicity of leaf movements was an innate trait with a period shorter than 24 hours (Candolle, 1832). However, despite these revelations, little progress was made in the field for a considerable time. It was in the 1930s that Erwin Bünning, widely regarded as the first true circadian biologist, made significant strides in the field through his thorough research on bean plants, demonstrating that their leaf movements were internally regulated and genetically predetermined (Bünning, 1930, 1932, 1933). He was the pioneer in proposing that plants' internal clock regulates photoperiodism and relies on external stimuli to measure the duration of daylight. During the 1950s, the concept of a 24-hour endogenous clock system within living organisms gained widespread acceptance (Chandrashekaran, 1998). This discovery then got recognized as a general mechanism that governed a broad spectrum of biological functions in most animals, thanks to the work of Curt Richter, Colin Pittendrigh, and Jürgen Aschoff, who conducted extensive research on animals. Jürgen Aschoff, Colin Pittendrigh, and Erwin Bünning are regarded as the conceptual pioneers of modern chronobiology. These scientists contributed significantly to our understanding of biological rhythms and their regulation, laying the groundwork for the study of chronobiology.

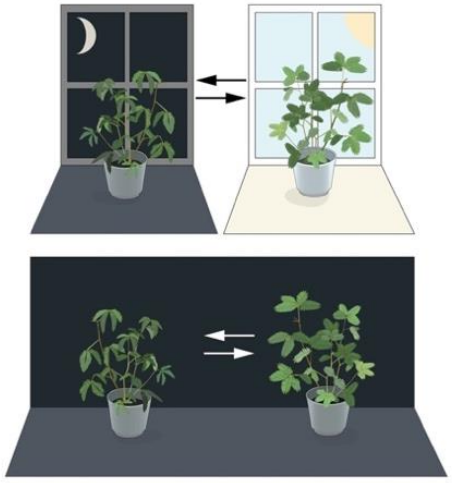

Figure 1.1 Representation of De Mairan's experiment on daily leaf movements of mimosa plants conducted in 1729. The leaves of mimosa plants display a daily rhythm of opening towards the sun during the day and closing at night, which persists even in the absence of light under constant dark conditions. (Taken from www.nobelprize.org)

Jürgen Aschoff mainly studied the human physiology of thermoregulation and was credited as the first to provide evidence of human circadian rhythms by discovering a daily pattern in the body temperature variation (Aschoff, 1947). His famous "bunker" experiments, which involved isolating human subjects from external temporal cues, demonstrated the endogenous nature of human circadian rhythms (Aschoff, 1965, 1967). He extended his studies to different organisms, including mice, to investigate the basic characteristics of circadian rhythms (Aschoff et al., 1973). Aschoff's research also focused on the effects of external stimuli, and in 1960, he coined the term 'zeitgeber' (a German word meaning 'time giver') to refer to external factors that provide ambient time cues to the internal clock (Aschoff & Wever, 1962). He proposed the concept that the circadian clocks are sensitive to external stimuli, and in the absence of such zeitgebers (time cues), the self-sustaining circadian rhythms will continue to oscillate or 'free-run' with their own endogenous period (Aschoff, 1960a, 1965, 1967; Aschoff et al., 1967). As a result, under constant conditions (absence of any 24-hour cue), such as in constant darkness or constant light, the circadian clock cannot synchronize with external environmental cues.

Colin Pittendrigh's pioneering research on the circadian rhythm of fruit flies was a significant breakthrough in the field of chronobiology, as it uncovered the model for synchronizing biological rhythms with daily light-dark (LD) cycles within a 24-hour period. The discovery that environmental cues like LD cycles could reset the internal biological clock was a crucial finding (Daan, 2000; Pittendrigh, 1960). The absence of zeitgeber-driven clock synchronization or resetting hinders the oscillations from achieving a stable phase relationship with the surroundings. This mechanism, termed entrainment, enables the organism to time daily behavior and physiology accurately and represents an adaptation of organisms to their surroundings. Given that endogenous rhythms are nearly but not precisely 24 hours in duration, they will become out of sync with natural cycles if left to their free-running properties unless the entrainment process maintains their timing daily (Golombek & Rosenstein, 2010; Pittendrigh, 1981). Additionally, Pittendrigh discovered that the circadian rhythm was temperature-compensated, meaning that the period of the rhythm remained constant even when the temperature was changed (Pittendrigh, 1954).

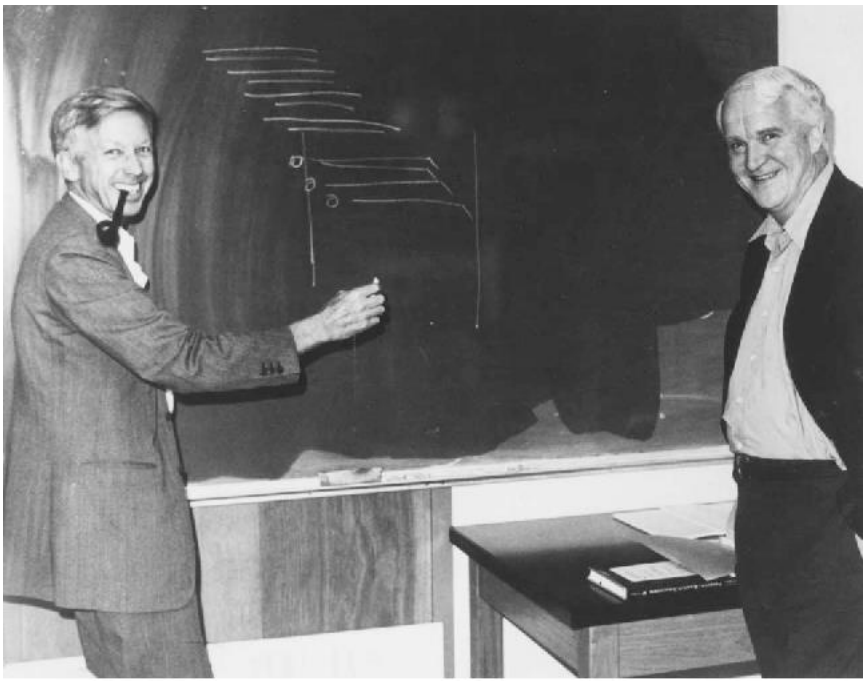

Figure 1.2 Jürgen Aschoff and Colin Pittendrigh in 1970 at Max Planck Institut für Verhaltensphysiologie in Erling-Andechs. (Taken from Kumar, 2017)

1.2.2 Fundamental properties of circadian rhythms

Many of the fundamental characteristics regarding the functions of a circadian clock were initially put forward by the pioneering work of Jürgen Aschoff and Colin Pittendrigh (Fig 1.2). In evolutionary terms, while molecular clock constituents show limited conservation, the time-keeping mechanism and its entrainment seemed to be conserved from bacteria to animals. On earth, as organisms evolved and survived in an ever-changing environment since its dawn, natural selection may have selected diverse mechanisms to generate circadian rhythms in different organisms. Although the genes responsible for clock components encode distinct proteins in different organisms, the processes by which these proteins interact to establish oscillatory mechanisms are similar in many species. Nonetheless, the characteristics that define circadian rhythms are not solely dependent on canonical molecular mechanisms but are characterized by observable, significant, and well-established criteria. At the early stages of modern chronobiology research, Aschoff and Pittendrigh characterized and established the general properties defining circadian rhythms through their studies conducted in various animal models (Aschoff, 1960b; Daan, 2000; Daan & Pittendrigh, 1976; Pittendrigh, 1960). Generally, three fundamental characteristics define

circadian rhythms found in all living organisms, which are as follows:

- Circadian rhythms are self-sustained and persist under constant environmental conditions, such as constant temperature and light or dark, with a period of approximately 24 hours, called the free-running period.
- The free-running period exhibited by circadian rhythms is independent of ambient temperature in constant conditions. This characteristic mechanism, called temperature compensation, allows the biological clock to maintain a constant period despite variations in factors that can influence their reaction rate, such as temperature.
- Although self-sustained, circadian rhythms can be entrained by 24-hour environmental cues, such as light-dark cycles, temperature cycles, or other rhythmic stimuli. This synchronization with external conditions provides the clock with an internal measurement of external local time. Entrained clocks exhibit overt rhythms with a period equivalent to the entraining cycle (zeitgeber cycle) with a fixed phase angle.

1.2.3 Generic model of the circadian system

The circadian system of any organism can be conceptually oversimplified as a linear model consisting of three main components. These components include an ‘input’ pathway that perceives and transmits environmental time cues to synchronize the clock, the endogenous ‘clock’ that generates rhythmicity, and an ‘output’ pathway that connects the clock to various biological processes (Hardin & Panda, 2013; Reppert & Weaver, 2002; Schibler & Sassone-Corsi, 2002).

The input pathway underlies the entrainment process, which aligns the internal clock to the local time. This sensory pathway detects specific environmental cues that provide reliable ambient time information and integrates them into the molecular clock residing inside a cell. Clock resetting via entrainment allows the clock to adjust its period and phase to the environmental cycle, thereby driving different biological processes at the appropriate time (Golombek & Rosenstein, 2010; Roenneberg et al., 2003). The core mechanism that generates circadian rhythms is based on a network of biochemical feedback loops. The molecular clock creates oscillations in gene expression that are synchronized to the

environmental cycle through the zeitgeber pathway. The circadian system's output pathways are diverse and regulate various biochemical, physiological, and behavioral processes. The output pathways of the circadian system are tightly interconnected and coordinated, allowing for the precise timing and synchronization of physiological and behavioral processes across different tissues and organs in the body (Dibner et al., 2010; A. N. King & Sehgal, 2020; Starnes & Jones, 2023).

Indeed, while the simplified linear model of the circadian system has been helpful in understanding the basic components of the system, it is now recognized as an oversimplification of the true complexity of the circadian system (Fig 1.3). Research has revealed that the circadian system is much more complex and dynamic than previously thought and involves a vast network of interacting components and feedback loops. This has led to the development of more sophisticated models, which take into account the various ways in which different components of the circadian system interact and influence one another. For instance, input signals such as light can impact a range of physiological and behavioral outputs without involving the circadian clock (known as "masking") (Redlin & Mrosovsky, 1999). On the other hand, clock-controlled output variables might also give feedback on the oscillator or even the input pathway, adding more evidence to a non-linear model (G. Y.-P. Ko, 2020).

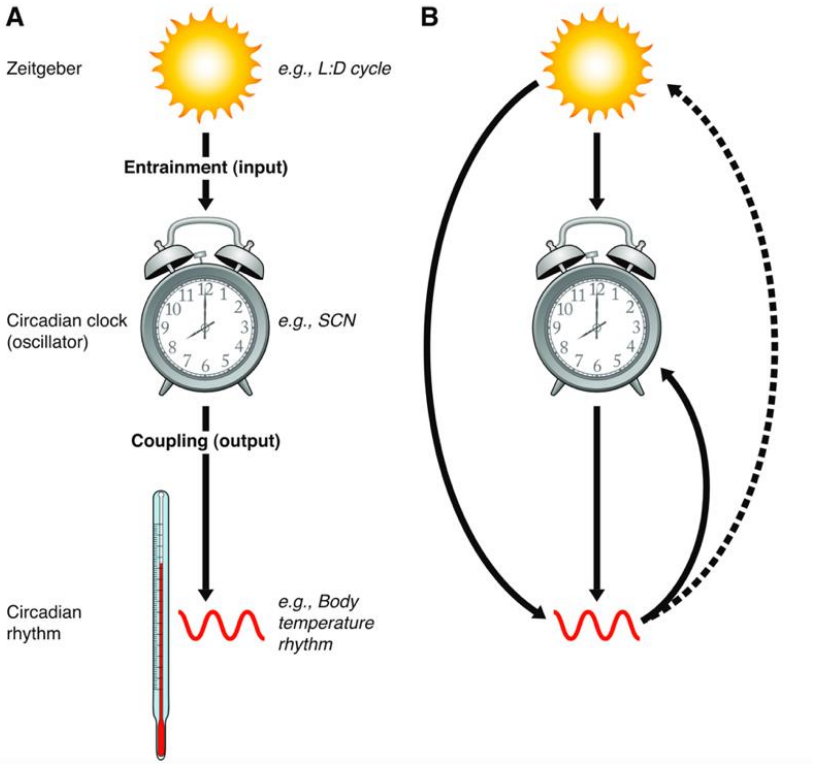

Figure 1.3 A: The simplified linear model of the circadian system. The internal clock residing at the model's center receives reliable time signals via the input pathway for entrainment (alignment of the clock's endogenous period to the external cycle). The genetically controlled clock then generates overt rhythms in behavior and physiology **B:** The complex scheme of circadian organization involving nonlinear relationships between its components. The input signal can influence the output component without clock mediation, and feedback from the output pathways is known to regulate the oscillator and impact the input pathways. (Taken from Golombek & Rosenstein, 2010)

1.2.4 Circadian entrainment

As endogenous circadian rhythms are not precisely 24 hours, external time cues (or zeitgeber) are required to reset the clock daily and adjust its phase to the local time. This daily re-setting is inevitable for the internal clock to stay aligned with the natural cycles. When the clock is not entrained, it deviates from external environmental cycles, which can nullify its adaptive and significant value. In humans, misalignment of circadian rhythms with the natural periodic changes is known to cause adverse effects on several physiological and behavioral processes, including sleep, metabolism, immunity, cognitive functions, etc. (Blume et al., 2019; Finger & Kramer, 2021; Roenneberg & Merrow, 2016).

The biological clock can be synchronized or entrained to external environmental cycles by a variety of stimuli. These cues are reliable proxies for the time of day that can reset the clock appropriately. These zeitgebers include light/dark, temperature, humidity, tides, food availability, social signals, and many others (Daan & Pittendrigh, 1976; Golombek & Rosenstein, 2010; Y. Liu et al., 1998; Mendoza, 2007; Mrosovsky, 1988; Roenneberg et al., 2003; Roenneberg & Foster, 1997). However, it has been widely recognized that the alternation between day and night is the most crucial resetting signal that entrains the circadian system in nearly all living organisms (Aschoff et al., 1972; Roenneberg & Foster, 1997).

Besides light, the most prominent zeitgeber would be natural temperature cycles. Research has shown that a slight variation of 2°C is enough to entrain the circadian clock in fruit flies (Glaser & Stanewsky, 2007; Rensing & Ruoff, 2002). Flies rely on their chordotonal organ to sense temperature changes, and these time signals are relayed to specific neurons in the brain for the entrainment of the circadian clock that controls activity rhythms. Ionotropic receptors seem to play an important role, but other receptors have been

involved, depending on the temperature conditions (Chen et al., 2015; Sehadova et al., 2009).

1.2.4.1 Photoentrainment

The dominant cyclical pattern that characterizes the temporal domain of our planet is the natural day-night cycle. Earth rotates on its axis, creating a cycle of 24 hours, which results in alternating periods of daylight and darkness. Consequently, the sunlight that reaches the Earth's surface undergoes systematic cyclic variations, including changes in the quantity, spectral composition, and direction of light. These changes are particularly significant during the twilight period. Thus, most organisms use characteristic variations of a natural light-dark (LD) cycle as their primary zeitgeber to track local time, a process known as photoentrainment (Fig 1.4) (Foster & Helfrich-Forster, 2001; Roenneberg & Foster, 1997; Wright et al., 2013).

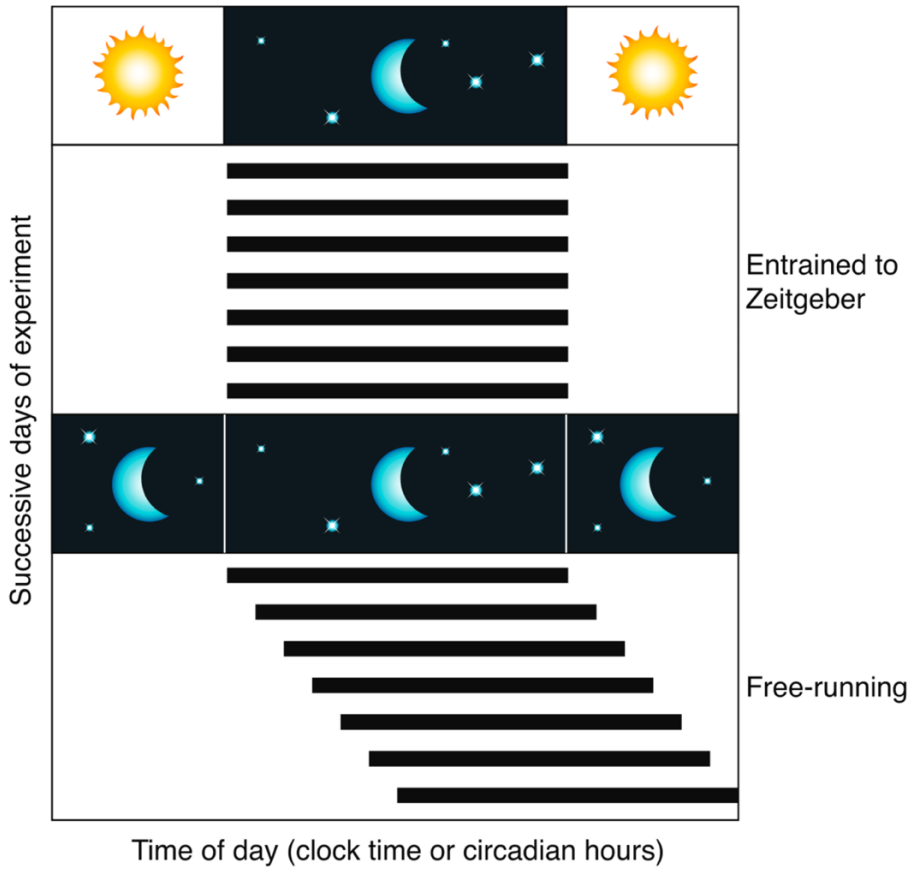

Figure 1.4 Circadian photoentrainment. Representation of an actogram displaying the locomotor activity rhythms of a nocturnal animal. The circadian rhythms are entrained to 24-hour external light-dark cycles during the initial days. Upon transfer to constant dark conditions, the circadian rhythms

deviate from external cycles and exhibit free-running behavior with their endogenous period (>24 hours in this case). (Taken from Golombek & Rosenstein, 2010)

There are two established models that explain how circadian entrainment occurs under natural photic conditions: the parametric model and the nonparametric model (Daan, 1977; Roenneberg et al., 2003). In essence, the parametric or continuous model proposes that extended light exposure alters the speed of the circadian clock, leading to changes in its period. Aschoff, who put forward this model, proposed that long durations of light have continuous (or tonic) action on the clock's speed, causing it to either run faster or slower. Thus, entrainment is attained by the modulation of angular velocity under the LD cycles, allowing the circadian clock to continuously adjust its endogenous period to that of the LD cycle (Aschoff, 1979; Daan, 2000; Hut et al., 1999).

According to the nonparametric or discrete model, the endogenous period is adjusted through light-induced daily phase shifts of the clock. In this model, a short light pulse or a transition of light at dawn or dusk is sufficient to trigger a phase shift in the circadian clock. This phase shift could be either advanced or delayed, enabling the endogenous period of the clock to remain aligned with that of the zeitgeber cycle (Daan, 2000; Daan & Pittendrigh, 1976).

Entrainment cues in nature for the nonparametric or discrete model are typically the transitions between light and dark at dawn and dusk, which are brief and discrete changes in the light environment. On the other hand, the entrainment cues for the parametric model are associated with the gradual changes in the intensity or duration of light over the course of the day, which provide a continuous signal for the circadian clock to entrain. However, it's important to note that the differences between the two models are not only determined by the nature of the stimulus but also by the specific mechanisms and parameters involved in the entrainment process. For instance, the parametric model consists of a mechanism that adjusts the clock's velocity and period in response to the strength of the entrainment signal, while the nonparametric model doesn't rely on such a mechanism (Daan, 2000; Dunlap et al., 2004). It is not excluded that the two types of entrainment process coexist for the same clock.

1.2.4.2 Phase response curve

As mentioned earlier, a short light pulse can perturb the phase of a clock. The effect of such light stimulus depends on the phase (φ) at which the stimulation is applied. A phase response curve (PRC) is a plot of phase shifts of a circadian rhythm as a function of the phase (or the time of the day) at which the stimulus was given. The phase shift is typically measured in hours and can be either positive (an advance in the clock's phase) or negative (a delay in the clock's phase) (Fig 1.5). The resulting PRC curve shows how the timing of a stimulus affects the magnitude and direction of the resulting phase shift. It is a valuable tool for understanding the entrainment of circadian rhythms and the effects of a particular stimulus on the clock (Aschoff & Pohl, 1978; Johnson, 1999).

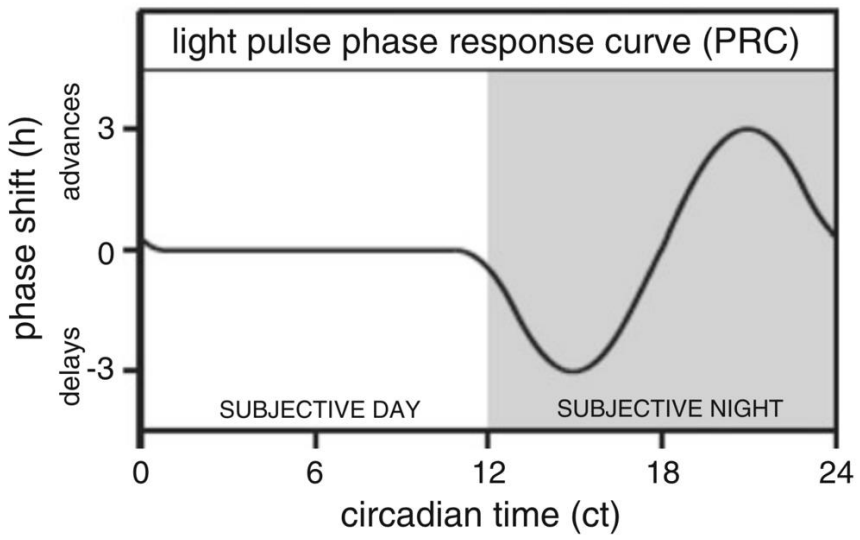

Figure 1.5 A representative graph showing the circadian phase response curve to light pulses. Conventionally, positive values represent phase advances, while negative values indicate phase delays. A biphasic pattern is typically observed in photic phase response curves (PRCs), with phase delays occurring at the start of the subjective night and phase advances towards the end of this period. There exists a dead zone in the middle of the subjective day characterized by no change in the clock's phase to the stimulus given. (Taken from Kumar, 2017)

1.2.5 Structural organization of the circadian clock

The molecular clock machinery resides in nearly all tissues throughout the body of a multicellular organism, temporally regulating the function of organs and tissues (Dibner et

al., 2010; Mohawk et al., 2012; Reppert & Weaver, 2002). In essence, the circadian rhythms are orchestrated by a multi-oscillator circadian system that is hierarchically organized into a central clock and subsidiary peripheral clocks.

The central clock functions as the body's master circadian pacemaker, regulating a wide range of key circadian rhythms, both overt and covert, throughout the body. In contrast, peripheral clocks are more specialized and tend to govern specific, localized circadian rhythms in physiology and behavior. In mammals, the central pacemaker located in the SCN plays a primary role in governing circadian rhythms across the entire body. It transmits signals and orchestrates the synchronization of peripheral clocks through neural and hormonal pathways. The synchronization of peripheral clocks in mammals relies to some extent on the central pacemaker. Conversely, in *Drosophila*, the situation diverges. Peripheral clocks in *Drosophila* demonstrate a greater capacity to directly receive environmental cues or 'zeitgeber' inputs, such as light and temperature, with less reliance on the central brain clock. This heightened autonomy of peripheral clocks in *Drosophila* enables them to respond more independently to external cues. Consequently, the extent to which the central pacemaker is essential for regulating circadian rhythms in various cells, tissues, physiological functions, and behaviors exhibits variations among species.

1.2.5.1 Central and peripheral clocks

The central or master clock emerges from a dedicated network of circadian pacemaker neurons in the brain. These so-called 'clock neurons' express core clock genes that compose the molecular clock to generate autonomous rhythmicity. The neuronal network within the master clock is characterized by their synchronization with one another through topographically organized coupling mechanisms facilitated by neurotransmitters and neuromodulators (Ahmad et al., 2021; Crespo-Flores & Barber, 2022a; Dibner et al., 2010). Moreover, the master clock is effectively synchronized with external environmental cycles by receiving direct inputs from zeitgeber signals. As such, the central clock plays a critical role in the entrainment mechanism, particularly photoentrainment, since they receive direct photic input from dedicated photoreceptors (Dannerfjord et al., 2021; Yoshii et al., 2016). The master clock could then transmit temporal information provided by such reliable cues to peripheral clocks located throughout the body, including other brain regions, through

neuronal and humoral pathways (Dubowy & Sehgal, 2017; A. N. King & Sehgal, 2020). Master clocks are also capable of integrating entraining signals that have been feedback onto them from periphery clocks.

Peripheral clocks, much like the central clock, are self-sustaining and share a similar molecular clock composition (Dibner et al., 2010; Ito & Tomioka, 2016). However, due to the hierarchical nature of the circadian system, the synchronization between different peripheral clocks is heavily dependent on the master clock in the brain (Yamazaki et al., 2000). While peripheral clocks are generally regarded as "slave" oscillators that receive input from the central clock to reset themselves, recent research suggests that they can also be synchronized autonomously, in addition to being entrained by hormonal and neural signals from the central clock (Ito & Tomioka, 2016; Whitmore et al., 2000). The extent to which the central clock is required to fine-tune the peripheral clocks can vary depending on the species and specific tissues, organs, and circadian rhythms involved.

Different physiological functions and behaviors may be regulated to varying degrees by the central and peripheral oscillators. For example, the sleep-wake cycle is strongly regulated by the central pacemaker, while peripheral clocks in the liver and pancreas play a more prominent role in regulating metabolism and glucose homeostasis (Fig 1.6). Overall, regulating circadian rhythms is a complex and dynamic process involving both central and peripheral clocks working in concert to coordinate physiology and behaviors in a rhythmic manner.

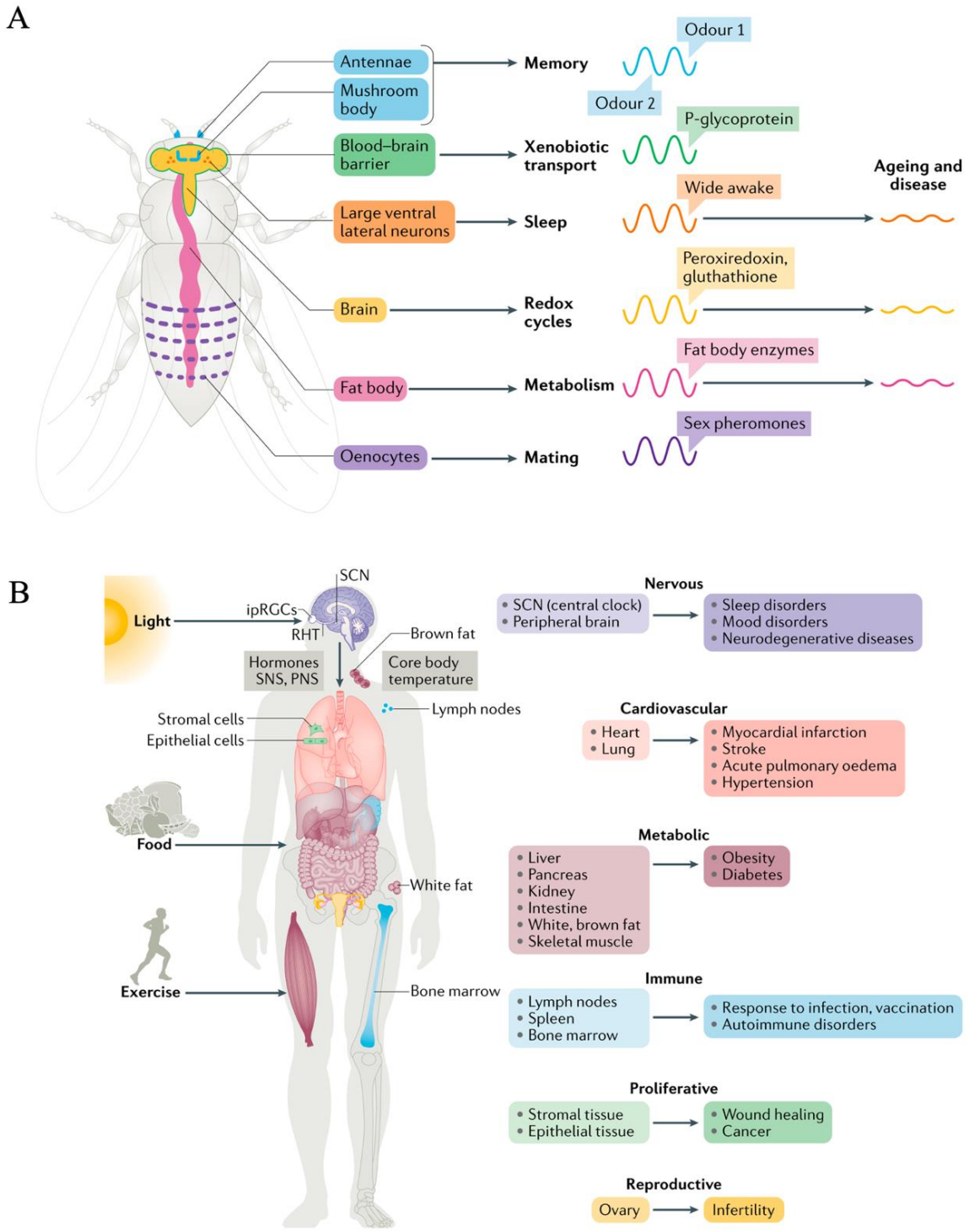

Figure 1.6 The central and selected peripheral clocks in *Drosophila melanogaster* and Humans. **A:** The central clock of flies resides in ~150 clock neurons in the brain. In addition to central pacemaker cells, clocks in other brain regions and peripheral tissues co-ordinately drive circadian rhythmicity in various biological functions by facilitating the cyclic expression of associated molecules like cycling of sex pheromones for mating, fat body enzymes for metabolism, etc. **B:** The circadian system in humans comprises a central clock located in the suprachiasmatic nuclei (SCN) region of the brain, as well as subsidiary clocks found in nearly all cells throughout the body. Physiological domains that

demonstrate circadian rhythmicity are color-coded, and representative organs containing local circadian oscillators are illustrated for each part. Furthermore, certain pathophysiologies linked to circadian dysfunction are also featured. (Adapted from Patke et al., 2020)

1.3 Molecular basis of the circadian rhythms

1.3.1 Emergence of neurogenetics: Unlocking complex behaviors

Although Erwin Bünning's research on plant hybrids with different endogenous periods unveiled the genetic foundation of circadian rhythms, the finer details of the underlying genetic and molecular mechanism remained elusive for an extended period. In the early 1900s, the renowned scientist Thomas Hunt Morgan proposed the idea of a gene (a region of DNA) as a fundamental unit of heredity. He did his ground-breaking research on fruit flies and found that specific traits (mainly physical attributes) in flies are inherited and linked to genes residing on chromosomes. This revelation became the cornerstone of modern genetics, but the idea of a single gene affecting something as complex as an animal's behavior was unheard of then. The era of neurogenetics or behavioral genetics linking genes, brain, and behavior began in 1971 when Seymour Benzer and Ron Konopka discovered that mutation in a particular gene in flies affected their circadian behaviors drastically. They utilized ethyl methane sulfonate–induced mutations on the X chromosome to perform a screen and identify clock mutants. By using pupal eclosion timing as the screening parameter, they located and mapped three clock mutants that impacted the rhythmicity of eclosion. These mutations were categorized as distinct, comprising a short-period mutant (about 18 hours), a long-period mutant (about 28 hours), and an arrhythmic mutant (Fig 1.7). Further analysis revealed that all three mutations were allelic variations of a single gene, which they named *period (per)*. This discovery marked the first identification of a clock gene in any organism, although clock mutants were isolated in *Neurospora crassa* and *Chlamidomonas reinhardi* almost simultaneously. The *per* gene was found to be essential for nearly all *Drosophila* circadian behaviors, indicating its critical role in the circadian clock function (Konopka & Benzer, 1971).

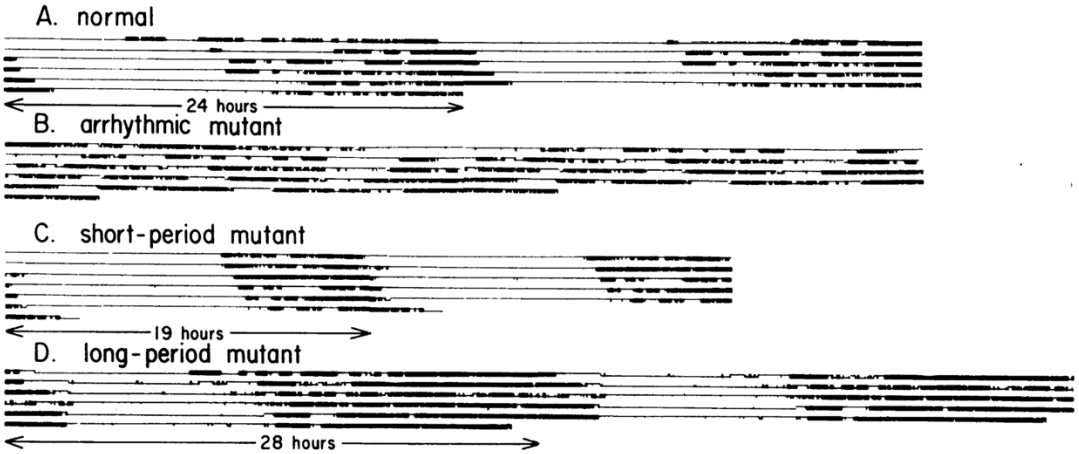

Figure 1.7 Three *period* mutants of *Drosophila melanogaster* discovered by Konopka and Benzer after their famous screen for clock mutants. Double plotted actograms showing locomotor activity of various per mutants in constant infrared light, previously entrained in 12:12 LD. The short-period mutant runs with a period of ~19 h, the long-period mutant with ~28 h, and the arrhythmic mutant display an arrhythmic activity pattern. (Taken from Konopka & Benzer, 1971)

1.3.2 Conceptualization of feedback loop model

The molecular characterization of *per* gene was performed another 13 years later as the recombinant DNA technology was only gaining progress during the 1980s. In 1984, the *period* locus was identified and cloned independently by the laboratories of Jeff Hall and Michael Rosbash at Brandies and Michael Young at Rockefeller (Bargiello et al., 1984; Reddy et al., 1984; Zehring et al., 1984). The cloning and sequencing of the *per* gene failed to provide substantial insights into the molecular workings of the circadian clock. Nonetheless, the sequence analysis uncovered a structurally conserved PAS domain in PER, a key region involved in protein-protein interaction and dimerization. In 1988, Hall, Rosbash, and their colleagues identified the periodic expression of PER protein in the visual system of flies (Siwicki et al., 1988). Two years later, they uncovered that both *per* mRNA and protein follow a rhythmic expression pattern in the fly head (Hardin et al., 1990). Over a 24-hour period, the protein encoded by *per* exhibited a pattern of accumulation during nighttime and degradation during the daytime, thereby following a circadian pattern. Additionally, they found that the cycling of *per* mRNA depended on the presence of PER

protein, which peaked a few hours later than the mRNA cycling (Zeng et al., 1994). It was shown that PER was actually a nuclear protein, and antibody staining results revealed that they shuttled between the nucleus and cytoplasm (X. Liu et al., 1992). These findings further supported the idea that PER migrate to the nucleus upon translation in the cytoplasm, where they function as a transcriptional repressor to regulate their own gene expression (Hardin et al., 1992; Zeng et al., 1994). In light of these characterizations, Hall and Rosbash proposed an intracellular transcriptional translational feedback loop (TTFL) model that defined the molecular basis for clock machinery.

Even though the role of PER as a transcription repressor got more evidence, it lacks a DNA binding domain, such as the basic helix-loop-helix (bHLH), to directly inhibit its transcription. Therefore, it was initially hypothesized that PER might inhibit transcription by binding to its transcription activators that contain the bHLH domain, using its PAS domain to mediate the interaction (Huang et al., 1993). Later in 1994, the identification of *timeless* (*tim*) as the second clock gene by Michael Young's laboratory added further insights to the TTFL model (Myers et al., 1995; Sehgal et al., 1994). Young and his team observed that levels of mRNA and protein encoded by the *tim* gene oscillate in phase with that of *per*. They also showed that mutations in the *tim* gene disrupted the oscillation of *per* mRNA levels and eliminated overt circadian rhythms (Price et al., 1995; Sehgal et al., 1994, 1995). Furthermore, it was discovered that in *tim* mutants, the nuclear localization of PER protein was eliminated (Vosshall et al., 1994). These results collectively suggested that PER protein's cyclic build-up and nuclear positioning relied on the PER-TIM interaction and was proven later (Gekakis et al., 1995).

Characterization of *per* and *tim* gave an initial idea of how the TTFL functions to establish an autonomous *Drosophila* circadian oscillator to drive circadian rhythms. The year when the core clock gene *tim* was identified in *Drosophila* also saw the discovery of the first mammalian clock gene by the laboratory of Joseph Takahashi, which was named *Clock* (*clk*) (Antoch et al., 1997; D. P. King et al., 1997; Vitaterna et al., 1994). Later they found *Bmal1* as another vital clock gene in mice and demonstrated that CLOCK/BMAL1 heterodimers recognized specific binding sites for bHLH domains, known as E-boxes, located upstream of the *per* gene to initiate its transcription (Gekakis et al., 1998). Identifying *Clock* and *Bmal1* as transcriptional activators led to the discovery of their orthologs in *Drosophila*. In 1998, the research team under Hall and Rosbash discovered two new clock genes in *Drosophila*, *Clock* (*clk*) and *Cycle* (*cyc*), which were orthologs of

mammalian *Cycle* and *Bmal1* (Allada et al., 1998; Rutila et al., 1998). Mutations in these genes led to arrhythmicity in both overt circadian rhythms and transcript levels of *per* and *tim*. After forming a heterodimer, CLK and CYC, both possessing a DNA binding domain (bHLH) and a protein-protein interaction domain (PAS), were observed to activate the transcription of *per* and *tim*. Consequently, later the proteins encoded by *per* and *tim* after additional posttranscriptional modifications suppress the activity of CLK/CYC heterodimer, thus completing the feedback loop (Darlington et al., 1998).

The canonical TTFL model underlying the circadian mechanism in *Drosophila* thus became apparent after the identification of four clock genes and the subsequent molecular characterizations. These landmark studies on *Drosophila* opened the door for extensive research into understanding biological clocks in all other organisms, including humans. Even though the clock components are not that conserved, there is a high degree of similarity in the fundamental TTFL structure (Fig 1.8) (Bell-Pedersen et al., 2005; Dunlap, 1999; Young & Kay, 2001). Hall, Rosbash, and Young's groundbreaking work on the molecular underpinnings of circadian rhythm were honored with the 2017 Nobel Prize in Physiology and Medicine.

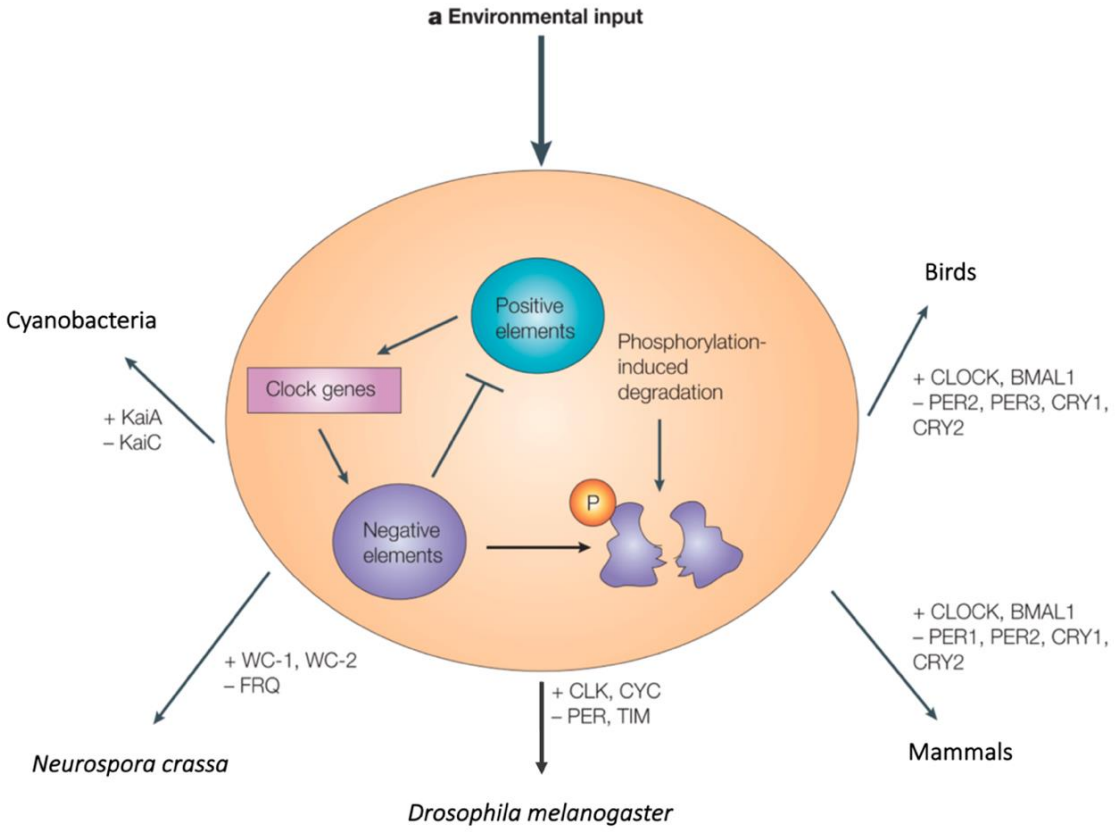

Figure 1.8 TTFL mechanism to generate 24-hour oscillations is conserved across diverse organisms, from bacteria and fungi to plants and animals. TTFL consists of a few interlinked feedback loops that rely on positive and negative components. In general, the transcription of certain clock genes encodes clock proteins that act as negative elements and inhibit the action of positive elements whose role is to activate the clock genes. Subsequent phosphorylation-induced degradation of negative elements allows positive elements to restart a new cycle. However, the components of these negative and positive regulatory arms vary across species. Positive and negative components involved in each model organism's core TTFL are indicated by the '+' and '-' symbol, respectively. (Adapted from (Bell-Pedersen et al., 2005)

1.3.3 Molecular clock in *Drosophila*

From the dawn of chronobiology, researchers worldwide relied heavily on *Drosophila* as the model organism to study circadian rhythms due to its ease of use and advanced molecular and genetic toolkit. Over the past three decades, the molecular clock in *Drosophila* has been extensively examined, making it one of the most comprehensively understood biological clocks. In a simplified view, the molecular clock could be represented by interlocked loops involving transcription and translation of core clock proteins. By means of this autoregulatory feedback mechanism, clock proteins can not only regulate their own transcription but also establish the rhythmic expression of a multitude of clock-controlled genes.

1.3.3.1 The core feedback loop

The core negative feedback loop propels the self-sustained oscillation of *per* and *tim*, which are critical clock genes. In the late morning, CLK/CYC heterodimer binds with the conserved E-boxes in the promoters of *per* and *tim* genes to drive their positive transcription (Darlington et al., 1998; Hao et al., 1997; McDonald et al., 2001). Although the levels of *per* and *tim* transcripts reach their maximum in the early night, their corresponding proteins do not accumulate until late at night (Edery et al., 1994; Hardin et al., 1990; Hunter-Ensor et al., 1996; Myers et al., 1996; Sehgal et al., 1995). This delayed accumulation of PER and TIM proteins is due to several posttranslational modifications, which are obligatory for their oscillatory expression (explained later). Thus, cytoplasmic accumulation of PER and TIM

is observed from the early night only, approximately 4-6 hours after the initiation of their transcription. PER and TIM will dimerize upon translation in the cytoplasm, with TIM binding to the PAS domain of PER (Gekakis et al., 1995; Zeng et al., 1996). The stabilization of PER is attributed to its dimerization with TIM since PER is susceptible to degradation following the posttranslational phosphorylation (Suri et al., 1999; Vosshall et al., 1994). After reaching a critical threshold, PER/TIM heterodimers translocate to the nucleus, impeding CLK/CYC activity to inhibit their transcription (Chang & Reppert, 2003; C. Lee et al., 1999; Saez & Young, 1996). PER/TIM shuts down the activity of CLK/CYC by inducing phosphorylation and reducing their affinity for E-boxes (Bae et al., 2000; C. Lee et al., 1998, 1999; Yu et al., 2006). This negative feedback completes the loop, and the new cycle resumes with the eventual degradation of PER and TIM, leading to the regain of transcriptional activity of CLK/CYC. Upon light exposure, TIM degrades rapidly via CRYPTOCHROME-JETLAG dependent pathway (explained later), which in turn lowers the stability of PER and causes it to degrade as well (Hunter-Ensor et al., 1996; C. Lee et al., 1996; Zeng et al., 1996, 1996). As a result, during the early morning, both TIM and PER experience degradation, and their levels reach their lowest point towards the end of the light phase.

The duration for which PER and TIM remain in the cytoplasm is a crucial factor in determining the length of the circadian rhythm's period (Curtin et al., 1995; Meyer et al., 2006; Saez et al., 2007). Thus, temporal regulation of nuclear entry of the PER-TIM proteins is a vital step to set the oscillation frequency. The cytoplasmic presence of both proteins and their subsequent dimerization is essential for their nuclear translocation (Saez & Young, 1996; Suri et al., 1999; Zeng et al., 1996). PER-TIM dimer formation is required for PER to translocate into the nucleus, whereas TIM can enter the nucleus alone without PER (Shafer et al., 2002a). Nevertheless, in the absence of PER, TIM's ability to remain in the nucleus is compromised. TIM is the primary component of nuclear import mechanisms here, where it acts as an adapter to transport PER to the nucleus (Jang et al., 2015). The nuclear localization sequence (NLS) in the TIM protein recognizes and binds the components of the canonical importin system, which in turn targets the nuclear pore complex to facilitate nuclear uptake. Mutations in this region affected the timed nuclear accumulation of both TIM and PER. This leads to abnormally high levels of TIM and PER in the cytoplasm for an extended period, eliciting circadian rhythms with a period of ~30 hours (Saez et al., 2011).

1.3.3.2 Interlocked feedback loops

In the *Drosophila* clock, *clk* mRNA level cycles with a peak expression immediately after dawn and thus are antiphase to the mRNA levels of *per* and *tim* (Bae et al., 1998). Moreover, it was also observed that null mutations in *per* (*per*^{0}) and *tim* (*tim*^{01}) repressed *clk* mRNA rhythms resulting in consistently low *clk* mRNA levels (Bae et al., 1998; Darlington et al., 1998). Notably, in the flies with mutations in *clk* (*clk*^{Jrk}) and *cyc* (*cyc*^{0}), *per* and *tim* mRNAs were constitutively low, while *clk* and *cyc* transcript levels remained constitutively high (Allada et al., 1998; Rutila et al., 1998). This suggested a different transcriptional regulation for *clk*, adding more intricacies to the feedback loop model. Thus, it was proposed that a secondary feedback loop is intricately linked with the core feedback loop to regulate the rhythmic expression of the *clk* mRNA (Glossop et al., 1999). According to this model, CLK/CYC may inhibit *clk* transcription, perhaps by activating a repressor of *clk*, while PER/TIM appears to alleviate this inhibition in some manner (Glossop et al., 1999).

It was discovered that *vrille* (*vri*), which encodes a transcription factor with a basic leucine zipper (bZip) motif and is directly controlled by CLK/CYC, functions as a repressor of *clk* (Blau & Young, 1999). *In vitro* studies revealed that VRI protein can bind directly to the VRI/PDP1 (V/P) boxes in the *Clk* promoter, inhibiting its activity to shut down the *clk* transcription (Cyran et al., 2003; Glossop et al., 2003). Furthermore, it was demonstrated that the decrease in *clk* RNA levels resulting from *vri* overexpression occurred irrespective of the presence of nuclear PER and TIM proteins. Later, another *clk* activator was discovered named *PAR domain protein 1ε* (*Pdp1ε*), possessing both bZip and PAR (proline and acidic rich) domains (Cyran et al., 2003). Similar to *vri*, *Pdp1ε* have E-box elements in their promoter region and is activated by CLK/CYC. *Pdp1ε* and *vri* transcripts cycle in phase with those of *per* and *tim* genes, although the peak of *Pdp1ε* expression is delayed by ~ 4-6 hours (Cyran et al., 2003).

At about midday, CLK/CYC heterodimers attach to E-boxes and activate the transcription of *vri* and *Pdp1ε*. As a result of differences in their transcriptional regulation, mRNAs and proteins of *vri* and *Pdp1ε* accumulate with different phases such that VRI protein accumulates first and suppresses *Clk* expression. Afterward, PDP1ε protein accumulates at a delayed pace and binds to V/P boxes by displacing VRI, leading to the derepression of *clk* transcription in the middle of the night (Cyran et al., 2003; Glossop et

al., 1999, 2003). However, the newly formed CLK protein is initially inactive due to the PER inhibition of CLK/CYC activity in the late part of the night. Following the degradation of PER/TIM at dawn, CLK/CYC starts to bind the E-boxes of the respective promoters to drive the transcription of both *per*/*tim* and *vri*/*Pdp1ε*, initiating a new cycle of both feedback loops. Therefore, the second feedback loop, mainly comprised of *vri*, *Pdp1ε*, and *clk*, underpins the daily rhythms of *clk* expression, which is antiphase to *per*/*tim* cycle (Cyran et al., 2003; Glossop et al., 1999, 2003). Here CLK/CYC complex simultaneously activates the transcription of its repressor and activator. In turn, as *Pdp1ε* and *vri* feedback to CLK/CYC, thus closing the loop to drive daily oscillations. VRI and PDP1ε proteins accumulate with a phase delay, which likely underlies the sequential repression and activation of *clk* transcription.

The initial assumption was that the *clk* transcription cycle was regulated by the competition between VRI and PDP1ε for V/P boxes, where VRI acted as a repressor, and PDP1ε served as an activator for the *clk* transcription (Cyran et al., 2003). According to this model, during the early night when VRI levels were high compared to PDP1ε, VRI would bind to V/P boxes, and vice versa during the late night when PDP1ε levels were high. However, consistent downregulation or overexpression of PDP1ε exerted little effect on *clk* transcription or VRI cycling (Benito et al., 2007; X. Zheng et al., 2009). Additionally, *clk* mRNA was constantly elevated in mutants that had reduced expression of VRI and PDP1ε (clk^{Jrk} and cyc^{01}), indicating that PDP1ε did not significantly impact *clk* transcription. Altogether, these results highlighted a model where *clk* transcription was rhythmically regulated primarily by the periodic repression by VRI rather than periodic activation by PDP1ε (Benito et al., 2007; Hardin, 2011a; X. Zheng et al., 2009).

A third feedback loop, regulated by the transcription inhibitor CLOCKWORK ORANGE (CWO) of the bHLH-orange family, exists alongside the *per*/*tim* and *clk* feedback loops (Kadener et al., 2007; Lim et al., 2007; Matsumoto et al., 2007). The CLK/CYC complex activates the transcription of *cwo* by binding to the E-boxes in the 5′ upstream regions. CWO, acting as a transcriptional repressor, subsequently feedback to inhibit the CLK/CYC-activated transcription. This inhibition occurs via competitive binding to the E-boxes, further strengthening the transcriptional repression of CLK/CYC caused by PER complexes (Kadener et al., 2007; Lim et al., 2007; Matsumoto et al., 2007).

Even though both *per*/*tim* and *clk* feedback loops regulate the rhythmic expression of specific clock genes, they do not hold equal importance in the function of the circadian clock (Hardin, 2006). The positive arm of the *per*/*tim* loop is formed by CLK/CYC-mediated transcription of *per* and *tim*; however, the *clk* loop, which is responsible for driving the rhythmic expression of CLK, is not a prerequisite for the operation of the *per*/*tim* loop (E. Y. Kim et al., 2002). This is accounted for by the observation that there is little impact on molecular or behavioral rhythms when the *clk* mRNA cycling is reversed (E. Y. Kim et al., 2002). However, abolishing both *per* and *tim* mRNA cycling heavily impedes circadian rhythms (Yang & Sehgal, 2001). Since PER complexes regulate the transcription of *vri* via CLK/CYC inhibition, the *per*/*tim* loop could be considered inevitable for the *clk* loop (Cyran et al., 2003; Yu et al., 2006). Notably, mutations in *per* (per^{0}) and *tim* (tim^{01}) disrupt the transcriptional rhythms in both loops (Cyran et al., 2003; Glossop et al., 2003). Although *clk* mRNA cycling is not essential for clock function, the *clk* loop drives the rhythmic transcription of clock-output genes required for circadian rhythms. This was further supported by genome-wide expression analysis and other microarray screens, which revealed that a significant fraction of rhythmically expressed mRNAs in *Drosophila* have a similar phase to that of *clk* (Ceriani et al., 2002; Claridge-Chang et al., 2001; Keegan et al., 2007; McDonald & Rosbash, 2001; Ueda et al., 2002; Wijnen et al., 2006).

1.3.3.3 Posttranslational regulation of clock

The interlocked feedback loops described thus far constitute the fundamental framework of the *Drosophila* molecular clock. This TTFL clock establishes the self-sustained rhythmic expression of clock genes, wherein the transcription of clock genes is negatively regulated by the feedback from their protein products. To generate 24-hour period oscillations, the aforementioned molecular clock must separate the phases of clock gene transcription and repression. Failure to do so will cause clock components to settle into a stable state. To prevent this damping out effect and ensure that the clock maintains a period of ~24 hours, inevitable regulatory mechanisms are needed (Hardin, 2011b; Özkaya & Rosato, 2012).

Completing a single feedback loop involves several steps, including the whole gene-to-protein cascade comprising activation, transcription, mRNA transport and translation. Following this, proteins are translocated to the nucleus to repress their transcriptional

activators and close the loop. Since all these steps collectively take much less than 24 hours to complete, it is critical to incorporate specific delays in one or more steps to stretch the feedback loop, covering an entire day. As a result, different mechanisms have evolved to ensure the temporal separation between transcriptional activation and repression of clock genes. Many such regulatory mechanisms occur at the post-transcriptional and post-translational levels to incorporate the required delay. In particular, it's been the post-translational regulation that heavily controls the period and amplitude of the clock to ensure proper timekeeping. These modifications implemented on the clock proteins regulate their activity, stability, and subcellular localization so that transcriptional feedback occurs at the appropriate time of day. Phosphorylation, dephosphorylation, ubiquitination, acetylation, and SUMOylation are the widely reported vital mechanisms utilized for modifying clock proteins at the posttranslational level (Fig 1.9) (Benito et al., 2007; Cyran et al., 2005; Hardin, 2011a; Helfrich-Förster, 2017; Martinek et al., 2001; Patke et al., 2020; Tataroglu & Emery, 2015; Weber et al., 2011; X. Zheng & Sehgal, 2012).

The PER/TIM loop, the core feedback loop, is characterized by a temporal delay between the transcription and repression of *per* and *tim* genes. This is mainly put forward by the delayed accumulation of PER and TIM proteins in the cytoplasm. As previously mentioned, the levels of these proteins remain low even after their transcription initiation, resulting in a time lag of ~6 hours between peak RNA and protein levels. This lag in protein accumulation is thought to be caused by the phosphorylation-dependent destabilization of PER by DOUBLE-TIME (DBT), a homolog of mammalian CASEIN KINASE 1ε (Kloss et al., 1998, 2001; Price et al., 1998).

Upon PER translation, DBT binds and phosphorylates PER to promote its proteasomal degradation. An F-box E3 ubiquitin ligase named SLIMB recognizes the phosphorylation at PER's Ser47 site and mediates this proteasomal degradation (Chiu et al., 2008; Grima et al., 2002; H. W. Ko et al., 2002). Consequently, this decelerates its accumulation in the cytoplasm, and it's also known to hinder the premature nuclear entry of PER. Few years prior to the identification of DBT, it was reported that PER levels were constantly low and cytoplasmic in tim^{01} mutants and that TIM binds to PER (Price et al., 1995; Rothenfluh et al., 2000). Considering this, it was later proposed that PER is unstable on its own until TIM accumulates in the cytoplasm and binds to it (Gekakis et al., 1995; Kloss et al., 2001; Price et al., 1995, 1998). As a result of dimerization between TIM and PER, phosphorylated PER

is stabilized, resulting in the cytoplasmic accumulation of the DBT-PER-TIM complex. Thus, TIM and DBT work antagonistically to stabilize PER and thereby control its abundance level (Chiu et al., 2008; Kloss et al., 1998, 2001; Price et al., 1998). In addition, PER is also dephosphorylated by phosphates, like PP2A and PP1, to promote stabilization, and, in particular, PP2A also facilitates the nuclear entry of PER (Fang et al., 2007; Sathyanarayanan et al., 2004).

The nuclear entry of PER is another critical event tightly regulated by the phosphorylation mechanism. The translocation of PER to the nucleus is influenced by different kinases, such as CASEIN KINASE 2 (CK2) and SHAGGY (SGG), along with phosphorylation by a proline-directed kinase that is yet to be identified (Akten et al., 2003; Chiu et al., 2008; H. W. Ko et al., 2010; J.-M. Lin et al., 2005; Martinek et al., 2001; Meissner et al., 2008; Top et al., 2016). Prior studies conducted *in vitro* suggest that the mitogen-activated protein kinases ERK2 and p38 are potential candidates for the unidentified proline-directed kinase (Dusik et al., 2014; H. W. Ko et al., 2010). It is believed that these kinases play a priming role in the process. For instance, phosphorylation at Ser661 by proline-directed kinase primes the phosphorylation of Ser657 by SGG and also the phosphorylation of Ser149, Ser151, and Ser153 by CK2. Therefore, PER undergoes a series of intricate phosphorylation events that impact each other in various ways (Chiu et al., 2008; Helfrich-Förster, 2017; Kivimäe et al., 2008; H. W. Ko et al., 2010; J.-M. Lin et al., 2005). Similar to PER, TIM also undergoes a sequence of phosphorylation and dephosphorylation post its translation (Fang et al., 2007; Martinek et al., 2001; Top et al., 2016). Mainly, SGG, a homolog of GLYCOGEN SYNTHASE KINASE-3β (GSK-3β), phosphorylates TIM to promote its nuclear localization (Martinek et al., 2001). In summary, various regulatory factors like DBT, CK2, SGG, and PP2A act on PER and TIM to regulate their stability and facilitate the proper timing of their translocation to the nucleus. The complete cascade of the interplay between kinases and phosphatases in determining the clock's period is still being studied extensively.

During the second half of the night, DBT-PER-TIM complexes start to build up in the nucleus. These complexes then interact with CLK, promoting its phosphorylation and reducing the binding affinity of CLK/CYC for the E-boxes (E. Y. Kim & Edery, 2006; Yu et al., 2006, 2009). Consequently, the transcription of all genes with E-boxes, including *per* and *tim*, is inhibited. At dawn, TIM undergoes light-induced degradation, which leads to the destabilization of phosphorylated PER. In contrast to PER in the cytoplasm, nuclear PER,

which is heavily phosphorylated, is more resilient without TIM and can continue suppressing CLK/CYC activity for several additional hours. As PER is subjected to subsequent phosphorylation by DBT, SLIMB is then recruited to drive the proteasomal degradation of PER (Grima et al., 2002; H. W. Ko et al., 2002). As PER degradation progresses, newly synthesized hypo-phosphorylated CLK gains accumulation and heterodimerizes with CYC to form CLK/CYC complexes. These heterodimers then bind to E-boxes, initiating another round of CLK/CYC-mediated transcription.

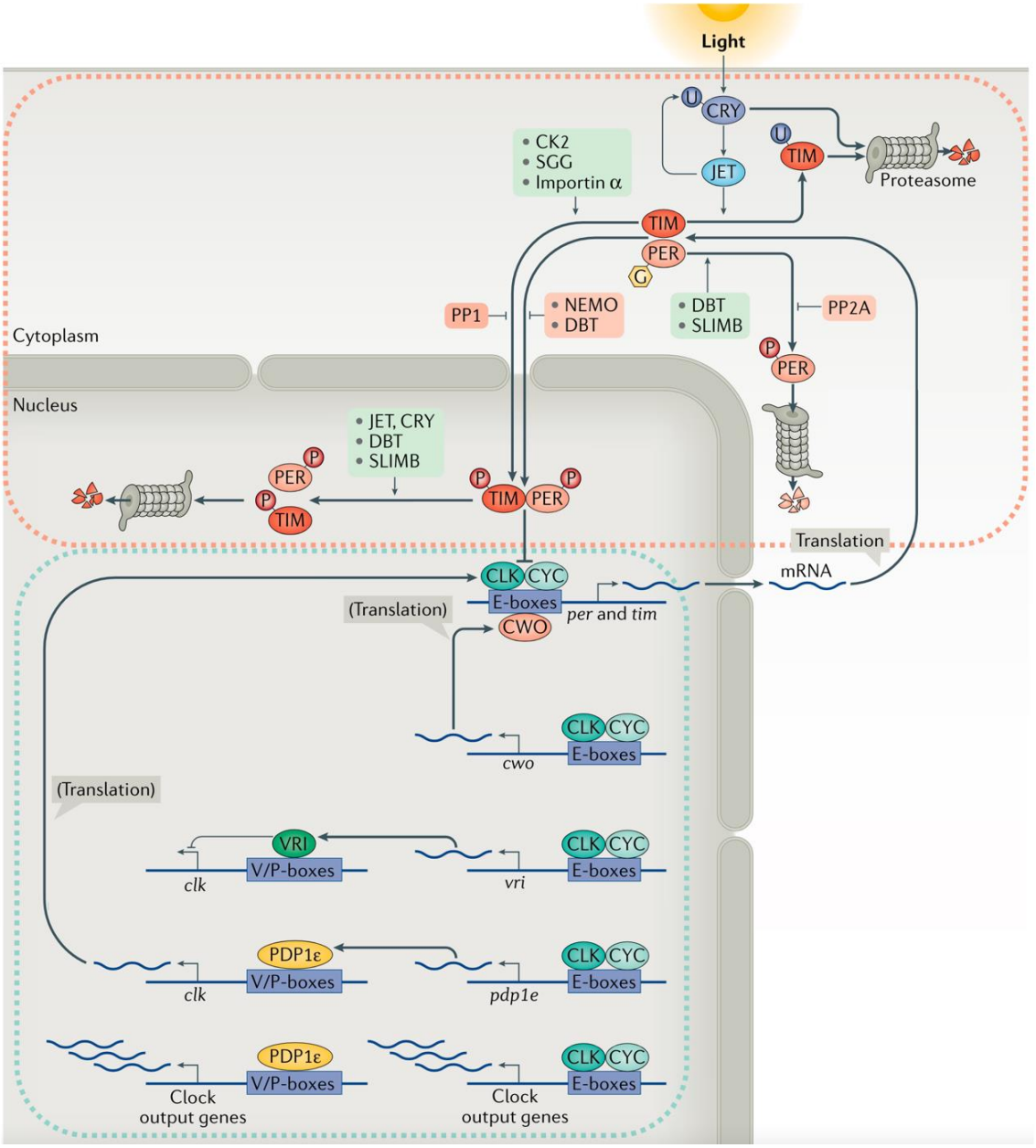

Figure 1.9 Interlocked feedback loops in the *Drosophila melanogaster* molecular clock. In the main *per*/*tim* feedback loop, the heterodimeric transcription factor complex CLK/CYC induces the transcription of their own transcriptional repressors PER and TIM. To maintain a period of ~24 hours,

the TTFL loop undergoes tight regulation at various levels, including post-transcriptional and post-translational. The post-translational regulators (selected) include kinases like DBT, SGG, CK2, and NEMO; phosphatases like PP1 and PP2A; nuclear importin factors like importin-α; and ubiquitin ligases like SLIMB and JET. These factors modify different clock proteins to control their stability and subcellular localization and, in turn, regulate the duration of the TTFL cycle. Additional interlinked loops exist where the CLK-CYC dimer activates the transcription of different transcriptional factors like VRI, PDP1ε , and CWO. VRI and PDP1ε repress and activate the *clk* transcription to regulate its mRNA cycle, while CWO feedbacks to inhibit the CLK/CYC-activated transcription by competitively binding to the E-box element of CLK target genes. CLK-CYC also regulates the transcription of several clock output genes that confer circadian rhythmicity to different biological functions. (Adapted from Patke et al., 2020)

1.3.4 Mammalian molecular clock

Similar to *Drosophila*, intertwined transcriptional translational feedback loops (TTFLs) driven by a set of dedicated clock genes and their proteins form the molecular basis of circadian timekeeping in mammals. CLOCK and BMAL1 (mammalian homolog of Drosophila CYC) are the bHLH/PAS proteins that form the positive arm of the core feedback loop (Fig 1.10) (Antoch et al., 1997; Gekakis et al., 1998; D. P. King et al., 1997; Vitaterna et al., 1994). CLOCK and BMAL1 form a heterodimeric complex, which acts as a transcriptional activator and initiates the expression of clock genes such as *PERIOD* (*PER*) and *CRYPTOCHROME* (*CRY*), as well as other clock-controlled output genes (Horst et al., 1999; Kume et al., 1999; Shearman et al., 1997; Yoo et al., 2005; B. Zheng et al., 2001). Following translation, PER and CRY proteins form a complex in the cytoplasm that subsequently enters the nucleus, where it acts as a repressor to inhibit the transcriptional activity of CLOCK/BMAL1, which comprise the negative arm of the loop (Griffin et al., 1999; Horst et al., 1999; Kume et al., 1999; Sato et al., 2006). Later PER and CRY proteins undergo degradation through a ubiquitin-dependent proteasomal pathway, which ultimately relieves the repression of CLOCK/BMAL1 activity and initiates a new cycle of the *PER* and *CRY* transcription (Busino et al., 2007; Eide et al., 2005; Hirano et al., 2013; Siepka et al., 2007).

Multiple paralogs of the *PER* and *CRY* genes exist in mammals due to gene duplication events that occurred during evolution. Specifically, the PER protein has three paralogs called PER1, PER2, and PER3, while the CRY protein has two paralogs called CRY1 and CRY2

(Horst et al., 1999; Shearman et al., 1997; B. Zheng et al., 2001). The different paralogs have distinct functions and expression patterns, which contribute to the complexity and robustness of the circadian clock system. For instance, PER1 is primarily expressed in the suprachiasmatic nucleus (SCN) and is involved in SCN entrainment. On the other hand, PER2 and PER3 have broader expression patterns in various tissues and participate in other functions (Bae et al., 2001; Cheng et al., 2009; Yoo et al., 2004). Moreover, the loss of one paralog of the *PER* and *CRY* genes can be partially compensated by other paralogs to some extent, a phenomenon known as paralog compensation (Bae et al., 2001; Vitaterna et al., 1999; B. Zheng et al., 2001).

A key difference between the circadian clocks of *Drosophila* and mammals is the role of the CRY proteins. In *Drosophila*, CRY (dCRY) primarily functions as an intracellular photoreceptor that interacts with the TIM to mediate light-induced responses in the molecular clock. Thus, dCRY does not function as a core component of the transcription-translation feedback loop (TTFL) but rather feeds external signals into it by regulating the stability of TIM in a light-dependent manner. In mammals, the CRY proteins (CRY1 and CRY2) took over the role of TIM, as they interact with the PER proteins to form a complex that inhibits the transcriptional activity of the CLK/BMAL1 complex. Research has shown that mammalian TIM shares significant similarities with a family of yeast proteins that regulate the DNA replication fork (Somyajit et al., 2017).

Analogous to the regulation of dCLK by VRI and PDP1ε in *Drosophila*, the second interlocked feedback loop in mammals involves CLOCK-BMAL1 mediated transcriptional activation of genes for the nuclear receptor REV-ERBα and REV-ERBβ, which, together with retinoic acid-related orphan receptors RORα, RORβ, and RORγ, regulate the rhythmic expression of BMAL1. The transcription of *bmal1* genes is either inhibited or activated by REV-ERBα/β and RORα/β/γ respectively, through their competition for binding to REV-ERB-ROR response elements located in the promoter and enhancer regions of these genes (Preitner et al., 2002; Sato et al., 2004). In contrast to *Drosophila*, where dCYC is expressed continuously, and dCLK is rhythmically transcribed through the secondary feedback loop, in mammals, BMAL1 (ortholog of dCYC and serves as the partner of CLK in the transcriptional activator complex) is regulated in a circadian manner through the secondary loop.

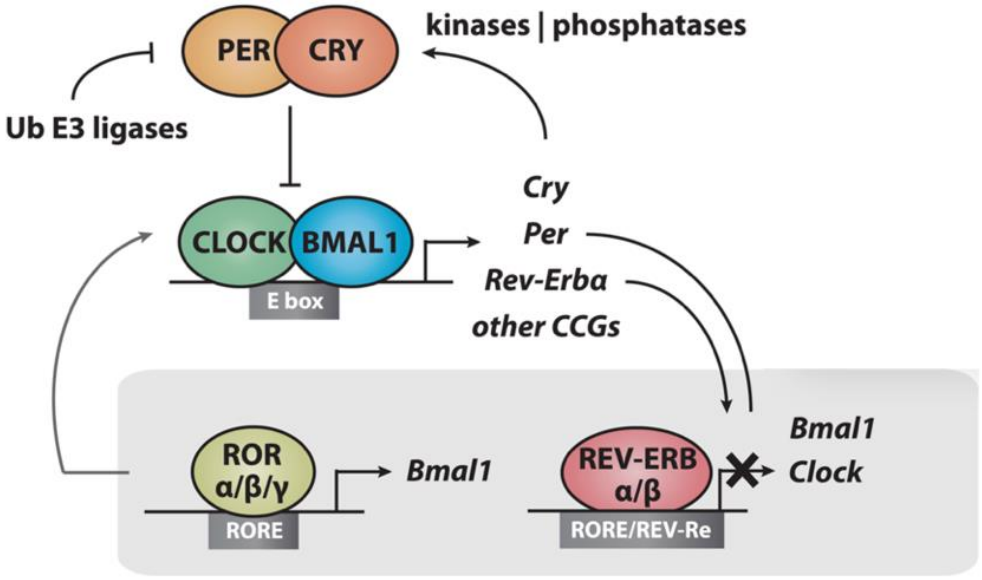

Figure 1.10 Simplified model of the mammalian molecular clock. In the core loop, the heterodimer CLK–BMAL1 drives the expression of their own negative regulators, the PER and CRY. Once PER and CRY are degraded, the transcriptional factors CLK-BMAL1 initiate a new cycle of *PER* and *CRY* transcription. Regulation of the rhythmic expression of BMAL1 is also achieved by subsidiary feedback loops composed of various components such as nuclear receptors REV-ERBα and REV-ERBβ, as well as retinoic acid-related orphan receptors RORα, RORβ, and RORγ. (Adapted from Gustafson & Partch, 2015)

1.4 Neuronal circuitry controlling circadian rhythms

The previous section covered the molecular makeup of circadian clocks, the underlying mechanism by which they achieve self-sustaining, endogenous rhythmicity, and how they regulate the length of their periods. As mentioned earlier, these molecular clocks reside in numerous cells throughout the body, and in general, these clocks are organized in a hierarchical architecture comprising central and peripheral clocks. In animals, coupled and plastic networks of clock neurons in the brain constitute the central or master clock. The brain circadian clock in *Drosophila* consists of ~150 clock neurons, whereas in mammals, the master clock resides in the suprachiasmatic nuclei (SCN) of the hypothalamus.

1.4.1 *Drosophila* central clock circuitry

Approximately 150 clock neurons in the *Drosophila* brain have been recognized as clock neurons based on the cyclic expression of core clock proteins like PER and TIM. In addition to the 150 clock neurons, the cycling of clock proteins has been observed in numerous glial cells in *Drosophila* (Jackson et al., 2015). Although the exact role of these glial cells is not well characterized, they appear to be important for regulating circadian rhythms. The canonical clock machinery residing in the pacemaker neurons forms a highly yet differentially coupled multi-oscillator system designated as the *Drosophila* central clock. These pacemaker neurons are distributed across the brain, with ~ 75 on each hemisphere (Fig 1.11). Drosophila clock neurons can be subdivided into different clusters based on their cell body location and size, as well as the expression of a circadian signaling molecule named Pigment Dispersing Factor (PDF) (Ahmad et al., 2021; Dubowy & Sehgal, 2017; Helfrich-Förster, 2003; Helfrich-Förster, Shafer, et al., 2007; Helfrich-Förster, Yoshii, et al., 2007; Helfrich-Förster, 2017; Hermann-Luibl & Helfrich-Förster, 2015; Kaneko et al., 1997; Kaneko & Hall, 2000; A. N. King & Sehgal, 2020; Reinhard, Schubert, et al., 2022; Schubert et al., 2018; Top & Young, 2018). Generally, bilateral clustering can divide these into two main categories: lateral neurons (LN) and dorsal neurons (DN). The lateral group is further subdivided into large ventrolateral neurons (l-LNvs), small ventrolateral neurons (s-LNvs), 5^{th} small ventrolateral neuron (5^{th} s-LNv), dorsolateral neurons (LNds), and posterior lateral neurons (LPNs). Dorsal neurons can be subdivided into three clusters: DN1, DN2, and DN3, where DN1 is further subdivided into anterior (DN1a) and posterior (DN1p) groups. The expression and release of PDF are exclusive to the l-LNvs and s-LNvs, which are the only neuronal groups in the master clock network that do so (Helfrich-Förster, 1995; Renn et al., 1999). This is the primary differentiating factor between the 5^{th} s-LNvs and other s-LNvs, among several other functional and anatomical aspects.

1.4.1.1 *Drosophila* clock neuron clusters

- **s-LNv** – The cell bodies of s-LNvs are located in the ventral brain, between the optic lobe and central brain (Helfrich-Förster, Shafer, et al., 2007; Helfrich-Förster, Yoshii, et al., 2007; Shafer et al., 2022). Each brain hemisphere contains four s-LNvs which express PDF, a circadian neuromodulator employed in

communication with other clock cells as well as in circadian clock output rhythms (Helfrich-Förster, 1995; Renn et al., 1999; Shafer & Yao, 2014). In addition, they also release another neuropeptide, short Neuropeptide F (sNPF), and neurotransmitter glycine (Choi et al., 2012a; Frenkel et al., 2017; Johard et al., 2009). These clock neurons have two main projection targets: (1) the accessory medulla (aMe), small neuropil recognized as a circadian pacemaker center where most clock neurons send arborizations for intercellular communication and also a key site for the integration of visual-system mediated light input into the clock circuit, and (2) the dorsal protocerebrum (Hermann-Luibl & Helfrich-Förster, 2015; Muraro et al., 2013; Shafer et al., 2022). The ventral neurites of s-LNvs that innervate the accessory medulla mostly contain postsynaptic structures and are known to receive light input from the *Drosophila* visual system (Helfrich-Förster, 2020a; Schlichting, 2020; Yoshii et al., 2016). The dorsal projections of s-LNvs form fine termini that extend toward the midline and contain both synaptic input and output sites but are biased toward presynaptic sites. Connectome studies depict that s-LNvs area highly unified connectomic type displaying uniformity in their synaptic partners and connections (Shafer et al., 2022).

Both GFP Reconstitution Across Synaptic Partners (GRASP) technique and electron microscopy (EM) studies revealed that s-LNvs have presynaptic connections with DN1ps and DN2s in the dorsal protocerebrum area (Guo et al., 2016; Shafer et al., 2022; Yasuyama & Meinertzhagen, 2010). Interestingly, analysis of the hemibrain connectome suggests that within the hemibrain volume, s-LNvs do not make strong synaptic connections with other clock neurons (Shafer et al., 2022). This may be due to synaptic plasticity shown by s-LNvs over a day or their communication to other clock neurons through peptidergic connectivity like PDF signaling. The axonal arborizations of s-LNv in the dorsal terminals undergo circadian remodeling, where axonal structures display high complexity during dawn and vice versa at dusk. This phenomenon, termed circadian structural plasticity, depends on clock-controlled PDF cycling at the dorsal terminals (Fernández et al., 2008; Muraro et al., 2013).

- **l-LNv** – In each hemisphere, there are four l-LNvs that release PDF, much like the s-LNvs. Their cell bodies reside in the ventral brain, positioned dorsally relative to the s-LNv. The size of l-LNv soma is visibly larger than that of s-LNvs, hence the name. Their initial primary projection from the cell body runs ventrally towards aMe, forming ventral elongation of the accessory medulla (aMe_{vel}). The second projection arises from this ventral extension, which travels through the posterior optic commissure (POC) towards the opposite hemisphere, eventually branching throughout the surface of the contralateral medulla. Another third projection arises from the POC fiber, innervating the ipsilateral medulla. Recent research has revealed that among the l-LNvs, one cell exhibits a unique arborization pattern in the ipsilateral and contralateral medulla. The majority of l-LNvs (3 per hemisphere) exhibit a dense branching pattern on the distal region of the medulla, whereas the remaining l-LNv exclusively invades the dorsomedial and ventromedial surfaces of the medulla (Helfrich-Förster, Shafer, et al., 2007; Helfrich-Förster, Yoshii, et al., 2007; Schubert et al., 2018).

- **5^{th} s-LNv** – It's now well established that the PDF-negative 5^{th} s-LNv is genetically, functionally, and anatomically diverse from the PDF-positive s-LNv (Shafer et al., 2022; Yao & Shafer, 2014). This clock neuron expresses the neuropeptide ion transport peptide (ITP) and is also found to be cholinergic (Hermann-Luibl et al., 2014; Johard et al., 2009). The cell body of the 5^{th} s-LNv is close to the l-LNvs. Similar to s-LNv, 5^{th} s-LNv too has two prominent projections: the accessory medulla (aMe) and the dorsal brain. However, 5^{th} s-LNv has more extensive ramifications on their projections compared to s-LNv. In contrast to the s-LNv, the 5th s-LNv's dorsal termini extend across the middle dorsal commissure, establishing synaptic connections in the contralateral hemisphere (Schubert et al., 2018; Shafer et al., 2022). According to the connectome data, 5^{th} s-LNv has a significantly higher number of synaptic connections and synaptic partners than a single s-LNv (Shafer et al., 2022).

- **LNd** – There are six LNds in each hemisphere of the brain, and their cell bodies are situated in the lateral brain, similar to LNvs. However, they are located relatively

more dorsally than the LNvs. All LNds project into the dorsal protocerebrum passing through the anterior optic tract (AOT). After encompassing the AOT, three neurons among them, extend neurites that diverge from the primary tract and innervate the ipsilateral ventral brain. These three neurons express CRYPTOCHROME (CRY), Drosophila's sole intracellular circadian photoreceptor, whereas the remaining three LNds are identified as CRY-negative (Helfrich-Förster, Yoshii, et al., 2007; Johard et al., 2009; Schubert et al., 2018).

The three CRY-negative LNds project only to the dorsal brain but do not cross the middle dorsal commissure and are confined to the ipsilateral brain hemisphere. In contrast, dorsal projections of all CRY-positive LNds cross the midline and pass into the contralateral hemisphere (Schubert et al., 2018; Shafer et al., 2022). Among the three CRY-positive LNds, which had additional projections to the ventral brain, only one neuron innervates the ipsilateral aMe and expresses ITP similar to the 5^{th} s-LNv. The other two CRY-positive LNds, which share a similar morphology, express sNPF (Johard et al., 2009).

- **LPN** – LPN consists of three neurons per hemisphere and are the latest characterized clock neurons. It was discovered that all three LPN neurons rhythmically express Allatostatin A (AstA), Allatostatin C (AstC), and Diuretic Hormone 31 (DH31). They are also known to be glutamatergic and exhibit heterogeneity in their morphology. Two among the three arborize in the superior medial, while the third neuron passes through the superior lateral protocerebrum and innervates towards the anterior optic tubercle (Reinhard, Bertolini, et al., 2022).

- **DN1a** – DN1a consists of only two neurons in each hemisphere. Their cell bodies are located in the anterior superior cell body rind in the dorsal brain. These neurons express neuropeptides IPNamide and CChamide1 and are also identified to be positive for glutamate and CRY (Collins et al., 2012; Fujiwara et al., 2018; Hamasaka et al., 2007; Shafer et al., 2006). Both these neurons project ventrally, passing through the superior lateral protocerebrum and lateral horn before finally innervating aMe. Two neurons extensively branch and innervate in the posterior SLP

and LH regions, but their arborizations differ slightly in morphology. In the aMe, most of the projections are presynaptic, but they make up only a small fraction of output synapses. On the other hand, the majority of synaptic connections for both input and output of the two DN1as occur in the SLP and posterior lateral protocerebrum (PLP)(Reinhard, Schubert, et al., 2022).

- **DN1p** – The DN1p cluster in each brain hemisphere contains roughly 14-16 cells, out of which half express the CRY and PDF receptor (PDFR), forming a diverse group (Im & Taghert, 2010; Shafer et al., 2008a; Yoshii et al., 2008). A subgroup of five to six CRY-positive DN1ps is glutamatergic and expresses neuropeptides Diuretic Hormone 31 (DH31) (Goda et al., 2016; Hamasaka et al., 2007; Kunst et al., 2014). Among these CRY and DH31 expressing DN1p cells, there are four neurons that also express Allatostatin C (AstC) and CNMamide (Abruzzi et al., 2017; Díaz et al., 2019; Jung et al., 2014; C. Zhang et al., 2021). DN1ps exhibit morphological heterogeneity as well. Some neurons remain in the ipsilateral hemisphere and innervate the anterior optic tubercle (AOTU). In contrast, the remaining neurons lack projections towards AOTU and cross the MDC, projecting towards the opposite hemisphere. The latter type of DN1ps can be again classified based on their projections on the ipsilateral side (Reinhard, Schubert, et al., 2022). Recently, clock neuron single-cell RNA sequencing (RNA-Seq) identified six subgroups within DN1ps (Ma et al., 2021).

- **DN2** – Each hemisphere contains two DN2s whose cell bodies are ventrally positioned in the dorsal brain relative to DN1s. Similar to DN1s, DN2 resides near the dorsal termini of the s-LNvs. They have two prominent projections that bifurcate from their initial neurite. One projects medially and cross the MDC through pars intercerebralis, ultimately branching out in the contralateral hemisphere. The other projection runs laterally towards SLP and finally arborizes the anterior part of AOTU (Reinhard, Schubert, et al., 2022). Both of these DN2s are CRY-negative and are thought to be PDFR-positive (Benito et al., 2007; Reinhard, Schubert, et al., 2022; Yoshii et al., 2008).

- **DN3** – The DN3 cluster is the largest cluster of clock neurons in the adult brain, consisting of approximately 40 neurons. Most DN3s have small cell bodies, with only a few neurons having larger somata (about four to five) (Helfrich-Förster, Yoshii, et al., 2007; Reinhard, Schubert, et al., 2022). The cell bodies are located in the dorsal superior protocerebrum, dispersedly positioned on the dorsal, posterior, and lateral cell body rind of LH (Reinhard, Schubert, et al., 2022). Most DN3s are known to produce the neuropeptide AstC, and a maximum of ten neurons express the DH31 receptor (Díaz et al., 2019; Goda et al., 2016; Meiselman et al., 2022).

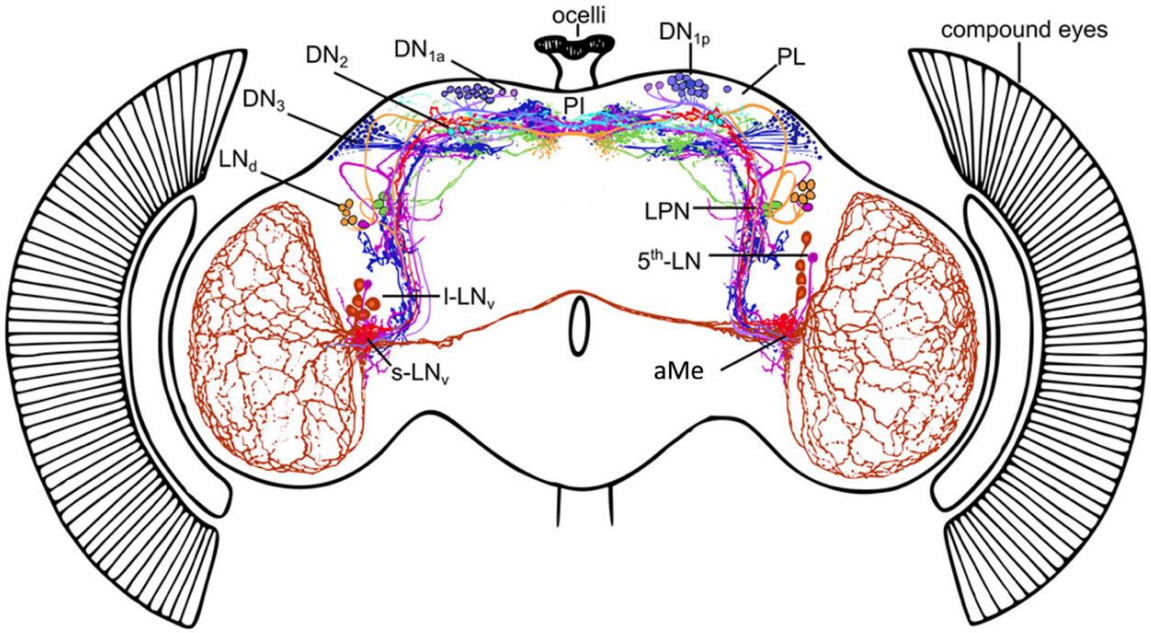

Figure 1.11 Clock neuron network in the brain of *Drosophila melanogaster*. Core clock components are expressed by approximately 150 clock neurons, which are further categorized into clusters such as s-LN_vs (red), l-LN_vs (brown), LN_ds (orange), 5^{th} s-LN_v (magenta), LPNs (green), DN_{1a}s (lilac), DN_{1p}s (violet), DN_2s (cyan), and DN_3s (blue). Across the network, clusters communicate with each other utilizing different neuropeptides and neurotransmitters. Through anatomical and neurochemical characterization, it has been shown that clock neuron groups exhibit heterogeneity both within and between them, allowing cells to perform varied functions and respond to distinct environmental signals. Most of the clock neurons in the brain send their projections into two primary regions: the dorsal protocerebrum (which includes the neurosecretory centers in the pars intercerebralis (PI) and pars lateralis (PL)) and the accessory medulla (aMe) neuropil. Among six LN_ds (orange), one is colored in magenta along with 5^{th} s-LN_v to denote that both of them are ITP-expressing cells.

1.4.1.2 Clock neuron communication and connectivity

The *Drosophila* brain clock consists of anatomically and neurochemically distinguishable subsets of cellular oscillators that operate in a coordinated manner to regulate daily rhythms in physiology and behavior. The coordinated activity of these cellular oscillators and the underlying circuit mechanisms are critical for the proper functioning of the circadian system. Even the molecular rhythmicity of each clock neuron depends on this coupling property to form a unified clock network that generates robust circadian rhythms. Moreover, the available studies indicate that the inherent coupling mechanism endows the clock network with dynamic flexibility in receiving varying inputs and generating resilient outputs as well (Ahmad et al., 2021; Beckwith & Ceriani, 2015b; Crespo-Flores & Barber, 2022b). Various neuropeptides and neurotransmitters are utilized by the clock system to achieve this synchrony between and among clock neuron clusters (Fig 1.12). The current understanding is that the coordination of the clock network relies on the differential coupling between clock neurons, adding more intricacies to their framework.

The Pigment Dispersing Factor (PDF) was the first neuropeptide to be identified as a critical regulator of circadian rhythms in *Drosophila* (Helfrich-Förster, 1995; Renn et al., 1999). Like other neuropeptides, they are signaling molecules released by neurons and acts in target cell by binding to specific receptors, triggering a response that modulates their activity. Mature PDF comprises only 18 amino acids and is expressed exclusively in s-LNvs and l-LNvs in the fly brain. Notably, PDF release from the dorsal terminals of s-LNv oscillates in a circadian fashion (Park et al., 2000). Flies depleted for PDF, such as pdf^{01} mutant, displayed short-period (~22) locomotor rhythms that dampened progressively under constant darkness conditions (DD) (Renn et al., 1999). Similar behavioral phenotypes in DD were observed in flies with ablated or silenced LNvs (Renn et al., 1999). These findings supported the notion that PDF is crucial in regulating the circadian rhythms in flies through its role as the primary signaling peptide released by the LNvs. s-LNvs exhibit endogenous molecular rhythms that continue for several days without external light cues, thus holding greater significance in regulating DD behavioral rhythms than PDF-positive l-LNvs (Grima et al., 2004; Shafer et al., 2002b; Stoleru et al., 2004; Yang & Sehgal, 2001).

The identification of the PDF receptor (PDFR) further emphasized the crucial role of PDF in maintaining overt circadian rhythms in flies, as loss of this receptor leads to phenotypes identical to pdf^{01} mutants (Hyun et al., 2005; Lear et al., 2009; Mertens et al.,

2005). The PDFR encodes a G-protein coupled receptor (GPCR) and is expressed in several clock neurons, primarily CRY-positive neurons. This includes all s-LNvs, half of LNds, half of DN1ps, and both DN1a and DN2 (Hyun et al., 2005; Im & Taghert, 2010; Mertens et al., 2005; Shafer et al., 2008a).

Although the lack of PDF impacts the locomotor activity rhythms, it does not entirely halt the oscillations of free-running clock proteins in individual oscillators. Nevertheless, the absence of PDF leads to a loss of synchrony in the phase relationships of the molecular clock among various clock neurons, causing some oscillators to run faster while others slow down (Y. Lin et al., 2004; Yoshii et al., 2009). This partially explains the marked deficiencies in the free-running locomotor patterns displayed by pdf^{01} flies and highlights the necessity of a synchronized network system for the proper functioning of the circadian clock. In DD, s-LNvs are capable of modulating the phase of downstream clock cells such that if the s-LNv clock is accelerated or deaccelerated, the pace of PDF-sensitive clock cells will likewise be adjusted. Therefore, LNvs play a significant role as the primary pacemaker cells in the *Drosophila* circadian system by regulating the phase and period of remote molecular clocks via PDF-dependent coupling mechanisms (Guo et al., 2014; Stoleru et al., 2005; Yao & Shafer, 2014). In summary, PDF is widely regarded as the chief circadian signaling molecule, which not only functions as an output factor of the clock but also plays a vital role in maintaining circadian network coordination and orchestrating behavioral activity (Peng et al., 2003; Shafer & Yao, 2014).

Numerous studies are being done to unravel the precise cellular responses mediated by PDF that affect individual molecular clock. In addition to circadian clock resetting, PDF signaling is also identified to regulate the cellular physiologies of target neurons by modulating its intracellular messenger molecule dynamics (Choi et al., 2012; Hyun et al., 2005; Mertens et al., 2005; Shafer et al., 2008). PDFR, belonging to the GPCR family, is coupled to the G_s protein. Upon binding PDF to its receptor, a conformational change is triggered, which leads to the activation of the G protein. This, in turn, activates an enzyme called adenylyl cyclase which increases the cellular levels of the secondary messenger molecule cAMP (cyclic adenosine monophosphate) (Duvall & Taghert, 2012, 2013). Prior studies have demonstrated that PDFR-positive clock neurons responded to PDF with increased cAMP levels (Shafer et al., 2008). Additionally, such a response to PDF exhibited circadian rhythmicity with a peak around dawn (Klose et al., 2016). It is hypothesized that PDF-dependent upregulation of cAMP may then directly activate a cyclic-nucleotide-gated

(CNG) channel to depolarize the cell and increase the action potential firing rate (Seluzicki et al., 2014). This acute effect of PDF on neuronal activity also contributes to its role in regulating circadian rhythms. On the other hand, the same study suggested that PDF regulates the molecular clockwork by targeting the core clock protein TIM via cAMP-activated protein kinase A, aka PKA (Seluzicki et al., 2014). Thus, besides being the clock protein that integrates environmental light input into the clock machinery, TIM also incorporates PDF-dependent network signals into the same clockwork for proper functioning. Notably, another study depicts that an increase in PKA via PDF signaling stabilizes PER, slowing the pace of PDFR-positive clock neurons (Y. Li et al., 2014).

Other prominent neuropeptides employed by the *Drosophila* clock system include the aforementioned sNPF, ITP, IPNamide, DH31, CChamide, CNMamide, and AstC. Additionally, Neuropeptide F (NPF), the mammalian homolog of neuropeptide Y (NPY), is expressed in a few l-LNvs, 5th s-LNv, and three LNds, in which one is CRY-positive and the other two CRY-negative neurons (Hamasaka et al., 2010; He et al., 2013; Hermann et al., 2012; W. J. Kim et al., 2013; G. Lee et al., 2006). The circadian role of NPF has yet to be clearly elucidated, but some studies found it may regulate sleep and evening activity behavior (He et al., 2013). sNPF, expressed in s-LNvs and two LNds, is known to be a sleep-promoting molecule (Shang et al., 2013). ITP is localized in 5th s-LNv, one CRY-positive LNd, and a few non-clock cells in the fly brain. Like PDF, ITP is also rhythmically released in the dorsal brain region, where it is likely to act on DN1s to regulate locomotor behavior (Hermann-Luibl et al., 2014). Flies in which ITP expression was knockdown displayed reduced evening activity and increased nocturnal activity (Hermann-Luibl et al., 2014). DH31, the mammalian homolog of calcitonin gene-related peptide (CGRP), is another neuromodulator that serves as an output factor rather than a communicator. DH31 acts as a signal to promote wakefulness before dawn but does not affect the locomotor activity rhythms (Kunst et al., 2014). In addition to its role in sleep regulation, DH31 also plays a significant part in regulating the preferred temperature decrease that occurs at night onset, which is accomplished through its function as a ligand of PDFR (Goda et al., 2016).

In addition to neuropeptides, classical neurotransmitters contribute to the communication between multiple oscillators in the circadian neuronal network.

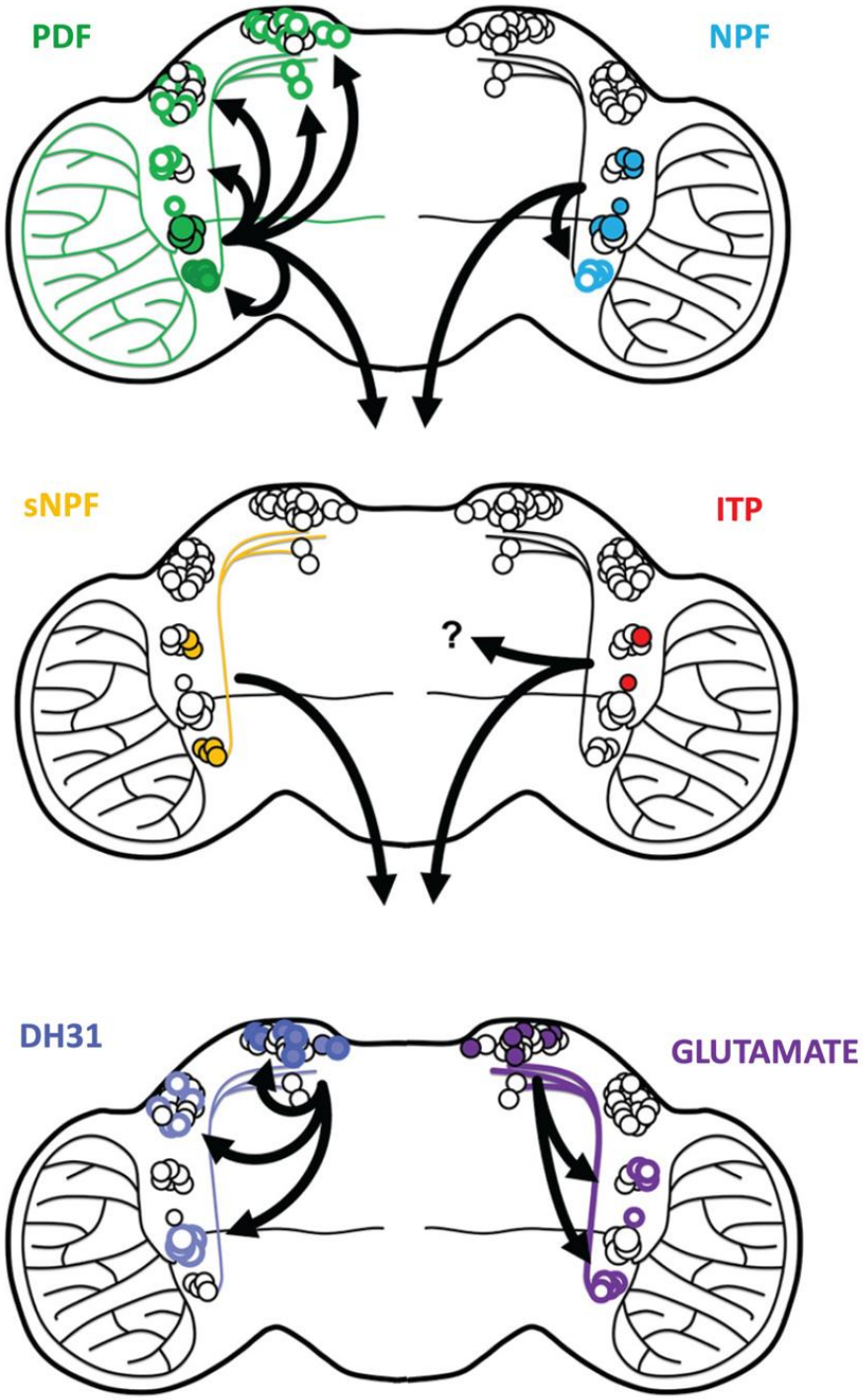

Figure 1.12 Schematic model of neuronal communication in the circadian clock network of *Drosophila melanogaster*. The clock neurons that express specific signaling molecules are filled with corresponding colors, whereas neurons with the indicated signaling molecule's receptor expression are only outlined with the corresponding color. (Adapted from Ahmad et al., 2021)

1.4.2 Functional organization in the *Drosophila* clock network

Drosophila has been a valuable model organism for studying neural mechanisms underlying circadian rhythms. As mentioned earlier, the *Drosophila* brain clock comprises several groups of clock neurons that exhibit diversity in their anatomy and neurochemical makeup. This heterogeneity also translates into differences in their circadian functions. To better understand the functional organization of the *Drosophila* circadian clock, researchers have long utilized the genetic toolkit available to manipulate clock neuron physiology and circadian signaling molecules and then, in turn, analyze the resulting circadian outputs. The primary circadian output commonly used to assess the function of the clock neurons in the *Drosophila* brain is locomotor activity. Therefore, most of the functional roles of clock neuron groups in the *Drosophila* brain that have been elucidated by research are related to their ability to regulate and shape daily locomotor activity patterns. Although locomotor behavior is a widely used and convenient circadian output to measure, it is possible that the manipulation of clock genes or clock neurons may have differential effects on other behaviors and physiological processes that are also under circadian control. The current understanding is that the *Drosophila* multi-oscillator network employs different circuit logic and principles depending on the environmental conditions. Overall, the functional organization and operation of the *Drosophila* clock network are highly adaptable to environmental conditions, allowing the fly to maintain stable and synchronized circadian rhythms in a wide range of settings. In this section, we will primarily examine the functional layout of the clock network under constant darkness (DD) and light-dark (LD) conditions.

1.4.2.1 Network configuration in constant darkness

The LNvs, particularly s-LNvs, were initially characterized as the master pacemaker cells because they expressed PDF, an essential circadian neuropeptide to maintain circadian rhythms. In constant darkness (DD), the s-LNvs have been shown to be the primary cluster coordinating neural activity and molecular oscillations in other clock clusters. Additionally, a functional molecular clock in s-LNvs alone was sufficient to maintain endogenous free-running rhythms in DD, further emphasizing their role as a hierarchically dominant group in the clock circuit (Grima et al., 2004). However, recent progress in the field presents a different perspective, portraying the *Drosophila* circadian clock circuit as a network of

oscillators without a clear hierarchy. In essence, this novel model considers the clock as a distributed network of individual oscillators, where different clusters with distinct functions assume control depending on the varying environmental signals (Ahmad et al., 2021; Chatterjee & Rouyer, 2016; Crespo-Flores & Barber, 2022b; Top & Young, 2018).

Two decades ago, it was clearly established that the presence of PDF-positive LNvs is required to drive persisting locomotor rhythms and that rescuing a functional molecular clock solely in them is sufficient for free-running behavior in DD (Grima et al., 2004; Renn et al., 1999). Depletion of PDF or ablation or silencing of the LNvs suppressed the locomotor rhythms in DD and also resulted in desynchronized molecular rhythms (Nitabach et al., 2002; Renn et al., 1999). These findings reinforced the concept that LNvs maintain a hierarchy within the clock network by resetting PDF-negative neurons on a daily basis and thereby regulating the pace of behavioral rhythms in the absence of environmental time cues.

Flies with particular mutations that disrupted their circadian light input pathways exhibited locomotor rhythms under constant light conditions (LL). Prior studies indicate that a functional clock in LNd was adequate to drive free-running rhythms in LL conditions, whereas the LNv clock was inadequate (Picot et al., 2007; Stoleru et al., 2007). This dominant role possessed by LNds in constant light challenged the previously thought hierarchical model that proposed LNvs as master pacemakers. Additionally, some studies showed that a subset of LNd has a significant role in circadian timing and has independent control over locomotor rhythmicity in DD. In 2014, Yao and Shafer demonstrated that in the absence of PDFR signaling, PDF-positive LNvs had no influence over locomotor rhythms, and the PDF-negative LNds determined the pace of endogenous locomotor rhythms in the absence of environmental time cues (Yao & Shafer, 2014). In addition, the same study showcased that LNds are made up of at least three functionally distinct oscillatory units, which are differentially coupled to PDF neurons. Furthermore, adjusting the speed of the M cell's clocks altered the pace of specific subsets of E cells and the locomotor period in DD, but only within a restricted temporal range. For instance, when the discrepancy of the M and E cell's periods exceeds ~2.5 hours, the PDF neurons lose their ability to determine the period of DD behavior. As a result, LNds, which were formerly believed to be subordinate to LNvs, are now known to possess varying degrees of autonomy and are involved in determining the period in DD together with highly influential LNvs. During the same time, two other groups, using neuronal silencing and clock speed manipulation strategies, also provide evidence for the involvement of LNds in the period determination. The discovery

that the nonadditive interaction among clock cells is more significant has led to a decline in the notion that a single cluster is dominant in regulating free-running rhythms in Drosophila (Beckwith & Ceriani, 2015a; Dissel et al., 2014).

In addition to lateral neurons, dorsal neurons, particularly DN1ps, were also found to be involved in the production of coherent free-running rhythms but are neither necessary nor sufficient for the maintenance of the rhythms in constant dark conditions (Yao et al., 2016; L. Zhang et al., 2010). Notably, it was also revealed evidence suggesting that network-wide synchrony in molecular oscillations is a prerequisite for generating robust circadian rhythms (Yao et al., 2016). DN1ps are highly dependent on PDF neurons, as manipulating the pace of the clock in PDF neurons imparts a similar effect on the DN1p clock. Moreover, in the absence of PDF signaling, clock gene oscillations in the DN1p clock become arrhythmic, indicating that PDF neurons dictate the circadian signals to DN1p (Yoshii et al., 2009). Later in 2018, Chatterjee et al. found that manipulating kinase activity to speed up and slow down the molecular clock in DN1p neurons altered the phase of the DD locomotor rhythm but not the period (Chatterjee et al., 2018). Based on this finding and previous research, it was suggested that in DD, PDF neurons play a role in determining the pace of locomotor rhythms, while DN1p neurons are responsible for determining the phase. Thus, in the absence of light (DD), a hierarchical organization with DN1ps lying downstream of PDF neurons organizes behavioral rhythms. However, further output pathways downstream of DN1ps generating DD rhythm still remain unclear.

Recently, two independently published studies revealed that CRISPR-mediated deletion of *per* and *tim* in both LNvs and LNds eliminated the DD locomotor behavior. At the same time, the presence of a functional molecular clock in LNvs or LNds alone was sufficient to maintain free-running locomotor rhythms. Altogether, it could be inferred that although LNv clocks were enough to drive rhythmicity in DD conditions, they are not essential (Delventhal et al., 2019; Schlichting, Díaz, et al., 2019). It became apparent that the LNv's molecular clock is not necessary for synchronizing the activity of other clock neurons to govern circadian rhythms, and further indicates that clock neurons operate cooperatively in a decentralized way to make up for the absence of the molecular clock in specific subsets of neurons. Furthermore, a different study conducted recently demonstrated that impairing the clock function in non-LNvs resulted in a decrease in the strength of the free-running rhythm, and silencing their neural activity led to the elimination of locomotor rhythms (Bulthuis et al., 2019). In summary, recent works question the necessity of LNvs in

maintaining DD locomotor rhythm and suggest that clock neurons function as a network to control circadian behavior rather than entirely depending on a particular cluster. It's important to note that the individual contribution of each cluster toward a fully functional network may not be similar, and PDF-positive lateral neurons are generally believed to be more influential.

1.4.2.2 Clock network organization in light-dark cycles

The bimodal activity pattern exhibited under light-dark (LD) cycles is considered the most prominent behavioral output of the *Drosophila* circadian clock. This crepuscular behavior comprising two activity bouts in their daily locomotor profile is found in many other animals. In 1976, Pittendrigh and Daan put forth the 'dual oscillator' model that suggests that the two activity peaks of the bimodal profile are sculpted by two different circadian oscillators in the brain (Pittendrigh & Daan, 1976). By studying the bimodal activity pattern of nocturnal rodents in various photoperiods, they observed that the activity rhythms split into two components as the photoperiod length changed. This leads them to propose that two mutually coupled oscillators with different periods independently control the activity peaks at dawn and dusk, aka morning and evening peaks.

Later in 2004, the anatomical basis of the dual oscillator model in fruit flies was revealed by two groups independently. In one of the studies, Grima et al. rescued clock function in different clusters by targeted PER expression in per^0 mutant background. PER rescue solely in PDF-positive LNvs restored the morning peak (M peak) and not the evening peak (E peak), whereas PER rescue in 5^{th} s-LNv and LNds only resulted in the presence of the E peak. Thus, it was concluded that a functional clock in LNvs acts as a morning oscillator (M oscillator), whereas LNds plus 5^{th} s-LNv comprise the evening oscillator (E oscillator) driving the E peak (Grima et al., 2004). Stoleru et al. put forth a similar conclusion, where they selectively ablated subsets of the clock neurons and found that LNvs were required for the M peak and 5^{th} s-LNv plus LNds were required for the E peak (Stoleru et al., 2004). This hallmark study was in accordance with already known activity patterns observed in pdf^0 mutants, lacking neurotransmission in the M oscillators and exhibiting little to no M peak in LD (Renn et al., 1999). Later it was revealed that among the LNds, only three CRY-positive ones contribute to generating an E peak and thus belong to the E

oscillator entity (Guo et al., 2014). Overall, these studies reinforced the dual oscillator model and suggested that PDF-positive neurons, particularly the s-LNv, were responsible for controlling anticipatory behavioral activity during the dawn (M peak), while PDF-negative and CRY-positive LNds, along with the 5th s-LNv, regulated anticipatory behavioral activity during dusk (E peak). Recently published data based on CRISPR mutation of clock genes in selected clusters found that impairing clock function in s-LNv reduced M peak amplitude and that in LNds reduced E peak amplitude in LD, implying the critical role played by lateral neurons in orchestrating bimodal activity pattern (Delventhal et al., 2019).

Soon it became apparent that the dual oscillator model of bimodal activity generation in Drosophila was a simplified model that did not fully capture the complexity of the underlying neural basis. Even though the presence of PDF neurons is a prerequisite, a functional clock in PDF neurons was not required to generate morning anticipation. Moreover, it was observed that four LNs (3 LNds plus 5th s-LNv) that were thought to belong to the E oscillator generated normal bimodal patterns encompassing both M and E peaks under low light LD conditions. Blocking neurotransmission or suppressing neuronal activity in E cells led to a notable reduction in both morning and evening anticipation in LD, as well as weakened locomotor rhythms in DD (Guo et al., 2014). This indicated that the functioning of M and E oscillators might not be confined to specific anatomical groups of clock neurons but rather depends on environmental conditions. Subsequently, doubts have been raised regarding the previous emphasis on the M cells as the primary pacemakers and the E cells as the secondary ones in the dual oscillator model. Notably, altering the speed of the clock in PDF neurons did not result in any phase shifts in the locomotor activity pattern in LD. In contrast, the acceleration of the molecular clock in E cells caused a significant advance in the evening peak phase, suggesting that the E cells may play a more crucial role in determining the activity phase in light-dark cycles compared to constant darkness (Guo et al., 2014). Thus, unlike in DD, the M cell clock was found to have no impact on the pace of molecular rhythm in E cells under LD conditions.

PDF signaling from M oscillators not only regulated the M behavior but also adjusted the phase of the E peak. In LD, the E peak of the flies with no PDF or PDFR was observed to be 2-3 hours advanced, while the M peak was suppressed (Renn et al., 1999). Thus, PDF signaling is required for normal entrained behavior in LD conditions, implying a hierarchical position to LNvs over LNds. Restoring PDFR signaling in non-LNvs rescued morning behavior and accurately phased evening peak, as well as DD rhythms (Lear et al., 2009).

This finding indicated that PDFR signaling controlled morning anticipation likely by facilitating the LNv output pathway, whereas it reset the evening phase and regulated period length through non-LNv clock resetting instructed by PDF signaling from LNv. In addition to autonomous entrainment via CRY, LNds also utilizes PDF-modulated visual inputs to control the evening behavior (Cusumano et al., 2009). PDF released from l-LNvs was found to be essential and sufficient for the proper timing of E peak under long photoperiods (Schlichting, Weidner, et al., 2019). Exclusively in long-day conditions, the eye-mediated light input modulates l-LNvs, triggering PDF release in the accessory medulla and directly signals to the PDFR on the LNd cells to delay the E peak (Schlichting, Weidner, et al., 2019). The crucial role of PDF signaling and related inter-oscillator communication in shaping bimodal patterns in LD became emphasized by all these discoveries. In fact, these findings illuminated the significance of multi-oscillator network interaction in regulating *Drosophila* diurnal behavior.

Over time, the model has been refined to incorporate additional oscillators and network intricacies, including diversified coupling mechanisms among neuron groups and integration of environmental factors into the circuit. As a result, the prevalent concept shifted from a simpler dual oscillator model to a more complex network model that does not require strictly designated M and E oscillators. The intriguing observation that morning anticipation could be driven without requiring a clock in M cells or an E oscillator comprising LNds and 5^{th} s-LNv alone is not sufficient for the morning behavior was solved when the functional role of DN1ps in regulating diurnal behavior was revealed. In 2010, Zhang et al. showed that a functional clock in most DN1p neurons is sufficient to elicit both morning and evening anticipation behavior. Interestingly, under high-intensity light conditions, the DN1p-driven evening behavior got suppressed, while it didn't affect the morning behavior. This finding was observed at 25^0C, and the same study also discovered that when the temperature was at 20^0C, evening behavior was restored even in high light intensities, whereas morning behavior was inhibited. Thus, the morning and evening behavior generated by DN1p is under both photic and thermal regulation (Y. Zhang et al., 2010).

Mutation in the sodium leak channel *narrow abdomen* (*na*), which facilitates the rhythmic neuronal activity of DN1ps, led to inhibition of the M peak (Nash et al., 2002; L. Zhang et al., 2010). Similar results are also observed when DN1ps are silenced by targeted expression of the Kir channel. Therefore, even though a molecular clock of DN1p neurons is not necessary, their neuronal activity is a prerequisite for morning behavior. It is

noteworthy that under LD conditions, PDF had a minimal impact on the molecular clock machinery of DN1p oscillators (Cusumano et al., 2009). A subset of DN1p neurons responds to PDF bath application by increasing cAMP levels and, thereby, neuronal firing rate (Chatterjee et al., 2018). It's also known that targeting the *pdfr* function only in DN1ps restores the M peak (L. Zhang et al., 2010). Additionally, flies that did not have LNvs but still had PDFR signaling in DN1ps due to the expression of membrane-anchored PDF exhibited morning behavior. Taken together, these findings imply that the activity of DN1p neurons, which is modulated by the PDF signaling regardless of its rhythmicity, regulates morning activity. Nevertheless, the aforementioned coupling mechanisms and resulting morning behavior are subject to significant regulation by environmental factors such as light and temperature.

Similarly, the DN1p-generated evening peak is subjected to modulation by light and temperature. According to recent studies, the inhibition of the DN1p-generated evening peak under high-light conditions was attributed to light signals transmitted via compound eyes (Chatterjee et al., 2018). Notably, it was also observed that in the absence of PDF or PDFR, the DN1p-driven evening peak persisted even under high-light LD conditions. Chatterjee et al. recently demonstrated that PDF levels in the axon terminals of s-LNv are upregulated under high-light conditions through an HR38-dependent increase of PDF expression. They also suggest that elevated PDF levels suppress evening activity by inhibiting non-glutamatergic CRY-negative DN1ps, which serve as the evening oscillator within the DN1p population (Chatterjee et al., 2018). Nevertheless, suppression of evening activity could also be via a downstream inhibitory pathway gated by the activation of DN1p neurons through PDF signaling in bright light. However, the exact mechanism through which this light-induced increase in PDF levels inhibits the evening activity is still unknown.

At present, DN1p neurons are considered to be grouped into two functional subsets that serve as the morning or evening oscillators. As mentioned earlier, recent data show that different subsets of DN1p neurons exhibit entirely opposite responses to the PDF bath application. PDF activates the DN1p morning oscillator comprising the CRY-positive glutamatergic subset, while the CRY-negative non-glutamatergic neurons that make up the DN1p evening oscillator are inhibited by PDF (Chatterjee et al., 2018). The mechanism underlying this antagonistic response is yet to be elucidated.

Overall, it's well ascertained now that in addition to lateral neurons, dorsal neurons like

DN1ps also play a crucial role in regulating circadian behavior (Lamaze & Stanewsky, 2020). These neurons receive inputs from various sensory modalities, including light and temperature, and integrate this information to help synchronize the fly's internal clock with the external environment. It is now evident that M and E clocks are flexible entities made up of subsets of clock neurons that alter their predominance and contribution based on the surrounding environmental conditions.

1.4.3 Neuronal properties of *Drosophila* circadian network

The intrinsic properties of *Drosophila* clock neurons equip them to operate as a circadian system and perform different tasks related to regulating circadian rhythms. These neuronal characteristics facilitate the circadian system in numerous ways, such as accurate timing of clock gene expression, integration of various time cues, optimization and generation of clock output, and more. Earlier, we discussed certain clock neuron characteristics, such as their neurochemical composition and morphology. However, clock neurons also exhibit a number of other essential attributes, including those that are affected by the clock and have an impact on it, which are important for their required functioning.

1.4.3.1 Electrical signals

When activated, a neuron generates an electrical signal called an action potential, which travels down the neuron and triggers the release of chemical messengers at the synapse, allowing it to transmit information to downstream neurons. Silencing such electrical activity of clock neurons via targeted expression of hyperpolarizing potassium channel Kir2.1 abolished free-running locomotor rhythms in DD (Nitabach et al., 2002). Expression of Kir2.1 suppressed the ability of neurons to depolarize or fire action potential and thus, in addition, disrupted classical neurotransmission and neuropeptidergic release as well. Strikingly, adult-specific expression of Kir2.1 in clock neurons didn’t affect the molecular oscillation even though it disrupts the behavioral rhythms (Depetris-Chauvin et al., 2011).

Despite the small soma size of *Drosophila*, successful patch-clamp recordings have been performed in l-LNvs and DN1ps. The earliest cellular electrophysiological studies were done in l-LNvs, and in 2008, two research groups reported that the firing rate of action potentials in l-LNvs followed a diurnal pattern, with the highest rate in the morning and the

lowest in the early night (Cao & Nitabach, 2008; Sheeba et al., 2008). Additionally, they observed that the resting membrane potential was more depolarized during the subjective day, while it was hyperpolarized during the subjective night. Furthermore, these changes in membrane excitability were found to be controlled by the circadian clock.

Later, patch-clamp recordings from DN1ps uncovered the mechanism responsible for clock-controlled membrane excitability, which is also conserved in mammals (Flourakis et al., 2015). Due to the CLK-driven transcription, the ER protein NLF-1 is high in the morning, enhancing the membrane's sodium conductance and reducing potassium conductance, leading to increased excitability. During the night, the sodium current is reduced, and simultaneously, the potassium conductance is increased, leading to decreased cellular excitability. NLF-1, under the control of the circadian clock, drives the rhythm of sodium ion channels (NALCN and NA), thereby linking the core clock to sodium conductance regulation. However, the mechanism linking the clock to the control of potassium conductance still needs to be discovered.

An exciting study by Mizrak et al. demonstrated that the clock neuron's electrical activity could act as endogenous zeitgebers to entrain molecular rhythmicity in LNvs (Mizrak et al., 2012). They found that specific electrical activity patterns, such as hyperexcitation, produced a morning-like expression pattern, while hyperpolarization resulted in an evening-like profile for clock gene expression in pacemaker neurons. Thus, at a particular time of day, there is a significant association between the transcription state of clock genes and the membrane potential of the neurons. Such correlation was observed even in per^0 mutants, suggesting that clock machinery could incorporate the electrical state of its neuron as a proxy for local time.

1.4.3.2 Neuronal activity: Intracellular calcium levels

For a long time, scientists were puzzled about how synchronous molecular clocks in most neurons within the clock network mediate network encoding to enable specific behavioral outputs, such as M and E peaks in the bimodal activity pattern. However, in 2016, Paul Taghert's group conducted groundbreaking research by performing brain-wide calcium imaging of clock neuron clusters *in vivo* for 24 hours, which shed light on this issue (Liang et al., 2016). They found that the intracellular calcium levels in clock neurons, which directly reflects the state of neuronal activity, exhibited daily cycling (Fig 1.13). However, this

oscillation was not synchronous among clock neurons like molecular oscillations. Strikingly, the intracellular calcium levels in M and E oscillators were out of phase by ~9 hours. The calcium level in the M cells reached its peak about 4 hours prior to the morning peak, while that in E cells reached its maximum 4 hours before the evening activity peak (Fig 1.13). The observed discrepancy between the peak times of neural activity in M and E cells suggests that there is a functional segregation between these two oscillator entities at the cellular physiology level. In summary, the timing of neuronal activity peaks in different clock groups is distinct and sequential, with s-LNv neurons reaching their peak around dawn, l-LNv around midday, LNd around dusk, and DN1 and DN3 around midnight. The following studies have demonstrated that the clock network establishes distinct daily activity phases by utilizing light and neuropeptide-mediated inhibition events in particular circuit nodes, producing sequentially timed outputs.

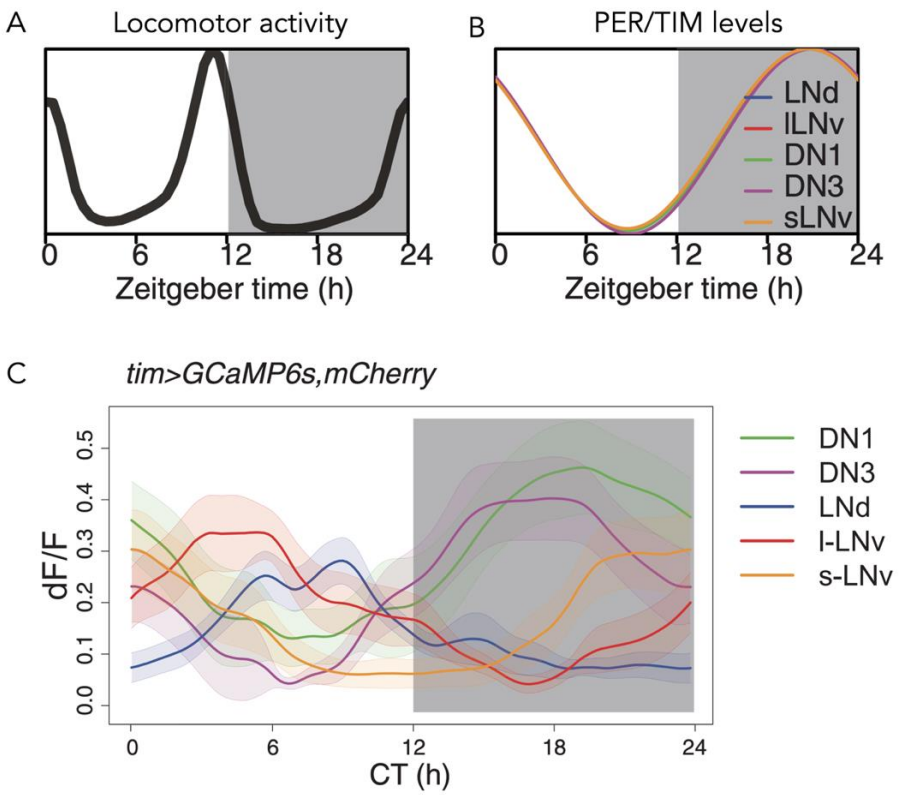

Figure 1.13 Non-synchronous intracellular Ca^{2+} rhythms exhibited by *Drosophila* pacemaker neurons in vivo. A: Schematic representation of bimodal activity pattern displayed by *Drosophila melanogaster* in 12:12 LD conditions. The multi-oscillator network of the *Drosophila* brain clock drives activity around dawn (M peak) and dusk (E peak). **B:** Schematic representation of the expression levels of PER and TIM proteins in different clock neuron clusters. **C:** Average fluorescence displayed by the Ca^{2+} sensor GCaMP6s expressed in cell bodies of five clock groups (color-coded) over a period of ~ 24

hours, providing a proxy for their daily intracellular Ca^{2+} levels. (Adapted from Liang et al., 2016)

1.4.3.3 Structural plasticity

Pioneer work from Fernanda Ceriani's lab established that s-LNv undergoes daily structural remodeling of their axonal termini in the dorsal brain (Fernández et al., 2008). Under LD, dorsal projections display extensive branching during the morning and minimal complexity in the early night (Fig 1.14). This structural plasticity depends on the circadian clock and persists even in constant conditions. The active synaptic zones in the dorsal termini also exhibit a similar circadian rhythm, with the highest number of presynaptic zones observed in the morning and lesser in the evening (Gorostiza et al., 2014). An even more remarkable aspect of the daily remodeling of s-LNv is that it enables time-dependent synapses with various synaptic partners. Thus, it was believed that the circadian remodeling of s-LNv is a mechanism of the circadian output pathway, permitting them to recompose their downstream targets and facilitate the regulation of time-specific biological processes. This notion got seriously challenged by Fernandez et al., who recently demonstrated that impeding the plasticity of s-LNv's axonal arborization alone did not impact the locomotor behavior in both LD and DD (Fernandez et al., 2020). Hence, the PDF release from s-LNv's dorsal termini proved to be sufficient in driving locomotor rhythms without requiring any circadian remodeling in the axonal termini of s-LNvs or synaptic transmission with target neurons. Given that different clock and non-clock neurons and visual inputs converge at the accessory medulla, which is recognized as the pacemaker center, it is plausible that this site plays a critical role in PDF's action rather than the dorsal brain. At the same time, the selective abrogation of axonal remodeling affected the entrainment of locomotor rhythms in temperature cycles. It was already established that DN1ps play a crucial role in temperature entrainment and that exciting these neurons, as well as the application of glutamate, leads to inhibitory responses in the s-LNvs. Building upon this understanding, the authors demonstrated that the dorsomedial terminals of PDF neurons serve as input regions that receive temperature signals via glutamatergic pathways originating from DN1p neurons (Fernandez et al., 2020). This remarkable discovery suggests that the structural plasticity of s-LNv neurons is linked to the sensory input pathway facilitated by the structural plasticity-modulated inhibitory synapses from DN1ps to s-LNv.

A recent discovery revealed that DN1a axons undergo daily remodeling, with more presynaptic sites and extended axons during the night compared to the morning (Fig 1.14)

(Song et al., 2021). Notably, the clock-driven rhythmicity in DN1a structural remodeling was antiphase to that of LNv. Antiphasic axonal remodeling of LNv and DN1a promotes their reciprocal connection in a time-of-day dependent manner, generating an internal predictive model of environmental light. The mechanism described enables s-LNv and DN1a to regulate the light-induced startle response during the daytime and nighttime, respectively (Song et al., 2021). The E oscillator residing on the lateral cluster, comprising three CRY-positive LNds and 5th s-LNv, displays a similar daily structural remodeling of their presynaptic active zones (Fig 1.14). The number of synaptic puncta is maximum during the day-to-night transition, coinciding with their highest level of neuronal activity. This, in turn, mediates the plastic functional connectivity between E and M cells that changes across the day, with the highest acetylcholine-mediated excitatory input from E to M cells occurring in the evening (Duhart et al., 2020).

The *Drosophila* circadian clock controls entrained circadian rhythms via a complex network of clock cells that undergo daily morphological remodeling, which is accompanied by changes in synaptic density and partners in their terminals. This process enables the fine-tuning of functional connections between oscillator pairs and the reconfiguration of the clock's output pathways. Moreover, structural plasticity in some pacemaker cells modulates sensory inputs into the *Drosophila* clock neuron network, contributing to the regulation of circadian rhythms.

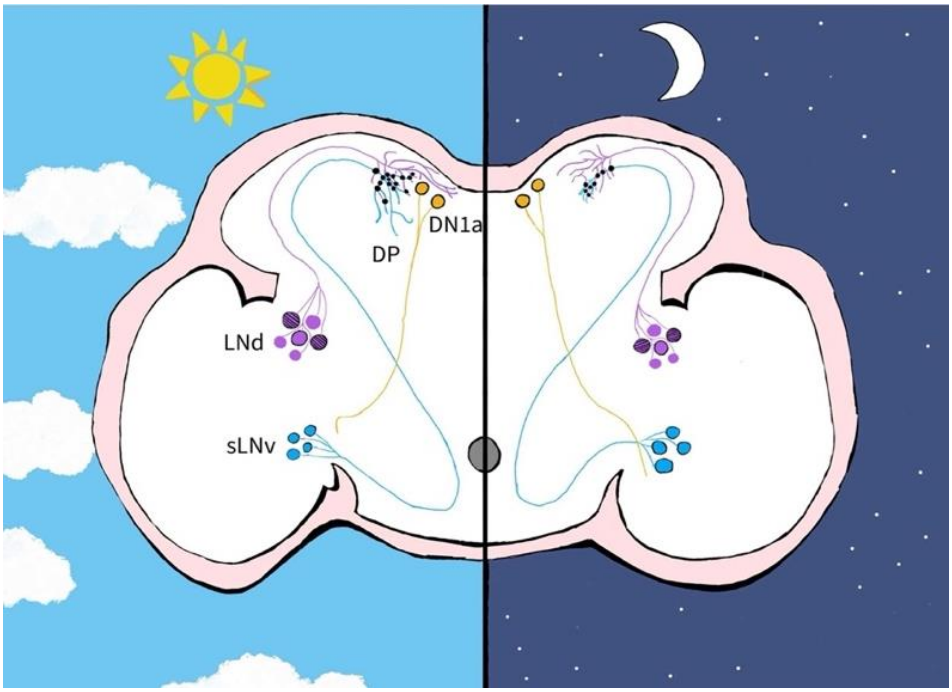

Figure 1.14 Circadian remodeling of clock neuron circuit in *Drosophila melanogaster*. Different clock neuron groups display daily remodeling in their morphology and presynaptic active zones. Compared to night-time, during the day-time, s-LNvs (blue) exhibits highly branched dorsomedial projections (DP), whereas LNds (colored in magenta) show a higher density of presynaptic terminals, thereby increasing their synaptic connections with s-LNv dorsal terminals (black dots). Similarly, DN1a exhibits a circadian structural remodeling with an extended terminal at night compared to day (Taken from Crespo-Flores & Barber, 2022c)

1.5 Photoentrainment of the *Drosophila* clock

Circadian clocks rely on multiple time cues to align the endogenous circadian rhythms with external environmental cycles, a mechanism referred to as entrainment. Most animals, including *Drosophila*, utilizes ambient light signals as the most reliable time cue to facilitate entrainment. So as to integrate this external light information into the central clock circuitry residing inside the brain, an organism employs dedicated sensory input pathways. These pathways can be either cell-autonomous, meaning that the light-sensitive cells are also part of the clock circuitry, or non-cell-autonomous, meaning that the light-sensitive cells are separate from the clock circuitry and transmit light signals through neuronal interactions.

Circadian photoreception in *Drosophila* is achieved by multiple photopigments present in various cells, including both clock and non-clock cells. Among these photopigments are rhodopsins located in the visual organs, such as compound eyes, ocelli, and Hofbauer-Buchner (H-B) eyelets, and CRYPTOCHROME (CRY), which is a circadian photoreceptor expressed in most clock neurons and a few other brain regions including the visual system. In general, circadian light input pathways in *Drosophila* could be broadly categorized into two major pathways: (1) the rhodopsin-mediated visual system pathway and (2) the CRY-mediated light input pathway (Fig 1.15) (Emery et al., 1998, 2000; Helfrich-Förster et al., 2001; Rieger et al., 2003; Stanewsky et al., 1998).

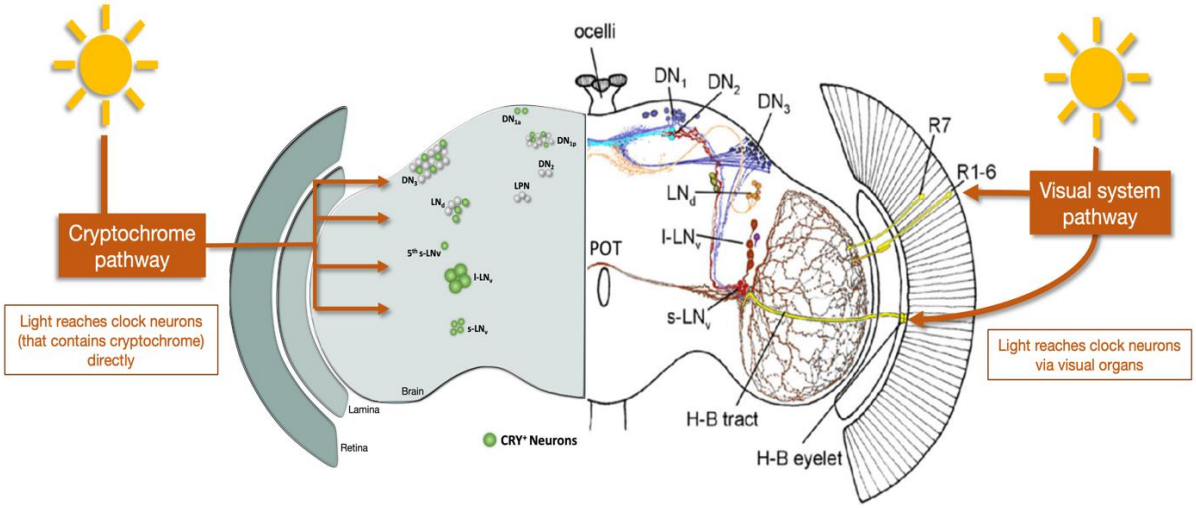

Figure 1.15 Circadian light input pathways in *Drosophila*. In *Drosophila*, external light information reaches the clock circuitry located deep within the brain through two primary pathways. One pathway involves CRY, while the other involves the light input pathways mediated by the visual system. In the CRY-dependent pathway, light signals penetrate the cuticle and directly integrate into the clock machinery via light-activated CRY-mediated TIM degradation. In the *Drosophila* brain, CRY, which is a UV-blue light-sensitive circadian photoreceptor, is expressed in most clock neurons (All CRY-positive clock neurons are depicted in green in the left hemisphere of the brain). On the other hand, in the visual system pathway, light inputs are detected by rhodopsins containing photoreceptor cells possessed by visual organs. These signals are then transduced and subsequently relayed to the central clock circuit either directly or through various interneurons. Compound eyes and H-B eyelets are known to contribute to circadian light entrainment, represented in the brain's right hemisphere.

1.5.1 Entrainment by the visual system

In *Drosophila*, three visual organs house specialized neurons containing light-detecting Rhodopsin proteins (Fig 1.16) (Hofbauer & Buchner, 1989). These sensory neurons, known as photoreceptor cells, are responsible for sensing different wavelengths of light through the phototransduction pathway, where they convert photons to electrical signals in the neuron (Hardie & Raghu, 2001; Nériec & Desplan, 2016). Through their highly specialized visual system, flies can process various visual modalities, including color, polarized, and motion vision (Behnia & Desplan, 2015; Borst et al., 2020; Borst & Helmstaedter, 2015; Hardcastle et al., 2021; Paulk et al., 2013; Schnaitmann et al., 2020; Silies et al., 2014; Zhu, 2013). In addition to this image-forming vision, the visual system also contributes to the non-image-

forming vision, such as the circadian clock's photoentrainment and the light-induced effects on the activity level (Helfrich-Förster, 2020b; Schlichting, 2020; Senthilan et al., 2019; Yoshii et al., 2016). It is now well established that various rhodopsin in the fly's photoreceptive organs relays relevant light information to the circadian network for phase resetting and synchronization of the clock. In the absence of CRY, *Drosophila* can still entrain to the LD cycle, indicating the importance of the visual system in photoentrainment (Helfrich-Förster et al., 2001). Apart from entrainment and re-entrainment, the visual system also regulates other aspects of the clock neuron network by transmitting light information to control the behavioral output of certain subsets of clock neurons. Altogether seven rhodopsins have been identified in *Drosophila* so far and have a complex expression pattern within the system consisting of seven eye structures: two compound eyes, two H-B eyelets, and three ocelli (Fig 1.16).

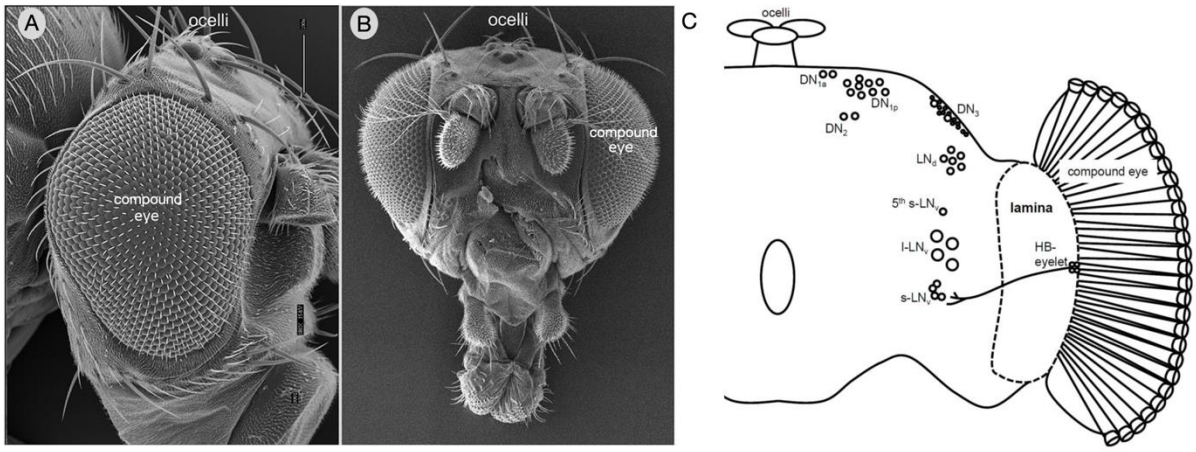

Figure 1.16 *Drosophila* visual organs. The fly visual system comprises seven eye structures: two compound eyes, three ocelli, and two H-B eyelets. **A, B:** Scanning electron micrographs of side and head-on views of the fly head with eye structures depicted. H-B eyelets located beneath the retina are not shown here. **C:** Schematic left hemisphere of the fly brain showing all three fly visual organs. Additionally, clock neuron cell bodies residing in the central brain region are shown. (Adapted from Jean-Guillaume & Kumar, 2022; Yoshii et al., 2016)

1.5.1.1 *Drosophila* rhodopsins and phototransduction mechanism

Light sensing is one of the most important senses for nearly all complex organisms that play a vital role in their survival and success. *Drosophila*, like other insects, expresses multiple

light-sensitive proteins known as rhodopsins to achieve a comprehensive and sensitive visual system. There are seven opsin genes present in the *Drosophila* genome that encode light-capturing rhodopsins. All seven rhodopsins, Rh1 to Rh7, have distinct spectral sensitivity and expression patterns (Fig 1.17) (Feiler et al., 1992; Salcedo et al., 1999; Sharkey et al., 2020). All rhodopsins except Rh2 are expressed in different photoreceptor cells of the compound eye, whereas Rh2 is expressed exclusively in ocelli. The four receptor cells in H-B eyelets express Rh6 in addition to its expression in compound eyes. Rh7, the least studied pigment among rhodopsins, was first identified in 2000 with the publication of the *Drosophila* genome. However, there is still ongoing debate about its expression pattern in *Drosophila* (Kistenpfennig et al., 2017; Ni et al., 2017).

Rhodopsins are a type of G-protein coupled receptor (GPCR), a large and diverse family of membrane proteins involved in a wide range of cellular signaling pathways. These proteins are characterized by seven transmembrane domains that are covalently coupled to a light-sensitive chromophore called retinal (3-hydroxy 11-*cis*-retinal in *Drosophila* and 11-*cis*-retinal in rods and cones) (Vogt & Kirschfeld, 1984; Zuker et al., 1985). When a light photon strikes the retinal molecule, it undergoes photoisomerization to form an all-*trans* configuration, promoting the conversion of rhodopsin to the active metarhodopsin state. This photoactivated rhodopsin state triggers the activation of a heterotrimeric G_q protein by exchanging guanosine diphosphate (GDP) for guanosine triphosphate (GTP). This leads to the subsequent dissociation of G_q subunits $G_q\alpha$, $G_q\beta$, and $G_q\gamma$ (Cockcroft & Gomperts, 1985; Kibelbek et al., 1991; Kiselev & Subramaniam, 1994; Scott et al., 1995). The activated $G_q\alpha$ subunit activates the PLC encoded by *norpA*, which hydrolyses phosphatidylinositol 4,5-bisphosphate (PIP_2), generating inositol 1,4,5-triphosphate (IP3) and diacylglycerol (DAG) (Bloomquist et al., 1988; Devary et al., 1987). This initiates the opening of the TRP channel and the related TRP-like (TRPL) cation channel in photoreceptor cells through an unknown mechanism (Hardie & Minke, 1992; Montell et al., 1985; Montell & Rubin, 1989; Niemeyer et al., 1996; Phillips et al., 1992). As a result, cells are depolarised, and neurotransmitters are released to the downstream neurons to convey light signals.

A

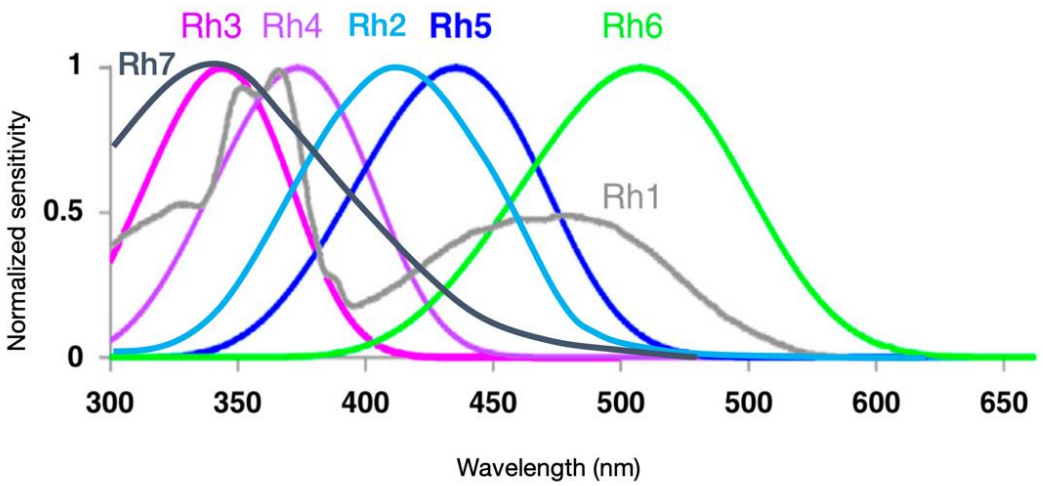

B

Compound Eyes	H-B- eyelets	Ocelli
Rh1, Rh3, Rh4, Rh5 and Rh6	Rh6 only	Rh2 only

Figure 1.17 Spectral sensitivity of different rhodopsins expressed in the fly visual system. All known rhodopsins have distinct absorption spectrums. The spectral sensitivity of rhodopsins covers a wide range of wavelengths from ultraviolet (UV) (Rh3, Rh4, Rh7) to blue (Rh2, Rh5) and green (Rh1, Rh6). Rh1 has a broad and characteristic shape due to the presence of an accessory pigment that mediates additional UV sensitivity. Rh3 and Rh4 are UV sensitive, whereas Rh2 and Rh5 have absorption maxima in the blue spectral range and Rh6 in the green spectral range. Recently characterized Rh7 has a sensitivity peak in the short UV range. **B:** *Drosophila* has specific rhodopsin expression patterns in various photoreceptor cells throughout its visual organs. The compound eyes consist of numerous individual ommatidia, each containing several photoreceptor cells. These photoreceptor cells have a complex rhodopsin expression pattern comprising Rh1, Rh3, Rh4, Rh5, and Rh6. Photoreceptor cells in ocelli exclusively express Rh2, whereas H-B eyelets containing only four cells express Rh6.

1.5.1.2 Anatomy of photoreceptive organs

- **Compound eyes**

Compound eyes are the most prominent and largest eye structure in *Drosophila*. Each compound eye consists of approximately 800 identical structural units called ommatidia (Fig

1.18A, B). A single ommatidium possesses eight photoreceptor cells (PRs) named R1-8. Within each PR is a collection of microvilli called rhabdomeres, which expresses rhodopsin (Rh) photopigments encoded by opsin genes. Apart from PRs, the ommatidium also comprises accessory cells, such as lens-secreting cone cells and pigment cells, that provide optical protection to a single ommatidium by preventing the entry of light from adjacent ommatidia (Fig 1.18C). These eight PRs, comprising six outer PRs (R1-6) and two inner PRs (R7 and R8) neurons, project the retina into the optic lobe (Fig 1.18F). The optic lobe in a fruit fly's brain is responsible for processing the visual information received through the eye's retina, where photoreceptors (PRs) are located. Four neuropils, namely the lamina, medulla, lobula, and lobula plate, form the optic lobe. Each of these regions contains different types of neurons that perform specific functions in visual processing. Outer PRs, R1-6, span the entire depth of the retina and project into the lamina, where they are connected to the lamina monopolar neurons that send their projections into the medulla neuropil. Inner PRs, R7 and R8, are superimposed in the center of the ommatidium, with R7 in the distal and R8 in the proximal part. Axonal projection of R1 and R8 neurons terminates in the M6 and M3 strata of the medulla, respectively (Fig 1.18F).

Rh1 is exclusively expressed in outer PRs, whereas one of four different rhodopsins is expressed in inner PRs. Depending on the rhodopsin expression pattern in inner PRs, there are two types of ommatidia. The pale type (p), which constitutes ~30% of ommatidia, features Rh3 in the R7 cells and Rh5 in the R8 cells, while the remaining ~70% of ommatidia are classified as the yellow type (y), containing Rh4-expressing R7 cells and Rh6-expressing R8 cells. These two types are stochastically distributed throughout the retina (Fig 1.18D, E). Located near the dorsal rim of the retina, two additional types of ommatidia, namely the DRA type and the dorsal yellow type, deviate from the standard distribution pattern, with the former featuring both R7 and R8 expressing Rh3 and the latter exhibiting co-expression of Rh3 and Rh4 in R7 (Fig 1.18F). While R1-6 are responsible for low light sensitivity and motion vision, R7 and R8 photoreceptors play a critical role in providing input to the color vision system in the medulla (Heisenberg & Buchner, 1977; Kelber & Henze, 2013; Morante & Desplan, 2008; Pagni et al., 2021; Paulk et al., 2013; Schnaitmann et al., 2013, 2018, 2020; Silies et al., 2014; Yamaguchi et al., 2008, 2010; Zhu, 2013). Recently published transcriptomic data suggest that outer PRs and R7 are histaminergic, while R8 receptor cells use both histamine and acetylcholine as neurotransmitters (Davis et al., 2020).

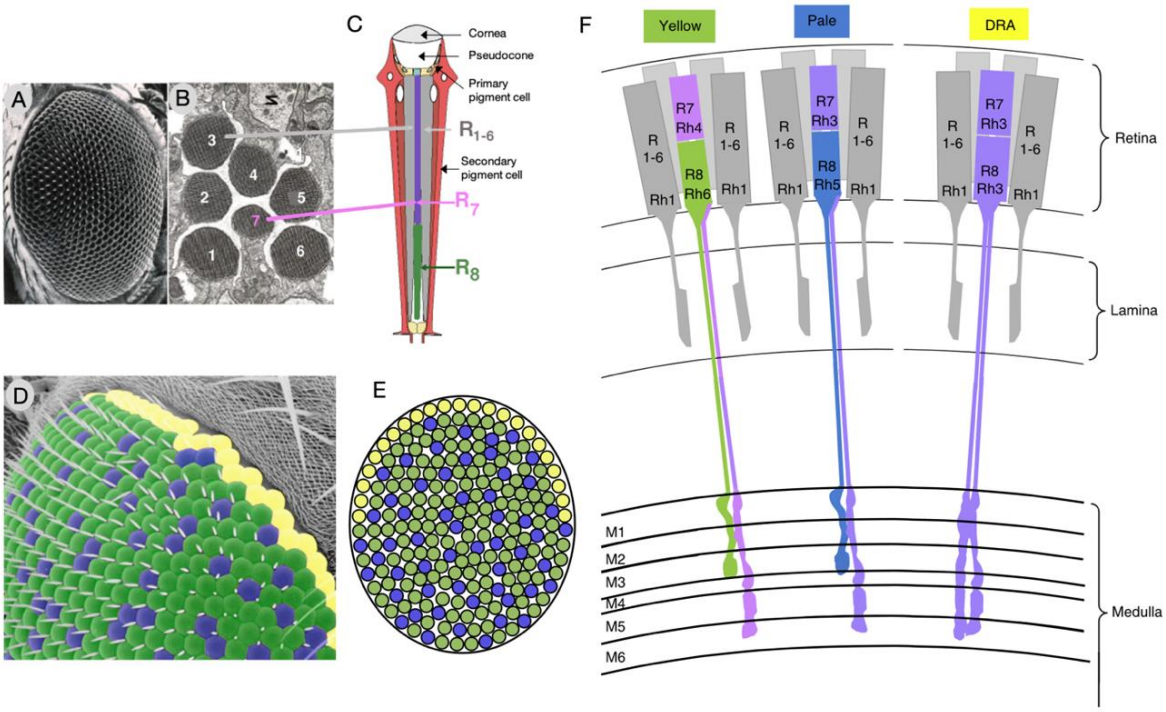

Figure 1.18 Anatomy of *Drosophila* compound eye and retinal photoreceptor cells. A: Scanning electron microscope (SEM) image of the adult compound eye. A single compound eye consists of ~800 ommatidia, inside which photoreceptor cells are housed. **B:** SEM cross-section of *Drosophila* ommatidium showing outer photoreceptor cells R1-6 and inner photoreceptor cell R7. R8 cell is located in the bottom half of ommatidia, below R7 (thus not shown in the cross-section). **C:** Schematic diagram showing the longitudinal section of ommatidia with all photoreceptor cells and accessory cells labeled. **D:** SEM of compound eye depicting the distribution of three different types of ommatidia: yellow type (green color), pale type (blue color), and DRA type (yellow color). Yellow and pale types are stochastically distributed in the retina, whereas DRA resides on the dorsal margin of the eye. **E:** Schematic representation of the retina depicted with three different types of ommatidia in a color-coded manner. **F:** A schematic section of the retina, lamina, and medulla along the anterior-posterior axis. In yellow and pale type ommatidia, inner photoreceptors R7 and R8 project from the retina to the medulla and terminates in the M6 and M3 strata of the medulla, respectively. In the DRA type, inner photoreceptors run into the medulla, and both R7 and R8 terminate in the M6 layer. The axons of outer receptor cells R1-R6 project to lamina neuropil, where they make synapses with lamina monopolar neurons. (Adapted from Desplan, n.d.; Helfrich-Förster, 2019; Sancer & Wernet, 2021)

- **Hofbauer-Buchner (H-B) eyelets**

The H-B eyelet is an extra-retinal photoreceptor organ composed of four Rh6-expressing cells positioned between the retina and lamina in the fly's optic lobe (Hofbauer & Buchner, 1989). This relatively simple eye structure is considered to be remnants of Bolwig's organs,

which are the larval eyes of *Drosophila*. Bolwig's organs contain only twelve photoreceptors, including eight Rh6-expressing cells and four Rh5-expressing cells, and do not have accessory cells like lens and pigment cells. Earlier studies have shown that Bolwig's organ is directly connected to larval pacemaker neurons and mediates light entrainment in the third instar larva (Malpel et al., 2002; Mazzoni et al., 2005). During pupal development, it is proposed that Rh5-expressing cells of Bolwig's organ switch to Rh6-expressing cells, which later become H-B eyelets, while the remaining eight Rh6-expressing cells perish (Sprecher & Desplan, 2008). Thus, all four receptor cells in H-B eyelets express Rh6 and are also known to release histamine and acetylcholine as neurotransmitters. The axonal projection of H-B eyelets arborizes the accessory medulla and ends in close proximity to the lateral neurons of the clock circuit (Helfrich-Förster et al., 2002; Schlichting et al., 2016; Yoshii et al., 2009).

- **Ocelli**

Ocelli are simple eyes found in most flying insects. In *Drosophila*, three ocelli structures are arranged in a triangle pattern on the vortex of the fly head between two compound eyes. The development of ocelli begins with precursor cells in the eye-antenna imaginal disc of the third instar larval stage (Jean-Guillaume & Kumar, 2022). Each ocellus possesses a single corneal lens located above the thin layer of lens-secreting corneagenous cells, below which ~80 photoreceptor cells reside. The photoreceptor cells are flanked by pigment cells on their lateral sides and are covered on their upper surface by corneagenous cells (Sabat et al., 2017). Ocellar photoreceptors, like those in compound eyes, contain rhabdomeres that are composed of microvilli stacks housing light-sensitive rhodopsin pigments (Fig 1.19). All the ocellar photoreceptor cells exclusively express Rhodopsin 2 (Rh2), which is sensitive to UV-blue light and has an absorption spectrum of 350nm to 450nm (Mismer et al., 1988; Pollock & Benzer, 1988). Unlike compound eyes, however, the rhabdomere size varies along the longitudinal length of the photoreceptor cells, with a shorter size in the periphery than in the middle (Sabat et al., 2017). Although ocelli's participation in vision is limited due to their poor resolving power, they mediate photosensitivity and assist in numerous behaviors like locomotion, polarization vision, flight, and body alignment (Honkanen et al., 2018; Hu & Stark, 1980; Kleef et al., 2008; Lazzari et al., 1998; Parsons et al., 2006; Taylor, 1981; Wehrhahn & Barlow, 1997).

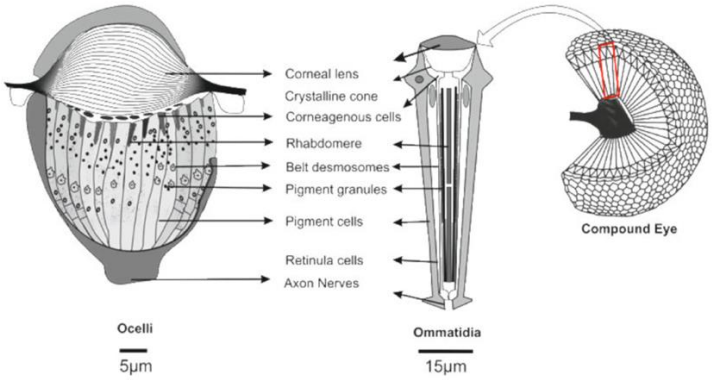

Figure 1.19 Structural difference between ocelli and compound eye. Schematic representation of ocelli and a single ommatidium. Each ocellus contains ~80 photoreceptor cells under a thin layer of corneagenous cells that lie below a large domelike corneal lens. Unlike compound eyes, the rhabdomere size in ocellar photoreceptors varies along the longitudinal length of the receptor cells. Ocelli uses a single lens to collect light signals and relay them to photoreceptor cells, while in compound eyes, each ommatidium contains a lens. (Taken from Sabat et al., 2017)

1.5.1.3 Role of Rhodopsins as circadian photoreceptors

Several seminal studies have highlighted the significance of specific rhodopsins on circadian photoentrainment and as well as on light-induced effects on activity levels. In the absence of CRY (*cry*^{02} or *cry*^{b}), flies can still synchronize their behavioral rhythms to LD cycles indicating that the visual system alone is sufficient for circadian photoentrainment. Developmental mutants like *eyes absent* (*cli*^{eya}) that ablated all the retinal PRs displayed an advanced E peak and a decreased M peak amplitude in normal 12:12 LD cycles (Rieger et al., 2003). These mutant flies also failed to facilitate long-day adaptation, i.e., they could not delay the timing of E peak like wild type. Recently it was discovered that light signals from R8 receptor cells trigger PDF release from l-LNvs to facilitate long-day adaptation (Schlichting, Weidner, et al., 2019). Moonlight stimulation, which replaces darkness in LD with moonlight, has been found to phase-advance the M peak and phase-delay the E peak in wild-type flies. However, the activity profile of eyes absent flies remains unchanged in such conditions. In addition, it has been observed that unlike wild-type flies, mutants lacking Rh1 or Rh6 exhibit significantly reduced nocturnal activity under moonlight simulation (Schlichting et al., 2014). Similarly, R7 and R8 receptor cells were found to be involved in adjusting the M peak and E peak in twilight-simulated LD cycles (Schlichting et al., 2015). Thus, different rhodopsins and underlying neural pathways play distinct roles in regulating

and synchronizing activity rhythms.

By rescuing *norpA* function in specific rhodopsin-expressing cells in a $norpA^{24}$ cry^{02} double mutant under low light intensities, Saint-Charles et al. showed that all rhodopsin except Rh5 and Rh2 (expressed in ocelli) mediated re-entrainment to 8-hour phase-shifted (both advanced and delayed) LD cycles. Thus, four of the six rhodopsin-expressing PRs (Rh7 was not considered in this study) contributed to re-entrainment through the NORPA pathway and were more efficient for advancing than delaying the behavioral clock in low lights (Saint-Charles et al., 2016). Analysis of such phase-shift experiments under colored LD cycles revealed that circadian entrainment to red light required Rh1 and Rh6 and, moreover, did not require CRY-mediated light input to the clock (Hanai et al., 2008). Similarly, it was also shown that visual system-mediated entrainment of the *Drosophila* clock in yellow and green light depends on Rh1, Rh5, and Rh6 (Hanai & Ishida, 2009).

In low light, flies depend on either CRY or *norpA*-dependent phototransduction pathway for clock synchronization. In contrast, $norpA^{24}$ cry^{02} (or $norpA^{P41}$ cry^{b}) flies resynchronize their behavioral rhythms to phase-shifted high-light LD cycles, suggesting the existence of a *norpA*-independent pathway for circadian light entrainment (Emery et al., 2000; Ogueta et al., 2018; Saint-Charles et al., 2016; Stanewsky et al., 1998; Szular et al., 2012). Therefore, Drosophila appears to utilize both canonical *norpA*-dependent and non-canonical *norpA*-independent pathways to synchronize the clock by visual input. Recent studies propose that the molecular and behavioral synchronization mediated by *norpA*-independent pathway relies on Rh1, Rh5, and Rh6. Unlike the canonical PLC-β encoded by the *norpA* gene, this alternate pathway employs a different PLC-β encoded by the *PLc21C* gene (Ogueta et al., 2018).

Histamine is the primary neurotransmitter released by all photoreceptors (Buchner et al., 1993; Pollack & Hofbauer, 1991; Sarthy, 1991). Upon light absorption by the rhodopsin molecule, the phototransduction cascade is initiated, resulting in the depolarization of PRs. This triggers the release of histamine, which inhibits the postsynaptic neurons by hyperpolarizing them. During the offset of light, PRs are repolarized, and thus the release of histamine neurotransmitters is reduced, leading to disinhibition and subsequent depolarisation of downstream neurons. *Drosophila* expresses two genes encoding histamine-gated chloride channels: *ora transientless* (*ort*) and *Histamine-gated chloride channel subunit 1* (*HisCl1*) (Davis et al., 2020; Gengs et al., 2002; Gisselmann et al., 2002; Witte et

al., 2002). In the visual system, based on the transcriptomics and in-situ hybridization study, ort was found to be observed in the lamina, medulla/lobula, and ocelli pediculus. At the same time, HisCl1 was localized in the retinal PRs, glial cells of the lamina, and ocelli pediculus. Flies with mutations in both *cry* and *hdc* (gene encoding histamine synthesizing enzyme histidine decarboxylase) do not support entrainment in LD cycles, implying that there is no histamine-independent pathway to transmit visual input to reset the clock machinery (Rieger et al., 2003). Recently, Aljeveski et al. demonstrated that flies depleted of both histamine receptors, ORT and HISCL1, failed to synchronize their rest-activity rhythms to LD cycles (Alejevski et al., 2019). Consequently, cry^{02} $HisCl1^{134}$ ort^{1} triple mutants (CHO) were identified as "circadian blind" flies, meaning their internal clock is insensitive to light signals. Furthermore, they show that each of the two histamine receptors could mediate the entrainment of activity rhythms through *norpA*-dependent and *norpA*-independent pathways. In contrast to HisCl1, ORT can facilitate photoentrainment when expressed solely in the optic lobe interneurons. Thus, ORT-positive neurons in the lamina and medulla can relay sufficient visual input from retinal PRs to the clock network for light entrainment. However, rescuing HisCl1 expression in the Rh6-expressing retinal photoreceptors but not other receptor cells restored entrainment in CHO mutants. Interestingly this could infer that Rh6-expressing cells may use a histamine-independent neurotransmission mechanism (possibly cholinergic), perhaps triggered by receiving histaminergic input from other photoreceptor cells or through autocrine negative histaminergic feedback, to transmit light signals to the clock circuit. Thus, in addition to serving as photoreceptor cells, Rh6-expressing cells also serve as interneurons, specifically in the HisCl1-dependent circadian light input pathway (Alejevski et al., 2019).

The first evidence of H-B eyelets being involved in circadian photoreception comes from the behavioral analysis of so^{1} cry^{b} mutant flies, which lack CRY, compound eyes, and ocelli, but retain H-B eyelets (Rieger et al., 2003). The results showed that around 50% of these flies could be entrained to normal 12:12 LD cycles. In contrast, only a few could be entrained to other photoperiods, indicating a relatively minor role for H-B eyelets in light entrainment. Later studies demonstrated that by blocking the synaptic output of H-B eyelets (using the Rh5gal4 driver expressed in H-B eyelets and 30% of R8 cells) in $norpA^{P41}$ cry^{b} double mutant background, the resynchronization of TIM cycling in pacemaker neurons and the behavioral rhythms to a phase-shifted high-light LD regime could be eliminated (Veleri et al., 2007). New research shows that H-B eyelets alone mediate high-intensity light

adaptation of the circadian clock. High-intensity light significantly increases the fly siesta by delaying the onset of the E anticipation, and this behavior strictly depends on H-B eyelets (Schlichting, Menegazzi, et al., 2019).

Despite the roles of the compound eye-mediated and H-B eyelet-mediated input pathways being well understood, the involvement of Rh2-expressing ocelli in circadian photoentrainment remains to be determined. Studies conducted on developmental mutants with impaired photoreceptor function have indicated minor participation of ocelli in circadian photoreception. When comparing cli^{eya} mutants (lacking compound eyes) with so^{1} mutants (lacking both compound eyes and ocelli), it was observed that significantly fewer so^{1} flies were able to entrain to short and long photoperiods in comparison to cli^{eya} mutants (Rieger et al., 2003). As mentioned earlier, Saint-Charles et al. have established that Rh2 alone is insufficient to enable entrainment in low-light conditions via the norpA-dependent pathway (Saint-Charles et al., 2016). However, more detailed studies are required to unravel this unknown circadian light input pathway.

Various studies have yielded conflicting results regarding the role of Rh7 in circadian entrainment. Two research groups conducted experiments on newly created Rh7 mutants, which formed the primary basis of the findings in this area. Ni et al. demonstrated that their $Rh7^{1}$ mutants required slightly more time to realign their behavioral rhythms in LD cycles with a 6-hour delayed phase shift (Ni et al., 2017). Conversely, Kistenpfennig et al. observed a comparable phenotype in their $Rh7^{0}$ mutant, but only under blue light conditions, not white light (Kistenpfennig et al., 2017). Furthermore, by examining the bimodal activity pattern in LD, Kistenpfennig et al. detected a lengthened siesta and marginally decreased morning anticipation behavior in $Rh7^{0}$ cry^{0} double mutants. Later it was shown that Rh7 expressed in R8 receptor cells reduced the ERG amplitude of cells only in high-light stimulation. Thus, it was proposed that in addition to circadian entrainment, Rh7 may have a putative role in fine-tuning the sensitivity of compound eyes to bright light (Senthilan et al., 2019). It has also been found that Rh7 plays a critical role in *Drosophila*'s daytime aversion to blue light.

1.5.1.4 Visual system-mediated light input pathways to clock neurons

The axonal projections of retinal photoreceptors terminate in the lamina or medulla neuropil of the optic lobe. The only clock neuron with neural projections in these regions is PDF-

positive l-LNv which has extensive arborizations in the distal medulla close to the terminals of inner photoreceptors. However, based on GRASP and *trans*-Tango techniques, there is no direct synapse between compound eye photoreceptors (outer and inner PRs) and PDF neurons in the medulla (Schlichting, 2020). This implies that visual interneurons in the optic lobe are involved in transmitting eye-mediated light input to the clock neurons (Alejevski et al., 2019). Further research shows that L2 lamina monopolar cells, which are postsynaptic partners of the outer retinal photoreceptors, send visual input to l-LNv neurons that may provide light information for arousal control (Muraro & Ceriani, 2015).

Recently published patch-clamp recordings done in ex vivo fly brains with intact eye structures revealed that most clock neurons, including s-LNv, l-LNv, 5^{th} s-LNv, ITP-LNds, sNPF-LNds, DN1a, and few DN3, responded to light with an increase of action potential firing (M.-T. Li et al., 2018). But most of the DN1ps, DN2, DN3, and CRY-negative LNds did not exhibit any response to light signals. Removing three ocelli did not impact the light-induced electrical responses, while the removal of compound eyes eliminated the light responses, indicating that compound eyes are responsible for the light-induced activation of most clock neurons. Interestingly, even in the absence of PDF or silencing/ablating the PDF expressing LNvs, the light response persisted in other clock neurons, such as LNds and DN1as. This finding challenges the hierarchical model of light signal transmission and instead suggests that the pacemaker neurons in the brain can receive visual information independently. As a result, the circuitry organization of the pacemaker neurons for visual system-mediated photoentrainment may follow a parallel model rather than a hierarchical one. Notably, all the photosensitive clock neurons send neurites to the accessory medulla (aMe) neuropil, while the light-insensitive ones did not send any neuronal projections to the aMe. Laser ablation of aMe led to the abolishment of electrical response to light, suggesting that aMe acts as a central hub for integrating eye inputs to the *Drosophila* clock circuit. The same study demonstrated that AstC/CcapR interneurons in the optic lobe could relay visual signals from compound eyes to clock neurons (M.-T. Li et al., 2018). Nevertheless, further investigation is necessary to fully elucidate the neural circuitry connecting the compound eyes to various clock neurons.

As discussed earlier, the neurites of H-B eyelets extend along the front surface of the medulla and terminate in the aMe. The findings from GRASP and *trans*-Tango experiments suggest that H-B eyelets form direct synaptic connections with both s-LNv and l-LNv but not with other clock clusters (Schlichting et al., 2016). Studies have shown that H-B eyelets-

mediated light input exerts opposing effects on s-LNvs and l-LNvs. Excitation of Rh-6 expressing photoreceptors (H-B eyelets cause an increase in the intracellular calcium, and cAMP increases in the small but not the large LNvs. Thus, it was proposed that s-LNvs receive excitatory acetylcholine input from H-B eyelets while l-LNvs receive inhibiting histaminergic inputs from H-B eyelets (Schlichting et al., 2016). However, a recent analysis of connectomics data reveals that H-B eyelets form notably fewer synaptic connections with LNvs than previously believed, challenging the longstanding model and indicating a minor role for H-B eyelets in circadian light input (Scheffer et al., 2020). In the case of ocelli, studies are yet to be done to investigate the underlying neural pathway connecting ocelli to clock neurons. However, based on the morphology of Rh2 expressing photoreceptors, they are unlikely to make direct contact with clock neurons, as their neurites terminate at the end of the ocelli pediculus and do not extend to the central brain region.

Although the involvement of the visual system in resetting the brain clock is evident, the mechanism by which how visual signals received by clock neurons are incorporated into the molecular clock remains largely unknown. Still, which clock protein integrates the visual input into clock machinery for its phase alignment with environmental cycles needs to be discovered. In contrast, the molecular mechanism underlying the CRY-mediated circadian light input to the clockwork has been comprehended well.

1.5.2 Cryptochrome-dependent circadian entrainment

1.5.2.1 Discovery of *Drosophila* CRY

As mentioned earlier, analysis of PRC in wild-type flies reveals that light stimuli can disrupt the phase of a molecular clock by either delaying or advancing it. The molecular mechanism underlying this action of light signals on the molecular clock resetting remained unknown until the mid-1990s. In 1996, three groups discovered that TIM is rapidly degraded after light exposure indicating that TIM is the clock protein that integrates light signals into the clock machinery (Hunter-Ensor et al., 1996; Myers et al., 1996; Zeng et al., 1996). However, TIM was not itself a photoreceptor, and genetic ablation of visual organs or mutations in the visual phototransduction pathway did not affect the *Drosophila* photoentrainment, suggesting there may be dedicated circadian photoreceptors in the fly. Later in 1998,

Stanewsky et al. discovered a novel non-opsin photoreceptor CRY by performing a mutagenesis screen for mutations that impact the bioluminescence rhythms of transgenic flies carrying *per-luc* reporter constructs (Stanewsky et al., 1998). Flies mutated for CRY (cry^b) had perturbed bioluminescence rhythms in LD conditions, while the rhythm prevailed when flies were kept in temperature cycles alone. The behavioral rhythms of cry^b flies were unaffected, but unlike wild-type flies, such flies failed to phase shift their clock in response to a brief light pulse (10 min) (Emery et al., 1998; Stanewsky et al., 1998). Moreover, while wild-type flies become arrhythmic under constant light conditions, cry^b flies were observed to be rhythmic (Emery et al., 2000). It was later discovered that CRY, when activated by light, interacts with TIM in clock neurons, and this interaction is crucial for the light-induced degradation of the TIM (Busza et al., 2004; Ceriani et al., 1999; Naidoo et al., 1999). Along with these and many other results that followed, CRY became recognized as a major cell-autonomous circadian photoreceptor as it mediates photoentrainment by interacting directly with molecular feedback.

CRY, first identified in plants from a mutant of *Arabidopsis thaliana*, is a highly conserved flavoprotein found in prokaryotes and eukaryotes (Ahmad & Cashmore, 1993; Chaves et al., 2011). In *Drosophila*, CRY is expressed in a majority of clock neurons, as well as in the eyes and various other tissues throughout the body (Agrawal et al., 2017; Emery et al., 1998). CRY mRNA exhibits a clock-controlled rhythmic expression, peaking late at night (Emery et al., 1998). CRY shares a structural resemblance with photolyases, which are enzymes responsible for repairing damaged DNA. However, CRY does not possess DNA repair capabilities and instead operates as a signaling photopigment molecule involved in various biological processes. (Chaves et al., 2011). Both CRY and photolyases have a conserved domain that binds to a flavin adenine dinucleotide (FAD) cofactor, which plays a critical role in their respective functions.

Although initially identified for its critical role as a circadian photoreceptor, *Drosophila* CRY exhibits an exceptional diversity of functions. Several seminal studies have demonstrated its involvement in regulating visual photoreception, magnetoreception, and neuronal activity. Interestingly, CRY can also function in a light-dependent or light-independent manner.

1.5.2.2 CRY-mediated phototransduction mechanism

CRY is sensitive to UV and blue light, with two absorbance peaks at 365 nm and 450 nm (Berndt et al., 2007; Bouly et al., 2007; Hoang et al., 2008; VanVickle-Chavez & Gelder, 2007). The cofactor FAD is non-covalently attached to the protein and is indispensable for CRY-mediated photoreception. Light photoreduces FAD from its oxidized state to an anionic semiquinone state by initiating electron transfer along a chain of highly conserved tryptophan residues (Ozturk et al., 2011, 2014; Vaidya et al., 2013). The so-called tryptophan tetrad, comprising four conserved tryptophan residues, mediates electron transfer from the protein's surface to the flavin binding pocket (C. Lin et al., 2018; B. Liu et al., 2010; Zoltowski et al., 2011). The photoreduction of flavin induces protonation of a neighboring histidine residue, promoting the displacement of the short helical C-terminal tail (CTT) from the FAD pocket, which otherwise hinders interactions with TIM (Ganguly et al., 2016). As a result of a light-induced conformational change at its C terminus, CRY can bind to TIM, triggering the degradation of both proteins and resulting in circadian clock resetting (Busza et al., 2004; Ceriani et al., 1999; Hemsley et al., 2007; Koh et al., 2006; Peschel et al., 2009). The significance of the tryptophan tetrad in CRY-mediated TIM photic degradation and circadian entrainment remains uncertain, as their mutation had little effect (Baik et al., 2019; C. Lin et al., 2018; Ozturk et al., 2014). Notably, mutations in the tryptophan residues that hindered photoreduction in vitro did not impede photoreduction in vivo, possibly because of the presence of alternative electron transfer pathways (Hoang et al., 2008; Öztürk et al., 2008).

The absence of the C-terminal tail (cry^{m} and cry^{Δ} mutant flies) of CRY affects the turnover of TIM in response to light, as the TIM-interaction surfaces in CRY are exposed regardless of the presence of light (Busza et al., 2004; Dissel et al., 2004). Flies carrying such mutations exhibit elongated periods of locomotor rhythms under DD (Dissel et al., 2004). However, conformational change in the C-terminal tail is not required for the CRY-mediated light-evoked electrical depolarization and subsequent neuronal firing. Moreover, neuronal activities regulated by CRY persist in flies depleted for TIM. Current research suggests that CRY employs different mechanisms for photoreception to regulate clock synchronization, visual function, neuronal firing, and magnetoreception. In this context, our primary focus is understanding CRY's mechanisms to mediate circadian entrainment.

1.5.2.3 Cell-autonomous CRY-dependent circadian light responses

In the *Drosophila* brain clock, CRY is expressed in a subset of clock neurons, such as four s-LNvs, four l-LNvs, 5th s-LNv, half LNds, and some of the DN1s. Clock neurons situated deep inside the fly brain sense light signals that penetrate through the cuticle via photodetection by CRY. Thus, cell-autonomous entrainment of the *Drosophila* clock solely depends on the intracellular function of CRY. CRY entrains the clock to LD cycles by targeting TIM protein to proteasomal degradation in response to light. As mentioned in the previous section, upon light exposure, CRY gets activated and undergoes a conformational change leading to its interaction with TIM. This promotes the recruitment of Skp1/Cullin/F-box (SCF) E3 ubiquitin ligase complex that contains JETLAG (JET), an F-box protein that recognizes TIM. Afterward, JET bound to the TIM-CRY complex and promotes their rapid degradation through the proteasomal pathway (Busza et al., 2004; Ceriani et al., 1999; Koh et al., 2006; F.-J. Lin et al., 2001; Peschel et al., 2009). However, JET exhibits a greater affinity for TIM than CRY, resulting in the sequential degradation of TIM and CRY (Peschel et al., 2009). As a result of light-induced TIM degradation, PER, which was TIM's binding partner, gets destabilized and degraded in the proteasome via the E3 ubiquitin ligase complex (Grima et al., 2002; H. W. Ko et al., 2002; C. Lee et al., 1996). This leads to a decrease in both PER and TIM levels during the light phase, ultimately relieving the PER-TIM mediated transcriptional repression and enabling the photic reset of the TTFL (Darlington et al., 1998; C. Lee et al., 1996). The proposed model of TIM degradation and photic resetting through the CRY-JET pathway suggests that CRY-dependent circadian photoreception operates in a cell-autonomous fashion (Fig 1.20).

The CRY-dependent cell-autonomous mechanism may explain the arrhythmic behavioral pattern observed in wild-type flies under LL conditions (Konopka et al., 1989). In LL, CRY undergoes constitutive photoactivation, which leads to persistent degradation of TIM, disrupting the rhythmic cycling of clock proteins. In contrast, flies lacking CRY were observed to be insensitive to constant light and exhibit rhythmic behavior under such conditions (Emery et al., 2000). Flies depleted for JET share a similar phenotype in LL, suggesting that cell-autonomous CRY-mediated photic resetting employs the CRY-JET pathway (Koh et al., 2006). *Drosophila* rhythms are highly sensitive to light, and the shape of the PRC indicates that the direction of the light-induced phase shift in the molecular clock relies on the timing of the light pulse. A brief light pulse administered during the early part

of the night when TIM levels are rising may hinder the accumulation of PER and TIM, thereby delaying the phase of circadian oscillations. Conversely, during the late-night period, when TIM levels are about to decrease, a brief light pulse at this stage can speed up the degradation of PER and TIM, thus causing phase advances. The generation of delayed and advanced phase shifts in the clock during the early and late night, respectively, can thus be explained through the degradation of TIM/PER resulting from cell-autonomous CRY photoreception to short light pulses. Loss of CRY or JET results in reduced TIM degradation and behavioral phase shift in response to brief light pulses (10 minutes) (Koh et al., 2006; Lamba et al., 2014; Stanewsky et al., 1998). This implied that the sensitivity of clock neurons to short light pulses is facilitated by CRY photoreception, not by light inputs relayed by the visual system. Moreover, the absence of CRY severely affected the capability of flies to re-entrain to phase-shifted LD cycles (Emery et al., 1998; Stanewsky et al., 1998).

1.5.2.4 Non-cell-autonomous CRY photoreception

Multiple studies supported the notion that the circadian light responses mediated by CRY result from its cell-autonomous function. Restricted expression of CRY in photoreceptor cells rescued local light-induced TIM degradation, but not in clock neurons, and as a result, such flies lacked a circadian light response to brief light pulses. Similarly, CRY expression in PDF neurons was insufficient to promote TIM degradation in eyes but not to mediate clock-controlled behavioral response to short light pulses (Emery et al., 2000). Additionally, it should be noted that not all clock neurons express CRY, and there is variation in the levels of CRY expression among clock neurons (Benito et al., 2008; Yoshii et al., 2008). Moreover, the response of different clock neurons to light pulses administered at subjective night varies considerably. Consequently, specific groups of clock neurons were found to participate in the circadian response to light at distinct times. Several studies highlighted the importance of a network-wide interaction among clock neurons on light-mediated phase shifting (discussed earlier). Such cross-talk was implicated in CRY photoreception too. Eventually, it became accepted that a non-cell-autonomous mechanism exists in addition to the cell-autonomous model for photic TIM degradation and resulting behavioral photoresponses (Fig 1.20).

Yoshii et al. demonstrated in 2008 that TIM is rapidly degraded not only in CRY-

positive neurons but also in CRY-negative neurons in response to a 1- hour light pulse. This indicated that CRY might facilitate TIM degradation via a non-cell-autonomous signaling pathway. Later in 2014, Lamba et al. revealed that JET expression restricted to PDF neurons was sufficient to induce light-dependent TIM degradation in LNds in response to a short 5-minute light pulse. This again implied that CRY-dependent light information could be transferred from a CRY-positive neuron to a CRY-negative neuron via intercellular interactions.

In a study that focused on phase delays of the clock in response to light in the early night, Tang et al. found that TIM degradation in s-LNvs was not necessary nor enough for phase delays. They also discovered that dorsal neurons, particularly LNds and DN1s, showed greater sensitivity to the delay zone light pulse and therefore were more crucial for phase delays (Tang et al., 2010). The finding that l-LNvs are necessary for advanced phase shifts further supports the notion that a system-level perspective is needed to understand these brief light pulse-induced phase shifts fully (Shang et al., 2008). While the molecular model underlying CRY-dependent TIM degradation is confined to individual cells, the studies mentioned above emphasize that network interactions also enable CRY-mediated circadian photoreception. However, the neural and molecular mechanisms underlying this non-cell autonomous circadian light input remain largely elusive.

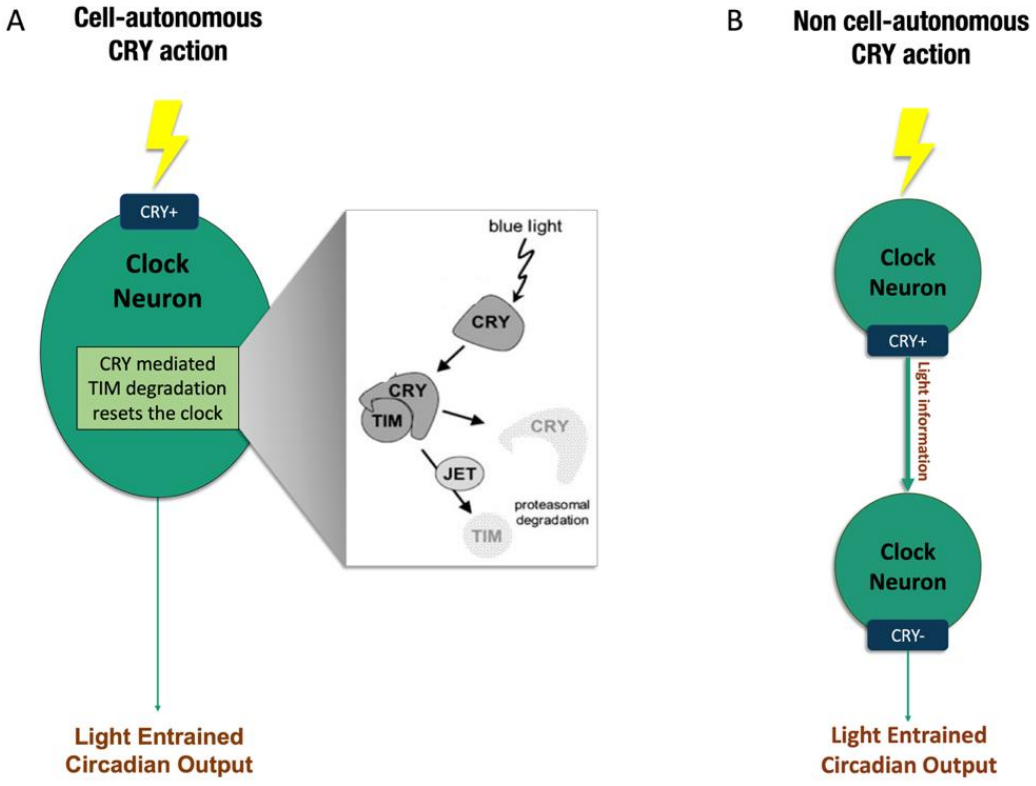

Figure 1.20 Cell-autonomous vs. non-cell autonomous CRY photoreception. CRY-mediated photoreception in clock neurons can be broadly divided into two types, namely cell autonomous and non-cell autonomous pathways. In the cell-autonomous pathway, each clock neuron that expressed CRY receives CRY-dependent light information in a cell-autonomous manner. The molecular mechanism underlying this pathway is well studied, and the schematic representation of this is shown. CRY undergoes structural changes upon light input and thus binds with TIM and initiates its proteasomal degradation by recruiting JET. In a non-cell autonomous pathway, different clock neurons receive CRY-dependent light information from each other's CRY status via cell-cell interaction. Hence, the circadian circuitry integrates and transmits CRY-dependent light input to effectively generate light-entrained circadian output.

Objectives

In most animals, the regulation of sleep-wake cycles is governed by a self-sustaining circadian clock situated within the brain. In the case of *Drosophila*, this clock is composed of a network of about 150 neurons, in which a molecular mechanism oscillates with a period of 24h approximately. A notable characteristic of the circadian clock is its ability to synchronize with external environmental cues, thus anticipating changes in the surroundings. Light serves as a fundamental cue that aligns the clock with external natural light-dark cycles. Recognizing the fundamental significance of light in entraining the circadian clock and its pivotal impact on animal well-being, it is of great importance to study circadian photoentrainment. In *Drosophila*, light reaches the brain's clock through different pathways involving Rhodopsin-mediated visual input and a light-sensitive photoreceptor named Cryptochrome (CRY), present in most clock neurons.

The process of light entrainment of the *Drosophila* circadian system has been the subject of extensive study in past years, gradually unveiling the intricate ways in which various light inputs are processed by the circadian clock. The clock assesses environmental light cues concurrently through multiple distinct, parallel pathways. Like many other animals, *Drosophila* employs multiple photoreceptors to finely adjust its clock. The circadian clock in fruit flies becomes non-responsive to light only when all photoreceptors, including CRY and rhodopsins, are removed.

This thesis is dedicated to exploring the diverse pathways through which light entrainment occurs in *Drosophila* and the neural circuits that underlie them. The main objective is to enhance our comprehension of how clock neurons extract reliable light information from the complex array of light inputs and comprehend the sensory cues responsible for regulating biological timekeeping. Utilizing *Drosophila melanogaste*r, a widely used model organism for circadian rhythms, this thesis comprises three distinct projects that delve into various aspects of the circadian light input pathways.

1. Ocelli-mediated photoentrainment pathway in *Drosophila*.

Several studies have shed light on the significance of various external photoreceptors and visual organs in refining fly locomotor activity patterns across diverse light conditions. Despite these findings, there is currently no conclusive study that has established the ocelli's (one of the three visual organs in *Drosophila melanogaster*) role in supplying light inputs to

the clock neuronal network. The primary aim of this project is to determine whether ocelli are involved in photoentrainment and, if so, to decipher the neuronal circuits that connect ocelli to clock neurons.

2. Non-cell autonomous CRY-dependent light responses in rest-activity rhythms of *Drosophila*.

A blue-light sensitive circadian photoreceptor, called Cryptochrome (CRY), is expressed within specific clock neurons and serves as the primary source of light input to the brain clock in *Drosophila*. The CRY-mediated light input pathway predominantly operates in a cell-autonomous manner by facilitating the degradation of TIMELESS, a key clock protein, upon exposure to light, leading to clock resetting. Although there is some evidence for non-cell autonomous CRY-dependent light input employing inter-oscillator communication, the behavioral outcomes and the underlying molecular and neural mechanisms of this pathway remain largely unclear. The present study is focused on comprehensively characterizing this intricate light input pathway and investigating how this signal is interpreted by various oscillators, particularly the crucial morning (M) and evening (E) brain clock oscillators responsible for regulating *Drosophila'*s bimodal activity in LD cycles.

3. Light entrainment pathway mediated by retinal photoreceptor cells

Compound eyes that possess rhodopsin-expressing histaminergic photoreceptor cells are known to play a pivotal role in *Drosophila* circadian photoentrainment. However, the exact neuronal pathways that connect these retinal photoreceptors to the clock circuit are still unknown. Previous results from our lab indicate that Rh6-expressing R8 photoreceptors contribute to circadian entrainment as both photoreceptors and interneurons. In addition to light detection, R8 cells receive inputs from other retinal photoreceptors and relay the signals to clock neurons. Based on this finding, our objective was to unravel the complete neural circuit connecting R8 cells with the clock network and the neurotransmitters employed for the achievement of photoentrainment.

Results

ARTICLE 1

Ocelli-mediated light input to *Drosophila* circadian clock

Ajay Sunilkumar[1], Faredin Alejeveski[1,a], Alexandra Saint-Charles[1,b], Elisabeth Chelot[1], François Rouyer[1*]

Affiliations:

[1] Institut des Neurosciences Paris-Saclay, Université Paris-Saclay, CNRS, 91400 Saclay, France

***Correspondence**: francois.rouyer@universite-paris-saclay.fr

[a] Present address: Institut de Biologie de l'École Normale Supérieure, ENS, CNRS, INSERM, Université PSL, Paris, France

[b] Present address: Recherche Translationnelle en Oncologie Pediatrique, Institut Curie, Paris, France.

Introduction

Circadian rhythms of behavior and physiology are considered to be an evolutionary trait that provides an organism with fitness advantages. These rhythms are regulated by the endogenous circadian clock that enable the organism to anticipate and adapt to 24-hour natural cycles imparted by the rotation of earth on its axis. Its ability to perceive and synchronize with daily cycles of external abiotic factors like light, temperature, etc., termed entrainment, allows the circadian clock to infer the local time (Golombek & Rosenstein, 2010; Pittendrigh, 1993). Only an entrained clock can adjust its period, which in most organisms is not precisely 24 hours, to the external 24-hour period of natural cycles (Roenneberg et al., 2003). Impaired circadian functioning and accompanying health concerns are common causes if a proper connection between the internal clock and the outside environment is not maintained (Blume et al., 2019).

Temporal variation of ambient light conditions is the most reliable time cue (zeitgeber) that resets a clock synchronously with the environment. Thus, in most animals, the outside world's photic information must be accessible to the master circadian clock located deep inside their brain (Foster & Helfrich-Forster, 2001; Roenneberg & Foster, 1997). In mammals, opsins in the rods and cones photoreceptors located in the retina and melanopsin in intrinsically photoreceptive retinal ganglion cells (ipRGCs) relay relevant light signals to the brain clock positioned in the suprachiasmatic nuclei (SCN) of the hypothalamus (Berson et al., 2002; Fu et al., 2005; Hattar et al., 2002; Provencio et al., 1998). Peripheral clocks then receive light indirectly through SCN signals. In *Drosophila*, the brain clock that controls behavioral rhythms sees light through different rhodopsins of the visual structures, allowing entrainment by a broad spectrum of light (300-600nm) (Helfrich-Förster, 2020; Helfrich-Förster et al., 2001; Rieger et al., 2003; Yoshii et al., 2016). In addition, the blue light photoreceptor Cryptochrome (CRY) is expressed in both brain and peripheral clock cells that can thus be autonomously synchronized with light-dark cycles (Emery et al., 1998, 2000;; Stanewsky et al., 1998; Klarsfeld et al., 2004).

The brain clock driving behavioral rhythms in *Drosophila* rests in approximately 150 neurons (Hermann-Luibl & Helfrich-Förster, 2015; Kaneko et al., 1997). CRY is expressed in most clock neurons, allowing cell-autonomous entrainment (Emery et al., 1998, 2000; Klarsfeld et al., 2004; Stanewsky et al., 1998). Besides this, rhodopsins-based

photoreceptors of the visual organs transmit light signals to the brain clock via direct and indirect neural connections (Helfrich-Förster et al., 2002; Rieger et al., 2003; Schlichting, 2020; Senthilan et al., 2019). Six Rhodopsins (Rh) have been identified to be expressed in seven photoreceptive structures: two compound eyes, two Hofbauer-Buchner eyelets, and three ocelli. Another Rhodopsin named Rhodopsin 7 (Rh7) was discovered later, whose circadian function and localization are not comprehended fully (Grebler et al., 2017; Kistenpfennig et al., 2017; Ni et al., 2017).

A single compound eye comprises about 800 unit eyes or ommatidia, housing eight photoreceptor cells. Six outer photoreceptors (R1-6) positioned at the periphery express Rh1 and send axons to the lamina neuropil (O'Tousa et al., 1985). Two inner photoreceptors, R7 and R8, innervate directly to the medulla neuropil and express Rh3-Rh6 (Rh3/Rh4 in R7 and Rh5/Rh6 in R8) (Behnia & Desplan, 2015; Rister et al., 2013; Salcedo et al., 1999). HB eyelets located underneath the retina and nearer to the medulla express only Rh6 in their four photoreceptor cells (Hofbauer & Buchner, 1989; Sprecher & Desplan, 2008). Ocelli, also known as "simple eyes," are found at the vertex of the head and have a triangle formation comprising two lateral and one median ocellus. The 80 photoreceptor cells of a single ocellus only express Rh2, which is not found in either of the remaining eye structures (Pollock & Benzer, 1988; Sabat et al., 2017). Unlike compound eyes, ocelli have a single large corneal lens through which photoreceptors residing underneath it receive light (Stark et al., 1989). In most insects, the postsynaptic partners of ocelli are comparatively few and have a large axonal diameter. Also, the neural connection between ocelli and effector neurons is much simpler, employing fewer neurotransmitters and synapses supporting faster signal transmission suitable for different behavioral responses (Hung & Ibbotson, 2014; Mizunami, 1995; Simmons, 2002).

Retinal photoreceptors play a crucial role in photoentrainment under various light conditions (Kistenpfennig et al., 2018; Schlichting et al., 2014, 2019). Photoreceptor ablation in compound eyes induced defects in the *Drosophila* bimodal activity pattern, including evening peak advancement and a decrease in the morning peak amplitude (Rieger et al., 2003; Wheeler et al., 1993). Except for Rh5 and Rh2, all rhodopsins mediate entrainment in low-light conditions via the canonical norpA-dependent transduction pathway (Saint-Charles et al., 2016). Later Rh1, Rh5, and Rh6 were found to be capable of clock synchronization in high-light conditions via the norpA-independent pathway (Ogueta et al., 2018). Histamine is the primary neurotransmitter employed by photoreceptors, and

flies devoid of histamine or histamine receptors (ORT and HISCL1) fail to support the visual system-mediated photoentrainment (Alejevski et al., 2019; Hardie & Raghu, 2001; Rieger et al., 2003). Most clock neurons send dendrites to the accessory medulla (aMe) neuropil, making direct synapses with HB eyelets and indirect connections with compound eyes (through optic lobe interneurons) (Damulewicz et al., 2020; Li et al., 2018; Muraro & Ceriani, 2015; Schlichting et al., 2016). The complete neural circuit connecting compound eyes to clock neurons still needs to be elucidated.

It is now well ascertained that compound eyes and HB eyelets transmit sensory inputs to clock neurons, thus contributing to its entrainment. Comparing the entrainment ability of certain mutant flies affecting specific eye structures suggested the existence of an ocelli-mediated photoentrainment (Rieger et al., 2003). However, the role of ocelli in circadian photoreception is still unclear. Although ocelli's participation in vision is limited due to their poor resolving power, they mediate photosensitivity and assist in numerous insect behaviors like locomotion, polarization vision, flight, and body alignment (Honkanen et al., 2018; Hu & Stark, 1980; Kleef et al., 2008; Lazzari et al., 1998; Parsons et al., 2006; Taylor, 1981; Wehrhahn & Barlow, 1997). In the present study, we assessed whether the *Drosophila* locomotor rhythms are regulated in response to changes in external light conditions by Rh2-expressing ocelli. We also dissected the circuitry linking ocelli to the clock network by utilizing the available circuit mapping techniques and the recently published Janelia hemibrain connectome. The neural circuit revealed by our studies suggests that ocelli send light inputs to most of the clock cells identified in the hemibrain. Finally, we also show that Rh2 is involved in adapting bimodal activity patterns during long photoperiods, especially the timing of the evening peak. In summary, we uncovered a novel circadian light-input pathway involving ocelli as the photoreceptive organ and examined this sensory input at the neuronal and behavioral levels.

Results

Ocelli (Rh2) alone can synchronize rest-activity rhythms to LD cycles.

As the primary experimental approach, we examined whether ocelli, which possesses Rh2 only, can entrain the circadian clock under light-dark cycles. To achieve this, we generated two different multiple-mutant fly lines; for better clarity, their genotypes were named Rh2+ and Rh7+. To generate Rh2+, all known null mutants of different rhodopsins, except Rh2 and Rh7, were recombined with the CRY-knockout cry^{02} mutant. Rh7+ was also created using a similar recombination strategy, combining null mutations of CRY and all rhodopsins except Rh7. Thus, the only functional rhodopsins expressed in Rh2+ were Rh2 and Rh7, whereas Rh7+ exclusively expressed Rh7. Then, to ascertain whether Rh2 can promote photoentrainment, we investigated and compared the re-entrainment capability of Rh2+ in LD cycles with that of wild-type (WT) flies (*Canton-S*), cry^{02}, and Rh7+. Because Rh7 alone cannot support photoentrainment (Alejeveski et al., unpublished data), Rh7+ was chosen as the negative control for our experimental approach to test the photoentrainment capacity of a fly, where we analyzed the ability of the fly to resynchronize their activity rhythms to the new advanced or delayed LD cycles. To do so, since there were some putative "circadian blind" genotypes, all the selected genotypes were initially entrained to both 12-hour:12-hour light-dark cycles associated with 25°C:20°C temperature cycles. After 2 days in these combined LD and temperature cycles, the flies were then exposed to a new 12:12 LD cycle for 8 days (temperature kept constant at 25°C), which was either 8 hours advanced or delayed to the previous regime. Here, our primary goal was to determine whether different genotypes had successfully resynchronized their bimodal activity patterns to the new phase-shifted LD cycle. We may draw the conclusion that the flies are light entrained if they can shift their behavioral activity patterns; otherwise, they cannot.

Consistent with previous studies, WT and cry^{02} mutant flies re-entrained their rest-activity rhythms in response to an 8-hour advanced or delayed LD cycle, both at low and high light intensities (Emery et al., 2000; Stanewsky et al., 1998) (fig. 1, Supplementary Table 1). However, under similar LD-shift protocols, re-entrainment was wholly eliminated in Rh7+, reconfirming that Rh7 alone cannot entrain the clock in both dim and high light conditions (fig. 1, Supplementary Table 1). In contrast, Rh2+ flies can resynchronize with advanced LD cycles under high light intensities only but not at low light intensities. At the

same time, their ability to re-entrain activity rhythms was abolished in delayed LD cycles under both low- and high-light conditions (fig. 1, Supplementary Table 1). These findings for Rh2+, compared with those for Rh7+, suggest a potential role for Rh2-expressed photoreceptors in re-entrainment to phase advances and therefore imply an ocellar function in photoentrainment.

Postsynaptic neurons of Rh2-expressing photoreceptors are Ort-positive.

Since the previously explained behavioral and functional studies conclusively demonstrated the involvement of Rh2-expressing photoreceptors in circadian clock resetting, we then decided to decipher the complete neural circuit connecting ocelli to clock neurons. As a preliminary step, we attempted to visualize the first-order downstream neurons of the ocelli. To this end, we took advantage of a recently developed anterograde tracing method, *trans*-Tango, to identify the putative postsynaptic targets of Rh2 cells (Talay et al., 2017). By expressing *trans*-Tango in Rh2-expressing photoreceptors using an *Rh2-Gal4* driver (Supplementary fig. S1), all their potential postsynaptic neurons were labeled, which interestingly had a distinctive morphology (fig. 2A). As expected, all postsynaptic partners arborized the ocellar ganglion (OCG), where Rh2 photoreceptors have projections. The cell bodies of these *trans*-Tango-labeled neurons were located in the central brain area, and their neurites were prominently directed in two directions, one to the OCG and the other to the different parts of the central brain. Unlike the similarities in their projections near the OCG, terminals of these neurons near the central brain exhibit a wide variety of projection patterns. Notably, one particular set of neurons (4 in number) sends projections to the Posterior Lateral Protocerebrum (PLP) neuropil, in contrast to the remaining set of downstream neurons that had arborizations in the superior and ventromedial neuropils (fig. 2A-iii). These neurons drew our attention because some major clock neurons are known to receive synaptic inputs from the PLP neuropil (Scheffer et al., 2020; Shafer et al., 2022).

All photoreceptors in the fly visual system, including Rh2-expressing cells, release histamine neurotransmitters in response to light stimuli. This histaminergic transmission is mediated by two inhibitory histamine-gated chloride channels, HisCl1 and Ort (Gengs et al., 2002; Gisselmann et al., 2002; Witte et al., 2002; Zheng et al., 2002). In light of this, we examined which of the two histamine receptors is expressed in the postsynaptic targets of

Rh2 photoreceptors. Utilizing the in-situ hybridization technique, we detected *ort* messenger RNA (mRNA) in all the downstream neurons of Rh2-expressing photoreceptors (fig. 2B). However, we did not find any evidence for the expression of *HisCl1* mRNA in those neurons labeled by *trans*-synaptic tracing (fig. 2C, Supplementary fig. S2). Together, these data indicate that Rh2-expressing photoreceptors relay light signals to their downstream neurons via ort-dependent neurotransmission.

Deciphering the circuit connecting ocelli to clock neurons.

To better comprehend the entire neuronal circuit that transmits signals from ocelli to clock neurons, we then examined the available connectome data from the Janelia hemibrain dataset (Scheffer et al., 2020). This recently published connectome data, made using large-scale reconstruction of neurons from electron microscopic (EM) data, provides detailed information about the neural connection, including their morphology, synaptic strength, and direction. A few open-source software and web interface tools (neuPRINT and Virtual Fly Brain) are also available to query and visualize this connectome dataset. With the aid of these tools and related research articles, we were able to identify and locate the postsynaptic neurons of Rh2 cells in the hemibrain connectome. These neurons were annotated as ocellar ganglion (OCG) neurons in the Janelia hemibrain connectome as they had a characteristic neural innervation in that region (fig. 3A). Based on the projection pattern of their terminals in the central brain area, OCG neurons were categorized into nine types by hemibrain annotations (Supplementary table 2). However, the presynaptic connections of OCG neurons with Rh2-expressing photoreceptors couldn't be established from the given connectome, as the ocellary region (including Rh2 cells) was not included in the reconstruction of hemibrain volume.

A detailed examination of the neuronal morphology of the OCG neurons clearly revealed close similarities with those neurons labeled by the trans-tango technique. Similar to trans-Tango results, we could visually distinguish between OCG neurons in EM data by looking at their patterns of neuropil innervations, where some had projections to SLP neuropil and a few other arborizing PLP neuropil. As previously mentioned, we were particularly interested in OCG neurons innervating PLP neuropil since we reasoned that they could be the primary candidates that make immediate connections with clock neurons. After

a detailed query of connectome data, we could identify the PLP innervating OCG neurons in hemibrain volume, which were annotated as OCG04 type (fig. 3B, C). The neuronal morphology of OCG04 neurons, as revealed by EM connectome data, aligned with the findings from the trans-Tango data, given that their morphologies exhibited a high degree of resemblance. (Supplementary fig. S3).

We continued further connectomic analysis using the fly hemibrain data to determine the neural pathways that connect OCG with clock neurons. All clock neuron clusters are identified in the hemibrain dataset except DN2, DN3, and a few DN1ps. Thus, with the primary candidate for the interneuron that relays signals from ocelli to clock cells being OCG04, we examined whether these neurons made direct synapses with any clock neuron cluster. We searched the entire connectivity of OCG04 but could not find any clock neurons as their postsynaptic targets (Supplementary table 3). However, we discovered that OCG04 made significant indirect neural connections to all the identified clock neurons within the hemibrain, including 4 s-LNvs, 4 l-LNvs, 6 LNds, 5^{th} s-LNv, 4 LPNs, 2 DN1as, 5 DN1pAs, and 2 DN1pBs. Using neuPRINT, an open-access tool for EM connectomics, we examined the shortest pathway linking individual OCG04 neurons to the aforementioned clock neurons. Our analysis specifically concentrated on neural connections characterized by strong synapses, defined as connections with ten or more synapses formed between the neurons. We observed the utilization of various types of neurons (both annotated and non-annotated in the hemibrain dataset) within these pathways responsible for transmitting signals from OCG04 to clock neurons. To simplify and facilitate a better understanding of the circuits, we will focus our discussion on circuits connecting OCG04 to two critical groups of lateral neurons: the small ventral lateral neurons (s-LNvs) that express Pigment Dispersing Factor (PDF) and the three dorsal lateral neurons (LNds) along with the 5^{th} s-LNv that expresses Cryptochrome (CRY) but lacks PDF. It is widely ascertained that these two classes of neurons are critical for predicting dawn and dusk. The morning oscillator residing in s-LNvs and an evening oscillator in CRY-positive LNds plus 5^{th} s-LNv are capable of driving morning and evening anticipation behavior, respectively.

The circuit associated with the neural pathway connecting OCG04 to s-LNvs included at least two interneurons. Two of the four OCG04 neurons could utilize a 4-node circuit, while the other two employed a 5-node circuit as their shortest route to establish connections with four s-LNvs (fig. 4A). In the pathway connecting OCG04 to CRY^{+} LNds and the 5^{th} s-LNv, two out of the four OCG04 neurons formed connections through a 3-node circuit, while

the remaining two utilized a 4-node circuit (fig. 4B). Within the aforementioned 3-node circuit formed by two OCG04 neurons, they made synaptic connections with a neuron class known as accessory medulla-type 8 neurons (aMe8), which were identified as major presynaptic partners of the three CRY^+ LNds and the 5^{th} s-LNv. This identical circuitry pathway was also observed in the other two OCG04 neurons, but these two neurons were only able to establish medium synapses with aMe8 neurons, characterized by three to ten synapses between the neurons. This neural pathway proceeding from OCG04 via aMe8 to three CRY^+ LNds and 5^{th} s-LNv is the sole significant (having strong synapses) and shortest pathway that connects OCG neurons to the circadian circuit. We also did a detailed examination of synaptic connections of other OCG neurons, but none of them had a simple connectivity pathway to communicate with clock neurons, as OCG04 had. Thus, with the support of circuit mapping revealed by connectomic analyses, we propose a putative neural circuitry connecting Rh2-expressing photoreceptors to the circadian clock network, with OCG04 as the first-order downstream neurons.

In vivo characterization of OCG04.

OCG04 interneurons serve as the major first-order downstream neurons in the ocelli input pathway to the clock network. We then looked for their specific drivers to validate and address the role of OCG04 in the circuit of our interest in an in vivo manner. Since we identified these interneurons in the EM hemibrain dataset, we were able to find their matching GAL4/LexA drivers using NeuronBridge, a web application for neuron similarity search across EM and confocal light microscopy (LM) datasets. We also performed a visual screening on LM images of GAL4 drivers in the Janelia FlyLight database. Combining these approaches, we uncovered several candidate drivers that targeted OCG04 neurons. However, none of the matched drivers showed exclusive expression in these neurons and were rather broadly expressed across the brain.

Out of the numerous candidate drivers identified for OCG04, our focus was exclusively on two specific drivers: *R19B01* and *R39D12* (fig. 5A, B). Since we already knew that the downstream neurons of Rh2-expressing photoreceptors are Ort positive, we then sought to check whether OCG04 also expresses Ort. We used the genetic intersection strategy to show that the selected drivers for OCG04, *R19B01,* and *R39D12* express Ort (fig. 5A, B). The

intersection between both *R19B01* and Ort and *R39D12* and Ort labeled the OCG04 neurons in a relatively more specific manner, which we concluded by comparing their neuronal morphology with *trans*-Tango staining and EM hemibrain data.

We then assessed the anatomy of the OCG04 neurons by expressing presynaptic (Syt-GFP) and postsynaptic markers (DenMark-RFP) in their drivers. This double-labeling result of OCG04 neurons revealed that their postsynaptic vesicles were located in the ocellar ganglion region, while the presynaptic sites in the terminals projected towards the PLP neuropil (fig. 5 C, D). The anatomy of the dendrites and axonal terminals of OCG04 revealed by this result is in accordance with the data provided by the connectome analysis.

We then used the GFP reconstitution across synaptic partner (GRASP) technique to validate that OCG04 neurons with dendritic arborizations in the ocellar ganglion region made anatomical connections with Rh2 cells (Feinberg et al., 2008). Robust GRASP signals were observed in the ocellar ganglion between Rh2-cells (labeled by *R14B02-LexA*) and OCG04 (labeled by *R19B01-GAL4* and *R39D12-GAL4*), indicating synaptic connections between OCG04 and Rh2-expressing cells (fig. 5E).

Rh2-expressing photoreceptors are required for long-day adaptation.

Under equinox conditions (12:12 LD), WT flies exhibit a bimodal activity pattern comprising morning (M peak) and evening peaks (E peak). These activity bouts, anticipating dawn and dusk, are driven by circadian oscillators residing in different clock neuron clusters (Cusumano et al., 2009; Grima et al., 2004; Rieger et al., 2006; Stoleru et al., 2004). Circadian light entrainment mediated by the inputs transmitted by various photoreceptors, along with intricate inter-oscillator communication, permits the fly to time these peaks precisely according to seasonal changes in day length. Earlier studies have demonstrated that the phase adjustment to longer photoperiods is accomplished mainly by delaying the E peak (Rieger et al., 2003).

It's already been shown that CRY mutant flies delay their E peak under long-day conditions more than WT, whereas flies with ablated visual organs display a relatively advanced E peak (Kistenpfennig et al., 2018). We redemonstrated this finding by comparing the activity patterns of WT with cry^{02} mutants and ort^{1} $HisCl1^{134}$ double mutant flies (no

visual-mediated inputs) in equinox (12:12) and summer (16:8) conditions. Under long-day conditions, cry^{02} mutants timed the E peak exactly at lights OFF while ort^{1} $HisCl1^{134}$ flies had a significantly advanced E peak compared to WT. This data reaffirms the notion that interaction between CRY-dependent and visual system-dependent light input is involved in the phase adjustment of fly behavior to longer photoperiods.

A previous study has established that R8 photoreceptor cells of compound eyes housing Rh5 and Rh6 are involved in the long-day adaption (Schlichting et al., 2019). Here, we investigated whether ocelli have any function in the visual system-mediated contributions to long-day adaptation, which until now is known to be solely enabled by R8 cells. Thus, we recorded the activity patterns of $Rh2^{1}$ (no Rh2) mutant flies in different photoperiods. $Rh2^{1}$ flies with no ocelli-mediated photoreception exhibited a significantly advanced E peak in 16:8 LD compared to WT flies, suggesting that ocelli are required for long-day adaptation (fig. 6).

Discussion

Most organisms have a timekeeping mechanism to perceive the recurring changes in environmental conditions. This essential survival strategy is achieved by an organism's master clock located in its brain. To keep track of time and synchronize with the environment (entrainment), the brain clock utilizes various time-givers or "zeitgebers." Ambient light status is the primary sensory input assessed by the brain clock to enable entrainment. Several studies have been done in *Drosophila* to unravel the astonishing complexity involved in different light-input pathways mediating photoentrainment. In addition to the blue-light photopigment CRY, expressed in most clock neurons, rhodopsin-mediated visual input pathways could also transduce external light stimuli onto the *Drosophila* clock machinery. Photoentrainment by the fly visual system can be broadly divided into different input pathways based on the photoreceptive organs employed. Compared to the compound eye and HB eyelet input, the contribution of ocelli in circadian light entrainment and its underlying neural pathway is almost unknown, which therefore signifies the relevance of current work.

Ocelli (Rh2) mediates photoentrainment.

Rh2, which encodes for the only photopigment expressed in ocelli, has a spectral sensitivity that peaks at 418nm (range from 350-445nm). It is recognized that this violet-type photopigment is more crucial for sensing changes in light intensity than for image creation. Unlike compound eyes, this "non-imaging" photoreceptor system has a faster signal transmission to effector neurons and thus could be considered as a unique yet potent circadian photoreceptor. Ocelli are thought to serve a number of functions in insects, but not circadian photoreception. Results from our photoentrainment assay indicate that the *Drosophila* brain clock receives ocelli-mediated light input to drive entrained circadian behaviors, which was not conclusively proven until now in any insect. By combined assessment of prior studies and our behavioral experiments with Rh2+ and Rh7+ flies, we could infer that all fly rhodopsins except Rh7 can single-handedly facilitate photoentrainment. Nonetheless, we cannot rule out the possibility of Rh7 participation in the ocelli-mediated re-entrainment observed in our test. The photoentrainment function of Rh2

discovered here further intensifies the complexity with which the circadian clock extracts reliable light information. Since the composition of ambient light fluctuates both quantitatively and qualitatively, the utilization of different visual organs adds more robustness to entrainment plasticity. Such behavioral regulation enabled by integrating multiple bandwidth-limited sensory inputs is common among all living systems, which are still being studied intensively. *Drosophila* circadian entrainment is one such intricate process that is being thoroughly explored and understood.

Like mammals, *Drosophila* circadian clock can encode an extensive range of irradiance for resetting. Based on its magnitude, the irradiance signal is relayed to the clock by distinct photoreceptor subtypes. In mammals, circadian responses to very low irradiance are regulated by rods, whereas melanopsin mediates the transmission of high-irradiance signals to the clock center. A similar mechanism can be seen in *Drosophila*, where different receptors transmit different light-intensity information. Here we determined the individual contribution of Rh2 photoreceptors in circadian response to low (<5 lux) and high-intensity (~2000 lux) light. Our results indicate that ocelli's circadian photoreception is sensitive to high light only but not low light. Thus, we discovered that Rh2 is also capable of resynchronizing the clock in high light, just like CRY, Rh1, Rh5, and Rh6, which are known to be able to do so. Prior works suggest that Rh5 is the other rhodopsin, which exclusively sends high-irradiance signals to the clock network. Furthermore, a recent study shows that Rh6-expressing HB-eyelets are the photoreceptor organ responsible for relaying extremely high-intensity light (10,000 lux) in order to adapt fly behavior in such conditions.

It was already known that under extremely low light levels, where only the NorpA-dependent transduction pathway functions, Rh2-expressing photoreceptors cannot contribute to synchronizing the clock (Saint-Charles et al., 2016). In agreement with this previous study, our results demonstrate the failure of Rh2+ flies to synchronize in dim light levels, further supporting the idea that Rh2 alone is insufficient to mediate photoentrainment in LD cycles under low light conditions. Since Rh2+ flies were synchronized in advanced high-light LD cycles, they could use either NorpA-dependent, NorpA-independent, or both signaling pathways to send light information to clock cells. Interestingly, another study has excluded the possibility of the Rh2-mediated photoentrainment pathway exclusively employing a NorpA-independent pathway that works only in high light (Ogueta et al., 2018). This finding, taken together with our data, argues that Rh2-mediated photoentrainment relies on both NorpA-dependent and NorpA-independent pathways or just the NorpA-dependent

pathway alone for sending high-intensity light signals to clock neurons.

Neural circuit underlying ocelli input

In addition to revealing the ocelli function in light entrainment, we also traced its underlying neuronal circuit. We leveraged *Drosophila*'s recently developed circuit mapping techniques and the EM hemibrain dataset to propose the neural circuit involved in ocelli-mediated circadian photoreception. Initially, anterograde tracing techniques helped to assess the downstream neurons of ocelli. These neurons were then identified in the hemibrain dataset, which was annotated as OCG, allowing us to decipher the entire neural pathway to the clock network. Within the OCG neurons, there were different classes differing in morphology. Among them, the OCG04 neurons emerged as the leading candidates for transmitting signals from the ocelli to clock neurons. Notably, these neurons displayed projections to the PLP neuropil, a region recognized for providing synaptic inputs to clock neurons. It was discovered that all four neurons belonging to the OCG04 class established indirect connections with every clock neuron identified in the hemibrain. We mainly discussed two circuitry pathways, the neural connections from OCG04 to s-LNvs and that to CRY+ LNds plus 5^{th} s-LNv. The s-LNv, a crucial pacemaker neuron in the *Drosophila* brain clock, indirectly receives ocelli-mediated signals from OCG04 through a minimum of two interneurons. In contrast, the 5^{th} s-LNv and three CRY^{+} LNds, clock neurons primarily responsible for regulating evening peaks in LD cycles, were found to be connected to OCG04 through at least one interneuron. The first and second-order ocellar interneurons involved in this circuit were identified as OCG04 and aMe8, respectively. Thus, a feedforward circuit from Rh2 photoreceptors to OCG04 to aMe8 to evening neurons was found as the simplest neural pathway connecting ocelli to the clock network. Nonetheless, other circuits connecting ocelli and clock neurons exist; all these pathways utilize at least three or more interneurons. Nevertheless, further investigation is required to understand how ocelli inputs regulate the synchronization of the molecular clock in different subsets of clock neurons. However, it is evident that OCG04 neurons serve as the primary conduits for relaying major ocelli-mediated synaptic signals to the clock network. In addition, we conducted various physiological studies to characterize OCG04 neurons in an in vivo setting to validate this proposed circuit.

Recent work from our lab established that histamine receptors Ort and HisCl1 are indispensable for visual system-mediated entrainment. Both Ort and HisCl1-dependent pathways can contribute to photoentrainment by compound eyes. In the case of ocelli, we found that Ort is the only histamine receptor involved in signal transmission. Our in-situ hybridization experiments revealed that postsynaptic neurons of Rh2 photoreceptors were Ort-positive and HisCl1-negative.

Rh2 is essential for long-day adaptation.

It is widely established that besides resynchronizing the molecular clock, the visual organs of *Drosophila* have a crucial role in sculpting the bimodal activity pattern. Several studies have pointed out the role of external photoreceptors in adjusting the *Drosophila* diurnal behavior to various environmental conditions. This includes the entrainment in 1) different photoperiods, 2) different irradiance, 3) twilight, 4) moonlight, and 5) different spectral compositions. But none of these studies indicated an Rh2-dependent locomotor adjustment in any condition except for a study published in 2003. By conducting experiments with various visual organ mutants, Rieger et al. revealed that ocelli had a minor contribution in adjusting the *Drosophila* activity phase to longer photoperiods. However, this conclusion was reached by comparing a mutant that affected both the compound eye and ocelli (so^{1}) to a mutant that only affected the compound eye (cli^{eya}). Considering this, we sought to explore the role of ocelli in long-day adaptation, which remained ambiguous. We found that under long-day conditions, flies without functional Rh2, and hence lacking ocelli input, could not delay the phase of their E peak properly, compared to WT flies. Thus, in addition to photoentrainment, the ocellary pathway is important in adapting flies' bimodal activity to summer-like days. In summary, we can infer that, like other visually guided behaviors, the *Drosophila* clock network processes inputs from all their visual organs: compound eyes, HB eyelets, and ocelli in a parallel way to provide optimum light-dark adaptation. But how the clock weighs these different visual stimuli and where the integration occurs at the cellular level still needs to be studied.

Methods

Fly stocks

The following *Drosophila* strains were used in this study: *Canton S* (wild type), cry^{02} (Dolezelova et al., 2007), $ninaE^{17}$ (O'Tousa et al., 1985), $Rh2^{1}$ (C. Montell, unpublished null mutant), $Rh3^{1}$ (Vasiliauskas et al., 2011), $Rh4^{1}$ (Vasiliauskas et al., 2011), $Rh5^{2}$ (Yamaguchi et al., 2010), $Rh6^{1}$ (Cook et al., 2003), ort^{1} (Iovchev et al., 2002), $Hiscl1^{134}$ (Hong et al., 2006), *Rh2-GAL4* (Wernet et al., 2012), *UAS-DenMark UAS-syt.eGFP* (BDSC-33065), *UAS-LexADBD* (Ting et al., 2011), Ort^{C1-3}*-gal4AD* (Ting et al., 2011), *Ort-LexA::VP16* (Gao et al., 2008), *UAS-*GFP_{1-10} (BDSC-93016), *LexAop-*GFP_{11} (BDSC-93019), *19B01-GAL4* (BDSC-48838), *39D12-GAL4* (BDSC-41228), *14B02-LexA* (BDSC-52468).

To generate multiple rhodopsin mutants, individual rhodopsin mutations were genetically recombined into a cry^{02} mutant. Thus, a mutant line that exclusively expresses Rh2 and Rh7 and another line with Rh7 alone were generated. All rhodopsin mutants used for recombination are null mutants. Except for the Rh5 gene on chromosome II, all other rhodopsin genes and CRY are positioned on chromosome III. The final genotype for mutant fly having only Rh2 and Rh7 was $Rh5^{2}$; ninaE^{17}, $Rh3^{1}$, $Rh4^{1}$, $Rh6^{1}$, cry^{02} and that of fly expressing Rh7 only was $Rh5^{2}$; $ninaE^{17}$, $Rh2^{1}$, $Rh3^{1}$, $Rh4^{1}$, $Rh6^{1}$, cry^{02}.

All flies were raised under a 12-hour light/12-hour dark cycle at 25 °C on a standard corn meal–yeast agar medium.

Photoentrainment assay

Drosophila Activity Monitor System (DAM2; Trikinetics) was used to assay the locomotor activity of flies. Individual 2 to 5 days old male flies were transferred to a glass tube with food at one end and a cotton plug at another. DAM2 monitors holding such tubes were kept inside an incubator, and activity was recorded at 30-minute intervals. All the experiment flies were entrained in light/dark (12 hour:12 hour) and temperature cycles (25-20^{0}C) for initial 2 days. Depending on the required experiment protocol (advanced or delayed shift in LD), flies were then exposed to a 4-hour day (advanced lights OFF) or 20-hour night

(delayed lights ON) on the third day. Then for the remaining 8 days, flies were subjected to the new 12:12 LD regime with a phase similar to the condition exposed on the 3rd day. Thus, the new phase-shifted LD cycle was either 8 hours advanced (advanced phase shift) or 8 hours delayed (delayed phase shift) from the initial LD cycle. From day 3 onwards, the temperature was kept constant at 25^0C. Illumination in the incubator was provided by light-emitting diodes (LEDs) with emission spectra ranging from 400nm to 680nm. The light intensity was about 2000 lux for high-light conditions and below 5 lux for low-light conditions. Flies were released into constant darkness (DD) for 6 days after 8 days in the phase-shifted LD cycle.

Activity analysis was performed using FaasX 1.21 software, derived from the Brandeis Rhythm Package. Activity profiles were plotted as double-plotted actograms. The hash density (HD) denoted the activity events per hash. As activity levels varied across genotypes, different definitions for HD were chosen for better comparison. ZT, at which the peak value of evening activity in LD cycles and activity in DD, was determined and used to generate the phase plot corresponding to each actogram. To determine the entrainment status of a specific genotype, we compared the phase of evening activity over the last five days of the shifted LD schedule with that of the WT. A genotype was considered to be entrained based on two conditions: (1) when the sequence of five values did not display a statistically significant difference from the control group (*Canton S*) in a one-way analysis of variance (ANOVA) using Dunnett's multiple comparisons tests, and (2) the variance of these five values needed to be less than 0.1, indicating that those values are relatively consistent and not widely dispersed from each other. Results are shown in supplementary table 1.

Long-day adaption assay

Locomotor activity was recorded using *Drosophila* Activity Monitor System (DAM2; Trikinetics) as described earlier. 2 to 5 days old male flies were considered for the assay. Flies were subjected to equinox conditions (12:12 LD) for 7 days and then to long-day conditions (16:8 LD) for the remaining 7 days. The temperature was kept constant at 25^0C throughout the experiment. Using FaasX 1.21 software, daily locomotor profiles were plotted as activity histograms over 24 hours. The activity of n flies recorded over 4-5 days was averaged to generate the daily activity profile. The activity during the first 2-3 days in

a particular LD regime was excluded from the analysis. Each white bar in the 24-hr activity histogram represents mean activity levels in a 0.5h interval during the light phase, and black bars represent that during the dark phase of the LD cycle. The evening peak was the highest activity bin in the second half of the photoperiod.

Immunolabeling

All immunolabeling was done on whole-mounted adult male brains. Fly brains were dissected in PBS (phosphate buffer saline) and transferred to 4% PFA (paraformaldehyde) for 1-hour fixation at room temperature. After fixation, samples were washed in PBST (0.3% Triton X-100 in PBS) four times (15 min/time) and later blocked with 1% bovine serum albumin (BSA) in 0.3% PBST for 2 hours at room temperature. The blocked samples were then incubated in primary antibodies for at least 48 hours at 4°C. The primary antibodies used include chicken anti-GFP (ThermoFisher) at 1:1000 dilution, mouse anti-Chaoptin (clone 24B10, gift from A. Hofbaeur) at 1:100 dilution, rabbit anti-DsRed (Clonetech) at 1:2000 dilution. Before incubating with 1:1000 diluted secondary antibodies for at least 24 hours at 4°C, the samples were washed in 0.3% PBST four times (15 min/ time). Secondary antibodies include Alexa Fluor 488-conjugated anti-chicken, Alexa Fluor 547-conjugated anti-mouse, and Alexa Fluor 568-conjugated anti-rabbit. Both the primary and secondary antibodies were diluted in antibody dilution buffer (0.1% bovine serum albumin and 0.3% Triton X-100 in PBS). Brains were mounted on PTFE printed slides (Electron Microscopy Sciences) in ProLong™ Diamond Antifade Mountant (ThermoFisher). Images were acquired with a Zeiss AxioImager Z1 semi-confocal microscope equipped with an AxioCam MRm digital camera and an apotome with an adjustable grid, providing structured illumination.

For GRASP experiments, the brain samples were not incubated with any antibodies. After dissection in PBS and fixation in PFA, brains were washed in 0.3% PBST five times (15 min/time) and later mounted for image acquisition.

Trans-Tango

For anterograde tracing of a specific neuron group, the corresponding GAL4 driver was crossed to *UAS-myrGFP, QUAS-mtdTomato::3xHA; UAS-hGCG::hICAM1::dN RXN1. nSyb-hGCGR::TEVcs::QF, Elav-hArr::TEV;* . After eclosion, male progeny flies were selected and kept in 12:12 hour LD conditions at 18 ℃. Immunolabeling was done on flies at least two weeks old, and brains were dissected, fixed, and labeled as previously described. Primary antibodies used were chicken anti-GFP (1:1000, ThermoFisher), rat anti-HA (1:200), rabbit anti-DsRed (1:2000, Clonetech), mouse anti-PDF (1:50000, Developmental Studies Hybridoma Bank), rat anti-TIM (1:10000, Grima et al., 2002). Secondary antibodies include Alexa Fluor 488-conjugated anti-chicken, Alexa Fluor 547-conjugated anti-mouse, and Alexa Fluor 568-conjugated anti-rabbit.

In situ hybridization

In situ hybridization was performed on the whole-mount fly brain with RNAscope® Multiplex Fluorescent Reagent Kit v2 (ACD bio) as previously described (Alejevski et al., 2019). The brain samples were incubated with probe diluent solution: *HisCl1* probe (Cat. No. 300031-C3 ACD Bio) was diluted (1:50 in probe diluent), and *ort* probe (Cat. No. 435481, ACD Bio) was undiluted. The samples were incubated overnight with probe solution at 40 °C, followed by two washes (10 min/wash) using 1× Wash Buffer. Later the samples were incubated at 40 °C for 30 minutes with 2-3 drops of RNAscope® Multiplex FL v2 and then washed again. These steps were repeated for RNAscope® Multiplex FL v2 Amp 2 and RNAscope® Multiplex FL v2 Amp 3 incubations. For *ort* and negative control stains, the samples were incubated at 40 °C for 15 minutes with RNAscope® Multiplex FL v2 HRP-C1, followed by the same washing procedure. Likewise, for *HisCl1* stains, the samples were incubated at 40 °C for 15 minutes with RNAscope® Multiplex FL v2 HRP-C3, followed by the same washing steps. Finally, the samples were incubated at 40 °C for 30 minutes with Opal 520 (Perkin Elmer, FP1487001KT, diluted 1:2000) for *ort* and negative control probes and Opal 650 (Perkin Elmer, FP1496001KT, diluted 1:2000) for the *HisCl1* probe. The brain samples were then washed as previously described and incubated overnight at 4 °C with rat anti-HA antibody (1:200 dilution). Following incubation with a primary antibody, the samples are washed in PBST and later incubated with a secondary

antibody, Alexa546-conjugated anti-rat antibody, for 3 hours at room temperature. Samples were washed in PBST before mounting them on glass slides with SlowFadeTM Gold antifade reagent (Invitrogen). Images were taken using SP8 Leica Confocal Microscope.

Figures and legends

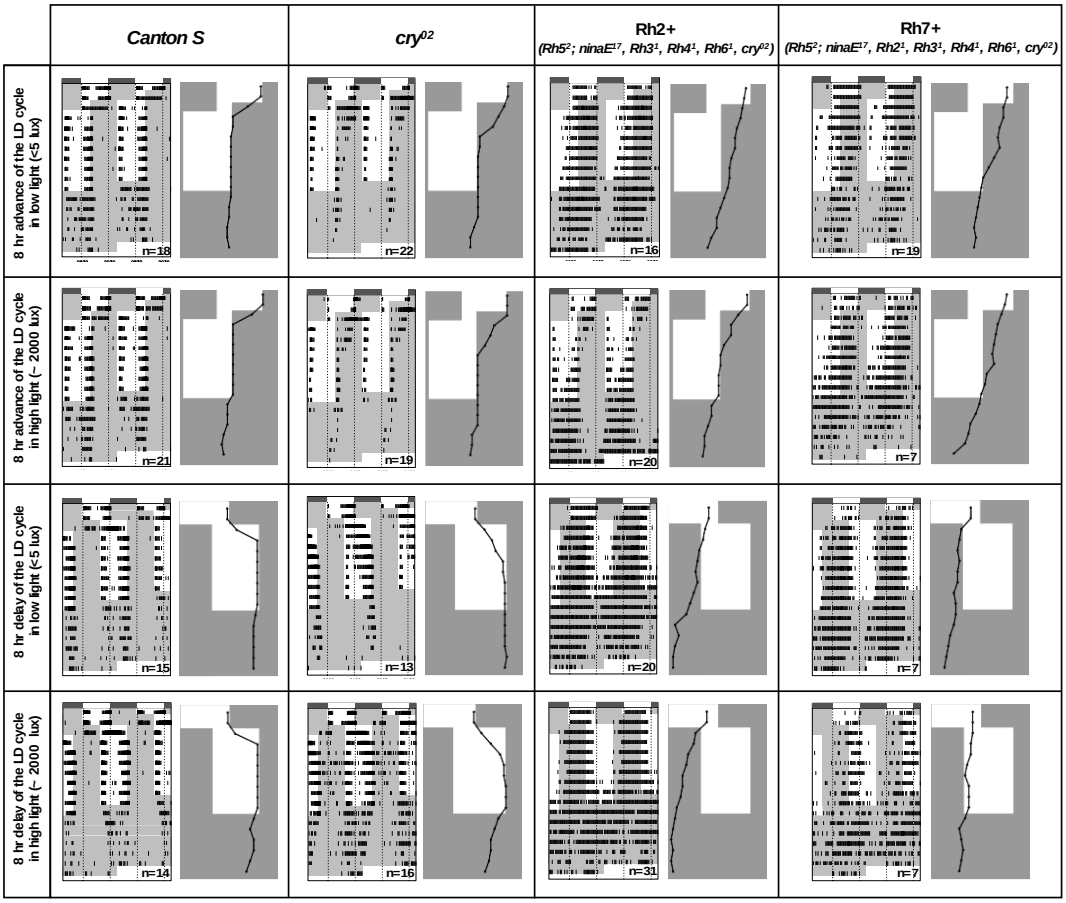

Fig. 1 Ocelli (Rh2) supports re-entrainment only to phase advanced LD cycles under high-light conditions. Average double plots illustrating the locomotor activity of each genotype with corresponding phase plots (see methods). The flies were initially subjected to a 12 hr:12hr LD cycle along with temperature cycles of 25:20 °C for 2 days. For low light (first and third row) and high light (second and fourth row) condition experiments, light intensity throughout the experiment was maintained at <5 lux and ~2000 lux, respectively. The temperature was kept constant at 25 °C from the beginning of the day 3 light phase till the end of the experiment. Depending on the required experiment protocol (advanced or delayed shift in LD), flies were then exposed to a 4-hour day (advanced lights OFF) or 20-hour night (delayed lights ON) on the third day. Then for the remaining 8 days, flies were subjected to the new 12:12 LD regime with a phase similar to the condition exposed on the 3rd day. Thus, the new phase-shifted LD cycle was either 8 hours advanced (advanced phase shift, first and second row) or 8 hours delayed (delayed phase shift, third and fourth row) from the initial LD cycle. Wild type (first column) and flies depleted for CRY (second

column) resynchronized their rest-activity rhythms to both phase advanced and phase delayed LD cycles in low and high light conditions. In all four different experimental conditions, wild-type flies shift their evening peak and re-entrains within 2 days, while flies without CRY require at least 4 days to do so. Rh2+ flies were observed to resynchronize their locomotor rhythms only to high-light phase advanced LD cycles (second row, third column), but not to any other protocol. Rh7+ flies do not synchronize with both advanced and delayed cycles under low and high-intensity light conditions (last column). The white area indicates the light phase, and the grey area corresponds to the dark phase of the LD cycles as well as DD condition. Dots in the phase plots indicate the peak value of evening activity in LD cycles and activity in DD. n is the number of flies used for each experiment. Results of the statistical analysis is shown in supplementary table 1.

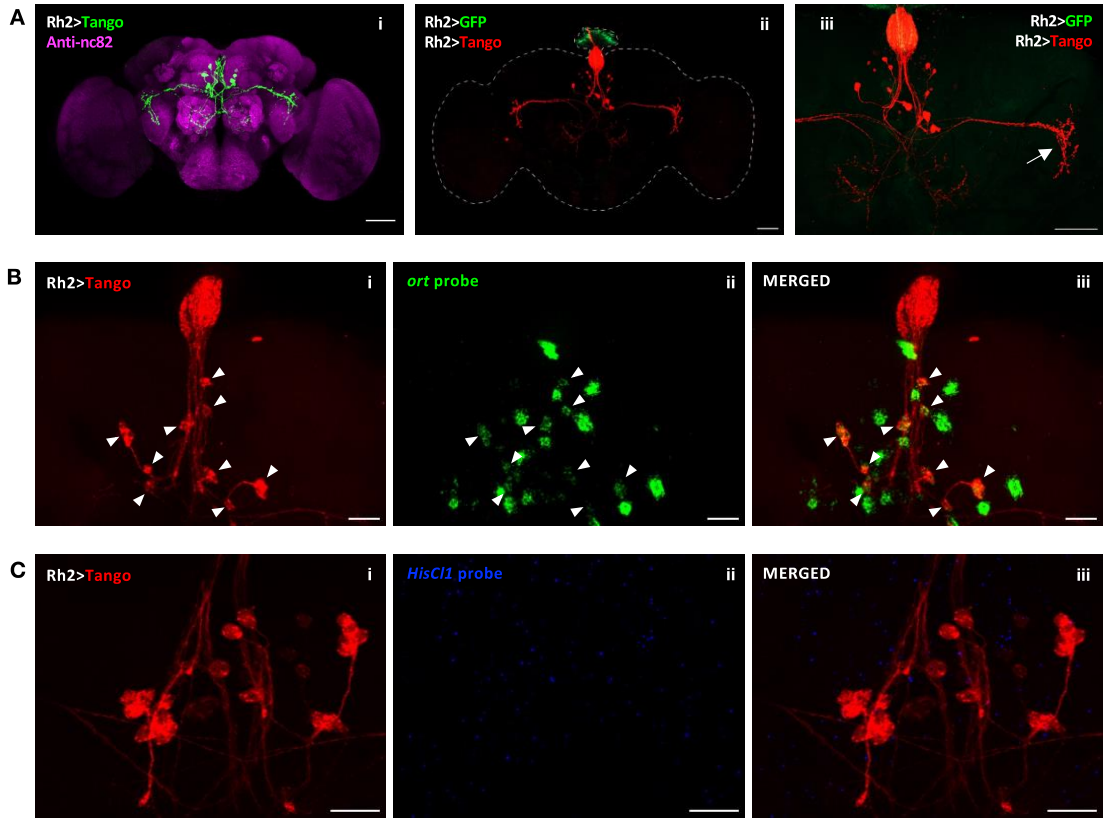

Fig. 2 Characterizing the postsynaptic neurons of Rh2-expressing photoreceptors. (A i-iii) Anatomy of postsynaptic neurons (green) of Rh2-expressing cells revealed by trans-Tango technique. **(i)** The brains stained with anti-RFP (green) and anti-nc82 (magenta), respectively, to visualize the downstream partners of Rh2-expressing cells and neuropils of the *Drosophila* adult brain. **(ii)** *Rh2-GAL4/trans-Tango* flies stained with anti-GFP (green) and anti-RFP (red). Expression of trans-Tango ligand in Rh2-expressing photoreceptor cells (green) allowed tracing their postsynaptic partners (red). **(iii)** More magnified image to visualize the projection patterns of downstream neurons of Rh2 cells. Unlike other postsynaptic neurons, a particular set of neurons (4 in number) projects to the lateral side of the brain (white arrow). Scale bars, 50 μm **(B-I, C-i)** *Rh2-GAL4/trans-Tango* flies stained with anti-RFP (red) to label postsynaptic neurons of Rh2-expressing cells. **(B-ii)** *ort* mRNA expression (green) in central brain region visualized by RNAscope® in situ hybridization (see Methods). **(B-iii)** Merged image revealing that all downstream neuron cell bodies (white arrowheads) of Rh2 cells express *ort* mRNA. **(C-ii)** *HisCl1* mRNA expression (blue) in central brain region visualized by RNAscope® in situ hybridization (see Methods). **(C-iii)** Merged image showing that downstream neurons of Rh2-expressing cells do not express *HisCl1* mRNA. Scale bars (B, C), 20 μm.

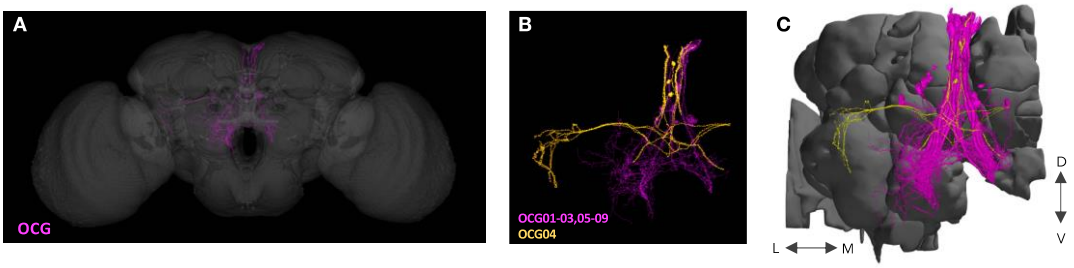

Fig. 3 Deciphering the circuit connecting ocelli to clock neurons. (A) EM morphology of ocellary ganglion (OCG) neurons (magenta) revealed from the Janelia hemibrain connectome dataset. Neuropils are shown in grey. (**B)** OCG04 (yellow) neurons highlighted from the rest of the OCG neurons (magenta). **(C)** Four neurons annotated as OCG04 (yellow) in EM data innervated the posterior lateral protocerebrum, while other OCG neurons projected towards the central region of the brain.

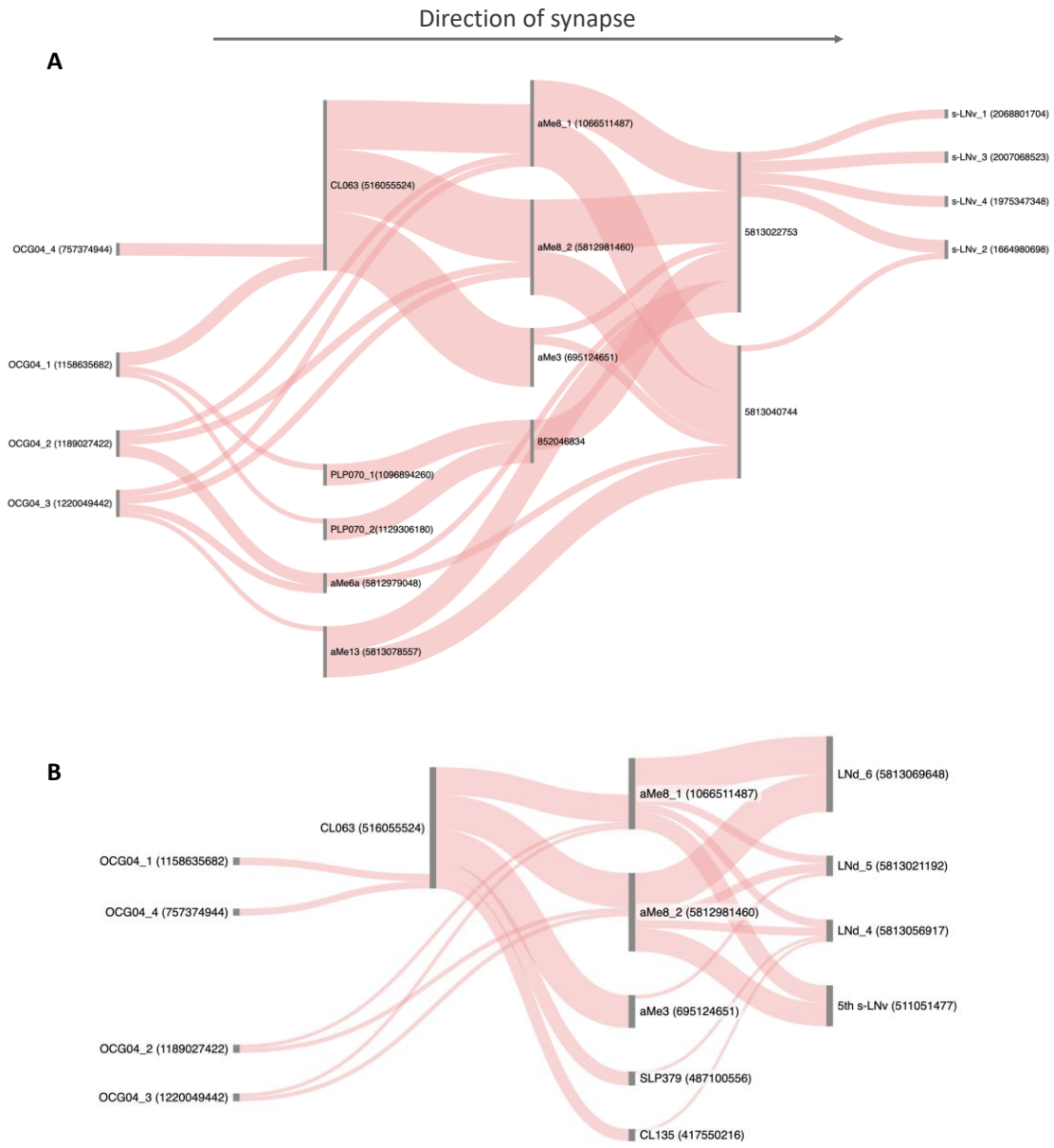

Fig. 4 Circuitry connecting ocelli to major pacemaker neurons. Sankey diagrams illustrating the neural pathway from four OCG04 neurons to four s-LNvs (A) and 3 CRY^{+} LNds + 5^{th} s-LNv (B). The strength of synaptic connections is represented by the thickness of the flow between the nodes. The diagrams presented exclusively represent strong synaptic connections, defined as having 10 or more synapses between neurons. Notably, certain OCG neurons displayed strong connections with each other, but these connections are omitted in the diagrams. The neurons are annotated in accordance with the hemibrain dataset, and their corresponding IDs from the dataset are provided. However, it should be noted that some neurons are currently not annotated in the dataset, and therefore only their unique IDs are provided here.

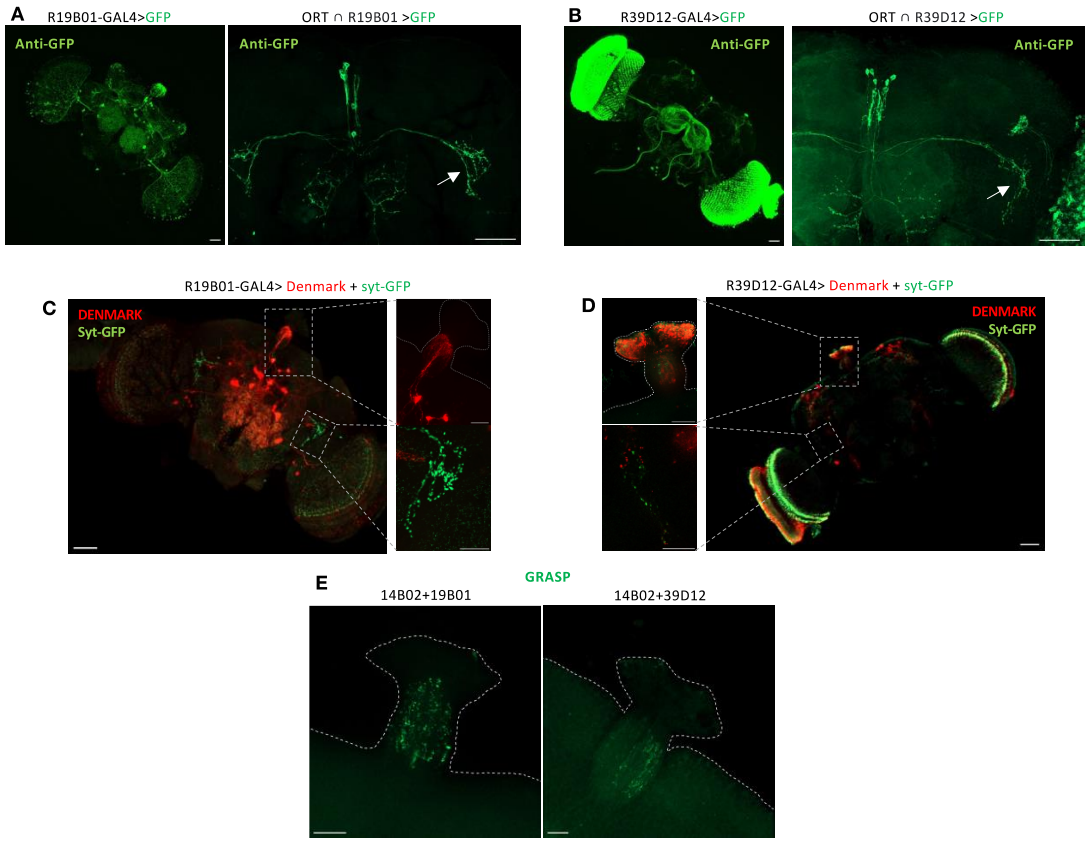

Fig 4 *In vivo* characterization of OCG04 neurons. (A) (left) *R19B01-GAL4* expression pattern (green). Image is taken from the Janelia FlyLight database. (right) Expression pattern of Ort$^{c1\text{-}3}$ ∩ R19B01 (green) label OCG04 neuron projections (white arrow) in a relatively more specific manner compared to *R19B01-GAL4* expression pattern. Scale bars, 50 μm (**B)** (left) *R39D12-GAL4* expression pattern (green). Image is taken from the Janelia FlyLight database. (right) Expression pattern of Ort$^{c1\text{-}3}$ ∩ R39D12 (green) label OCG04 neuron projections (white arrow) in a relatively more specific manner compared to *R39D12-GAL4* expression pattern. Scale bars, 50 μm (**C, D)** Expression of UAS-syt-GFP and UAS-Denmark, which are presynaptic and postsynaptic markers, respectively, under *R19B01-GAL4* (C) and *R39D12-GAL4* (D). The brains were stained with anti-GFP (green, syt-GFP) and anti-DsRED (red, Denmark) antibodies to visualize the respective markers. The ocellary ganglion region and the lateral side of the central brain region are highlighted in the insets (dotted box). Additionally, magnified images of these insets are provided for closer examination. Scale bars in the main figures, 50 μm and that in the insets, 20 μm **(E)** GRASP signals (green) between Rh2 expressing photoreceptor cells (labeled by R14B02-LexA) and OCG04 neurons labeled by *R19B01-GAL4* (left) and *R39D12-GAL4* (right). Scale bars, 20 μm.

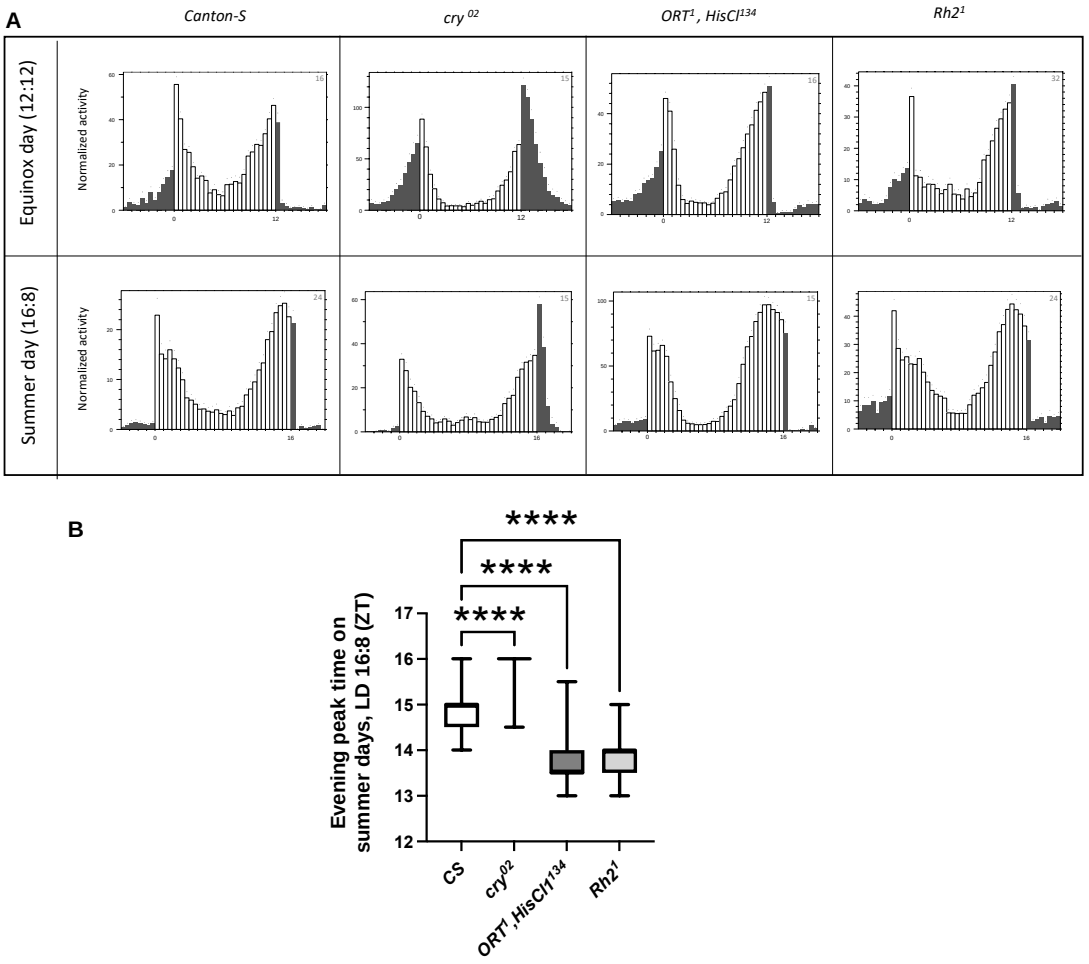

Fig. 6 Rh2 is essential for long-day adaptation. (A) Representative averaged locomotor activity profiles of flies exposed to equinox day conditions (LD12:12, upper panel) and summer day conditions (LD 16:8, lower panel). X-axis denotes the zeitgeber time (ZT). The white bar indicates the activity during the light phase, and the grey bars indicate the dark phase. The sample size of each behavioral experiment is indicated by the number displayed in the upper right corner of activity plots. Corresponding genotypes are written above each column. In LD 12:12, all genotypes exhibit a bimodal activity pattern with an M peak around lights ON and an E peak (green bar) around lights OFF. In LD 16:8, the E peak (green bar) of all genotypes except *cry*^{02} is delayed and uncoupled from the lights OFF. **(B)** Box plot illustrating the timing of the evening activity peak of each genotype in summer day conditions. One-way ANOVA reveals a significant difference between the genotypes ($F=120.9$; **** $p < 0.0001$). Post hoc Tukey test shows a significantly advanced E peak in *ort*^{1} *HisCl1*^{134} and *Rh2*^{1}compared to *Canton S* controls ($p = 0.0001$ for all)

Supplementary figures and legends

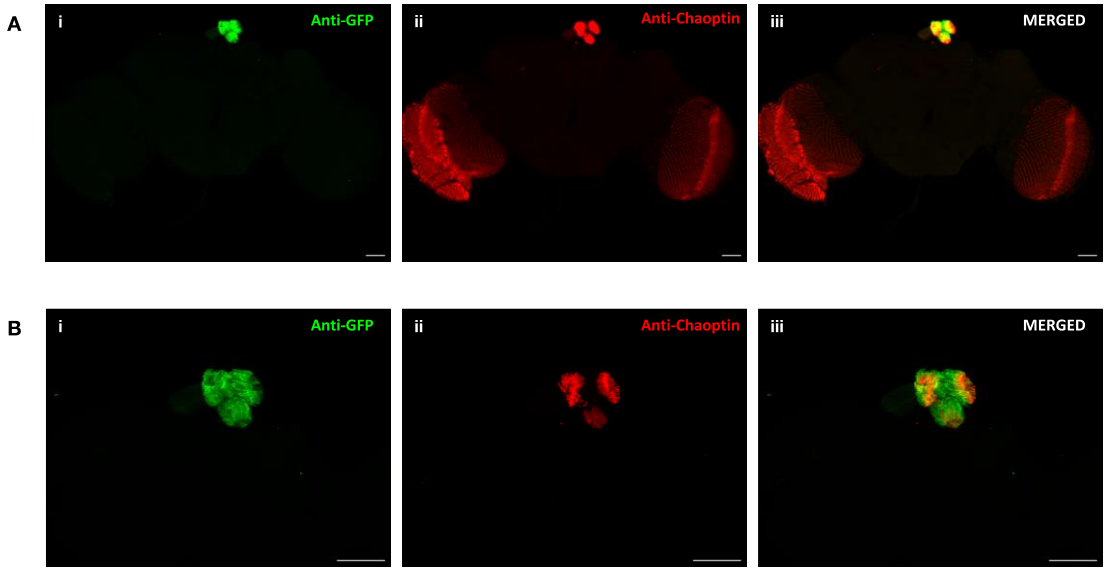

Fig. S1 (A, B) Expression pattern of Rh2-GAL4 in the *Drosophila* adult brain. (A) Maximum projection of RH2-GAL4>GFP stained with (i) anti-GFP (green) and (ii) anti-Chaoptin (red). (iii) Composite of all channels. Scale bars, 50 μm. (B) More magnified images showing RH2-GAL4>GFP ocelli labeled with (i) anti-GFP (green) and (ii) anti-Chaoptin (red). (iii) Composite of all channels. Scale bars, 50 μm.

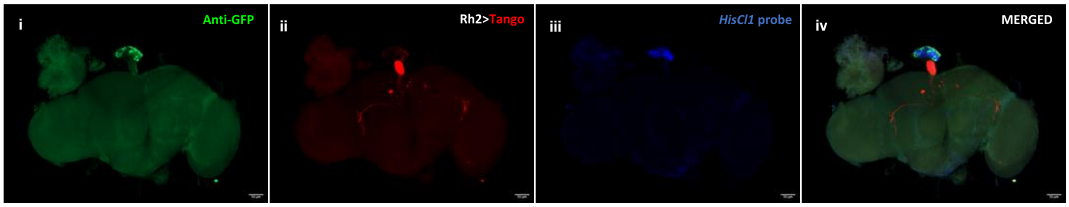

Fig. S2 HisCl1 mRNA expression in the whole mount brain. *Rh2-GAL4>trans-Tango* flies stained with (i) anti-GFP (green) to visualize Rh2-expressing cells and with (ii) anti-RFP (red) to label postsynaptic neurons of Rh2-expressing cells. (iii) HisCl1 mRNA expression (blue) visualized by RNAscope® in situ hybridization (see Methods). (iv) Composite of all channels.

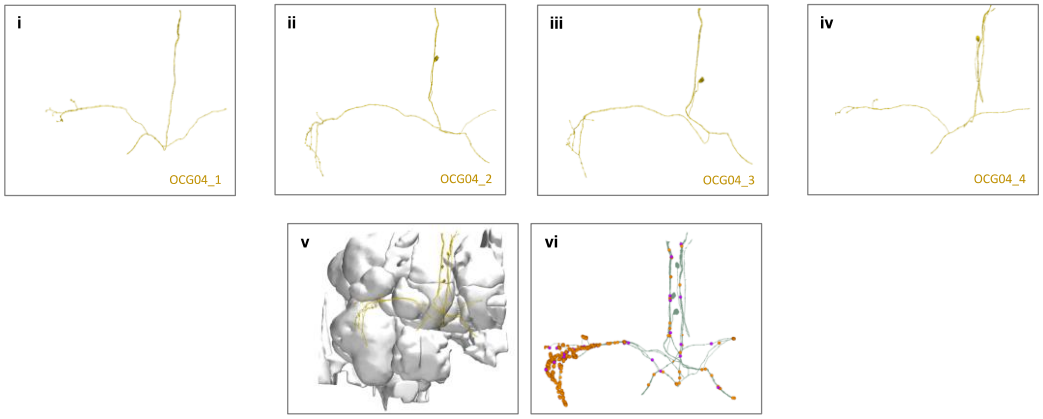

Fig. S3 Neuronal morphology of OCG04 neurons revealed by EM connectome data. (i-iv) EM morphology of four neurons annotated as OCG04 type neurons. (v) Morphology of neurons (yellow) along with neuropils (grey). (vi) Synaptic connections of four OCG04 neurons. Synaptic outputs are shown in orange, while inputs are in magenta.

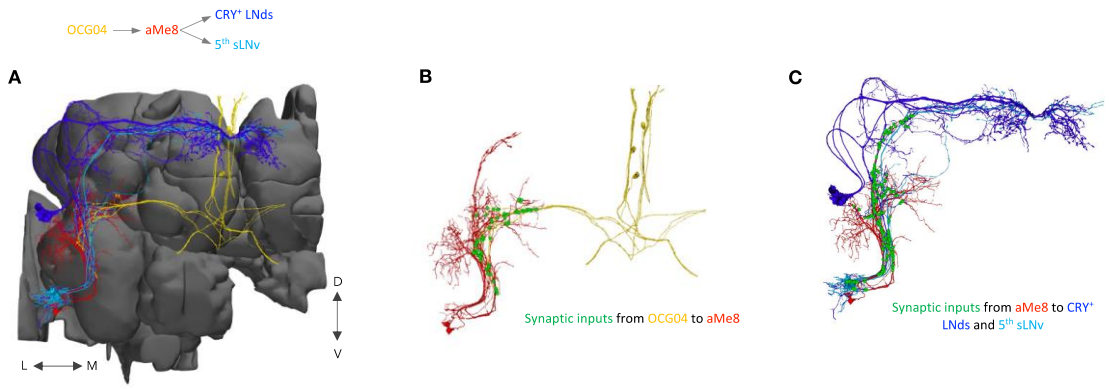

Fig. S4 (A) Neuronal morphology of different types of neurons involved in the circuit connecting ocelli to 3 CRY^+ LNds and 5^{th} s-LNv. Four OCG04 neurons are indicated in yellow, two aMe8 neurons are indicated in red, three CRY^+ LNds are indicated in dark blue, and one 5^{th} sLNv is indicated in light blue. Neuropils are shown in grey. **(B)** Sites of synaptic inputs (green) from OCG04 to aMe8 neurons. OCG04 neurons are indicated in yellow, whereas aMe8 neurons are in red. **(C)** Sites of synaptic inputs (green) from aMe8 neurons to three CRY^+ LNds and 5^{th} sLNv. aMe8 neuron morphology is shown in red, and that of CRY^+ LNds and 5^{th} sLNv in dark blue and light blue, respectively.

Supplementary tables

8 hr advance of the LD cycle in low light						
	Mean of evening peak time during last 5 days of shifted LD	Mean Difference (from Canton S)	95% CI of difference	Adjusted P value	Variance of evening peak time during last 5 days of shifted LD	Summary
Canton S	13	-			0	
cry^{02}	13.6	-0.6	-2.608 to 1.408	0.78	0	Entrained
Rh2+	15.8	-2.8	-4.808 to -0.7918	0.0063	0.575	Not entrained
Rh7+	15.8	-2.8	-3.508 to 0.5082	0.1673	5.375	Not entrained

8 hr advance of the LD cycle in high light						
	Mean of evening peak time during last 5 days of shifted LD	Mean Difference	95% CI of difference	Adjusted P value	Variance of evening peak time during last 5 days of shifted LD	Summary
Canton S	13.5	-			0	
cry^{02}	13.5	0	-1.004 to 1.004	>0.9999	0.05	Entrained
Rh2+	12.7	0.8	-0.2041 to 1.804	0.1336	0.075	Entrained
Rh7+	13.1	0.4	-0.6041 to 1.404	0.6129	1.425	Not entrained

8 hr delay of the LD cycle in low light						
	Mean of evening peak time during last 5 days of shifted LD	Mean Difference	95% CI of difference	Adjusted P value	Variance of evening peak time during last 5 days of shifted LD	Summary
Canton S	20	-			0	
cry^{02}	19.8	0.2	-0.6599 to 1.060	0.8776	0.075	Entrained
Rh2+	6.3	-10.3	12.84 to 14.56	<0.0001	0.7	Not entrained
Rh7+	6.3	-10.3	12.84 to 14.56	<0.0001	0.325	Not entrained

8 hr delay of the LD cycle in high light						
	Mean of evening peak time during last 5 days of shifted LD	Mean Difference	95% CI of difference	Adjusted P value	Variance of evening peak time during last 5 days of shifted LD	Summary
Canton S	20	-			0	
cry^{02}	20.3	-0.3	-1.160 to 0.5599	0.6978	0.075	Entrained
Rh2+	2.8	-6.8	16.34 to 18.06	<0.0001	0.825	Not entrained
Rh7+	8.7	11.3	10.44 to 12.16	<0.0001	0.2	Not entrained

Table 1. Determination of the phase of evening activity in the different genotypes and comparison with wild-type flies. See Methods for phase determination and statistical analysis.

	OCG01	OCG02	OCG03	OCG04	OCG05	OCG06	OCG07	OCG008	OCG09
1	232513628	788055763	1127402256	757374944	1685029571	1164503211	1467111071	757374955	880780647
2	232513671	1498120574	5813045787	1158635682	5813065110	1375738477	1529527067	1219462308	911815444
3	233877926			1189027422			1590858381	1250885621	972603320
4	262167456			1220049442			1652530588	1281191190	1003655362
5	262504004						5813008755	1405313687	
6	262517074						5813038661	1405321852	
7	262840563							1653342390	
8	263199096							1745989723	
9	263522664							1746088555	
10	540462600							5812986100	
11	5813025982							5812986958	
12	5813062887							5812990520	
13								5813006657	
14								5813016856	
15								5813035196	

Table 2. OCG neurons identified in the hemibrain dataset. Based on the hemibrain annotations, OCG neurons have been classified into nine distinct types (OCG01-09) based on their morphology. The table contains the unique IDs assigned to each neuron.

Post synaptic partners of OCG04_1 (1158635682)		
Neuron ID	Type	Number of Synapses (% of total)
516055524	CL063	27 (2.35%)
5813021196	aMe17c	22 (1.92%)
5813078095	aMe17a	19 (1.66%)
1220049442	OCG04	14 (1.22%)
5813020750	SLP250	14 (1.22%)
1128235633	aMe17c	13 (1.13%)
1096894260	PLP070	12 (1.05%)
1129306180	PLP070	10 (0.87%)
1283406432	aMe2	9 (0.78%)
757374944	OCG04	9 (0.78%)
821340054	PLP091	9 (0.78%)
756502912	PLP080	8 (0.70%)
5812981460	aMe8	7 (0.61%)
1128274593	-	6 (0.52%)
702760942	CL157	6 (0.52%)
1004450322	PLP135	6 (0.52%)
1066511487	aMe8	6 (0.52%)
5813044385	PLP135	6 (0.52%)
1282097987	-	6 (0.52%)
1189027422	OCG04	6 (0.52%)

Post synaptic partners of OCG04_2 (1189017422)		
Neuron ID	Type	Number of Synapses (% of total)
516055524	CL063	26 (1.52%)
5812979048	aMe6a	24 (1.40%)
1345087352	PLP098	22 (1.28%)
1128235633	aMe17c	21 (1.23%)
5812981460	aMe8	16 (0.93%)
5813021943	aMe20	15 (0.88%)
1129306180	PLP070	15 (0.88%)
1096894260	PLP070	15 (0.88%)
5813021196	aMe17c	14 (0.82%)
5813078095	aMe17a	14 (0.82%)
1066511487	aMe8	13 (0.76%)
1591701396	-	13 (0.76%)
5813069337	CL103	12 (0.70%)
5813020750	SLP250	11 (0.64%)
1345493520	-	11 (0.64%)
821340054	PLP091	11 (0.64%)
1220049442	OCG04	10 (0.58%)
667271225	SMP428	10 (0.58%)
759632919	-	10 (0.58%)
1658885859	PLP098	10 (0.58%)

Post synaptic partners of OCG04_3 (1220049442)		
Neuron ID	Type	Number of Synapses (% of total)
5813021196	aMe17c	34 (2.32%)
516055524	CL063	26 (1.77%)
1128235633	aMe17c	24 (1.64%)
1345087352	PLP098	23 (1.57%)
5813078095	aMe17a	22 (1.50%)
5813020750	SLP250	19 (1.30%)
5812979048	aMe6a	16 (1.09%)
1284373356	-	15 (1.02%)
5812981460	aMe8	15 (1.02%)
1345493520	-	14 (0.95%)
1096894260	PLP070	13 (0.89%)
1066511487	aMe8	13 (0.89%)
821340054	PLP091	12 (0.82%)
1191402226	SAD070	12 (0.82%)
1378251040	PLP211	11 (0.75%)
5813078557	aMe13	10 (0.68%)
1189027422	OCG04	10 (0.68%)
1158635682	OCG04	10 (0.68%)
5813044385	PLP135	10 (0.68%)

Post synaptic partners of OCG04_4 (757374944)		
Neuron ID	Type	Number of Synapses (% of total)
516055524	CLO63	25 (3.18%)
5813078095	aMe17a	19 (2.42%)
756502912	PLP080	15 (1.91%)
5813020750	SLP250	10 (1.27%)
1158635682	OCG04	9 (1.15%)
1128274593	-	8 (1.02%)
1128235633	aMe17c	8 (1.02%)
389195896	SLP304	7 (0.89%)
5813021196	aMe17c	7 (0.89%)
1066511487	aMe8	7 (0.89%)
1096894260	PLP070	7 (0.89%)
821340054	PLP091	7 (0.89%)
1220049442	OCG04	6 (0.76%)
636594676	SMP200	6 (0.76%)
5813044385	PLP135	5 (0.64%)
1283406432	aMe2	5 (0.64%)
5812981460	aMe8	5 (0.64%)

Table 3. Strong postsynaptic partners of each OCG04 neuron. The postsynaptic partners are ranked based on the number of synapses they have with OCG, and their corresponding ID is provided.

References

Alejevski, Faredin, Alexandra Saint-Charles, Christine Michard-Vanhée, Béatrice Martin, Sonya Galant, Daniel Vasiliauskas, and François Rouyer. 2019. 'The HisCl1 Histamine Receptor Acts in Photoreceptors to Synchronize Drosophila Behavioral Rhythms with Light-Dark Cycles'. *Nature Communications* 10(1):252. doi: 10.1038/s41467-018-08116-7.

Aschoff, J. 1960. 'Exogenous and Endogenous Components in Circadian Rhythms'. *Cold Spring Harbor Symposia on Quantitative Biology* 25(0):11–28. doi: 10.1101/SQB.1960.025.01.004.

Behnia, Rudy, and Claude Desplan. 2015. 'Visual Circuits in Flies: Beginning to See the Whole Picture'. *Current Opinion in Neurobiology* 34:125–32. doi: 10.1016/j.conb.2015.03.010.

Berson, David M., Felice A. Dunn, and Motoharu Takao. 2002. 'Phototransduction by Retinal Ganglion Cells That Set the Circadian Clock'. *Science* 295(5557):1070–73. doi: 10.1126/science.1067262.

Blume, Christine, Corrado Garbazza, and Manuel Spitschan. 2019. 'Effects of Light on Human Circadian Rhythms, Sleep and Mood'. *Somnologie* 23(3):147–56. doi: 10.1007/s11818-019-00215-x.

Cook, Tiffany, Franck Pichaud, Remi Sonneville, Dmitri Papatsenko, and Claude Desplan. 2003. 'Distinction between Color Photoreceptor Cell Fates Is Controlled by Prospero in Drosophila'. *Developmental Cell* 4(6):853–64. doi: 10.1016/S1534-5807(03)00156-4.

Cusumano, Paola, André Klarsfeld, Elisabeth Chélot, Marie Picot, Benjamin Richier, and François Rouyer. 2009. 'PDF-Modulated Visual Inputs and Cryptochrome Define Diurnal Behavior in Drosophila'. *Nature Neuroscience* 12(11):1431–37. doi: 10.1038/nn.2429.

Damulewicz, Milena, Juan I. Ispizua, Maria F. Ceriani, and Elzbieta M. Pyza. 2020. 'Communication Among Photoreceptors and the Central Clock Affects Sleep Profile'. *Frontiers in Physiology* 11.

Dolezelova, Eva, David Dolezel, and Jeffrey C. Hall. 2007. 'Rhythm Defects Caused by Newly Engineered Null Mutations in Drosophila's Cryptochrome Gene'. *Genetics* 177(1):329–45. doi: 10.1534/genetics.107.076513.

Emery, Patrick, W. Venus So, Maki Kaneko, Jeffrey C. Hall, and Michael Rosbash. 1998. 'CRY, a Drosophila Clock and Light-Regulated Cryptochrome, Is a Major Contributor to Circadian Rhythm Resetting and Photosensitivity'. *Cell* 95(5):669–79. doi: 10.1016/S0092-8674(00)81637-2.

Emery, Patrick, Ralf Stanewsky, Charlotte Helfrich-Förster, Myai Emery-Le, Jeffrey C. Hall, and Michael Rosbash. 2000. 'Drosophila CRY Is a Deep Brain Circadian Photoreceptor'. *Neuron* 26(2):493–504. doi: 10.1016/S0896-6273(00)81181-2.

Feinberg, Evan H., Miri K. VanHoven, Andres Bendesky, George Wang, Richard D. Fetter, Kang Shen, and Cornelia I. Bargmann. 2008. 'GFP Reconstitution Across Synaptic Partners (GRASP) Defines Cell Contacts and Synapses in Living Nervous Systems'. *Neuron* 57(3):353–63. doi: 10.1016/j.neuron.2007.11.030.

Foster, Russell G., and Charlotte Helfrich-Forster. 2001. 'The Regulation of Circadian Clocks by Light in Fruitflies and Mice'. *Philosophical Transactions of the Royal Society of London. Series B: Biological Sciences* 356(1415):1779–89. doi: 10.1098/rstb.2001.0962.

Fu, Yingbin, Haining Zhong, Min-Hua H. Wang, Dong-Gen Luo, Hsi-Wen Liao, Hidetaka Maeda, Samer Hattar, Laura J. Frishman, and King-Wai Yau. 2005. 'Intrinsically Photosensitive Retinal Ganglion Cells Detect Light with a Vitamin A-Based Photopigment, Melanopsin'. *Proceedings of the National Academy of Sciences* 102(29):10339–44. doi: 10.1073/pnas.0501866102.

Gao, Shuying, Shin-ya Takemura, Chun-Yuan Ting, Songling Huang, Zhiyuan Lu, Haojiang Luan, Jens Rister, Andreas S. Thum, Meiluen Yang, Sung-Tae Hong, Jing W. Wang, Ward F. Odenwald, Benjamin H. White, Ian A. Meinertzhagen, and Chi-Hon Lee. 2008. 'The Neural Substrate of Spectral Preference in Drosophila'. *Neuron* 60(2):328–42. doi: 10.1016/j.neuron.2008.08.010.

Gengs, Chaoxian, Hung-Tat Leung, David R. Skingsley, Mladen I. Iovchev, Zhan Yin, Eugene P. Semenov, Martin G. Burg, Roger C. Hardie, and William L. Pak. 2002. 'The

Target of Drosophila Photoreceptor Synaptic Transmission Is a Histamine-Gated Chloride Channel Encoded Byort (HclA)*'. *Journal of Biological Chemistry* 277(44):42113–20. doi: 10.1074/jbc.M207133200.

Gisselmann, Günter, Hermann Pusch, Bernd T. Hovemann, and Hanns Hatt. 2002. 'Two CDNAs Coding for Histamine-Gated Ion Channels in D. Melanogaster'. *Nature Neuroscience* 5(1):11–12. doi: 10.1038/nn787.

Golombek, Diego A., and Ruth E. Rosenstein. 2010. 'Physiology of Circadian Entrainment'. *Physiological Reviews* 90(3):1063–1102. doi: 10.1152/physrev.00009.2009.

Grebler, Rudi, Christa Kistenpfennig, Dirk Rieger, Joachim Bentrop, Stephan Schneuwly, Pingkalai R. Senthilan, and Charlotte Helfrich-Förster. 2017. 'Drosophila Rhodopsin 7 Can Partially Replace the Structural Role of Rhodopsin 1, but Not Its Physiological Function'. *Journal of Comparative Physiology A* 203(8):649–59. doi: 10.1007/s00359-017-1182-8.

Grima, Brigitte, Elisabeth Chélot, Ruohan Xia, and François Rouyer. 2004. 'Morning and Evening Peaks of Activity Rely on Different Clock Neurons of the Drosophila Brain'. *Nature* 431(7010):869–73. doi: 10.1038/nature02935.

Hattar, S., H. W. Liao, M. Takao, D. M. Berson, and K. W. Yau. 2002. 'Melanopsin-Containing Retinal Ganglion Cells: Architecture, Projections, and Intrinsic Photosensitivity'. *Science (New York, N.Y.)* 295(5557):1065–70. doi: 10.1126/science.1069609.

Helfrich-Förster, Charlotte. 2020. 'Light Input Pathways to the Circadian Clock of Insects with an Emphasis on the Fruit Fly Drosophila Melanogaster'. *Journal of Comparative Physiology A* 206(2):259–72. doi: 10.1007/s00359-019-01379-5.

Helfrich-Förster, Charlotte, Tara Edwards, Kouji Yasuyama, Barbara Wisotzki, Stephan Schneuwly, Ralf Stanewsky, Ian A. Meinertzhagen, and Alois Hofbauer. 2002. 'The Extraretinal Eyelet of Drosophila: Development, Ultrastructure, and Putative Circadian Function'. *Journal of Neuroscience* 22(21):9255–66. doi: 10.1523/JNEUROSCI.22-21-09255.2002.

Helfrich-Förster, Charlotte, Christine Winter, Alois Hofbauer, Jeffrey C. Hall, and Ralf

Stanewsky. 2001. ‘The Circadian Clock of Fruit Flies Is Blind after Elimination of All Known Photoreceptors’. *Neuron* 30(1):249–61. doi: 10.1016/S0896-6273(01)00277-X.

Hermann-Luibl, Christiane, and Charlotte Helfrich-Förster. 2015. ‘Clock Network in Drosophila’. *Current Opinion in Insect Science* 7:65–70. doi: 10.1016/j.cois.2014.11.003.

Hofbauer, A., and E. Buchner. 1989. ‘Does Drosophila Have Seven Eyes?’ *Naturwissenschaften* 76(7):335–36. doi: 10.1007/BF00368438.

Hong, Sung-Tae, Sunhoe Bang, Donggi Paik, Jongkyun Kang, Seungyoon Hwang, Keunhye Jeon, Bumkoo Chun, Seogang Hyun, Youngseok Lee, and Jaeseob Kim. 2006. ‘Histamine and Its Receptors Modulate Temperature-Preference Behaviors in *Drosophila*’. *The Journal of Neuroscience* 26(27):7245–56. doi: 10.1523/JNEUROSCI.5426-05.2006.

Honkanen, Anna, Paulus Saari, Jouni Takalo, Kyösti Heimonen, and Matti Weckström. 2018. ‘The Role of Ocelli in Cockroach Optomotor Performance’. *Journal of Comparative Physiology A* 204(2):231–43. doi: 10.1007/s00359-017-1235-z.

Hu, Karin G., and William S. Stark. 1980. ‘The Roles OfDrosophila Ocelli and Compound Eyes in Phototaxis’. *Journal of Comparative Physiology* 135(1):85–95. doi: 10.1007/BF00660183.

Hung, Yu-Shan, and Michael R. Ibbotson. 2014. ‘Ocellar Structure and Neural Innervation in the Honeybee’. *Frontiers in Neuroanatomy* 8. doi: 10.3389/fnana.2014.00006.

Iovchev, Mladen, Plamen Kodrov, Adrian J. Wolstenholme, William L. Pak, and Eugene P. Semenov. 2002. ‘Altered Drug Resistance and Recovery from Paralysis in Drosophila Melanogaster with a Deficient Histamine-Gated Chloride Channel’. *Journal of Neurogenetics* 16(4):249–61. doi: 10.1080/01677060216293.

Kaneko, Maki, Charlotte Helfrich-Förster, and Jeffrey C. Hall. 1997. ‘Spatial and Temporal Expression of the *Period* and *Timeless* Genes in the Developing Nervous System of *Drosophila* : Newly Identified Pacemaker Candidates and Novel Features of Clock Gene Product Cycling’. *The Journal of Neuroscience* 17(17):6745–60. doi: 10.1523/JNEUROSCI.17-17-06745.1997.

Kistenpfennig, Christa, Rudi Grebler, Maite Ogueta, Christiane Hermann-Luibl, Matthias Schlichting, Ralf Stanewsky, Pingkalai R. Senthilan, and Charlotte Helfrich-Förster. 2017. 'A New Rhodopsin Influences Light-Dependent Daily Activity Patterns of Fruit Flies'. *Journal of Biological Rhythms* 32(5):406–22. doi: 10.1177/0748730417721826.

Kistenpfennig, Christa, Mayumi Nakayama, Ruri Nihara, Kenji Tomioka, Charlotte Helfrich-Förster, and Taishi Yoshii. 2018. 'A Tug-of-War between Cryptochrome and the Visual System Allows the Adaptation of Evening Activity to Long Photoperiods in Drosophila Melanogaster'. *Journal of Biological Rhythms* 33(1):24–34. doi: 10.1177/0748730417738612.

Klarsfeld, André, Sébastien Malpel, Christine Michard-Vanhée, Marie Picot, Elisabeth Chélot, and François Rouyer. 2004. 'Novel Features of Cryptochrome-Mediated Photoreception in the Brain Circadian Clock of Drosophila'. *Journal of Neuroscience* 24(6):1468–77. doi: 10.1523/JNEUROSCI.3661-03.2004.

Kleef, Joshua van, Richard Berry, and Gert Stange. 2008. 'Directional Selectivity in the Simple Eye of an Insect'. *Journal of Neuroscience* 28(11):2845–55. doi: 10.1523/JNEUROSCI.5556-07.2008.

Lazzari, Claudio R., Carolina E. Reiseman, and Teresita C. Insausti. 1998. 'The Role of the Ocelli in the Phototactic Behaviour of the Haematophagous Bug Triatoma Infestans'. *Journal of Insect Physiology* 44(12):1159–62. doi: 10.1016/S0022-1910(98)00080-8.

Li, Meng-Tong, Li-Hui Cao, Na Xiao, Min Tang, Bowen Deng, Tian Yang, Taishi Yoshii, and Dong-Gen Luo. 2018. 'Hub-Organized Parallel Circuits of Central Circadian Pacemaker Neurons for Visual Photoentrainment in Drosophila'. *Nature Communications* 9(1):4247. doi: 10.1038/s41467-018-06506-5.

Mizunami, Makoto. 1995. 'Functional Diversity of Neural Organization in Insect Ocellar Systems'. *Vision Research* 35(4):443–52. doi: 10.1016/0042-6989(94)00192-O.

Muraro, Nara I., and M. Fernanda Ceriani. 2015. 'Acetylcholine from Visual Circuits Modulates the Activity of Arousal Neurons in Drosophila'. *Journal of Neuroscience* 35(50):16315–27. doi: 10.1523/JNEUROSCI.1571-15.2015.

Ni, Jinfei D., Lisa S. Baik, Todd C. Holmes, and Craig Montell. 2017. 'A Rhodopsin in the

Brain Functions in Circadian Photoentrainment in Drosophila'. *Nature* 545(7654):340–44. doi: 10.1038/nature22325.

Ogueta, Maite, Roger C. Hardie, and Ralf Stanewsky. 2018. 'Non-Canonical Phototransduction Mediates Synchronization of the Drosophila Melanogaster Circadian Clock and Retinal Light Responses'. *Current Biology* 28(11):1725-1735.e3. doi: 10.1016/j.cub.2018.04.016.

O'Tousa, Joseph E., Wolfgang Baehr, Richard L. Martin, Jay Hirsh, William L. Pak, and Meredithe L. Applebury. 1985. 'The Drosophila NinaE Gene Encodes an Opsin'. *Cell* 40(4):839–50. doi: 10.1016/0092-8674(85)90343-5.

Parsons, Matthew M., Holger G. Krapp, and Simon B. Laughlin. 2006. 'A Motion-Sensitive Neurone Responds to Signals from the Two Visual Systems of the Blowfly, the Compound Eyes and Ocelli'. *Journal of Experimental Biology* 209(22):4464–74. doi: 10.1242/jeb.02560.

Pittendrigh, C. S. 1993. 'Temporal Organization: Reflections of a Darwinian Clock-Watcher'. *Annual Review of Physiology* 55(1):17–54. doi: 10.1146/annurev.ph.55.030193.000313.

Pollock, John A., and Seymour Benzer. 1988. 'Transcript Localization of Four Opsin Genes in the Three Visual Organs of Drosophila; RH2 Is Ocellus Specific'. *Nature* 333(6175):779–82. doi: 10.1038/333779a0.

Provencio, Ignacio, Guisen Jiang, Willem J. De Grip, William Pär Hayes, and Mark D. Rollag. 1998. 'Melanopsin: An Opsin in Melanophores, Brain, and Eye'. *Proceedings of the National Academy of Sciences* 95(1):340–45. doi: 10.1073/pnas.95.1.340.

Rieger, Dirk, Orie Thomas Shafer, Kenji Tomioka, and Charlotte Helfrich-Förster. 2006. 'Functional Analysis of Circadian Pacemaker Neurons in Drosophila Melanogaster'. *Journal of Neuroscience* 26(9):2531–43. doi: 10.1523/JNEUROSCI.1234-05.2006.

Rieger, Dirk, Ralf Stanewsky, and Charlotte Helfrich-Förster. 2003. 'Cryptochrome, Compound Eyes, Hofbauer-Buchner Eyelets, and Ocelli Play Different Roles in the Entrainment and Masking Pathway of the Locomotor Activity Rhythm in the Fruit Fly Drosophila Melanogaster'. *Journal of Biological Rhythms* 18(5):377–91. doi:

10.1177/0748730403256997.

Rister, Jens, Claude Desplan, and Daniel Vasiliauskas. 2013. 'Establishing and Maintaining Gene Expression Patterns: Insights from Sensory Receptor Patterning'. *Development* 140(3):493–503. doi: 10.1242/dev.079095.

Roenneberg, Till, Serge Daan, and Martha Merrow. 2003. 'The Art of Entrainment'. *Journal of Biological Rhythms* 18(3):183–94. doi: 10.1177/0748730403018003001.

Roenneberg, Till, and Russell G. Foster. 1997. 'Twilight Times: Light and the Circadian System'. *Photochemistry and Photobiology* 66(5):549–61. doi: 10.1111/j.1751-1097.1997.tb03188.x.

Sabat, Debabrat, Subhashree Priyadarsini, and Monalisa Mishra. 2017. 'Understanding the Structural and Developmental Aspect of Simple Eye of Drosophila: The Ocelli'. *Journal of Cell Signaling* 01(02). doi: 10.4172/2576-1471.1000109.

Saint-Charles, Alexandra, Christine Michard-Vanhée, Faredin Alejevski, Elisabeth Chélot, Antoine Boivin, and François Rouyer. 2016. 'Four of the Six Drosophila Rhodopsin-Expressing Photoreceptors Can Mediate Circadian Entrainment in Low Light'. *Journal of Comparative Neurology* 524(14):2828–44. doi: 10.1002/cne.23994.

Salcedo, Ernesto, Armin Huber, Stefan Henrich, Linda V. Chadwell, Wen-Hai Chou, Reinhard Paulsen, and Steven G. Britt. 1999. 'Blue- and Green-Absorbing Visual Pigments OfDrosophila: Ectopic Expression and Physiological Characterization of the R8 Photoreceptor Cell-Specific Rh5 and Rh6 Rhodopsins'. *Journal of Neuroscience* 19(24):10716–26. doi: 10.1523/JNEUROSCI.19-24-10716.1999.

Scheffer, Louis K., C. Shan Xu, Michal Januszewski, Zhiyuan Lu, Shin-ya Takemura, Kenneth J. Hayworth, Gary B. Huang, Kazunori Shinomiya, Jeremy Maitlin-Shepard, Stuart Berg, Jody Clements, Philip M. Hubbard, William T. Katz, Lowell Umayam, Ting Zhao, David Ackerman, Tim Blakely, John Bogovic, Tom Dolafi, Dagmar Kainmueller, Takashi Kawase, Khaled A. Khairy, Laramie Leavitt, Peter H. Li, Larry Lindsey, Nicole Neubarth, Donald J. Olbris, Hideo Otsuna, Eric T. Trautman, Masayoshi Ito, Alexander S. Bates, Jens Goldammer, Tanya Wolff, Robert Svirskas, Philipp Schlegel, Erika Neace, Christopher J. Knecht, Chelsea X. Alvarado, Dennis A. Bailey, Samantha Ballinger, Jolanta A. Borycz, Brandon S. Canino, Natasha Cheatham,

Michael Cook, Marisa Dreher, Octave Duclos, Bryon Eubanks, Kelli Fairbanks, Samantha Finley, Nora Forknall, Audrey Francis, Gary Patrick Hopkins, Emily M. Joyce, SungJin Kim, Nicole A. Kirk, Julie Kovalyak, Shirley A. Lauchie, Alanna Lohff, Charli Maldonado, Emily A. Manley, Sari McLin, Caroline Mooney, Miatta Ndama, Omotara Ogundeyi, Nneoma Okeoma, Christopher Ordish, Nicholas Padilla, Christopher M. Patrick, Tyler Paterson, Elliott E. Phillips, Emily M. Phillips, Neha Rampally, Caitlin Ribeiro, Madelaine K. Robertson, Jon Thomson Rymer, Sean M. Ryan, Megan Sammons, Anne K. Scott, Ashley L. Scott, Aya Shinomiya, Claire Smith, Kelsey Smith, Natalie L. Smith, Margaret A. Sobeski, Alia Suleiman, Jackie Swift, Satoko Takemura, Iris Talebi, Dorota Tarnogorska, Emily Tenshaw, Temour Tokhi, John J. Walsh, Tansy Yang, Jane Anne Horne, Feng Li, Ruchi Parekh, Patricia K. Rivlin, Vivek Jayaraman, Marta Costa, Gregory SXE Jefferis, Kei Ito, Stephan Saalfeld, Reed George, Ian A. Meinertzhagen, Gerald M. Rubin, Harald F. Hess, Viren Jain, and Stephen M. Plaza. 2020. 'A Connectome and Analysis of the Adult Drosophila Central Brain' edited by E. Marder, M. B. Eisen, J. Pipkin, and C. Q. Doe. *ELife* 9:e57443. doi: 10.7554/eLife.57443.

Schlichting, Matthias. 2020. 'Entrainment of the Drosophila Clock by the Visual System'. *Neuroscience Insights* 15:2633105520903708. doi: 10.1177/2633105520903708.

Schlichting, Matthias, Rudi Grebler, Nicolai Peschel, Taishi Yoshii, and Charlotte Helfrich-Förster. 2014. 'Moonlight Detection by Drosophila's Endogenous Clock Depends on Multiple Photopigments in the Compound Eyes'. *Journal of Biological Rhythms* 29(2):75–86. doi: 10.1177/0748730413520428.

Schlichting, Matthias, Pamela Menegazzi, Katharine R. Lelito, Zepeng Yao, Edgar Buhl, Elena Dalla Benetta, Andrew Bahle, Jennifer Denike, James John Hodge, Charlotte Helfrich-Förster, and Orie Thomas Shafer. 2016. 'A Neural Network Underlying Circadian Entrainment and Photoperiodic Adjustment of Sleep and Activity in Drosophila'. *Journal of Neuroscience* 36(35):9084–96. doi: 10.1523/JNEUROSCI.0992-16.2016.

Schlichting, Matthias, Patrick Weidner, Madelen Diaz, Pamela Menegazzi, Elena Dalla Benetta, Charlotte Helfrich-Förster, and Michael Rosbash. 2019. 'Light-Mediated Circuit Switching in the Drosophila Neuronal Clock Network'. *Current Biology: CB*

29(19):3266-3276.e3. doi: 10.1016/j.cub.2019.08.033.

Schubert, Frank K., Nicolas Hagedorn, Taishi Yoshii, Charlotte Helfrich-Förster, and Dirk Rieger. 2018. 'Neuroanatomical Details of the Lateral Neurons of Drosophila Melanogaster Support Their Functional Role in the Circadian System'. *Journal of Comparative Neurology* 526(7):1209–31. doi: 10.1002/cne.24406.

Senthilan, Pingkalai R., Rudi Grebler, Nils Reinhard, Dirk Rieger, and Charlotte Helfrich-Förster. 2019. 'Role of Rhodopsins as Circadian Photoreceptors in the Drosophila Melanogaster'. *Biology* 8(1):6. doi: 10.3390/biology8010006.

Shafer, Orie T., Gabrielle J. Gutierrez, Kimberly Li, Amber Mildenhall, Daphna Spira, Jonathan Marty, Aurel A. Lazar, and Maria de la Paz Fernandez. 2022. 'Connectomic Analysis of the Drosophila Lateral Neuron Clock Cells Reveals the Synaptic Basis of Functional Pacemaker Classes'. *ELife* 11:e79139. doi: 10.7554/eLife.79139.

Simmons, Peter J. 2002. 'Signal Processing in a Simple Visual System: The Locust Ocellar System and Its Synapses'. *Microscopy Research and Technique* 56(4):270–80. doi: 10.1002/jemt.10030.

Stanewsky, Ralf, Maki Kaneko, Patrick Emery, Bonnie Beretta, Karen Wager-Smith, Steve A. Kay, Michael Rosbash, and Jeffrey C. Hall. 1998. 'The Cryb Mutation Identifies Cryptochrome as a Circadian Photoreceptor in Drosophila'. *Cell* 95(5):681–92. doi: 10.1016/S0092-8674(00)81638-4.

Stark, William S., Randall Sapp, and Stanley D. Carlson. 1989. 'Ultrastructure of the Ocellar Visual System in Normal and Mutant Drosophila Melanogaster'. *Journal of Neurogenetics* 5(2):127–53. doi: 10.3109/01677068909066203.

Stoleru, Dan, Ying Peng, José Agosto, and Michael Rosbash. 2004. 'Coupled Oscillators Control Morning and Evening Locomotor Behaviour of Drosophila'. *Nature* 431(7010):862–68. doi: 10.1038/nature02926.

Talay, Mustafa, Ethan B. Richman, Nathaniel J. Snell, Griffin G. Hartmann, John D. Fisher, Altar Sorkaç, Juan F. Santoyo, Cambria Chou-Freed, Nived Nair, Mark Johnson, John R. Szymanski, and Gilad Barnea. 2017. 'Transsynaptic Mapping of Second-Order Taste Neurons in Flies by Trans-Tango'. *Neuron* 96(4):783-795.e4. doi:

10.1016/j.neuron.2017.10.011.

Taylor, Charles P. 1981. ‘Contribution of Compound Eyes and Ocelli to Steering of Locusts in Flight: I. Behavioural Analysis’. *Journal of Experimental Biology* 93(1):1–18. doi: 10.1242/jeb.93.1.1.

Ting, Chun-Yuan, Stephanie Gu, Sudha Guttikonda, Tzu-Yang Lin, Benjamin H. White, and Chi-Hon Lee. 2011. ‘Focusing Transgene Expression in Drosophila by Coupling Gal4 With a Novel Split-LexA Expression System’. *Genetics* 188(1):229–33. doi: 10.1534/genetics.110.126193.

Vasiliauskas, Daniel, Esteban O. Mazzoni, Simon G. Sprecher, Konstantin Brodetskiy, Robert J. Johnston, Preetmoninder Lidder, Nina Vogt, Arzu Celik, and Claude Desplan. 2011. ‘Feedback from Rhodopsin Controls Rhodopsin Exclusion in Drosophila Photoreceptors’. *Nature* 479(7371):108–12. doi: 10.1038/nature10451.

Wehrhahn, C., and Horace Basil Barlow. 1997. ‘Ocellar Vision and Orientation in Flies’. *Proceedings of the Royal Society of London. Series B. Biological Sciences* 222(1228):409–11. doi: 10.1098/rspb.1984.0073.

Wernet, Mathias F., Mariel M. Velez, Damon A. Clark, Franziska Baumann-Klausener, Julian R. Brown, Martha Klovstad, Thomas Labhart, and Thomas R. Clandinin. 2012. ‘Genetic Dissection Reveals Two Separate Retinal Substrates for Polarization Vision in Drosophila’. *Current Biology: CB* 22(1):12–20. doi: 10.1016/j.cub.2011.11.028.

Wheeler, David A., Melanie J. Hamblen-Coyle, Mitchell S. Dushay, and Jeffrey C. Hall. 1993. ‘Behavior in Light-Dark Cycles of Drosophila Mutants That Are Arrhythmic, Blind, or Both’. *Journal of Biological Rhythms* 8(1):67–94. doi: 10.1177/074873049300800106.

Witte, Ines, Hans-Juergen Kreienkamp, Michael Gewecke, and Thomas Roeder. 2002. ‘Putative Histamine-Gated Chloride Channel Subunits of the Insect Visual System and Thoracic Ganglion’. *Journal of Neurochemistry* 83(3):504–14. doi: 10.1046/j.1471-4159.2002.01076.x.

Yamaguchi, Satoko, Claude Desplan, and Martin Heisenberg. 2010. ‘Contribution of Photoreceptor Subtypes to Spectral Wavelength Preference in Drosophila’. *Proceedings*

of the National Academy of Sciences of the United States of America 107(12):5634–39. doi: 10.1073/pnas.0809398107.

Yoshii, Taishi, Christiane Hermann-Luibl, and Charlotte Helfrich-Förster. 2016. 'Circadian Light-Input Pathways in Drosophila'. *Communicative & Integrative Biology* 9(1):e1102805. doi: 10.1080/19420889.2015.1102805.

Zheng, Yingcong, Birgit Hirschberg, Jeffrey Yuan, Alice P. Wang, David C. Hunt, Steven W. Ludmerer, Dennis M. Schmatz, and Doris F. Cully. 2002. 'Identification of Two Novel Drosophila Melanogaster Histamine-Gated Chloride Channel Subunits Expressed in the Eye*'. *Journal of Biological Chemistry* 277(3):2000–2005. doi: 10.1074/jbc.M107635200.

ARTICLE 2

Non-cell autonomous CRY-dependent light responses in rest-activity rhythms of *Drosophila*

Ajay Sunilkumar[1#], Abhishek Chatterjee[1,a#], Elisabeth Chelot[1], François Rouyer[1*]

Affiliations:

1 Institut des Neurosciences Paris-Saclay, Université Paris-Saclay, CNRS, 91400 Saclay, France

Joint first authors

***Correspondence**: francois.rouyer@universite-paris-saclay.fr

[a] Present address: Institute of Ecology and Environmental Sciences of Paris, iEES-Paris, INRAE, Sorbonne Université, CNRS, IRD, UPEC, Université de Paris, 78026 Versailles, France

Introduction

Under standard laboratory conditions, *Drosophila melanogaster*, a crepuscular insect, displays a bimodal activity pattern principally regulated by the endogenous circadian clock. Accordingly, their activity profile consists of elevated activity during the morning (morning peak) and evening (evening peak), allowing them to anticipate dawn and dusk, respectively. *Drosophila* locomotor behavior is driven by the circadian clock located inside the fly brain (Chatterjee & Rouyer, 2016; Dubowy & Sehgal, 2017). A network of approximately 150 clock neurons incorporated in this circadian clock circuit house the rhythmically expressed pacemaker genes known as 'clock genes.' (Helfrich-Förster, 2003; Hermann-Luibl & Helfrich-Förster, 2015; Nitabach & Taghert, 2008) Several interlocked transcriptional-translational feedback loops in these clock neurons form the foundation for the molecular mechanism underlying circadian timekeeping. Transcription of transcriptional repressors, PERIOD and TIMELESS, by their activators CLOCK and CYCLE, constitutes the primary feedback loop in the *Drosophila* circadian system. After some post-translational modifications essential for their stability and function, PER and TIM protein levels peak in the cytoplasm towards the night's end. Later they enter the nucleus as a heterodimer to repress the activity of the CLOCK/CYCLE complex and thereby sustain the feedback regulation. This self-sustained loop provides the rhythmic expression of clock genes, enabling rhythmic outputs to various behavior and physiology (Dubowy & Sehgal, 2017; Hardin, 2011; Patke et al., 2020).

Tightly interconnected 75 clock neurons found in each hemisphere of the fly brain are commonly grouped into different clusters based on their cell body location and a key circadian signaling molecule they possess, known as Pigment Dispersing Factor (PDF). Four lateral groups consist of PDF expressing small ventral lateral neurons (s-LNv) and large ventral lateral neurons (l-LNv) along with PDF negative dorsal lateral neurons (LNd) and lateral posterior neurons (LPN). A fifth small ventral lateral neuron (5^{th} sLNv) which is PDF negative and of similar size to other sLNvs, also resides among other lateral neurons. DN1, DN2, and DN3 comprise the dorsal group of the clock neurons (Beckwith & Ceriani, 2015; Helfrich-Förster et al., 2007; Hermann-Luibl & Helfrich-Förster, 2015; Shafer et al., 2006). It is now well ascertained that these anatomically diverse clock neuron clusters function distinctly to regulate the fly's locomotor behavior, and a central theory prevailing in the field suggests a model where these independent but tightly coupled oscillators are accountable

for architecting the morning and evening bouts in *Drosophila's* bimodal activity profile. Several studies infer that a relevant morning oscillator resides in PDF positive s-LNvs and an evening oscillator in the PDF negative LNd group plus the 5th s-LNv, facilitating them to regulate morning and evening peaks (Grima et al., 2004; Stoleru et al., 2004). Subsequently, these oscillators or clock cell groups were termed morning oscillators or morning cells (LN^{MO} cells) and evening oscillators or evening cells (LN^{EO} cells), respectively. Lately, it has been shown that some subsets of dorsal neurons receive and send signals to lateral neurons to fine-tune locomotor behavior under particular environmental conditions, adding some intricacy to this dual oscillator model. Specifically, posterior DN1s (DN1ps) receive inputs from various sensory modalities, including light and temperature, and integrate this information to assist in synchronizing the fly's internal clock with the external environment (Chatterjee et al., 2018; L. Zhang et al., 2010; Y. Zhang et al., 2010). It is now evident that the M and E clocks are flexible entities composed of specific subsets of clock neurons that dynamically alter their predominance and contribution in response to environmental conditions (Dissel et al., 2014; Schlichting et al., 2019; Yao et al., 2016; Yao & Shafer, 2014).

The circadian system evolved primarily to help the organism adjust its behavior and physiology to changing environmental conditions (Golombek & Rosenstein, 2010; Pittendrigh, 1993; Roenneberg et al., 2003). The clock's characteristic ability to synchronize with such external cues is termed entrainment. Most living organisms have evolved multiple pathways for their circadian clocks to perceive important light information, as light is typically the most potent agent for resetting these clocks (Lucas et al., 2012; Millar, 2003; Yoshii et al., 2016). Only a brain clock entrained to light-dark cycles (photoentrainment), for example, can generate morning and evening peaks in phases with light ON-OFF and light OFF-ON transitions. Thus, the photic information, an important environmental cue (zeitgeber) of the outside world, must be incorporated into the fly's clock machinery located inside their brain for the accurate timing of circadian rhythms. In *Drosophila*, circadian photoreception is achieved by the photoreceptors present in their visual organs and clock neurons, mediating non-cell-autonomous and cell-autonomous light-input pathways (Helfrich-Förster, 2020; Helfrich-Förster et al., 2001; Rieger et al., 2003; Schlichting, 2020; Senthilan et al., 2019; Yoshii et al., 2016). The main source of cell-autonomous light-sensing in the clock circuit is mediated by CRYPTOCHROME (CRY), a blue light-sensitive circadian photoreceptor expressed in most clock neurons (fig. 1A) (Emery et al., 1998, 2000;

Klarsfeld et al., 2004; Stanewsky et al., 1998). CRY detects the light passing through the fly cuticle and directly resets the molecular clock to enable entrainment. Upon light exposure, CRY undergoes conformational changes leading to its binding with TIM. The CRY-TIM complex then promotes proteasomal degradation of TIM and CRY mediated by JETLAG (JET) containing E3 ubiquitin ligase. This CRY-mediated TIM degradation also leads to subsequent PER degradation as its stability is compromised, causing the clock to reset accurately (Busza et al., 2004; Dissel et al., 2004; Koh et al., 2006; Myers et al., 1996; Ozturk et al., 2011; Peschel et al., 2009; Zeng et al., 1996).

Like the visual system pathway, CRY-dependent light detection alone is sufficient to synchronize the sleep/wake cycles in *Drosophila*. However, when CRY is altered, acute TIM degradation and phase shifts in behavioral rhythms generated by brief light pulses are substantially affected (Dolezelova et al., 2007; Stanewsky et al., 1998). Over the years, CRY-dependent light-input pathway has been studied extensively to comprehend its molecular and cellular basis. In addition to CRY's canonical cell-autonomous light detection role, few studies have proposed a non-cell-autonomous mode of CRY action in *Drosophila* (Lamba et al., 2014; Tang et al., 2010; Yoshii et al., 2008). A coordinated interaction among different oscillators is inevitable for generating entrained outputs, and such non-autonomous aspects of the circadian network are also thought to be vital for proper photoentrainment of the circadian circuit. It's still unclear how the non-autonomous CRY pathway utilizes these flexible neuronal interactions in providing photic information to different oscillators. The present work intends to elucidate the molecular and neurological underpinnings of this pathway and the behavioral repercussions it influences, which are largely unknown. Here we uncover the surprising finding that even the CRY-positive neurons get updates about each other's CRY status, albeit not equivalently. Subsequently, our main emphasis was directed toward a particular route that entails the transfer of CRY signals from PDF^+ cells to various other subgroups. Through our investigation, we provided evidence highlighting the participation of PDF signaling and the dependence on the circadian clock in PDF cells for transmitting CRY-transduced photic information to remote oscillators. With some comprehensive behavioral studies, we further propose the possibility of a hitherto unknown JET-independent mechanism in CRY-mediated photoentrainment.

Results

Oscillators are coupled diversely to exchange CRY-dependent light information

Prior studies indicated that there exists a cross-talk between the clock neurons, deploying non-cell autonomous CRY-dependent light signals to promote TIM degradation in different oscillators. Eventually, these resetting cues synchronize the molecular feedback loop to the external light conditions. Here we assessed the interaction and mode of coupling between different oscillators in integrating non-cell-autonomous CRY information for molecular clock synchronization. To do so, we restricted CRY expression in a specific group of clock neurons and analyzed whether PER cycling in other clock neuronal groups is synchronized to LD cycles (at constant temperature) exclusively via non-cell-autonomous CRY action. In order to functionally isolate CRY-transduced light input to specific subsets of clock neurons, we restored CRY expression in these cells within a genotype that was impaired for both the visual system and CRY pathway, that is, *GMR-hid* cry^{02} double mutant. Our primary focus was on investigating three distinct clock clusters: (1) PDF-expressing clock neurons encompassing s-LNvs (LN^{MO}-oscillator) and l-LNvs, identified by *Pdf-GAL4* labeling (fig. 1B); (2) the 5^{th} s-LNv along with three CRY^{+} LNds (LN^{EO}-oscillator), labeled by *Mai179-GAL4 + Pdf-GAL80* (fig. 1B); and (3) the 6-7 DN1p neurons (possessing both M oscillator, DN^{MO} and E oscillator, DN^{EO}), labeled by *Clk4.1M-GAL4* (fig. 1B). To assess the interaction among these oscillator groups, we selectively restricted CRY expression in one of them and evaluated the entrainment of the molecular clock in the remaining groups to 12:12 hour LD cycles by quantifying PER expression at different time points. Consequently, this approach would enable us to gain further insights into the impact of non-cell-autonomous CRY action by elucidating (1) which clock neurons are capable of perceiving this CRY information from remote oscillators through neuronal communication, (2) which clock neurons could be the critical source of exporting such information and (3) ultimately, to achieve a comprehensive understanding about the functional connectivity among the mentioned clock groups in facilitating the transmission of CRY-dependent light signals for circadian entrainment.

In this study, we compared the intracellular levels of PER within whole mount brains of experimental flies to those of negative and positive control strains. The brains were dissected at two different time points, 12 hours apart, specifically at the end of the day phase

(ZT10) and night phase (ZT22). Our primary focus was assessing PER levels in specific clock neurons, namely s-LNv, l-LNv, 5th s-LNv, LNds, and DN1ps. We identified clock neurons either directly, such as s-LNv and l-LNv, by their expression of the neuropeptide PDF or by their position within the brain relative to the PDF^{+} LNv cell bodies and dorsal projections of the s-LNv (in the case of 5th s-LNv, LNd, and DN1ps). Since it is difficult to distinguish between CRY^{+} and CRY^{-} LNds based on their cell body position, we considered the 5th s-LNv as a proxy for CRY^{+} LNds, as the 5th s-LNv shares the same anatomical, functional, and connectomic characteristics with them.

All analyzed clock neurons from wild-type flies maintain robust and synchronized cycling in LD, displaying prominent PER labeling at ZT22 and less pronounced PER labeling at ZT10, which aligns with PER cycling (fig. 1C). In contrast, the negative control flies, *GMR-hid cry^{02}* double mutant, displayed disrupted PER levels without any discernible rhythm, exhibiting nearly equal expression levels at ZT22 and ZT10 (fig. 1C).

Remarkably, by confining CRY expression exclusively to PDF^{+} LNvs of *GMR-hid cry^{02}* flies, light-synchronized PER oscillation was reinstated in all examined subgroups (fig. 1C). Evidently, the entrainment of PDF^{+} LNvs stemmed from the cell-autonomous action of CRY, which provided ample light information. Additionally, the canonical CRY signaling within the LNv cells effectively informs (entrain) downstream oscillator nodes about the ambient light status to elicit synchronized molecular oscillations. Surprisingly, at both ZT10 and ZT22, there was significant PER labeling observed in three out of the six LNds. Considering that the 5th s-LNv exhibited synchronized PER cycling, peaking at ZT22 and reaching a minimum at ZT10, we inferred that the three CRY^{+} LNds represented the group displaying peak PER expression at ZT22 and reduced expression at ZT10. Consequently, the CRY^{-} LNds exhibited an atypical phase-reversed PER oscillation, peaking at ZT10. Hence, the non-cell-autonomous function of CRY originating from LNvs is adequate and capable of inducing wild-type PER oscillations in other neuronal subgroups like 5th s-LNv, CRY^{+} LNds, and DN1ps, as well as a phase-reversed oscillation specific to CRY^{-} LNds.

In the scenario of CRY rescue in 5th s-LNv and CRY^{+} LNds, along with this particular group, PDF-expressing s-LNvs and DN1ps maintained light-entrained PER oscillations (fig. 1C). However, in such flies, the synchronization of molecular oscillations to LD cycles was disrupted in PDF-positive l-LNvs. Furthermore, we observed that PER levels remained constant in three LNds at both time points, unlike the remaining three LNds, which peak at

ZT22 and trough at ZT10. Given the robust oscillation observed in 5th s-LNv and considering that the driver (*Mai179-GAL4 + Pdf-GAL80*) used for CRY rescue exclusively labeled CRY^{+} LNds, we deduced that CRY^{-} LNds exhibited arrhythmic PER expression. Conversely, CRY^{+} LNds displayed PER oscillation resembling that of wild-type flies, indicating the cell-autonomous role of CRY.

Subsequently, we examined the accumulation of PER in the clock neurons of flies where CRY expression was limited to a few DN1p cells. With the exception of DN1ps, all other neuronal groups within the clock network exhibited consistent PER expression levels at both ZT22 and ZT10, indicating the absence of non-cell-autonomous CRY-mediated light input to those cells (fig. 1C). Interestingly, we observed that the PER levels in l-LNv were not constant but rather displayed an anti-phasic pattern compared to wild-type flies. These findings indicate that the role of DN1p cells in providing non-autonomous CRY input to entrain other oscillator groups was limited.

Altogether, here we sought to uncover the network dynamics underlying the flow of CRY-dependent light information in the *Drosophila* brain clock. The findings from our study suggest that the non-autonomous role of CRY in synchronizing molecular clocks could play a crucial role in conveying information about ambient light conditions throughout the circadian neuronal network. Additionally, our results emphasize the presence of diverse coupling mechanisms between oscillators to exchange information regarding each other's CRY status. It became apparent that the transmission of CRY-dependent light information varied depending on the source of CRY information. This variability in coupling patterns implied that different oscillators had distinct ways of exchanging and integrating CRY-related photic updates.

Non-cell-autonomous CRY action can synchronize bimodal activity patterns to LD conditions.

Under standard 12:12 LD conditions, the locomotor profile of flies displays a bimodal pattern, which is regulated by the clock neuron network. *Drosophila* brain clock consists of multiple independent oscillators capable of having unique functions in orchestrating such activity patterns. Recent studies provide substantial evidence that this distributed multi-oscillator network system facilitates the integration of diverse light signals to enable the

plasticity of circadian behavior in response to various environmental conditions (Chatterjee et al., 2018; Lamba et al., 2018; L. Zhang et al., 2010; Y. Zhang et al., 2010). Following our discovery that these oscillators perceive CRY-mediated light signals through network interactions, our objective was to investigate whether clock neurons translate these light cues to elicit synchronized bimodal activity patterns. To this end, we utilized the previously mentioned flies, in which CRY was confined to specific clusters of clock neurons, and analyzed their rest-activity rhythms.

Consistent with previous findings, flies lacking both CRY and the visual system (*GMR-hid cry*^{02}) do not exhibit the characteristic bimodal activity pattern observed in wild-type flies (fig. 2A, B, C). These 'circadian blind' flies fail to display an M anticipation peak around lights ON and an E anticipation peak around lights OFF. However, rescuing CRY expression in PDF^{+} cells, which is known to encompass an M oscillator in s-LNv neurons (LN^{MO}), wholly restored a synchronized E peak in addition to the M peak (fig. 2A, B, C). Despite the sole source of light signals to the clock network being the CRY-mediated input to LN^{MO} cells, distant E cells (either LN^{EO} or DN1p^{EO}) were able to retrieve light information through non-autonomous CRY photoreception, enabling them to generate properly phased evening behavior.

Interestingly, when CRY was solely expressed in the 5th s-LNv and three CRY^{+} LNds (LN^{EO}), the evening anticipation persisted while the morning peak remained notably absent (fig. 2A, B, C). This observation was intriguing as we had previously discovered that the PER levels in these flies' s-LNv (LN^{MO}) and DN1p (containing DN1p^{MO}) were synchronized with the external LD cycle. Thus, despite the molecular oscillation of LN^{MO} and DN1p^{MO} being synchronized through non-autonomous CRY inputs originating from LN^{EO} cells, it failed to induce synchronized morning anticipation behavior.

Confining the CRY function only in DN1ps (comprising both DN^{MO} and DN^{EO}) generated synchronized M and E peaks (fig. 2A, B, C). This could possibly be via cell-autonomous CRY-mediated entrainment of DN^{MO} and DN^{EO}, as these flies had an entrained PER expression only in DN1ps but not in other clock clusters. Based on our findings, it becomes apparent that only the non-autonomous effect of CRY originating from PDF^{+} cells (containing LN^{MO}) could sufficiently fine-tune the locomotor activity profiles, even when confronted with varying photoperiods and light intensities (Supplementary fig. 1, 2, 3). At the same time, other assayed non-autonomous CRY signaling, such as input from LN^{EO} to

LN^{MO} and DN^{MO}, proved inadequate in eliciting entrained behavioral outputs across different conditions.

Circadian photoresponses mediated by non-autonomous CRY signaling from PDF^+ cells

In order to further investigate the circadian photoresponses triggered by non-autonomous CRY signaling, our attention was directed toward a specific pathway involving the transmission of CRY signals from PDF^+ cells to other subgroups. CRY resets the molecular clock cell autonomously by triggering the light-induced degradation of TIM. Consequently, even a brief light pulse at night can promptly degrade TIM, resetting the clock and causing phase shifts in behaviour (Dolezelova et al., 2007; F.-J. Lin et al., 2001; Stanewsky et al., 1998). Such circadian photoresponses are abolished in the absence of CRY. Here, we sought to examine whether non-autonomous CRY inputs could elicit a comparable rapid degradation of TIM in effector clock neurons when exposed to brief light pulses.

When a short light pulse of 10-minute duration was given to flies at ZT15 in which CRY expression was confined only to PDF^+ LNvs, we observed a significant TIM degradation in 5^{th} s-LNv, PDF^- CRY^+ LNds and DN1ps besides PDF^+ cells (fig. 3A, B). This finding indicates that akin to cell-autonomous light input, non-autonomous CRY signals can also induce rapid TIM degradation in response to short light pulses. These results suggest a robust and rapid transmission of CRY information across oscillators. Therefore, CRY could non-autonomously regulate photic TIM degradation in 5^{th} s-LNvs, LNds, and DN1ps. Moreover, the data provide substantial evidence for the existence of the transfer of CRY-dependent light information, even among CRY-expressing neurons.

Subsequently, we examined the impact of this non-autonomous pathway on behavioral phase shifts resulting from clock resetting. It's to be noted that our analysis focused on light-induced shifts in the peak phase of the subjective evening activity. In wild-type flies, the phase-shifting response to light is most pronounced during the subjective night, where a short light pulse early in the night causes phase delays, and a light pulse later in the night drives phase advances. As expected, cry^{02} flies, lacking functional CRY, exhibited no behavioral phase shifts when subjected to a 10-minute light pulse at early (ZT15) and late (ZT21) night (fig. 3C, D). Conversely, *GMR-hid* flies with genetically impaired visual

systems displayed robust phase shifts in response to light pulses at ZT15 and ZT21 (fig. 3C, D). Interestingly, when CRY expression was explicitly confined to PDF^+ LNvs, we observed similar phase advances and delays in the evening peak, emphasizing the significance of the non-autonomous CRY pathway (fig. 3C, D). Therefore, the CRY-dependent photic signals relayed to an E oscillator (either LN^{EO} or DN^{EO}) from LN^{MO} were adequate to reset its molecular clock and trigger corresponding behavioral phase shifts.

CRY in either s-LNv or l-LNv alone is sufficient for synchronizing E oscillators

Next, we were interested in identifying the source of non-cell autonomous CRY input responsible for synchronizing E cells. While we already established that PDF^+ neurons transmit CRY information to E neurons, it remains uncertain whether this communication originates from the large cluster (l-LNv) or the small cluster (s-LNv) within the PDF-expressing cells. To address this question, we selectively restricted CRY expression to the mentioned subgroups individually and evaluated whether the evening bout of activity became synchronized with LD conditions by analyzing daily activity patterns (fig. 4A).

Examination of the locomotor activities of flies revealed that CRY expression exclusively in either s-LNv cells using *ss00681 split-GAL4* or l-LNvs with *R78G01-GAL4* generated synchronized evening anticipation behavior at dusk (fig. 4B, C). Hence, E oscillators within the clock network can extract relevant light information from non-autonomous CRY activity supplied by both the PDF^+ neuronal groups, s-LNvs, and l-LNvs.

PDF signaling is necessary to export the non-autonomous CRY information from PDF^+ LNvs to E-oscillators

Following that, we investigated how these photic signals are exported from LNvs to other classes of clock neurons. In order to gain insights into the neural interactions facilitating this circadian light input pathway, we investigated the involvement of potential mediators in conveying CRY signals between different neuronal groups. PDF is the main neuropeptide expressed in LNvs, assuming a pivotal role as a signaling molecule for preserving coordination within the circadian network and regulating behavioral activity

(Cusumano et al., 2009; Liang et al., 2017; Y. Lin et al., 2004; Renn et al., 1999). Consequently, PDF emerged as the primary candidate for transmitting photic information associated with CRY from LNvs. Furthermore, prior research has established that LNvs modulate the phase and period of remote oscillators through coupling mechanisms reliant on PDF (Im et al., 2011; Yao & Shafer, 2014). Also, the receptor for PDF (PDFR) exhibited widespread expression in various neuronal groups, such as the 5^{th} s-LNv, CRY^{+} LNds, and half of DN1ps (Im & Taghert, 2010).

We, therefore, analyzed the locomotor activity of flies that relied solely on CRY-dependent photoreception in PDF^{+} cells as their light input while simultaneously disabling their PDF receptor signaling using the *han*^{5304} mutant strain. Under normal LD conditions, these flies show a reduced M anticipation as expected, which recapitulates the *han*^{5304} phenotype. In addition to this, they also failed to produce an evening behavior confirming the requirement of PDFR signaling in E oscillators to utilize this photoreception pathway (fig. 5A, B). In addition to this, we also examined the behavior of flies in which CRY was present only in PDF^{+} LNvs and where a functional PDF neuropeptide was also absent. Similar to the previously mentioned genotype, these flies also displayed a phenotype characterized by the absence of anticipatory behaviors at dawn and dusk (fig. 5A, B). Collectively, these findings indicate the involvement of PDF, a vital circadian neuropeptide enabling communication among clock neurons, in exporting CRY-dependent light information from PDF^{+} morning cells to PDF^{-} evening cells.

Transmission of non-autonomous CRY signals is clock-dependent

Previous studies have revealed that PDF-modulated visual inputs can facilitate the synchronization of LN^{EO} to LD cycles (Cusumano et al., 2009). However, such PDF-dependent phasing of the evening oscillator in LNs (LN^{EO}) is independent of a functional clock in PDF^{+} neurons. In light of our discovery that E oscillators integrate external CRY signals transmitted through PDF, we aimed to determine whether a functional clock in PDF cells is necessary, contrary to the propagation of visual light information within the clock network.

To do so, in addition to the CRY rescue in LNv of *GMR-hid cry*^{02} flies, we also abolished the functional circadian clock in these oscillators by utilizing two approaches: (1)

by expressing *UAS-cyc*^{DN} under *Pdf-GAL4* and (2) by the aid of tissue-specific TIM knockout in PDF cells by CRISPR technique. Both strategies yielded comparable results where we observed that when the clock was absent in s-LNv and l-LNv, they failed to drive morning and evening bouts of activity in LD cycles (fig. 6A, B). These findings strongly suggest that a functional clock in PDF^{+} neurons is indispensable for them to send the non-autonomous CRY information to E-cells. Moreover, we provide evidence that when the light input to the clock network is restricted to CRY expression in PDF cells only, the LNv clock can establish the phase of the E oscillators. Our observations revealed that accelerating the molecular oscillator in s-LNv and l-LNv of flies with CRY limited to PDF neurons led to an advancement of the evening behavior phase (fig. 6A, B). Thus, in the absence of other light inputs, l-LNv exerted control over the phase of a remote E oscillator through non-autonomous CRY signaling. Taken together, the inter-oscillator CRY pathway described here is a clock-dependent mechanism.

Canonical CRY-JET pathway does not seem to be necessary for the non-cell-autonomous CRY action in LD entrainment

Based on our current findings, it is evident that CRY-mediated photic resetting of the *Drosophila* brain clock also relies strongly on network interactions. Nevertheless, a more substantial and vital input from CRY signaling is facilitated through a cell-autonomous mechanism. CRY, expressed in half of the clock neurons, translates photic signals to the internal clock machinery by initiating light-dependent degradation of TIM (Emery et al., 1998; F.-J. Lin et al., 2001; Stanewsky et al., 1998; Yoshii et al., 2008). The CRY-mediated TIM degradation and the resulting circadian behavioral responses to brief light pulses are entirely mediated via JETLAG (JET), as the absence of the JET function eliminates the cell-autonomous CRY photoreception (Koh et al., 2006; Lamba et al., 2014; Peschel et al., 2009).

To investigate the role of JET in the entrainment of bimodal activity patterns via the non-cell-autonomous CRY pathway, we employed a severe JET mutant that induces impairments in CRY-dependent molecular and behavioral responses to brief light pulses. In *jet*^{set} *GMR-Hid cry*^{02} background, we rescued the CRY function in LNvs and analyzed their locomotion in LD conditions. Remarkably, these flies exhibited a synchronized bimodal activity pattern with a properly phased E peak (fig. 7A, B). Hence, the non-autonomous

CRY signal's ability to synchronize the E oscillator remained unaffected by the absence of functional JET, thereby supporting the possibility that the non-cell autonomous CRY-mediated light input pathway operates independently of the canonical CRY-JET pathway for LD entrainment.

Discussion

Within the *Drosophila* sensory system, several photopigments transduce light signals, which can entrain the molecular oscillations vital for accurate circadian timekeeping. This photic resetting, in turn, ensures the stability and coordination of various behavioral and physiological rhythms controlled by the clock, which are crucial for the organism's survival. *Drosophila* brain clock, consisting of 150 clock neurons, integrates light signals both cell-autonomously and non-cell autonomously. About one-quarter of these neurons express CRY, a circadian photoreceptor that serves as the exclusive pathway for cell-autonomous circadian photoreception in *Drosophila*. Nevertheless, some earlier studies have suggested that CRY might also contribute to non-autonomous light detection. Studies have revealed that CRY-mediated rapid degradation of TIM protein occurs in CRY-positive and CRY-negative neurons as well, indicating the non-autonomous role of CRY (Yoshii et al., 2008). Additional evidence supporting the exchange of CRY information between clock neurons was provided by the discovery that the expression of JET in PDF neurons can trigger acute TIM degradation in LNds upon a brief 5-minute light pulse (Lamba et al., 2014). Thus, in addition to intracellularly transmitting ambient light information to clock machinery, CRY can supply light signals through intercellular communication.

Recent findings in *Drosophila* propose brain clock as a diversely coupled multi-oscillator network, influencing each other's clock machinery through peptidergic and synaptic signaling (Ahmad et al., 2021; Crespo-Flores & Barber, 2022). Despite their differing cellular identities and functional roles, these oscillators operate synchronously through network interactions to produce coherent rhythms. Additionally, few studies have highlighted the importance of neural interactions among clock neurons in transmitting photic signals (both CRY and visual inputs) for clock resetting (Cusumano et al., 2009; Lamba et al., 2014, 2018). Typical CRY-mediated circadian photoresponses like behavioral phase delays or advances in responses to light pulses at subjective night rely heavily on network-wide interactions. For instance, the *Drosophila* clock network elicits light-induced phase shifts in locomotor rhythms by employing distinct neuronal groups (Shang et al., 2008; Tang et al., 2010). Specifically, DN1s are associated with phase delays, while l-LNvs are linked to phase advances. Additionally, M and E oscillators residing in lateral neurons have been identified to operate in synergy to induce light-induced behavioral phase shifts (Lamba et al., 2014). Altogether it has been widely acknowledged that the neural interactions

underlying the non-cell-autonomous CRY action are vital for resetting the clock in response to short light exposure.

But how non-autonomous CRY signals are integrated across the circadian neuronal network to facilitate photoentrainment of the brain clock is largely unknown. To shed light on this light input pathway, our study sought to tackle a series of important inquiries. These included investigating the circuit logic governing the transmission of CRY-dependent light information in the circadian neural network, identifying the specific subgroup of clock neurons that utilize this pathway for extracting relevant light information, examining whether there is a hierarchical or distributed organization within the clock network to facilitate this process, exploring the potential for CRY^{+} neurons to also serve as recipients of such signals, in addition to their role as facilitators and finally uncovering the molecular and neural basis underlying this pathway. To address these questions, we utilized CRY rescue strategies in targeted clock neurons of circadian blind flies and examined their circadian photoresponses. In this way, we gained an understanding of how light perceived by specific oscillators not only affects the molecular clock synchronization of distant oscillators but also influences their behavioral outputs. While prior studies have primarily investigated the behavioral and molecular effects of the non-autonomous CRY pathway in response to brief light exposure, our focus lies on examining the significance of this input during longer exposures, such as regular LD cycles.

Network flow of CRY information

The findings from our study implied that the non-autonomous role of CRY could play a crucial role in conveying ambient light status throughout the circadian neuronal network. We present evidence that the different oscillators engage in the exchange of CRY-transduced light information, effectively impacting the photosensitivity of their clockwork. Importantly, this inter-oscillator CRY pathway exhibits considerable robustness, enabling it to independently synchronize numerous oscillators within the brain clock to the external LD cycles.

We find here that the sharing of CRY signals in the circadian neural network exhibits a distributed flow rather than a hierarchical one. Furthermore, we reveal an interesting finding that even the CRY-expressing neurons exchange CRY-dependent photic signals for light

sensing. CRY expressing 5th s-LNv and LNds, along with DN1ps, display robust and synchronized PER oscillations in response to external LD conditions by sensing light signals transmitted by CRY in PDF neurons (s-LNv + l-LNv). This indicates a strong coupling between PDF-negative and positive neurons for CRY-dependent clock synchronization. Intriguingly, CRY-negative LNd neurons displayed PER oscillations, albeit in a reversed-phase, in response to CRY inputs from PDF neurons. This could imply that different mechanisms may be involved in the integration of non-autonomous CRY signals. This could be linked to the fact that CRY-negative and CRY-positive LNds differ drastically in their neurochemical composition, including differential receptivity to PDF. PDF is necessary to transmit behaviorally relevant CRY signals from LNvs to CRY-positive LNds. Given that CRY-negative LNds lack PDF receptors, they need to employ an alternative neural transmission mechanism to receive CRY input from PDF cells, either directly or indirectly. This might potentially lead to the phase reversal of their PER oscillations in the absence of CRY in PDFR-expressing cells. A related mechanism has been postulated for the integration of visual inputs in LN^{EO} (CRY-expressing LNds and 5th s-LNv). Previous studies conducted in our laboratory have demonstrated the necessity of PDF receptor function in LN^{EO} for achieving proper phase alignment when entrained by the visual system only (Cusumano et al., 2009).

When CRY activity was confined to LN^{EO}, both LN^{MO} and DN1ps (DN^{MO} + DN^{EO}) exhibited entrainment to LD cycles. However, l-LNv and CRY-negative LNds did not synchronize their PER oscillations, indicating their insensitivity to non-autonomous CRY input provided by LN^{EO}. Furthermore, our findings reveal that the DN1p cluster was unable to drive molecular synchronization of other subgroups through non-autonomous CRY action. Dorsal neurons, in this regard, exhibited characteristics akin to a limited group positioned at the receiving end of the CRY network flow within the circadian circuit. Hence, the transmission and integration of CRY-dependent light information appeared to vary depending on both the source and destination of this pathway. Further studies should be carried out to infer whether these coupling mechanisms are modulated under varying external conditions, such as different photoperiods. To sum up, oscillators with diverse coupling patterns, known for influencing the clockwork of other oscillators, such as molecular rhythms and neural output, show similar intricate interactions in encoding network-mediated CRY signals.

Entrainment of locomotor activities through non-cell autonomous CRY pathway

To achieve properly phased M and E peaks under regular LD cycles, both the morning (M) and evening (E) oscillators need to be well-entrained. Our findings reveal that LN^{MO} holds a higher hierarchical position in the network when it comes to entraining locomotor activities through the non-cell autonomous CRY pathway. LN^{MO} can transmit sufficient CRY-related photic information to downstream E oscillator nodes, leading to a synchronized E peak while also autonomously entraining the M peak. The E oscillator responsible for generating the E peak in these flies could be located either in LN^{EO}, DN^{EO}, or possibly a combination of both through some unknown mechanisms. Surprisingly, when CRY expression was limited to LN^{EO}, it failed to generate M peaks through non-autonomous action. This result was intriguing, considering our previous findings that showed s-LNvs (containing LN^{MO}) and DN1ps (containing DN^{MO}) could synchronize their molecular oscillation through the non-autonomous CRY signals from LN^{EO}. Despite CRY in LN^{EO} influencing the molecular clock of M cells, it surprisingly does not translate into the behavioral output. It was conceivable that the absence of an M peak could result from the masking effect caused by lights ON, which might overshadow a less prominent peak. However, even in short photoperiods and during the initial days of DD (constant darkness), the M peak of these flies remained elusive and was not observable. Flies with PER expression restricted to PDF cells produce morning activity (Grima et al., 2004; Stoleru et al., 2004), even in the absence of either CRY or the visual system (Cusumano et al., 2009). However, altered PER oscillations in other clock neurons might affect their behavioral output. Alternatively, visual input and CRY in the PDF cells might be required for the morning anticipation.

The restricted CRY expression in a small subset of DN1ps using *Clk4.1M-GAL4* did not synchronize the molecular clockwork of M and E oscillators residing in lateral neurons (LN^{MO} and LN^{EO}), as shown earlier. Nevertheless, it was discovered that CRY in these DN1ps could still generate entrained M and E peaks in response to external LD cycles. The CRY-mediated cell autonomous entrainment of M and E oscillators within the DN1p group (DN^{MO} and DN^{EO}) could potentially facilitate this. Together, these findings strongly suggest that PDF^{+} neurons are the most critical group in the *Drosophila* circadian network that can transmit non-autonomous CRY signals to distant oscillators, leading to network-wide synchronization of the molecular clock and entrained behaviors in normal day-night cycles.

The bimodal activity patterns of flies are finely regulated by the non-autonomous effect of CRY originating from PDF^+ cells containing LN^{MO}, synchronizing both M and E oscillators. On the other hand, CRY actions arising from other oscillator groups, such as LN^{EO}, cannot induce entrained output from their counterpart oscillators like LN^{MO}, although LN^{EO} can influence the photosensitivity of LN^{MO}'s clockwork. Additionally, in the case of dorsal neurons, they lack the capability to transmit CRY signals to other critical pacemakers (LN^{MO} and LN^{EO}), resulting in the inability to synchronize both their molecular clock and output behavior.

Non-cell autonomous CRY signaling from PDF neurons

Our work revealed that non-autonomous CRY signaling from a specific cluster, namely PDF^+ neurons, can induce both behavioral phase shifts and network-wide acute TIM degradation in response to a short light pulse. Hence, the non-autonomous light reception by CRY emerges as a significant pathway through which light information can be disseminated across the neural network of the brain clock.

Prior research has demonstrated the collaborative function of M and E oscillators in the lateral neuron group, working together to reset circadian locomotor behavior in response to light (Lamba et al., 2014). Furthermore, it has been observed that resetting circadian behavior in response to light input relies on neural interactions, with various oscillators engaging depending on the timing of light exposure during the night (Shang et al., 2008; Tang et al., 2010). Our findings corroborate this idea, as we discovered that CRY in LN^{MO} alone could drive both phase delays and advances. This occurred through two mechanisms: firstly, by autonomously transducing light signals within the cells, and secondly, by exporting these signals to distant oscillators (like E cells) through neuronal communication.

A swift transfer of signals between oscillators facilitates the spread of CRY information within the network. This was evidenced by our observation of light-induced TIM degradation occurring just 1 hour after administering the light pulse. Subsequent experiments provided additional insights, indicating that PDF serves as the signaling molecule utilized by PDF^+ neurons to export CRY information. E oscillators in both lateral and dorsal groups express receptors for PDF and are known to establish functional connections with LN^{MO} through PDF-mediated coupling (Im & Taghert, 2010; Yao &

Shafer, 2014). Our study, too, demonstrated the critical importance of functional PDF receptors (PDFR) in enabling M cell-originated CRY signals to effectively synchronize the E oscillator.

Numerous studies have indicated a strong correlation between PDF and light input, highlighting the essential role of PDF in the circadian light input pathways(Ahmad et al., 2021; Cusumano et al., 2009; Guo et al., 2014; Lamba et al., 2018). CRY, and PDF/PDFR signaling pathways converge at E cells to influence their molecular oscillations and behavioral outputs (Im et al., 2011). Previous work by Liang et al. has shown that light inputs and PDF/PDFR signaling determine the appropriate phase of LNd Ca^{2+} rhythms (Liang et al., 2017). However, in all these cases, it remains uncertain whether the light signals perceived by LNds are entirely transmitted directly via visual and CRY inputs or involve some form of inter-oscillator interactions. Based on our findings, it appears that aside from cell-autonomous light detection, E oscillators acquire substantial CRY-dependent light signals from LN^{MO} through PDF input. Consequently, the process of CRY input in E cells is not solely dependent on the spatial convergence of PDF and CRY signaling within these cells; instead, it additionally involves a multiplexed light input signal that has undergone synergism at the PDF^{+} neurons.

Likewise, PDF signaling between LN^{MO} and LN^{EO} was identified as being engaged in the integration of visual inputs by LN^{EO}. When CRY is absent, the proper functioning of PDF signaling in LN^{EO} becomes crucial for generating evening behavior and establishing entrained PER oscillations. Notably, this PDF-mediated processing of visual inputs in LN^{EO} is independent of a functional molecular clock in LN^{MO} (Cusumano et al., 2009). The present work indicates the necessity of a functional clock in PDF cells to transfer non-cell autonomous CRY inputs to E oscillators. Hence, E cells employ diverse PDF signaling mechanisms (clock-dependent and clock-independent) to gather light information from their reliable neighboring LN^{MO} and entrain themselves. Collectively, this further underscores the function of PDF as a multifaceted facilitator and coordinator of circadian light input pathways (visual and CRY) as well as neural network signaling.

It has been proposed that under LD cycles, LN^{EO} cells play a pivotal role in generating circadian and locomotor activities. Meanwhile, LN^{MO} cells primarily function to integrate light information and modulate the phase of E-cell oscillations and behavioral rhythms. Prior works show that LN^{MO} cells could achieve this by initiating neural firing, which leads to the

release of PDF. Subsequently, this PDF release acts on downstream LN^{EO} cells, promoting the degradation of TIM via a mechanism that is independent of CRY-mediated protein degradation. The ubiquitin ligase CUL-3 is implicated in mediating TIM degradation in LN^{EO} cells in response to the firing-induced PDF signaling, ultimately leading to molecular and behavioral phase shifts (Guo et al., 2014). We checked whether a similar CUL3-dependent mechanism mediates non-cell-autonomous CRY action. Results obtained indicate that even in the absence of CUL-3, non-cell autonomous CRY signals from PDF cells could entrain the E oscillator and generate evening behavior.

Given that the interaction between light and CRY prompts neural firing in PDF cells, we conducted an investigation to determine whether electrophysiological light responses mediated by CRY contribute to inter-oscillator CRY communication (Fogle et al., 2011; Foley & Emery, 2020). Up until now, two distinct pathways have been put forth to explain how CRY regulates neuronal activity. In one of these pathways, CRY triggers a series of redox reactions that lead to the activation of Hyperkinetics (HK), a regulatory subunit of potassium channels. This activation, in turn, affects HK/EAG and HK/ERG channels, resulting in the depolarization of the clock neuron's membrane potential and an increase in firing activity (Fogle et al., 2011, 2015). The other pathway involves CRY-mediated activation of Quasimodo (Qsm), a membrane-anchored protein, which then acts on Shaw and NKCC to alter clock neuron activity in response to light (Buhl et al., 2016; Chen et al., 2011). Interestingly, Qsm's presence in CRY-negative clock neurons suggests its involvement in non-cell autonomous CRY action. Flies that lacked functional HK, EAG, Qsm, NKCC, and Shaw proteins were still able to exhibit synchronized locomotor behaviors under LD cycles by utilizing non-cell autonomous CRY-dependent photic input (Supplementary fig. 4). Thus, by introducing mutations or reducing the expression of membrane proteins like HK, Qsm, NKCC, and Shaw, we demonstrate that the CRY-mediated light-dependent changes in the firing rate of clock neurons are not involved in the distribution of CRY signals across the clock network.

JET-independent CRY-mediated photoreception

CRY-mediated circadian photoreception targets TIM to reset the molecular clock. When exposed to light, photoactivated CRY engages JET, an E3 ligase, leading to the ubiquitination and subsequent proteasomal degradation of TIM (Koh et al., 2006). This

straightforward model of autonomous CRY-dependent light input operates via the mediation of JET. This is evident from the fact that mutations in the *jet* gene lead to impaired photoresponses, characterized by the absence of behavioral phase shifts and rapid TIM degradation in response to light pulses (Lamba et al., 2014). Our findings suggest that the canonical CRY-JET pathway might not be implicated in the non-cell-autonomous effects of CRY in LD entrainment. The non-cell-autonomous pathway remained unaffected even with a significant loss of function of JET (jet^{set}), which essentially abolishes intra-oscillator CRY function. This observation supports the notion of a JET-independent action of CRY. This discovery is surprising as a JET-independent pathway for conveying CRY-mediated light signals to clock neurons has not been previously identified. However, our analysis of the entrainment of *Drosophila* diurnal behavior under LD cycles suggests the presence of an unknown JET-independent mechanism involved in the light entrainment of circadian rhythms by CRY.

This outcome came as a surprise, given that previous research has implied that JET functions cell-autonomously to promote TIM degradation in LN^{MO}- and LN^{EO}, and non-autonomously in LN^{EO} when expressed in LN^{MO}. Additionally, the non-autonomous JET pathway from M cells to E cells was insufficient to induce behavioral phase shifts as JET expression was required in both groups of neurons to phase-shift locomotor rhythms in response to a short light pulse (Lamba et al., 2014). However, our investigation diverged from previous work by focusing on the non-autonomous CRY pathway's involvement in entraining diurnal behavior instead of examining light pulse-induced TIM degradation and behavioral phase shifts. Additionally, in contrast to the aforementioned study, we conducted CRY rescue in a *GMR-hid* jet^{set} cry^{02} triple mutant background, rather than performing JET rescue within a jet^{set} mutant background.

It's worth noting that our ability to definitively conclude the presence of a JET-independent pathway is limited, as the nature of the jet^{set} mutant remains unclear—it's uncertain whether it's a complete null mutant of JET. Earlier findings indicated that under LD conditions, TIM cycling was not completely eliminated but rather exhibited reduced amplitude in jet^{set} mutants. The authors attributed this to the retention of residual activity of JET in jet^{set} mutants, which could possibly be detectable with prolonged light exposure (Lamba et al., 2014). In our experiments, we also employed extended exposure to light in the form of LD cycles. Thus, it's plausible that the unaffected entrainment of diurnal behavior via the non-autonomous CRY pathway in a jet^{set} mutant background could be

attributed to the residual JET activity present in *jet*^{set} mutants. An alternative scenario could involve the existence of a JET-independent pathway in both autonomous and non-autonomous CRY photoreception, with its functions becoming discernible only when subjected to prolonged light exposure. Additional experiments are required involving a comprehensive null mutant of JET in order to arrive at a definitive conclusion regarding this potential scenario.

Materials and methods

Fly stocks

All the flies were raised on standard cornmeal-yeast agar medium at 25ºC under light: dark cycle. The following Drosophila strains were used in this study. *cry*^{02} (Dolezelova et al., 2007), *pdf*^{01} (Renn et al., 1999), *GMR-hid* (Bergmann et al., 1998), *Pdfr*^{han5304} (Hyun et al., 2005), *jet*^{set} (Lamba et al., 2014) *Pdf-GAL4* (Renn et al., 1999), *Clk4.1M-GAL4* (Y. Zhang et al., 2010), *Mai179-GAL4* (Grima et al., 2004), *Pdf-GAL80* (Stoleru et al., 2004), *UAS-cry* (Emery et al., 2000), *UAS-jet* (Koh et al., 2006), *UAS-cyc*^{DN} (Tanoue et al., 2004), *UAS-DBTs* (Muskus et al., 2007), *UAS-Cas9.P2* (BDSC-58986), *R-ss00681-GAL4* (Liang et al., 2019), *R78G01-GAL4* (Pfeiffer et al., 2008) *UAS-tim.gRNA* (BDSC-90768) was previously described.

Standard genetic crosses were utilized to obtain various combinations of GAL4/UAS lines and mutants. Additionally, certain combinations were obtained by employing genetic recombination to incorporate the transgenes into particular chromosomes. For example, meiotic recombinations were utilized to insert transgenes, specifically *Clk4.1M–GAL4*, *R78G01–GAL4*, *pdf*^{01,} and *GMR-hid* (III), onto the third chromosome where the *cry* gene is located. To verify the presence of GAL4/UAS lines and mutants in the recombinants, PCR and behavior analysis were conducted.

Behavioral recording and analysis

2-6 days old male flies of corresponding genotypes were selected for recording locomotor activities using Drosophila Activity Monitor System (DAM2; Trikinetics). After placing individual flies into glass tubes with food, they were placed inside monitors. These monitors, housing the flies, were then kept inside an incubator maintained at a constant temperature of 25°C to record their activity.

For standard light-dark experiments, the behavior of flies was recorded for 7 days under standard light-dark conditions of 12 hr light and 12 hr darkness (LD12:12). The light intensity inside the incubator was approximately 2000 lux. For experiments referred to as

low light LD 12:12, the light intensity was reduced to less than 5 lux by incorporating gray neutral-density filters into the monitors. Data analysis was performed with the FaasX software derived from the Brandeis Rhythm Package. Locomotor activity profiles were averaged from a group of flies over the last 3-5 days of LD condition, excluding the recording days for quantitative analyses. The daily activity profiles averaged for n flies over 3-5 light-dark cycles were plotted as activity histograms, representing the distribution of the activity over 24 hours using 30-minute intervals. For analyzing the behavior in photoperiods other than LD 12:12, flies were initially entrained in normal 12:12 LD cycles for at least 4 days and then shifted to either short photoperiod (8:16 LD) or long photoperiod (16:8 LD) for 7 days. In such cases, the locomotion of flies during the last 3-5 days in the shifted conditions was used to generate the 24-hour activity profiles. White and gray bars in the activity histograms indicate day and night phases, respectively. Dots indicate the s.e.m of the activity for each 30-minute bin. Each genotype's morning and evening anticipation index was calculated as previously described (Chatterjee et al., 2018).

For phase shift experiments, flies were initially entrained in 12:12 LD cycles for at least 5 days and then released to a constant darkness (DD) condition for the remaining 7 days. On day 2 of DD, flies were subjected to a brief 10-minute white light pulse (2000 lux) at ZT15 and ZT21. As a control group, another set of flies was kept in a similar condition but without any light pulse given on DD2. Under DD conditions, the flies exhibit rhythmic activity behavior with a prominent peak observed during the subjective evening activity phase. Thus, the phase difference was calculated by comparing the change in the subjective evening activity phase (during DD3 to DD7) of light pulse-treated flies with non-light pulse-treated flies.

Immunohistochemistry

All experiments were done on whole-mounted adult brains. For TIM staining, flies were entrained in LD 12:12 for 4-5 days and then released to darkness (DD) for the remaining period. On the second day of the DD, a 10-minute short light pulse was shown at ZT15 and ZT21. Approximately 1 hour after the light pulse, the flies were anesthetized and fixed in 4% paraformaldehyde for 2-3 hours in darkness at 4°C. Following fixation, flies were washed in PBS containing 0.5% Triton X-100 and then dissected in PBS. Dissected brains

were then blocked with 1% bovine serum albumin (BSA) in 0.3% PBST for 2 hours at room temperature. The blocked samples were then incubated in primary antibodies (rabbit anti-PER used at 1:15,000 dilution (Stanewsky et al., 1997), rat anti-TIM used at 1:10,000 dilution (Grima et al., 2002), and mouse anti-PDF used at 1:20,000 dilution (Developmental Studies Hybridoma Bank)) for at least 48 hours at 4°C. Afterward, brains were rinsed for 6 x 10 mins with 0.3% PBST and subsequently incubated with 1:1000 diluted secondary antibodies (Alexa) for at least 24 hours at 4°C. Finally, brains were washed 6 x 10 mins with 0.3% PBST and mounted on PTFE printed slides (Electron Microscopy Sciences) in ProLong™ Diamond Antifade Mountant (ThermoFisher). Imaging was performed using a Zeiss AxioImager Z1 semi-confocal microscope equipped with an AxioCam MRm digital camera and an apotome featuring an adjustable grid that facilitated structured illumination.

For CRY staining, flies were kept in constant darkness (DD) after entrainment in standard 12:12 LD cycles for 3-5 days. Flies were collected and dissected on the fourth day of DD at ZT 0-2. Immunostainings and imaging were done as explained above. The primary antibodies used were rabbit anti-CRY (1:2,000 dilution) and mouse anti-PDF (1:20,000 dilution, Developmental Studies Hybridoma Bank).

To examine PER oscillation, the flies were subjected to 12:12 LD cycles for a few days to synchronize their behavior. Subsequently, flies from different genotypes were collected at two specific time points, ZT10 and ZT22. Following collection, the staining process and imaging were performed as described earlier. The primary antibodies used were rabbit anti-PER used at 1:15,000 dilution (Stanewsky et al., 1997), rat anti-TIM used at 1:10,000 dilution (Grima et al., 2002), and mouse anti-PDF used at 1:20,000 dilution (Developmental Studies Hybridoma Bank).

Quantification and statistical analysis

Fluorescence intensity was quantified from digital images with the ImageJ software. To obtain staining intensity, we applied the formula: $I = 100x(S-B)/B$, which gives the fluorescence percentage above the background (where S is the mean intensity inside the cell, and B is the mean intensity of the region adjacent to the positive cell). Images for PER protein oscillations and light-induced TIM degradation were acquired with a 63x objective, and for CRY staining experiments, images were taken with a 25x objective. Statistical

analysis was done with R and Prism (GraphPad).

The morning anticipation index was calculated by computing the 3-hr/6-hr activity ratio prior to the lights-on transition, providing an estimation of the amplitude of the morning peak. The evening anticipation index was obtained as the slope of a linear regression applied to the last eight 30-minute bins before the lights were turned OFF, giving a measure of the strength of the evening peak. The existence of a putative association between binned time and activity level preceding light-on/off transition was quantified by Spearman's rank-correlation coefficient (rho), whose significance (at $\alpha = 0.05$) was ascertained by the t test. Two sample means were compared by unpaired two-tailed t test, and multiple sample means were compared by ANOVA with post hoc comparison obtained from Tukey's HSD test ($\alpha = 0.05$).

Figures and legends

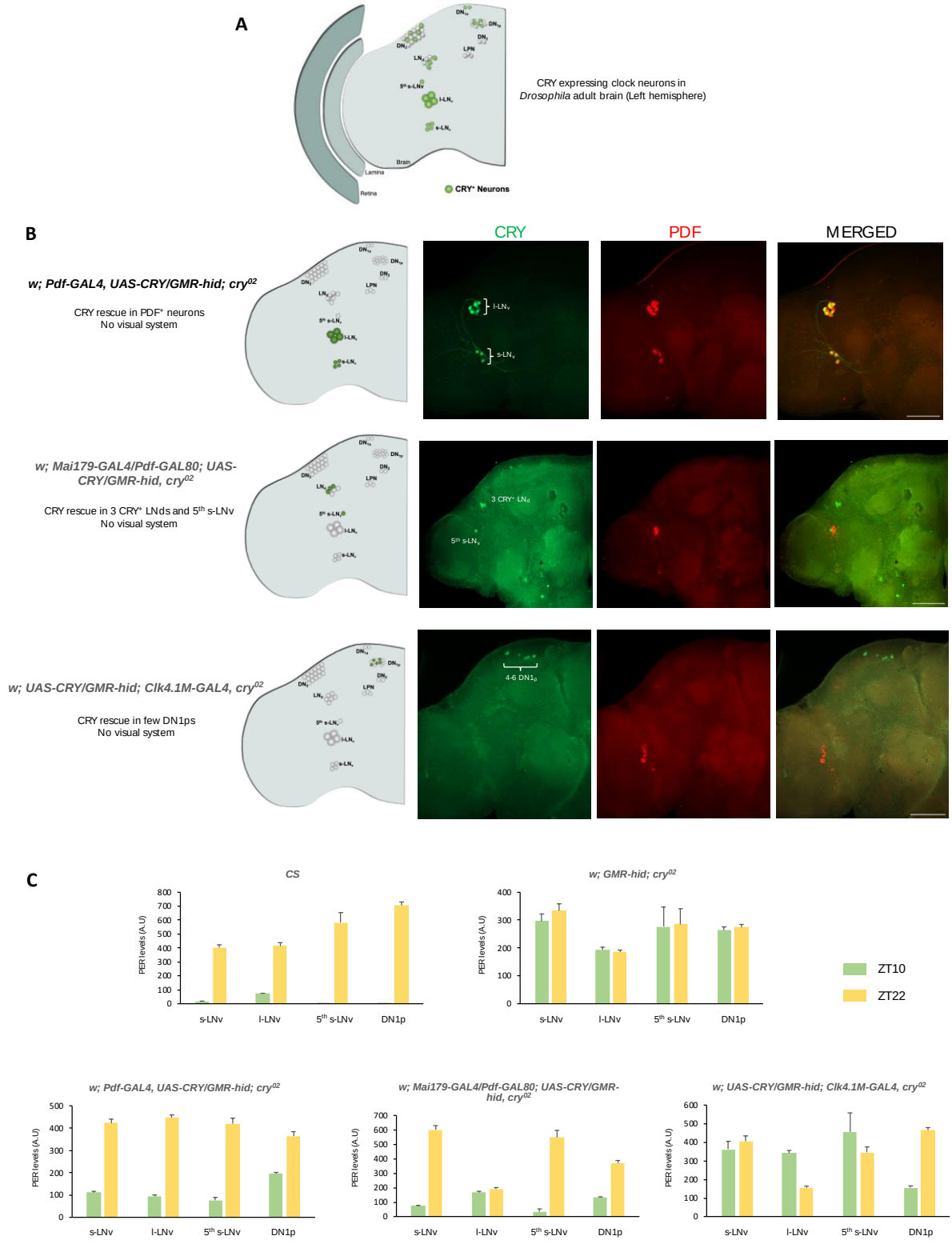

Fig. 1 Network-wide distribution of CRY-related photic inputs. (A) Schematic of CRY expressing neurons in the *Drosophila* circadian clock neuron network. The illustration depicts neurons that express CRY (highlighted in green) and those that do not express CRY (grey). **(B)** Schematic of CRY rescue in different neuronal subgroups along with representative images of adult brain showing restricted CRY expression (green) (co-stained with Anti-PDF, red) in the corresponding neurons. (top) CRY rescue in PDF neurons (including LN^{MO}) using *Pdf-GAL4* in *GMR-hid* cry^{02} mutant background. CRY and PDF co-localize in the PDF neurons. (middle) Rescue of CRY expression in the 5^{th} s-LNv and 3 CRY^{+} LNds (LN^{EO}) with *Mai179-GAL4 + Pdf-GAL80* in a *GMR-hid* cry^{02} background. (bottom) *Clk4.1M-GAL4* driven CRY expression in a few DN1ps (including DN^{MO} and DN^{EO}) of *GMR-hid* cry^{02} fly. Scale bars, 50 μm. **(C)** PER protein levels in various subgroups of neurons, including s-LNv, l-LNv, 5th s-LNv, and DN1ps, among different genotypes were examined. These genotypes were entrained under a 12:12 LD cycle, and staining was conducted at two specific time points: ZT10 and ZT22. In the case of wild-type flies (CS), the observed neuronal subsets exhibited minimal PER labeling at ZT10, followed by robust labeling at ZT22 (top left). *GMR-hid* cry^{02} flies, which were used as a negative control, displayed no notable difference in PER levels between ZT10 and ZT22, indicating unsynchronized PER oscillation across neuronal groups with the external LD condition (top right). Rescuing CRY expression in PDF neurons of *GMR-hid* cry^{02} flies resulted in wild-type-like PER levels in each subgroup at both ZT10 and ZT22 (bottom left). Whereas restoring CRY function only in LN^{EO} led to synchronized PER oscillation in all examined neuronal clusters except l-LNv (bottom middle). However, rescuing CRY expression only in a few DN1ps yielded LD-entrained PER levels solely in DN1ps, characterized by weak expression at ZT10 and strong expression at ZT22 (bottom right). All the brains were stained with anti-PER, anti-TIM, and anti-PDF antibodies. At least 10-12 hemispheres were examined for each genotype. Error bars correspond to SEM. See Materials and Methods for details of the quantification method.

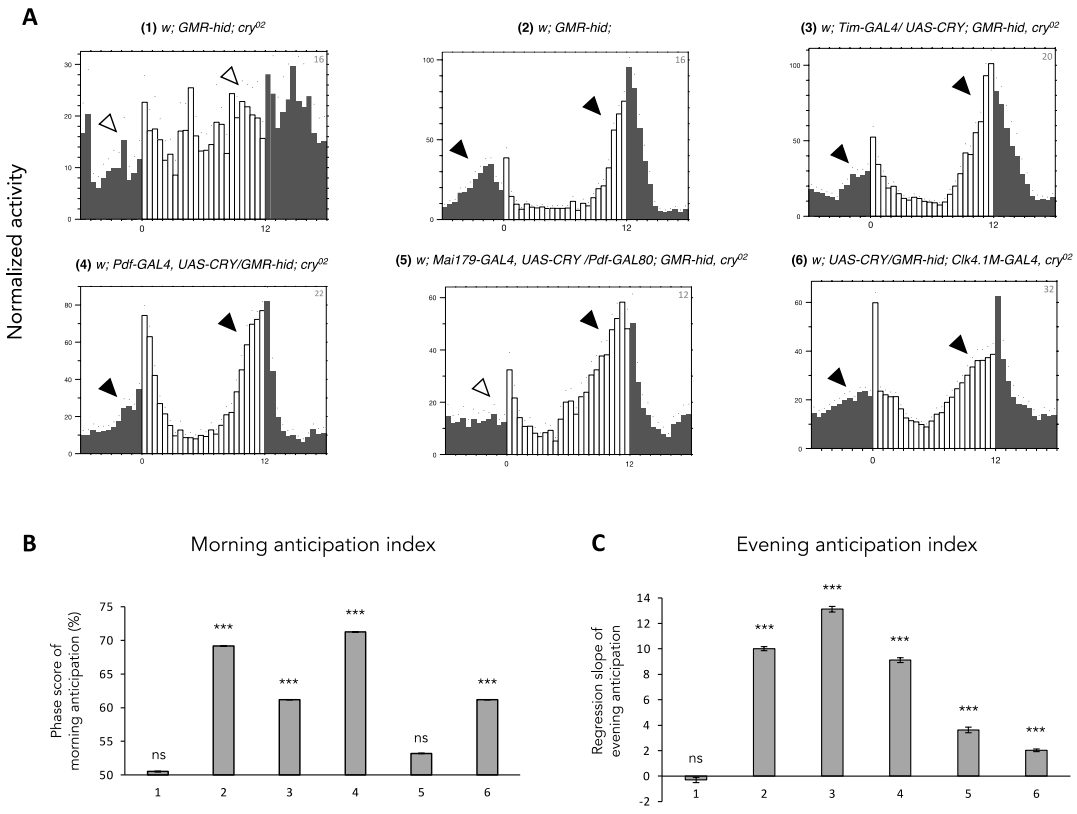

Fig. 2 Entrainment of daily locomotor activities to external LD conditions through non-autonomous CRY input. (A) Averaged group activity profiles of various genotypes under 12:12 LD. The light phase is represented by the white bar, while the dark phase is depicted by the grey bars. The sample size for each behavioral experiment is denoted by the number in the upper right corner of the activity plots, and the respective genotypes are labeled above each activity profile. The presence or absence of anticipatory behaviors (M and E peak) determined by Spearman's non-parametric rank-correlation test is indicated by solid and empty arrowheads, respectively. **(B** and **C)** Column chart showing the anticipation index values of the morning (B) and evening (C) anticipatory behaviors of each genotype (number coded as in A) in LD cycles. The morning anticipation index was calculated by computing the 3-hr/6-hr activity ratio prior to the lights-on transition, providing an estimation of the amplitude of the morning peak. Meanwhile, the evening anticipation index was obtained as the slope of a linear regression applied to the last eight 30-minute bins before the lights were turned OFF, giving a measure of the strength of the evening peak. Error bars indicate SEM. The significance of anticipatory activity was determined by Spearman's non-parametric rank-correlation test (Rank correlation quantifies anticipation indexes as the Spearman's

correlation coefficient rho (not provided here) that measures relationship between activity level and time during period of interest preceding light transitions). Following this, the significance of Spearman's rank-correlation coefficient (rho) was ascertained by t test. n.s., not significant ($p>0.05$), ***$p < 0.001$. No statistical analysis was conducted to compare anticipatory indexes between different genotypes. *GMR-hid cry^{02}* flies (1), which lack both visual and CRY input, failed to elicit both M and E anticipation. Positive controls, including *GMR-hid* flies (2) and *Tim-GAL4* driven expression of CRY in all clock neurons of *GMR-hid cry^{02}* flies (3), exhibited entrained bimodal activity patterns with M and E anticipation. CRY expression in PDF neurons (4) alone could generate significant M and E peaks. CRY in a few DN1ps (6) also exhibited synchronized bimodal activity. Whereas CRY expression restricted to LN^{EO} (5th s-LNv + 3 CRY^{+} LNds) (5) was sufficient for E anticipation but not for M anticipation.

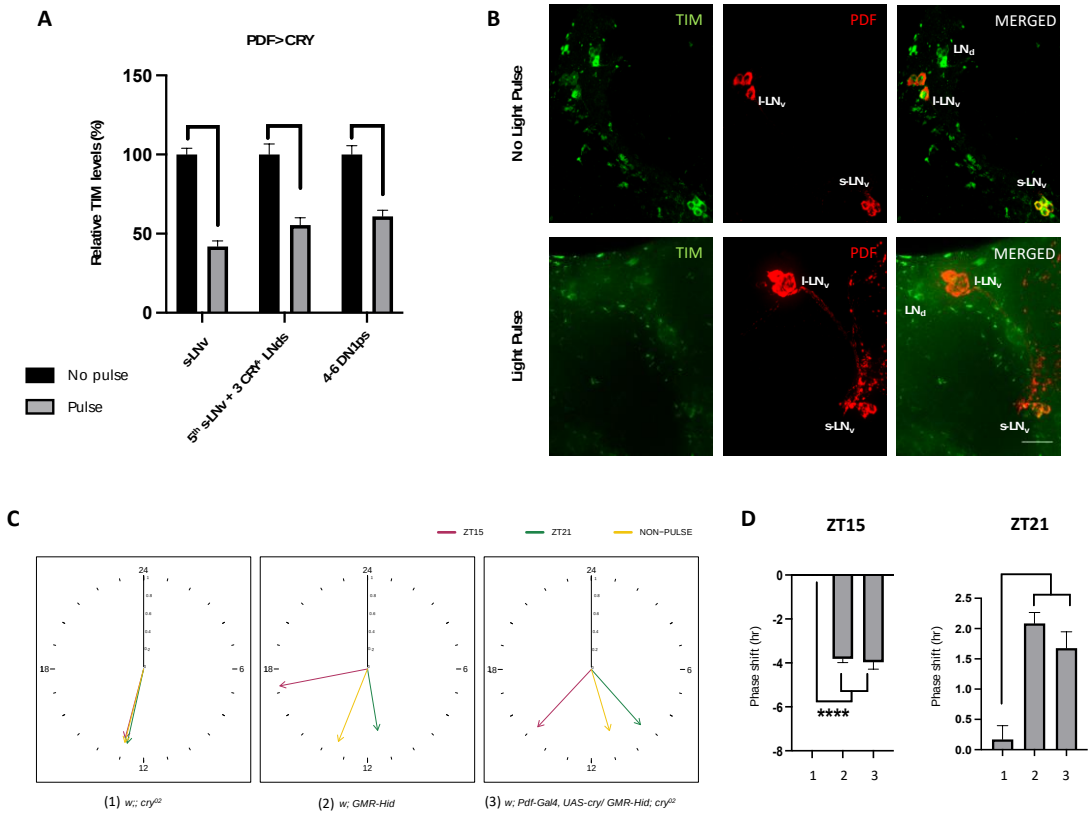

Fig. 3 Non-cell autonomous CRY-mediated circadian light responses. (A) Quantification of TIM levels after a short light pulse at ZT15 (grey) and in the absence of any light pulse (black) in different clock neuron clusters of flies in which CRY expression was restricted to PDF^{+} LNvs (*Pdf-GAL4, UAS-cry/GMR-hid; cry^{02}*). For each neuronal subset, relative TIM levels normalized to 'no pulse' controls were determined and used for the column chart. Error bars represent the SEM. ****p < 0.0001 was determined by the t-test. See Materials and Methods for details of the quantification method. **(B)** Representative images showing the TIM staining in experimental flies subjected to a brief light pulse at ZT15 (bottom) compared to those without any light exposure (top). Anti-TIM antibody (green) and anti-PDF antibody (red) were used to stain the brains. Scale bars, 50 μm. **(C)** Phase shifts in locomotor activity in response to a short light pulse (10 min) at ZT15 and ZT21. Circular plots with a 24-hour dial are utilized to construct the phase vectors that represent the peak phase of the main activity around subjective evening in DD. The respective genotypes are labeled below each plot. The phase vectors corresponding to each condition: (1) after pulse at ZT15 (red), (2) pulse at ZT21 (green), (3) and no pulse (yellow) are plotted for each genotype. **(D)** Quantification of phase shifts acquired by each genotype (number coded as in C) in response to a light pulse at ZT15 (left) and ZT21 (right). Error bars indicate SEM. ****p < 0.0001 by one-way analysis of variance (ANOVA), Tukey post hoc test.

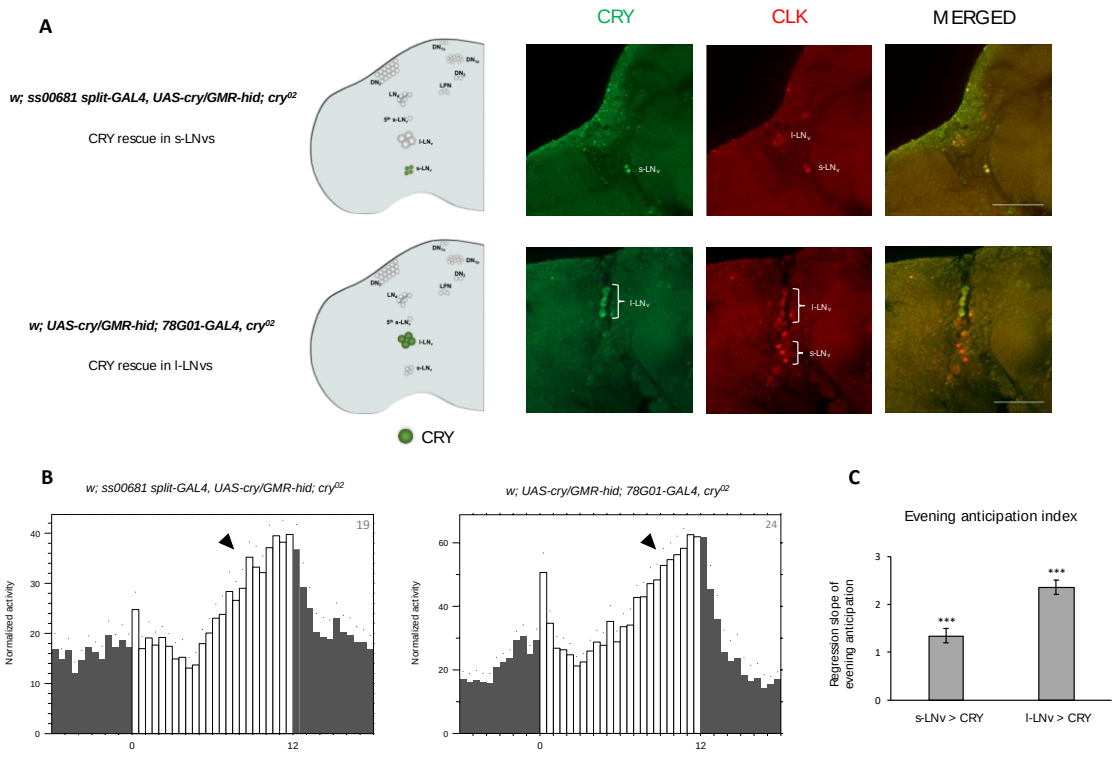

Fig. 4 CRY restricted to either small or large clusters of ventral lateral neurons alone are sufficient for synchronizing the E-oscillator. (A) Schematic of CRY rescue in s-LNvs (Top) and l-LNvs (Bottom) along with representative images of adult brain showing restricted CRY expression (green) (co-stained with Anti-CLK, red) in the corresponding neurons. Scale bars, 50 μm. **(B)** Averaged activity profiles during 12:12 LD cycles reveal that CRY expression in s-LNvs and l-LNvs alone could elicit significant evening behavior based on Spearman's non-parametric rank-correlation test. The numerical value located in the top right corner of the activity plots represents the sample size of flies analyzed in a single run of the behavioral experiment. The solid black arrowhead indicates the presence of a persistent evening peak, whose significance was determined by Spearman's non-parametric rank-correlation test. **(C)** Column chart showing the evening anticipation index values for each genotype. The anticipation index was calculated using the same method as previously described, depicting the strength of evening peak. The significance of evening anticipation was verified using Spearman's non-parametric rank-correlation followed by t test. ***$p < 0.001$. No statistical analysis was conducted to compare anticipatory indexes between different genotypes.

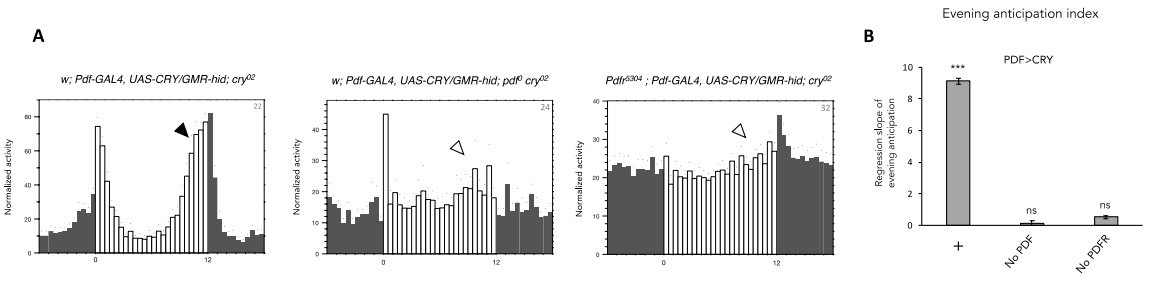

Fig. 5 Functional PDF and PDFR are critical for exporting non-autonomous CRY signals from PDF cells. (A) Average activity profile of different genotypes in 12:12 LD cycles. As revealed by the daily locomotor pattern, non-cell-autonomous effects of CRY from the M-oscillator are sufficient for the E-oscillator to generate entrained E behavior (left). However, in cases where flies lack either PDF (middle) or PDFR (right), there is an absence of E anticipation, suggesting that PDF/PDFR signaling is utilized for transmitting CRY signals from PDF neurons to E cells. The number in the upper right corner of the activity plots denotes the sample size for each behavioral experiment, while the corresponding genotypes are labeled above each activity profile. Solid and empty arrowheads are used to depict the presence or absence of evening anticipatory behavior, respectively, which was determined by Spearman's non-parametric rank-correlation test. **(B)** Column chart showing the evening anticipation index calculated from A. The significance of evening anticipation was verified using Spearman's non-parametric rank-correlation followed by t test. n.s., not significant ($p>0.05$), ***$p < 0.001$. No statistical analysis was conducted to compare anticipatory indexes between different genotypes

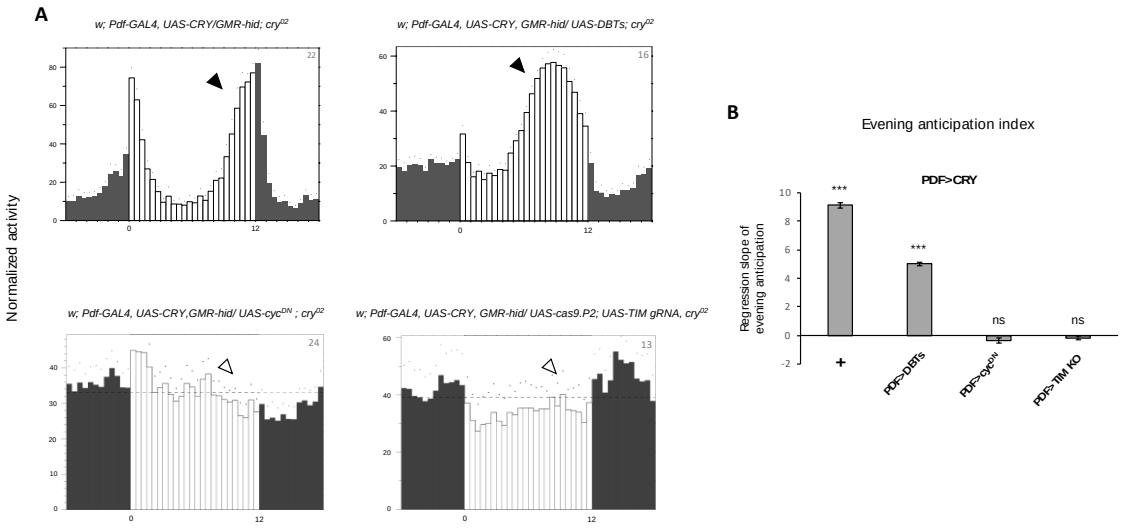

Fig 6. Inter-oscillator transfer of CRY signals from M cells to E cells requires a clock in M cells. (A) Daily activity profiles of various genotypes in LD 12:12. Acceleration of the molecular clock in PDF cells by expressing DBTs led to an advanced evening peak (top right), whereas in the absence of DBTs expression in PDF neurons, the evening peak remained properly phased (top left). Disrupting the functional clock in LNMO either through the expression of *UAS-cyc*^{DN} under *Pdf-GAL4* (bottom left) or by cell-specific knockout of the *tim* gene in LN^{MO} using the CRISPR technique (bottom right) resulted in the elimination of evening anticipatory behavior. **(B)** Quantification of evening anticipation displayed by each genotype mentioned in A. The presence of evening anticipation was ascertained using Spearman's non-parametric rank-correlation followed by test. n.s., not significant ($p>0.05$), ***$p < 0.001$. No statistical analysis was conducted to compare anticipatory indexes between different genotypes.

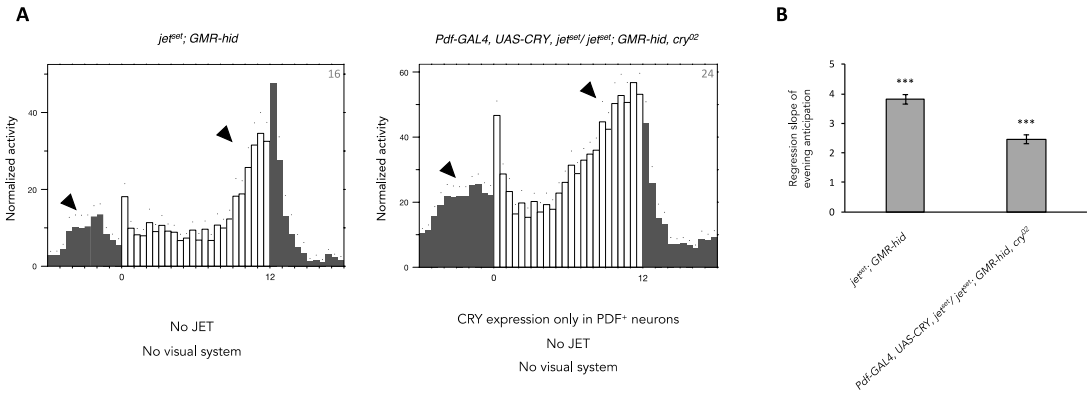

Fig. 7 A non-canonical CRY-JET independent pathway may be involved in the non-cell autonomous CRY action. (A) Activity profiles of *jet*^{set} *GMR-hid* flies (left), which are depleted for JET and visual-mediated inputs, demonstrate the possibility of a JET-independent CRY-mediated light input to the circadian clock network as these flies showed typical bimodal activity patterns. *jet*^{set} *GMR-hid* flies with CRY expression in PDF^{+} neurons alone could evoke evening behavior (right), suggesting that the canonical CRY-JET pathway may not be essential for the non-cell-autonomous effects of CRY in the entrainment of diurnal behavior in LD conditions. **(B)** Quantification of evening anticipatory behavior determined from A. The presence of evening anticipation was verified using Spearman's non-parametric rank-correlation followed by t test. ***$p < 0.001$. No statistical analysis was conducted to compare anticipatory indexes between different genotypes.

Supplementary figures and legends

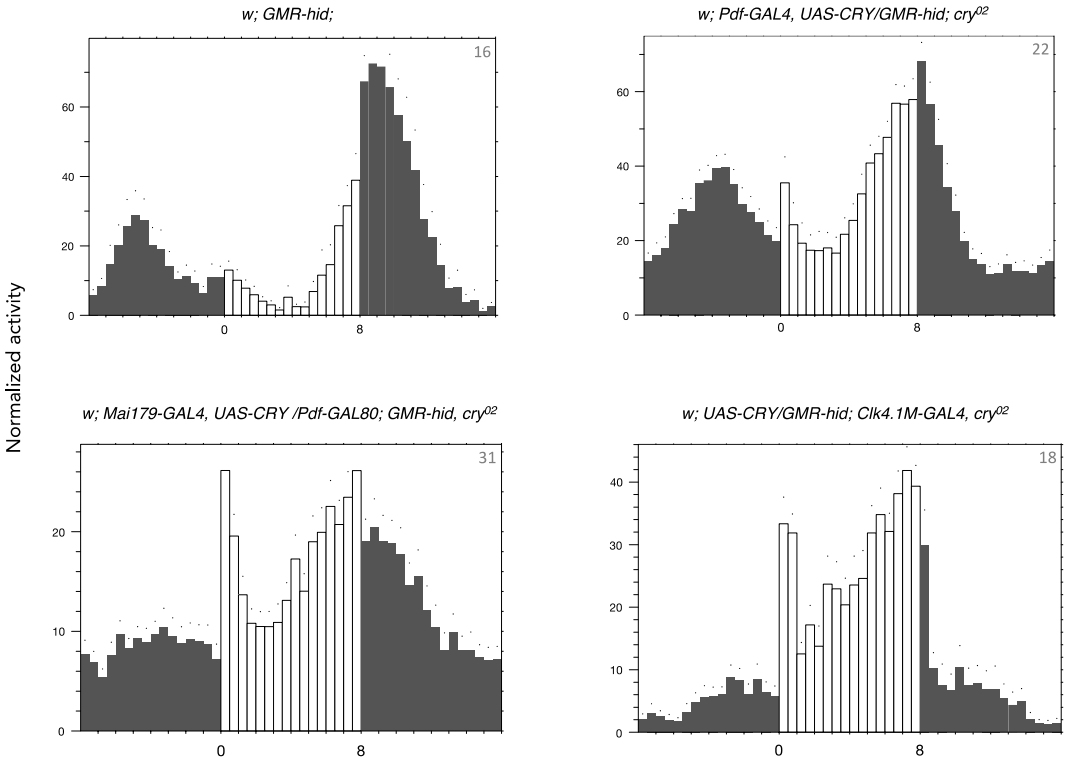

Sup fig. 1 Averaged daily activity profiles of different genotypes in LD 8:16 (short photoperiod). *GMR-hid cry*^{02} flies with CRY expression rescued in definite subsets like LN^{MO} (top right), LN^{EO} (bottom left), and DN^{MO}+DN^{EO} (bottom right), along with *GMR-hid* (top left) control flies entrained under short photoperiod.

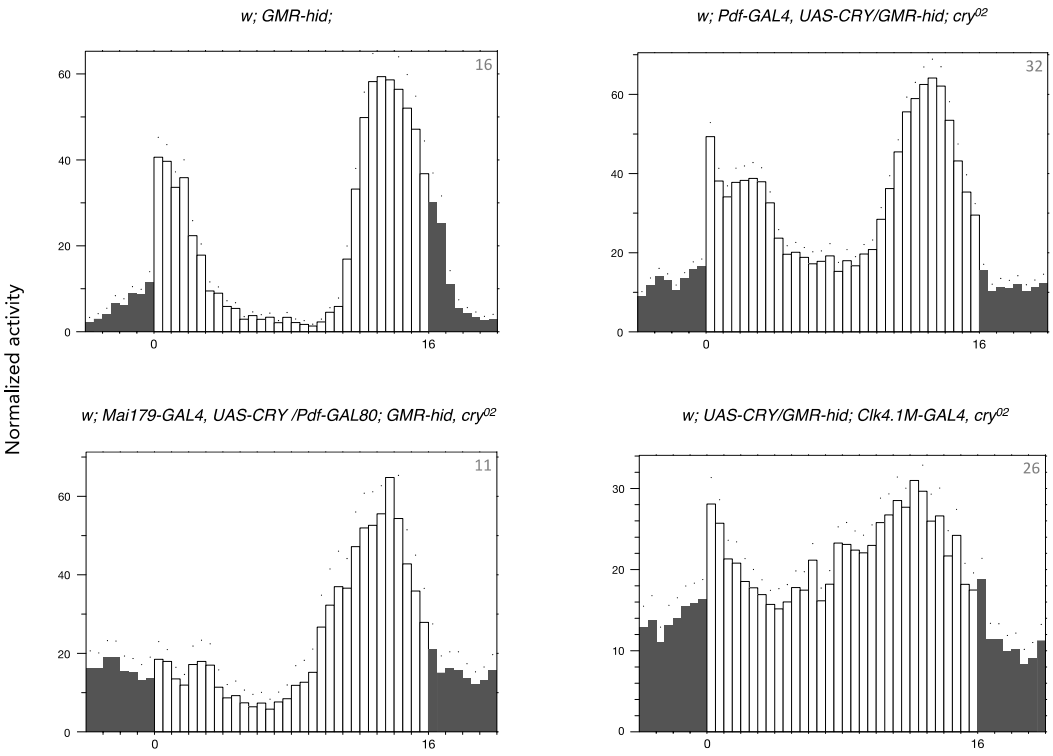

Sup fig. 2 Averaged daily activity profiles of different genotypes in LD 16:8 (long photoperiod). *GMR-hid cry*^{02} flies with CRY expression rescued in definite subsets like LN^{MO} (top right), LN^{EO} (bottom left), and DN^{MO}+DN^{EO} (bottom right), along with *GMR-hid* (top left) control flies entrained under long photoperiod.

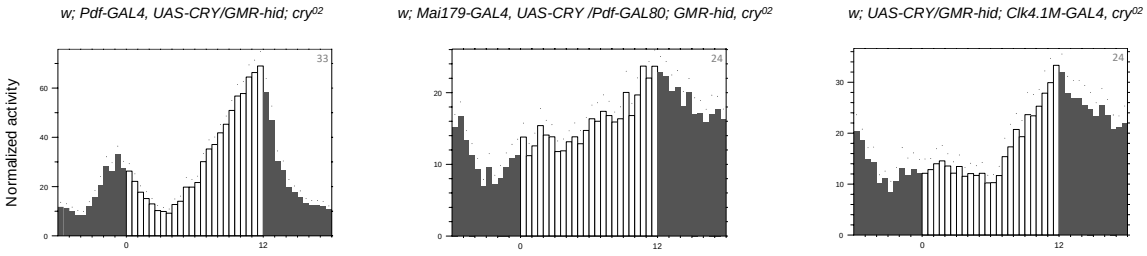

Sup fig. 3 Averaged activity profiles of different genotypes in 12:12 low light LD. *GMR-hid cry^{02}* flies with CRY expression rescued in definite subsets like LN^{MO} (top right), LN^{EO} (bottom left), and DN^{MO}+DN^{EO} (bottom right) entrained in 12:12 LD cycles with low-intensity light phase. Low light is indicated by gray shading on the lights ON phase.

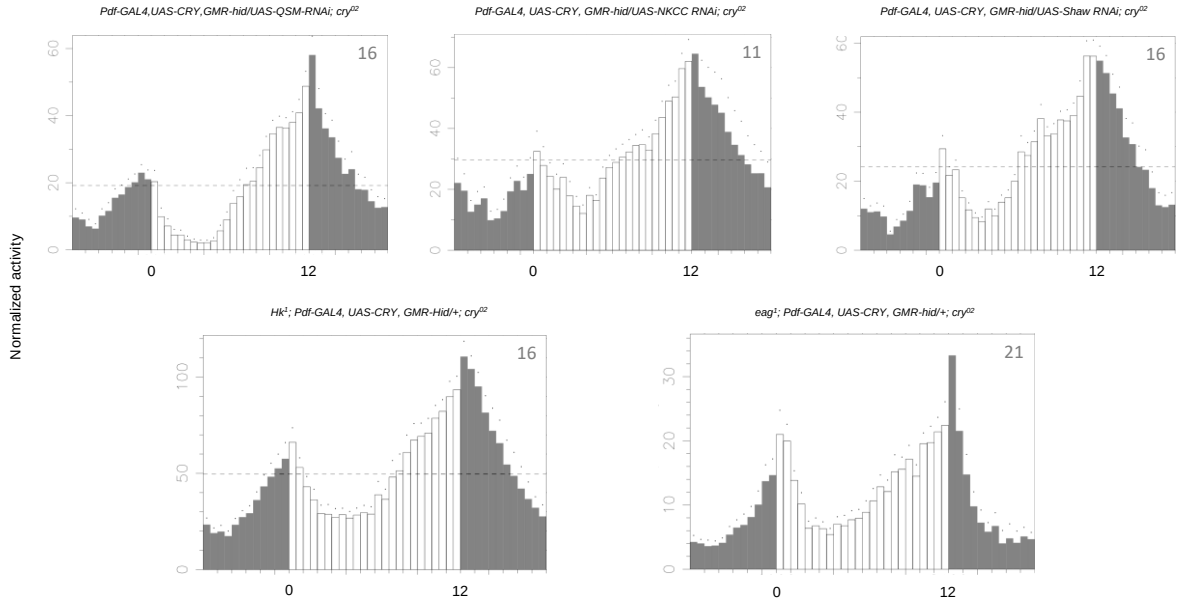

Sup fig. 4 Averaged locomotor activity profiles of different genotypes in LD 12:12.

References

Ahmad, Myra, Wanhe Li, and Deniz Top. 2021. 'Integration of Circadian Clock Information in the Drosophila Circadian Neuronal Network'. Journal of Biological Rhythms 36(3):203–20. doi: 10.1177/0748730421993953.

Beckwith, Esteban J., and M. Fernanda Ceriani. 2015. 'Communication between Circadian Clusters: The Key to a Plastic Network'. FEBS Letters 589(22):3336–42. doi: 10.1016/j.febslet.2015.08.017.

Bergmann, Andreas, Julie Agapite, Kimberly McCall, and Hermann Steller. 1998. 'The Drosophila Gene Hid Is a Direct Molecular Target of Ras-Dependent Survival Signaling'. Cell 95(3):331–41. doi: 10.1016/S0092-8674(00)81765-1.

Busza, Ania, Myai Emery-Le, Michael Rosbash, and Patrick Emery. 2004. 'Roles of the Two Drosophila CRYPTOCHROME Structural Domains in Circadian Photoreception'. Science 304(5676):1503–6. doi: 10.1126/science.1096973.

Chatterjee, Abhishek, Angélique Lamaze, Joydeep De, Wilson Mena, Elisabeth Chélot, Béatrice Martin, Paul Hardin, Sebastian Kadener, Patrick Emery, and François Rouyer. 2018. 'Reconfiguration of a Multi-Oscillator Network by Light in the Drosophila Circadian Clock'. Current Biology 28(13):2007-2017.e4. doi: 10.1016/j.cub.2018.04.064.

Chatterjee, Abhishek, and François Rouyer. 2016. 'Control of Sleep-Wake Cycles in Drosophila'. in A Time for Metabolism and Hormones, edited by P. Sassone-Corsi and Y. Christen. Cham (CH): Springer.

Chen, Ko Fan, Nicolai Peschel, Radka Zavodska, Hana Sehadova, and Ralf Stanewsky. 2011. 'QUASIMODO, a Novel GPI-Anchored Zona Pellucida Protein Involved in Light Input to the Drosophila Circadian Clock'. Current Biology 21(9):719–29. doi: 10.1016/j.cub.2011.03.049.

Crespo-Flores, Sergio L., and Annika F. Barber. 2022. 'The Drosophila Circadian Clock Circuit Is a Nonhierarchical Network of Peptidergic Oscillators'. Current Opinion in Insect Science 52:100944. doi: 10.1016/j.cois.2022.100944.

Cusumano, Paola, André Klarsfeld, Elisabeth Chélot, Marie Picot, Benjamin Richier, and François Rouyer. 2009. 'PDF-Modulated Visual Inputs and Cryptochrome Define

Diurnal Behavior in Drosophila'. Nature Neuroscience 12(11):1431–37. doi: 10.1038/nn.2429.

Dissel, Stephane, Veryan Codd, Robert Fedic, Karen J. Garner, Rodolfo Costa, Charalambos P. Kyriacou, and Ezio Rosato. 2004. 'A Constitutively Active Cryptochrome in Drosophila Melanogaster'. Nature Neuroscience 7(8):834–40. doi: 10.1038/nn1285.

Dissel, Stephane, Celia N. Hansen, Özge Özkaya, Matthew Hemsley, Charalambos P. Kyriacou, and Ezio Rosato. 2014. 'The Logic of Circadian Organization in Drosophila'. Current Biology 24(19):2257–66. doi: 10.1016/j.cub.2014.08.023.

Dolezelova, Eva, David Dolezel, and Jeffrey C. Hall. 2007. 'Rhythm Defects Caused by Newly Engineered Null Mutations in Drosophila's Cryptochrome Gene'. Genetics 177(1):329–45. doi: 10.1534/genetics.107.076513.

Dubowy, Christine, and Amita Sehgal. 2017. 'Circadian Rhythms and Sleep in Drosophila Melanogaster'. Genetics 205(4):1373–97. doi: 10.1534/genetics.115.185157.

Dunlap, Jay C., Jennifer J. Loros, and Patricia J. DeCoursey. 2004. Chronobiology: Biological Timekeeping. Sunderland, Mass.: Sinauer Associates.

Emery, Patrick, W. Venus So, Maki Kaneko, Jeffrey C. Hall, and Michael Rosbash. 1998. 'CRY, a Drosophila Clock and Light-Regulated Cryptochrome, Is a Major Contributor to Circadian Rhythm Resetting and Photosensitivity'. Cell 95(5):669–79. doi: 10.1016/S0092-8674(00)81637-2.

Emery, Patrick, Ralf Stanewsky, Charlotte Helfrich-Förster, Myai Emery-Le, Jeffrey C. Hall, and Michael Rosbash. 2000. 'Drosophila CRY Is a Deep Brain Circadian Photoreceptor'. Neuron 26(2):493–504. doi: 10.1016/S0896-6273(00)81181-2.

Fogle, Keri J., Lisa S. Baik, Jerry H. Houl, Tri T. Tran, Logan Roberts, Nicole A. Dahm, Yu Cao, Ming Zhou, and Todd C. Holmes. 2015. 'CRYPTOCHROME-Mediated Phototransduction by Modulation of the Potassium Ion Channel β-Subunit Redox Sensor'. Proceedings of the National Academy of Sciences of the United States of America 112(7):2245–50. doi: 10.1073/pnas.1416586112.

Fogle, Keri J., Kelly G. Parson, Nicole A. Dahm, and Todd C. Holmes. 2011. 'CRYPTOCHROME Is a Blue-Light Sensor That Regulates Neuronal Firing Rate'. Science 331(6023):1409–13. doi: 10.1126/science.1199702.

Foley, Lauren E., and Patrick Emery. 2020. 'Drosophila Cryptochrome: Variations in Blue'.

Journal of Biological Rhythms 35(1):16–27. doi: 10.1177/0748730419878290.

Golombek, Diego A., and Ruth E. Rosenstein. 2010. 'Physiology of Circadian Entrainment'. Physiological Reviews 90(3):1063–1102. doi: 10.1152/physrev.00009.2009.

Grima, Brigitte, Elisabeth Chélot, Ruohan Xia, and François Rouyer. 2004. 'Morning and Evening Peaks of Activity Rely on Different Clock Neurons of the Drosophila Brain'. Nature 431(7010):869–73. doi: 10.1038/nature02935.

Grima, Brigitte, Annie Lamouroux, Elisabeth Chélot, Christian Papin, Bernadette Limbourg-Bouchon, and François Rouyer. 2002. 'The F-Box Protein Slimb Controls the Levels of Clock Proteins Period and Timeless'. Nature 420(6912):178–82. doi: 10.1038/nature01122.

Guo, Fang, Isadora Cerullo, Xiao Chen, and Michael Rosbash. 2014. 'PDF Neuron Firing Phase-Shifts Key Circadian Activity Neurons in Drosophila' edited by L. Ptáček. ELife 3:e02780. doi: 10.7554/eLife.02780.

Hardin, Paul E. 2011. 'Molecular Genetic Analysis of Circadian Timekeeping in Drosophila'. Advances in Genetics 74:141–73. doi: 10.1016/B978-0-12-387690-4.00005-2.

Helfrich-Förster, C., T. Yoshii, C. Wülbeck, E. Grieshaber, D. Rieger, W. Bachleitner, P. Cusumano, and F. Rouyer. 2007. 'The Lateral and Dorsal Neurons of Drosophila Melanogaster: New Insights about Their Morphology and Function'. Cold Spring Harbor Symposia on Quantitative Biology 72:517–25. doi: 10.1101/sqb.2007.72.063.

Helfrich-Förster, Charlotte. 2003. 'The Neuroarchitecture of the Circadian Clock in the Brain of Drosophila Melanogaster'. Microscopy Research and Technique 62(2):94–102. doi: 10.1002/jemt.10357.

Helfrich-Förster, Charlotte. 2020. 'Light Input Pathways to the Circadian Clock of Insects with an Emphasis on the Fruit Fly Drosophila Melanogaster'. Journal of Comparative Physiology. A, Neuroethology, Sensory, Neural, and Behavioral Physiology 206(2):259–72. doi: 10.1007/s00359-019-01379-5.

Helfrich-Förster, Charlotte, Orie T. Shafer, Corinna Wülbeck, Eva Grieshaber, Dirk Rieger, and Paul Taghert. 2007. 'Development and Morphology of the Clock-Gene-Expressing Lateral Neurons of Drosophila Melanogaster'. Journal of Comparative Neurology 500(1):47–70. doi: 10.1002/cne.21146.

Helfrich-Förster, Charlotte, Christine Winter, Alois Hofbauer, Jeffrey C. Hall, and Ralf

Stanewsky. 2001. ‘The Circadian Clock of Fruit Flies Is Blind after Elimination of All Known Photoreceptors’. Neuron 30(1):249–61. doi: 10.1016/S0896-6273(01)00277-X.

Hermann-Luibl, Christiane, and Charlotte Helfrich-Förster. 2015. ‘Clock Network in Drosophila’. Current Opinion in Insect Science 7:65–70. doi: 10.1016/j.cois.2014.11.003.

Hyun, Seogang, Youngseok Lee, Sung-Tae Hong, Sunhoe Bang, Donggi Paik, Jongkyun Kang, Jinwhan Shin, Jaejung Lee, Keunhye Jeon, Seungyoon Hwang, Eunkyung Bae, and Jaeseob Kim. 2005. ‘Drosophila GPCR Han Is a Receptor for the Circadian Clock Neuropeptide PDF’. Neuron 48(2):267–78. doi: 10.1016/j.neuron.2005.08.025.

Im, Seol Hee, Weihua Li, and Paul H. Taghert. 2011. ‘PDFR and CRY Signaling Converge in a Subset of Clock Neurons to Modulate the Amplitude and Phase of Circadian Behavior in Drosophila’. PLOS ONE 6(4):e18974. doi: 10.1371/journal.pone.0018974.

Im, Seol Hee, and Paul H. Taghert. 2010. ‘PDF Receptor Expression Reveals Direct Interactions between Circadian Oscillators in Drosophila’. The Journal of Comparative Neurology 518(11):1925–45. doi: 10.1002/cne.22311.

Klarsfeld, André, Sébastien Malpel, Christine Michard-Vanhée, Marie Picot, Elisabeth Chélot, and François Rouyer. 2004. ‘Novel Features of Cryptochrome-Mediated Photoreception in the Brain Circadian Clock of Drosophila’. Journal of Neuroscience 24(6):1468–77. doi: 10.1523/JNEUROSCI.3661-03.2004.

Koh, Kyunghee, Xiangzhong Zheng, and Amita Sehgal. 2006. ‘JETLAG Resets the Drosophila Circadian Clock by Promoting Light-Induced Degradation of TIMELESS’. Science 312(5781):1809–12. doi: 10.1126/science.1124951.

Lamba, Pallavi, Diana Bilodeau-Wentworth, Patrick Emery, and Yong Zhang. 2014. ‘Morning and Evening Oscillators Cooperate to Reset Circadian Behavior in Response to Light Input’. Cell Reports 7(3):601–8. doi: 10.1016/j.celrep.2014.03.044.

Lamba, Pallavi, Lauren E. Foley, and Patrick Emery. 2018. ‘Neural Network Interactions Modulate CRY-Dependent Photoresponses in Drosophila’. The Journal of Neuroscience 38(27):6161–71. doi: 10.1523/JNEUROSCI.2259-17.2018.

Liang, Xitong, Margaret C. W. Ho, Yajun Zhang, Yulong Li, Mark N. Wu, Timothy E. Holy, and Paul H. Taghert. 2019. ‘Morning and Evening Circadian Pacemakers Independently Drive Premotor Centers via a Specific Dopamine Relay’. Neuron 102(4):843-857.e4.

doi: 10.1016/j.neuron.2019.03.028.

Liang, Xitong, Timothy E. Holy, and Paul H. Taghert. 2017. 'A Series of Suppressive Signals within the Drosophila Circadian Neural Circuit Generates Sequential Daily Outputs'. Neuron 94(6):1173-1189.e4. doi: 10.1016/j.neuron.2017.05.007.

Lin, Fang-Ju, Wei Song, Elizabeth Meyer-Bernstein, Nirinjini Naidoo, and Amita Sehgal. 2001. 'Photic Signaling by Cryptochrome in the Drosophila Circadian System'. Molecular and Cellular Biology 21(21):7287–94. doi: 10.1128/MCB.21.21.7287-7294.2001.

Lin, Yiing, Gary D. Stormo, and Paul H. Taghert. 2004. 'The Neuropeptide Pigment-Dispersing Factor Coordinates Pacemaker Interactions in the Drosophila Circadian System'. Journal of Neuroscience 24(36):7951–57. doi: 10.1523/JNEUROSCI.2370-04.2004.

Lucas, Robert J., Gurprit S. Lall, Annette E. Allen, and Timothy M. Brown. 2012. 'Chapter 1 - How Rod, Cone, and Melanopsin Photoreceptors Come Together to Enlighten the Mammalian Circadian Clock'. Pp. 1–18 in Progress in Brain Research. Vol. 199, The Neurobiology of Circadian Timing, edited by A. Kalsbeek, M. Merrow, T. Roenneberg, and R. G. Foster. Elsevier.

Millar, A. J. 2003. 'Input Signals to the Plant Circadian Clock'. Journal of Experimental Botany 55(395):277–83. doi: 10.1093/jxb/erh034.

Muskus, Michael J., Fabian Preuss, Jin-Yuan Fan, Edward S. Bjes, and Jeffrey L. Price. 2007. 'Drosophila DBT Lacking Protein Kinase Activity Produces Long-Period and Arrhythmic Circadian Behavioral and Molecular Rhythms'. Molecular and Cellular Biology 27(23):8049–64. doi: 10.1128/MCB.00680-07.

Myers, M. P., K. Wager-Smith, A. Rothenfluh-Hilfiker, and M. W. Young. 1996. 'Light-Induced Degradation of TIMELESS and Entrainment of the Drosophila Circadian Clock'. Science (New York, N.Y.) 271(5256):1736–40. doi: 10.1126/science.271.5256.1736.

Nitabach, Michael N., and Paul H. Taghert. 2008. 'Organization of the Drosophila Circadian Control Circuit'. Current Biology: CB 18(2):R84-93. doi: 10.1016/j.cub.2007.11.061.

Ozturk, Nuri, Christopher P. Selby, Yunus Annayev, Dongping Zhong, and Aziz Sancar. 2011. 'Reaction Mechanism of Drosophila Cryptochrome'. Proceedings of the National

Academy of Sciences 108(2):516–21. doi: 10.1073/pnas.1017093108.

Patke, Alina, Michael W. Young, and Sofia Axelrod. 2020. 'Molecular Mechanisms and Physiological Importance of Circadian Rhythms'. Nature Reviews Molecular Cell Biology 21(2):67–84. doi: 10.1038/s41580-019-0179-2.

Peschel, Nicolai, Ko Fan Chen, Gisela Szabo, and Ralf Stanewsky. 2009. 'Light-Dependent Interactions between the Drosophila Circadian Clock Factors Cryptochrome, Jetlag, and Timeless'. Current Biology 19(3):241–47. doi: 10.1016/j.cub.2008.12.042.

Pfeiffer, Barret D., Arnim Jenett, Ann S. Hammonds, Teri-T. B. Ngo, Sima Misra, Christine Murphy, Audra Scully, Joseph W. Carlson, Kenneth H. Wan, Todd R. Laverty, Chris Mungall, Rob Svirskas, James T. Kadonaga, Chris Q. Doe, Michael B. Eisen, Susan E. Celniker, and Gerald M. Rubin. 2008. 'Tools for Neuroanatomy and Neurogenetics in Drosophila'. Proceedings of the National Academy of Sciences 105(28):9715–20. doi: 10.1073/pnas.0803697105.

Pittendrigh, C. S. 1993. 'Temporal Organization: Reflections of a Darwinian Clock-Watcher'. Annual Review of Physiology 55:16–54. doi: 10.1146/annurev.ph.55.030193.000313.

Renn, S. C., J. H. Park, M. Rosbash, J. C. Hall, and P. H. Taghert. 1999. 'A Pdf Neuropeptide Gene Mutation and Ablation of PDF Neurons Each Cause Severe Abnormalities of Behavioral Circadian Rhythms in Drosophila'. Cell 99(7):791–802. doi: 10.1016/s0092-8674(00)81676-1.

Rieger, Dirk, Ralf Stanewsky, and Charlotte Helfrich-Förster. 2003. 'Cryptochrome, Compound Eyes, Hofbauer-Buchner Eyelets, and Ocelli Play Different Roles in the Entrainment and Masking Pathway of the Locomotor Activity Rhythm in the Fruit Fly Drosophila Melanogaster'. Journal of Biological Rhythms 18(5):377–91. doi: 10.1177/0748730403256997.

Roenneberg, Till, Serge Daan, and Martha Merrow. 2003. 'The Art of Entrainment'. Journal of Biological Rhythms 18(3):183–94. doi: 10.1177/0748730403018003001.

Schlichting, Matthias. 2020. 'Entrainment of the Drosophila Clock by the Visual System'. Neuroscience Insights 15:2633105520903708. doi: 10.1177/2633105520903708.

Schlichting, Matthias, Madelen M. Díaz, Jason Xin, and Michael Rosbash. 2019. 'Neuron-Specific Knockouts Indicate the Importance of Network Communication to Drosophila Rhythmicity' edited by A. Sehgal and C. Dulac. ELife 8:e48301. doi:

10.7554/eLife.48301.

Senthilan, Pingkalai R., Rudi Grebler, Nils Reinhard, Dirk Rieger, and Charlotte Helfrich-Förster. 2019. 'Role of Rhodopsins as Circadian Photoreceptors in the Drosophila Melanogaster'. Biology 8(1):6. doi: 10.3390/biology8010006.

Shafer, Orie Thomas, Charlotte Helfrich-Förster, Susan Christine Portia Renn, and Paul H. Taghert. 2006. 'Reevaluation of Drosophila Melanogaster's Neuronal Circadian Pacemakers Reveals New Neuronal Classes'. Journal of Comparative Neurology 498(2):180–93. doi: 10.1002/cne.21021.

Shang, Yuhua, Leslie C. Griffith, and Michael Rosbash. 2008. 'Light-Arousal and Circadian Photoreception Circuits Intersect at the Large PDF Cells of the Drosophila Brain'. Proceedings of the National Academy of Sciences of the United States of America 105(50):19587–94. doi: 10.1073/pnas.0809577105.

Stanewsky, Ralf, Brigitte Frisch, Christian Brandes, Melanie J. Hamblen-Coyle, Michael Rosbash, and Jeffrey C. Hall. 1997. 'Temporal and Spatial Expression Patterns of Transgenes Containing Increasing Amounts of the Drosophila Clock Geneperiod and a LacZ Reporter: Mapping Elements of the PER Protein Involved in Circadian Cycling'. Journal of Neuroscience 17(2):676–96. doi: 10.1523/JNEUROSCI.17-02-00676.1997.

Stanewsky, Ralf, Maki Kaneko, Patrick Emery, Bonnie Beretta, Karen Wager-Smith, Steve A. Kay, Michael Rosbash, and Jeffrey C. Hall. 1998. 'The Cryb Mutation Identifies Cryptochrome as a Circadian Photoreceptor in Drosophila'. Cell 95(5):681–92. doi: 10.1016/S0092-8674(00)81638-4.

Stoleru, Dan, Ying Peng, José Agosto, and Michael Rosbash. 2004. 'Coupled Oscillators Control Morning and Evening Locomotor Behaviour of Drosophila'. Nature 431(7010):862–68. doi: 10.1038/nature02926.

Tang, Chih-Hang Anthony, Erica Hinteregger, Yuhua Shang, and Michael Rosbash. 2010. 'Light-Mediated TIM Degradation within Drosophila Pacemaker Neurons (s-LNvs) Is Neither Necessary nor Sufficient for Delay Zone Phase Shifts'. Neuron 66(3):378–85. doi: 10.1016/j.neuron.2010.04.015.

Tanoue, Shintaro, Parthasarathy Krishnan, Balaji Krishnan, Stuart E. Dryer, and Paul E. Hardin. 2004. 'Circadian Clocks in Antennal Neurons Are Necessary and Sufficient for Olfaction Rhythms in Drosophila'. Current Biology 14(8):638–49. doi:

10.1016/j.cub.2004.04.009.

Yao, Z., and O. T. Shafer. 2014. ‘The Drosophila Circadian Clock Is a Variably Coupled Network of Multiple Peptidergic Units’. Science 343(6178):1516–20. doi: 10.1126/science.1251285.

Yao, Zepeng, Amelia J. Bennett, Jenna L. Clem, and Orie T. Shafer. 2016. ‘The Drosophila Clock Neuron Network Features Diverse Coupling Modes and Requires Network-Wide Coherence for Robust Circadian Rhythms’. Cell Reports 17(11):2873–81. doi: 10.1016/j.celrep.2016.11.053.

Yoshii, Taishi, Christiane Hermann-Luibl, and Charlotte Helfrich-Förster. 2016. ‘Circadian Light-Input Pathways in Drosophila’. Communicative & Integrative Biology 9(1):e1102805. doi: 10.1080/19420889.2015.1102805.

Yoshii, Taishi, Takeshi Todo, Corinna Wülbeck, Ralf Stanewsky, and Charlotte Helfrich-Förster. 2008. ‘Cryptochrome Is Present in the Compound Eyes and a Subset of Drosophila’s Clock Neurons’. The Journal of Comparative Neurology 508(6):952–66. doi: 10.1002/cne.21702.

Zeng, Hongkui, Zuwei Qian, Michael P. Myers, and Michael Rosbash. 1996. ‘A Light-Entrainment Mechanism for the Drosophila Circadian Clock’. Nature 380(6570):129–35. doi: 10.1038/380129a0.

Zhang, Luoying, Brian Y. Chung, Bridget C. Lear, Valerie L. Kilman, Yixiao Liu, Guruswamy Mahesh, Rose-Anne Meissner, Paul E. Hardin, and Ravi Allada. 2010. ‘DN1p Circadian Neurons Coordinate Acute Light and PDF Inputs to Produce Robust Daily Behavior in Drosophila’. Current Biology 20(7):591–99. doi: 10.1016/j.cub.2010.02.056.

Zhang, Yong, Yixiao Liu, Diana Bilodeau-Wentworth, Paul E. Hardin, and Patrick Emery. 2010. ‘Light and Temperature Control the Contribution of Specific DN1 Neurons to Drosophila Circadian Behavior’. Current Biology 20(7):600–605. doi: 10.1016/j.cub.2010.02.044.

ARTICLE 3

A single photoreceptor splits perception and circadian tasks by two neurotransmitters

Na Xiao[1-5], Shuang Xu[1-4], Ze-Kai Li[1-4], Min Tang[1-4], Renbo Mao[1,2], Tian Yang[1-4], Si- Xing Ma[1-4], Peng-Hao Wang[1-4], Meng-Tong Li[1-4,8], Ajay Sunilkumar[6], François Rouyer[6], Li-Hui Cao[7] & Dong-Gen Luo[1-5,9]

Affiliations:

[1]State Key Laboratory of Membrane Biology, School of Life Sciences, Peking University, Beijing 100871, China

[2]IDG/McGovern Institute for Brain Research, Peking University, Beijing 100871, China

[3]Peking-Tsinghua Center for Life Sciences, Academy for Advanced Interdisciplinary Studies, Peking University, Beijing 100871, China

[4]School of Life Sciences, Peking University, Beijing 100871, China

[5]Center for Quantitative Biology, Academy for Advanced Interdisciplinary Studies, Peking University, Beijing 100871, China

[6]Institut des Neurosciences Paris-Saclay, Université Paris-Sud, Université Paris-Saclay, CNRS, 91190 Gif-sur-Yvette, France

[7]School of Basic Medical Sciences, Beijing Key Laboratory of Neural Regeneration and Repair, Capital Medical University, Beijing 100069, China

[8]Present address: Zuckerman Mind Brain and Behavior Institute, Columbia University, NY 10032, USA

[9]Chinese Institute for Brain Research, Beijing 102206, China

***Correspondence:** dgluo@pku.edu.cn

Abstract

As a vital sense, vision enables both image-forming perception, driven by a contrast-based pathway, and subconscious non-image-forming circadian entrainment, driven by an irradiance-based pathway[1,2]. Although there are two distinct photoreceptor populations specialized for each visual task[3-6], image-forming photoreceptors can additionally contribute to photoentrainment of the circadian clock across species[7-18]. However, it is unknown how the image-forming photoreceptor pathway can functionally implement the segregation of irradiance signals required for circadian entrainment from contrast signals required for image perception. Here we report that the *Drosophila* R8 photoreceptor separates image-forming and irradiance signals by co-releasing two neurotransmitters, histamine and acetylcholine (ACh). This segregation is further established postsynaptically by histamine receptor-expressing unicolumnar retinotopic neurons and ACh receptor-expressing multicolumnar integration neurons. The latter is also regulated by histaminergic negative feedback. At the behavioral level, the elimination of histamine or ACh transmission impairs R8-driven motion detection and circadian photoentrainment, respectively. Thus, a single type of photoreceptor can achieve the dichotomy of visual perception and circadian entrainment as early as the first visual synapses, revealing a simple yet robust mechanism to segregate and translate distinct sensory features into different animal behaviors.

Introduction

The principle that irradiance signals for circadian entrainment can be generated by the conventional image-forming visual pathway is conserved across species[7-18]. In mammals, vision begins with light detection by retinal rod and cone photoreceptors[19], and sacrifices the absolute irradiance information to extract local contrast by constructing center-surround antagonistic receptive fields in bipolar cells[20,21]. Interestingly, bipolar cells also transmit irradiance information from rods and cones to intrinsically photosensitive retinal ganglion cells (ipRGCs) that are required for circadian entrainment[7-10]. Unlike conventional RGCs responsible for image-forming vision, ipRGCs that photoentrain circadian clocks do not exhibit center-surround antagonistic receptive fields even for rod/cone inputs[22-24], consistent with their role in coding overall irradiance instead of contrast. However, it is unclear whether and how conventional rod/cone and bipolar cell circuits upstream of ipRGCs can generate irradiance signals and separate them from their image-forming signals. The circadian clock in the *Drosophila* brain also receives irradiance signals from conventional retinal photoreceptors[11-18] but, like in mammals, the underlying neural mechanisms that generate and segregate irradiance signals remain unknown. Here, we identify a novel mechanism that enables such segregation in the *Drosophila* visual system. A single type of retinal photoreceptor cell separates visual perception and circadian entrainment by co-releasing two neurotransmitters at the first visual synapse, exemplifying a simple yet robust solution to the retina's multi-tasking needs.

Results

Histamine-independent irradiance signals

Drosophila has three types of eye structures: ocelli, Hofbauer-Buchner (H-B) eyelets, and compound eyes[25], the last of which generate signals for both image-forming vision and circadian entrainment[11-18]. Because in addition to the canonical neurotransmitter histamine used for image-forming vision[26], acetylcholine (ACh) has recently been implicated in a subgroup of compound-eye photoreceptors[11,27,28], we examined whether light-induced depolarization in clock neurons[15] depend on the canonical histamine signaling or other neurotransmitter signaling from photoreceptors (Fig. 1a). Surprisingly, clock neurons (including arousal neurons[29]: large ventrolateral neurons or l-LNvs; morning cells[30,31]: small ventrolateral neurons or s-LNvs; and evening cells[30,31]: ion transport peptide-expressing dorsolateral neuron or ITP-LNd and the 5th s-LNv) exhibited robust, though reduced, light-induced depolarization in the null mutant of histamine synthesizing enzyme histidine decarboxylase (HDC) *Hdc^{JK910}* (ref. 32) or null mutants of both histamine receptors in photoreceptor/glia (*HisCl1*) and second- order retinal neurons (*ort*)[11,33,34] (*HO*; *HisCl1^{134},ort^{1}*) (Fig. 1b). These responses were independent of cryptochrome[5,6] as they remained in the triple mutant flies lacking cryptochrome, HisCl1, and ort (*CHO*; *cry^{02},HisCl1^{134},ort^{1}*) (Extended Data Fig. 1), suggesting that clock neurons receive non-histaminergic inputs from the eyes. Furthermore, non-histaminergic inputs were completely absent in flies lacking phospholipase C (PLC; *norpA^{P41}*) under light intensities tested in this work (Fig. 1c), revealing their dependence on PLC-mediated canonical phototransduction. Physical removal of compound eyes and H-B eyelets abolished non-histaminergic inputs to clock neurons (Fig. 1c), but these inputs remained, though reduced, following genetic (Fig. 1d and Extended Data Fig. 2a) or laser ablation of H-B eyelets (Fig. 1d and Extended Data Fig. 2b-e). Thus, compound eyes can generate non-histaminergic signals that excite clock neurons.

To investigate which photoreceptor subtype generates these non-histaminergic signals in compound eyes, we genetically manipulated the functions of individual photoreceptor subtypes in flies with H-B eyelets laser-ablated (Fig. 1e). Histamine- independent responses of clock neurons were intact after transmission blockade[35] in R1-R7 photoreceptors expressing Rh1/3/4, but reduced following blockade in pale R8 (pR8, expressing Rh5) or

yellow R8 (yR8, expressing Rh6) photoreceptors[36] (Extended Data Fig. 2f). Furthermore, *norpA* rescue in pR8s or yR8s partially restored histamine- independent responses in *norpA*^{P41};; *HO* flies with H-B eyelets laser-ablated (Fig. 1e), confirming that R8s provide non-histaminergic inputs to the circadian clock. Finally, these responses were completely lost when both pR8s and yR8s were blocked (Extended Data Fig. 2f) or when both Rh5 and Rh6 were mutated (Fig. 1e), demonstrating their origin exclusively from R8s. Because R8-mediated responses to brief pulses of light were comparable in the presence or absence of histamine receptors in *norpA*^{P41} flies with H-B eyelets laser ablated (Fig. 1f), we concluded that although histamine is the canonical neurotransmitter of the compound eyes, R8s do not use it to transmit irradiance signals to clock neurons.

R8s release two neurotransmitters

Histamine is the known canonical neurotransmitter used by compound eyes[26], we confirmed this by observing the vesicular histamine transporter LOVIT (loss of visual transmission)[37] in the medulla (Extended Data Fig. 3a), where R8 axons terminate. In addition, we observed a similar expression pattern for HDC (Extended Data Fig. 3a). Double labeling confirmed that R8s express both LOVIT and HDC (Extended Data Fig. 3b), and thus have the ability to employ histaminergic neurotransmission. We, therefore, sought to identify the neurotransmitter responsible for their non-histaminergic signals by utilizing the recently developed chemoconnectomics tool[38] (Fig. 2a). Genetic intersection revealed that R8s express the ACh synthesizing enzyme ChAT (Fig. 2a, b), as well as the vesicular ACh transporter VAChT (Fig. 2c), supported by the prior RNA- seq results[27]. Interestingly, VAChT- and ChAT-labeled R8s were also immunopositive for LOVIT (Fig. 2c, d), suggesting that single R8s release both histamine and ACh during neurotransmission. In contrast, ChAT was not expressed in R1–R7 photoreceptors (Extended Data Fig. 3c), and other transmitters, including GABA, glutamate, serotonin, and dopamine, were absent in R8s (Extended Data Fig. 3d).

Because R8s have been implicated in both color vision[34,39,40] and circadian photoreception[11,12,17], we wondered whether their two transmitters may perform distinct roles and investigated these roles with behavioral tests. Due to the lack of a robust assay for color vision[41] and the interactions between motion detection and color vision[42], we

monitored fly behavioral responses to motion stimuli[43]. By rescuing *norpA* in R8s of *norpA*^{P41} mutant flies, we could study the specific role of R8s in motion detection (Fig. 2e) and circadian entrainment by monitoring locomotion activity when H-B eyelets were genetically ablated (Fig. 2f). We found that *norpA* rescue in R8s restored the ability of *norpA*^{P41} mutant flies to track moving bars (Fig. 2e and Extended Data Fig. 4a) and re-entrain to phase shifts of dim light-dark (LD) cycles (Fig. 2f and Extended Data Fig. 4b). Genetically disabling the histamine synthesizing enzyme HDC in R8s or the histamine receptor *ort* abolished R8-mediated motion detection (Fig. 2g and Extended Data Fig. 4c) but not circadian entrainment (Fig. 2h and Extended Data Fig. 4d). Conversely, ChAT knock-out in R8s abolished circadian entrainment (Fig. 2i and Extended Data Fig. 4e) but not motion detection (Fig. 2j and Extended Data Fig. 4f). We, therefore, concluded that R8s use histamine and ACh to drive motion detection and circadian entrainment, respectively.

ACh and histamine act on distinct neurons

To dissect the downstream circuits that support the segregation of R8-mediated visual perception from circadian entrainment, we labeled postsynaptic neurons of R8s with the anterograde trans-synaptic tracing tool *trans*-Tango[44] (Extended Data Fig. 5a). To selectively label ACh-responsive postsynaptic neurons, we further used *ort-QS* to exclude histamine-responsive neurons by suppressing QF-driven tdTomato expression in *trans*-Tango-labeled ort-expressing postsynaptic neurons[11,35]. We found one subgroup of postsynaptic multicolumnar neurons that innervate the accessory medulla (aMe), the hub that relays eye inputs to clock neurons[15], and also shows both multicolumnar arborization in the medulla and contralateral projection via a dorsal commissure with the shape of a working-recurve bow (Fig. 3a). A subpopulation of neurons labeled by *VT037867-Gal4* (ref. 45) showed similar morphological features. These *VT037867* neurons overlapped with the *trans*-Tango-labeled postsynaptic ort- independent neurons of R8s by sharing the same arcuate dorsal commissure (Fig. 3b and Extended Data Fig. 5b). Our single-cell morphological analysis of VT037867- labeled neurons by MultiColor FlipOut (MCFO)[46] revealed their characteristic features with aMe innervation, multicolumnar arborization, and an arcuate dorsal commissure (Extended Data Fig. 5c), which are consistent with single-cell morphology revealed by neurobiotin injection to a single neuron (Extended Data Fig. 5d). We named these ***a***Me- innervating, ***m***ulticolumnar, and ***a***rcuate neurons AMA neurons. In

addition, these AMA neurons contact both pR8 and yR8 visual columns (Extended Data Fig. 6). Moreover, GFP Reconstitution Across Synaptic Partners (GRASP)[47] confirmed close contacts between R8s and AMA neurons in the M1–M3 layers of the medulla (Fig. 3c), where R8 axons terminate. Furthermore, photoactivation of the photoactivable GFP (PA-GFP)[48]-expressing AMA neurons, specifically in the commissure track, revealed a total of 10 pairs of AMA neurons (Extended Data Fig. 7a). Interestingly, we found that the aMe 12 neurons identified as the postsynaptic neurons of R8s[49] were a subgroup of AMA neurons (Extended Data Fig. 7b). To identify histamine-responsive postsynaptic neurons, we performed double labeling with *ort-LexA*-driven GFP and R8-driven *trans*- Tango. A large population of visual neurons was co-labeled (Extended Data Fig. 8), including L1, Tm5, Tm9, and Tm20, all known to be postsynaptic partners of R8s[27,39,40,49-51]. Chemoconnectomics confirmed that L1, Tm5, Tm9, and Tm20 express *ort* (Fig. 3d), and GRASP confirmed their close contact with R8s (Fig. 3e), consistent with prior reports[27,49,51]. Together, these data show that R8s make connections with two populations of visual neurons: multicolumnar AMA neurons receiving non-histaminergic inputs and unicolumnar L1/Tm neurons receiving histaminergic inputs.

In contrast to the conventional view that light hyperpolarizes the second-order retinal neurons[26], we found that AMA neurons depolarize upon light stimulation. This depolarization was lost when both Rh5 and Rh6 were mutated, and restored with *norpA* rescued in R8s of *norpA*^{P41} mutant flies (Fig. 3f and Extended Data Fig. 9a, b). Furthermore, the nicotinic ACh receptor antagonist mecamylamine (MCA)[15], but not the histamine receptor blocker cimetidine (CIM), blocked light-induced depolarization of AMA neurons (Fig. 3g). Finally, the depolarizing response was completely lost following conditional knockout of either ChAT or VAChT in R8s, but remained unchanged when HDC or histamine receptors were mutated (Fig. 3g). We also observed conventional light-induced hyperpolarization of postsynaptic neurons of R8s, including L1, Tm9 and Tm20 (Fig. 3h). Exogenous histamine directly induced CIM-sensitive hyperpolarization in L1, Tm9 and Tm20 (Extended Data Fig. 9c), and genetic or pharmacological disruption of histamine receptors abolished R8-mediated hyperpolarization (Fig. 3h and Extended Data Fig. 9d). A small MCA-sensitive depolarization was apparent in the absence of histamine signaling (Fig. 3h), indicating that even though R8s drive a minor excitatory response, they predominantly hyperpolarize L1, Tm9 and Tm20 via histamine signaling. Together, these results demonstrate that physiological activation of R8s depolarizes VT037867 neurons via ACh

but hyperpolarizes L1, Tm9, and Tm20 via histamine. The histamine transmission from R8s to L1 may account for the observed motion detection by R8s (Fig. 2e) since L1 is one of the two major motion pathways[52].

We next investigated whether R8s release ACh and histamine at the same or different presynaptic sites. We developed a modified GRASP method[47] by expressing the two complementary split-GFP fragments only at postsynaptic sites of two different neurons so that reconstituted GFP signals would occur only when the two neurons share the same presynaptic terminal (Extended Data Fig. 10a, b). We termed this method polyadic synaptic GRASP (p-GRASP). Strong p-GRASP signals were observed in M1-M3 between AMA and Tm9 or Tm20 neurons (Fig. 3i and Extended Data Fig. 10c, d), implying that these neurons can possibly encounter both ACh and histamine in the same polyadic R8 synapse, which is also implicated in another study[27]. To verify this, we ectopically expressed *ort* in AMA neurons of triple mutant *CHO* flies (Extended Data Fig. 11). Unlike the monophasic depolarization in *WT* flies, *ort*-expressing AMA neurons showed biphasic responses to light stimulation (Fig. 3j). Furthermore, a depolarizing component via ACh was revealed in the presence of CIM and a hyperpolarizing component via histamine in the presence of MCA (Fig. 3j). Thus, AMA neurons encounter both ACh and histamine, while the monophasic responses in *WT* flies are due to ACh but not histamine.

Based on these data, we propose a model in which histamine and ACh co-release is segregated postsynaptically (Fig. 3k). Upon light stimulation, R8s depolarize and release both histamine and ACh at the same axonal terminals, but postsynaptic neurons expressing distinct transmitter receptors segregate these signals. Consequently, AMA neurons are depolarized, and L1/Tm neurons are hyperpolarized by light.

Irradiance detection by a three-node circuit

To investigate how AMA neurons relay non-histaminergic signals to the circadian clock, we immunostained the clock protein TIMELESS (TIM) and pigment dispersing factor (PDF) to examine whether anterograde *trans*-Tango tracing can label clock neurons as their postsynaptic neurons, and found that clock neurons, including s-LNv, l-LNv, 5^{th} s-LNv, and ITP-LNd, are postsynaptic to AMA neurons (Fig. 4a and Extended Data Fig. 12a-c). Moreover, retrograde trans-synaptic tracing using Botulinum-Activated Tracer

(BAcTrace)[53] confirmed that AMA neurons are presynaptic to clock neurons (Fig. 4b). We verified their functional connections using optogenetic activation of AMA neurons, which induced excitatory postsynaptic currents (EPSCs) with increasing amplitudes from s-LNvs, to l-LNvs, ITP-LNd, and the 5th s-LNv (Fig. 4c). Thus, AMA neurons make stronger connections with evening cells (5th s-LNv and ITP-LNd) than with arousal (l-LNvs) and morning cells (s-LNvs). Indeed, R8-driven light responses in clock neurons also showed the same order of strength (Extended Data Fig. 12d). MCA abolished AMA-driven EPSCs in clock neurons and genetic intersection confirmed that AMA neurons are acetylcholinergic (Fig. 4d). Moreover, when transmission from AMA neurons was blocked, light activation of R8s failed to excite clock neurons (Fig. 4e). Together, these data indicate that R8s, AMA, and clock neurons form a three-node circuit that drives circadian entrainment and that they do so by means of cholinergic transmission.

Because each AMA neuron innervates many columns in the medulla, we examined how it integrates spatial and spectral irradiance information. A single MCFO-labeled AMA neuron showed widespread arborization in ~100 visual columns (Fig. 4f) and innervation of both blue-sensitive pR8 and green-sensitive yR8 columns (Fig. 4g). Little overlap in columnar arborization was found between two random AMA neurons (Fig. 4f). On the other hand, neurobiotin injection revealed dye coupling among AMA neurons, which was absent in *shakB*^{2} mutant flies (Fig. 4h). This implies that innexin 8 mediates electrical coupling between AMA neurons, which we verified by dual patch- clamp recordings (Fig. 4i). We also found that AMA neurons were mutually coupled via cholinergic chemical synapses: *trans*-Tango tracing revealed AMA neurons as their own postsynaptic neurons (Fig. 4h) and mutual excitation between AMA neurons was reduced by a non-selective chemical transmission blocker cadmium (Fig. 4i). Furthermore, we found that light-triggered calcium responses of a single AMA neuron increased with the size of stimulating light spots and reached maximum only when the eye was fully covered by light stimulation (Extended Data Fig. 13), implying irradiance integration via its medulla-wide dendritic arborization. Thus, AMA neurons can integrate spatial and spectral irradiance signals via their multicolumnar and dual pR8/yR8 columnar arborization, respectively, and also share irradiance signals via their mutual electrical and chemical coupling.

Histamine feedback supports ACh release

Although double mutant flies (*CO*; *cry*^{0}, *ort*^{1}) can re-entrain to new LD cycles (Fig. 2h), *CHO* flies that additionally lack the histamine receptor HisCl1 were unable to photoentrain and HisCl1 rescue in R8s restored entrainment (Fig. 5a), consistent with a prior report[11]. Thus, HisCl1 appears to be indispensable for ACh-mediated circadian photoentrainment via an unknown mechanism. We investigated this mechanism by comparing light-induced responses of AMA neurons in the *CO* and *CHO* flies. Brief pulses of light elicited similar responses (Extended Data Fig. 14), but long steps of light elicited an initial transient depolarization followed by a relaxed steady depolarization in *CO* flies and just an initial transient in *CHO* flies (Fig. 5b). Because HisCl1 rescue in R8s restores circadian entrainment (Fig. 5a and ref. 11), we tested the same rescue on light-induced responses of AMA neurons and observed restoration of the steady depolarization in *CHO* flies (Fig. 5c). Moreover, pharmacological blockade of HisCl1 in *WT* flies also abolished the steady depolarization (Fig. 5d), and the histaminergic feedback in R8s sufficed to sustain steady depolarization in the transgenic flies with only R8s but not R7s in light detection (Extended Data Fig. 15). In contrast, in the absence of HisCl1, we observed an increase of light-triggered steady hyperpolarization in *ort*-expressing AMA neurons in the presence of MCA (Fig. 5e), implying an increase of continuous histamine release. Together, these results revealed that the cell-autonomous histaminergic feedback in R8s is required for continuous ACh release but not for continuous histamine release during long light illumination.

Such feedback could maintain continuous presynaptic ACh release or prevent desensitization of postsynaptic ACh receptors. However, AMA neurons in *CHO* flies could respond to exogenous application of pulses of ACh in the same way before, during, and after a long step of light (Fig. 5f) and exogenous application of steps of ACh could produce prolonged depolarizing responses (Extended Data Fig. 16a), suggesting that postsynaptic ACh receptors are not affected by this feedback effect. We next investigated whether histaminergic feedback affects presynaptic transmitter release. Calcium imaging in R8 axons with GCaMP6f showed that steps of light-induced a slight increase of calcium influx in the absence of HisCl1 (Extended Data Fig. 16b). Together with the evidence that ACh release from R8s showed a higher sensitivity to calcium changes than histamine (Extended Data Fig. 16c), the loss of ACh-mediated steady responses may reflect no continuous ACh release possibly due to local depletion in the absence of HisCl1-mediated negative feedback.

Given that AMA neurons can respond to short pulses of light in the absence of HisCl1 (Extended Data Fig. 14), we wondered whether they could maintain their responses to long trains of brief pulses of light. For a given intensity and pulse duration, AMA neurons had sustained responses to trains of low-frequency (≤ 1 Hz) but not high-frequency pulses (Fig. 5g). Moreover, clock neurons responded to short pulses of light with a similar frequency dependence in *CHO* flies (Extended Data Fig. 17). Interestingly, *CHO* flies displayed circadian entrainment when the light phase of LD cycles comprised brief light pulses at 1 Hz but not other tested frequencies including the 0.2 Hz that triggered robust sustained responses every 5 seconds (Fig. 5h), indicating that the circadian clock can be entrained only via proper temporal integration of clock-resetting molecules produced by light pulse-triggered transient electrical responses. In contrast, wild-type flies are entrained to all the tested frequencies (Extended Data Fig. 18). Together, these data indicate that the dual transmitter signaling in R8s interacts through negative histaminergic feedback (Fig. 5i).

Discussion

We have shown that R8 photoreceptors split tasks of visual perception and circadian entrainment by co-releasing two different neurotransmitters. This segregation is further supported by postsynaptic circuitry in the medulla, such that each unicolumnar neuron mainly receives histaminergic inputs from a single R8 photoreceptor (thus transmitting the retinotopic signal), whereas each multicolumnar aMe-innervating neuron integrates cholinergic inputs from hundreds of R8 photoreceptor cells (thus integrating the irradiance signal). These aMe-innervating neurons directly excite downstream clock neurons, forming a shallow three-node circuit for circadian entrainment. Thus, this clock-entrainment circuit integrates irradiance signals directly from conventional photoreceptors, bypassing the downstream image-forming processing circuit to avoid a less efficient reconstruction of irradiance signals from highly-processed signals in contrast-encoding visual pathways.

Our observation that compound eye-driven responses in clock neurons were reduced by half in the absence of histamine receptors (Fig. 1b) suggests that conventional photoreceptors other than R8s, for example, R1-R6, can use histamine-mediated circuitry pathways to excite clock neurons for circadian entrainment[12,15,18]. The downstream circuits of R1-R6 photoreceptors might reconstruct irradiance signals from image-forming signals via yet-to-be-uncovered mechanisms as mammalian rod/cone pathways do[22-24], given that the mechanisms underlying the conserved irradiance coding for circadian entrainment by conventional photoreceptor pathways evolved convergently.

We also identified unexpected crosstalk between the image-forming vision and circadian entrainment. The chloride channel HisCl1 mediates negative feedback of histamine in R8 photoreceptor cells, thus dynamically reducing photoreceptor depolarization during long light stimulation. This feedback regulation tunes ACh release to avoid its local depletion so that the irradiance signal can be continuously transmitted from R8s to clock neurons during the entire light phase.

Our work demonstrates that visual perception and circadian entrainment can be segregated as early as the first-order synapses in the visual system, providing a simple yet robust mechanism to enact distinct sensory functions. Furthermore, although the co-release of neurotransmitters is an emerging principle in brain research[54,55], its behavioral significance remains largely unknown. Our finding that co-release enables segregation and

translation of distinct visual features from the same photoreceptor cells into different behaviors paves the way for understanding this key, indispensable aspect of the nervous system.

References

1. Lazzerini Ospri, L., Prusky, G., & Hattar, S. Mood, the Circadian System, and Melanopsin Retinal Ganglion Cells. *Annu. Rev. Neurosci.* **40**, 539-556 (2017).
2. Do, M.T.H. Melanopsin and the Intrinsically Photosensitive Retinal Ganglion Cells: Biophysics to Behavior. *Neuron* **104**, 205-226 (2019).
3. Berson, D.M., Dunn, F.A., & Takao, M. Phototransduction by retinal ganglion cells that set the circadian clock. *Science* **295**, 1070-1073 (2002).
4. Hattar, S., Liao, H.W., Takao, M., Berson, D.M., & Yau, K.W. Melanopsin- containing retinal ganglion cells: architecture, projections, and intrinsic photosensitivity. *Science* **295**, 1065-1070 (2002).
5. Emery, P., So, W.V., Kaneko, M., Hall, J.C., & Rosbash, M. CRY, a *Drosophila* clock and light-regulated cryptochrome, is a major contributor to circadian rhythm resetting and photosensitivity. *Cell* **95**, 669-679 (1998).
6. Stanewsky, R. et al. The cryb mutation identifies cryptochrome as a circadian photoreceptor in *Drosophila*. *Cell* **95**, 681-692 (1998).
7. Ruby, N.F. et al. Role of melanopsin in circadian responses to light. *Science* **298**, 2211-2213 (2002).
8. Panda, S. et al. Melanopsin (Opn4) requirement for normal light-induced circadian phase shifting. *Science* **298**, 2213-2216 (2002).
9. Hattar, S. et al. Melanopsin and rod-cone photoreceptive systems account for all major accessory visual functions in mice. *Nature* **424**, 76-81 (2003).
10. Güler, A.D. et al. Melanopsin cells are the principal conduits for rod-cone input to non-image-forming vision. *Nature* **453**, 102-105 (2008).
11. Alejevski, F. et al. The HisCl1 histamine receptor acts in photoreceptors to synchronize *Drosophila* behavioral rhythms with light-dark cycles. *Nat. Commun.* **10**, 252 (2019).
12. Hanai, S., & Ishida, N. Entrainment of *Drosophila* circadian clock to green and yellow light by Rh1, Rh5, Rh6 and CRY. *Neuroreport* **20**, 755-758 (2009).
13. Helfrich-Förster, C. Light input pathways to the circadian clock of insects with an emphasis on the fruit fly *Drosophila melanogaster*. *J. Comp. Physiol. A. Neuroethol. Sens. Neural. Behav. Physiol.* **206**, 259-272 (2020).

14. Helfrich-Förster, C., Winter, C., Hofbauer, A., Hall, J.C., & Stanewsky, R. The circadian clock of fruit flies is blind after elimination of all known photoreceptors. *Neuron* **30**, 249-261 (2001).
15. Li, M.T. et al. Hub-organized parallel circuits of central circadian pacemaker neurons for visual photoentrainment in *Drosophila*. *Nat. Commun.* **9**, 4247 (2018).
16. Schlichting, M., Grebler, R., Peschel, N., Yoshii, T., & Helfrich-Förster, C. Moonlight detection by *Drosophila'*s endogenous clock depends on multiple photopigments in the compound eyes. *J. Biol. Rhythms.* **29**, 75-86 (2014).
17. Szular, J. et al. Rhodopsin 5- and Rhodopsin 6-mediated clock synchronization in *Drosophila melanogaster* is independent of retinal phospholipase C-β signaling. *J Biol Rhythms.* **27**, 25-36 (2012).
18. Saint-Charles, A. et al. Four of the six *Drosophila* rhodopsin-expressing photoreceptors can mediate circadian entrainment in low light. *J. Comp. Neurol.* **524**, 2828-2844 (2016).
19. Yau, K.W. & Hardie, R.C. Phototransduction motifs and variations. *Cell* **139**, 246- 264 (2009).
20. Masland, R.H. The neuronal organization of the retina. *Neuron* **76**, 266-280 (2012).
21. Sanes, J.R. & Zipursky, S.L. Design principles of insect and vertebrate visual systems. *Neuron* **66**, 15-36 (2010).
22. Dacey, D.M. et al. Melanopsin-expressing ganglion cells in primate retina signal colour and irradiance and project to the LGN. *Nature* **433**, 749-754 (2005).
23. Pu, M. Physiological response properties of cat retinal ganglion cells projecting to suprachiasmatic nucleus. *J. Biol. Rhythms.* **15**, 31-36 (2000).
24. Zhao, X., Stafford, B.K., Godin, A.L., King, W.M., & Wong, K.Y. Photoresponse diversity among the five types of intrinsically photosensitive retinal ganglion cells. *J. Physiol.* **592**, 1619-1636 (2014).
25. Hofbauer, A. & Buchner, E. Does *Drosophila* have seven eyes? *Naturwissenschaften* **76**, 335-336 (1989).
26. Hardie, R.C. A histamine-activated chloride channel involved in neurotransmission at a photoreceptor synapse. *Nature* **339**, 704-706 (1989).
27. Davis, F.P. et al. A genetic, genomic, and computational resource for exploring neural circuit function. *eLife* **9**, e50901 (2020).
28. Pagni, M. et al., Interaction of "chromatic" and "achromatic" circuits in *Drosophila* color opponent processing. *Curr. Biol.* **31**, 1687-1698 (2021).

29. Shang, Y., Griffith, L.C., & Rosbash, M. Light-arousal and circadian photoreception circuits intersect at the large PDF cells of the *Drosophila* brain. *Proc. Natl. Acad. Sci. U.S.A.* **105**, 19587–19594 (2008).
30. Grima, B., Chélot, E., Xia, R. & Rouyer, F. Morning and evening peaks of activity rely on different clock neurons of the *Drosophila* brain. *Nature* **431**, 869–873 (2004).
31. Stoleru, D., Peng, Y., Agosto, J. & Rosbash, M. Coupled oscillators control morning and evening locomotor behaviour of *Drosophila*. *Nature* **431**, 862–868 (2004).
32. Sarthy, P.V. Histamine: a neurotransmitter candidate for *Drosophila* photoreceptors. *J. Neurochem.* **57**, 1757-1768 (1991).
33. Rister, J. et al. Dissection of the peripheral motion channel in the visual system of *Drosophila melanogaster*. *Neuron* **56**, 155-170 (2007).
34. Schnaitmann, C. et al. Color Processing in the Early Visual System of *Drosophila*. *Cell* **172**, 318-330 (2018).
35. Schiavo, G. et al. Tetanus and botulinum-B neurotoxins block neurotransmitter release by proteolytic cleavage of synaptobrevin. *Nature* **359**, 832-835 (1992).
36. Morante, J. & Desplan, C. The color-vision circuit in the medulla of *Drosophila*. *Curr. Biol.* **18**, 553-565 (2008).
37. Xu, Y. & Wang, T. LOVIT Is a Putative Vesicular Histamine Transporter Required in *Drosophila* for Vision. *Cell Rep.* **27**, 1327-1333 (2019).
38. Deng, B. et al. Chemoconnectomics: Mapping Chemical Transmission in *Drosophila*. *Neuron* **101**, 876-893 (2019).
39. Gao, S. et al. The neural substrate of spectral preference in *Drosophila*. *Neuron* **60**, 328-342 (2008).
40. Heath, S.L. et al. Circuit Mechanisms Underlying Chromatic Encoding in *Drosophila* Photoreceptors. *Curr Biol.* **30**, 264-275 (2020).
41. Zhu, Y. The *Drosophila* visual system: From neural circuits to behavior. *Cell. Adh. Migr.* **7**, 333-344 (2013).
42. Gruntman, E., Reimers, P., Romani, S., & Reiser, M.B. Non-preferred contrast responses in the *Drosophila* motion pathways reveal a receptive field structure that explains a common visual illusion. *Curr. Biol.* **31**, 5286-5298 (2021).
43. Longden, K.D., Rogers, E.M., Nern, A., Dionne, H., & Reiser, M.B. Synergy of color and motion vision for detecting approaching objects in *Drosophila*. *bioRxiv*, **2021.2011.2003.467132** (2021).

44. Talay, M. et al. Transsynaptic Mapping of Second-Order Taste Neurons in Flies by *trans*-Tango. *Neuron* **96**, 783-795 (2017).
45. Tang, M. et al. An extra-clock ultradian brain oscillator sustains circadian timekeeping. *Sci. Adv.* **8**, eabo5506 (2022).
46. Nern, A., Pfeiffer, B.D., & Rubin, G.M. Optimized tools for multicolor stochastic labeling reveal diverse stereotyped cell arrangements in the fly visual system. *Proc. Natl. Acad. Sci. U.S.A.***112**, E2967-E2976 (2015).
47. Gordon, M.D. & Scott, K. Motor control in a *Drosophila* taste circuit. *Neuron* **61**, 373-384 (2009).
48. Ruta, V. et al. A dimorphic pheromone circuit in *Drosophila* from sensory input to descending output. *Nature* **468**, 686-690 (2010).
49. Kind, E. et al. Synaptic targets of photoreceptors specialized to detect color and skylight polarization in *Drosophila*. *eLife* **10**, e71858 (2021).
50. Karuppudurai, T. et al. A hard-wired glutamatergic circuit pools and relays UV signals to mediate spectral preference in *Drosophila*. *Neuron* **81**, 603-615 (2014).
51. Takemura, S.Y. et al. Synaptic circuits and their variations within different columns in the visual system of *Drosophila*. *Proc. Natl. Acad. Sci. U.S.A.* **112**, 13711-13716 (2015).
52. Tuthill, J.C., Nern, A., Holtz, S.L., Rubin, G.M. & Reiser, M.B. Contributions of the 12 neuron classes in the fly lamina to motion vision. *Neuron* **79**, 128-140 (2013).
53. Cachero, S. et al. BAcTrace, a tool for retrograde tracing of neuronal circuits in *Drosophila*. *Nat. Methods.* **17**, 1254-1261 (2020).
54. Lee, S., Kim, K. & Zhou, Z.J. Role of ACh-GABA cotransmission in detecting image motion and motion direction. *Neuron* **68**, 1159-1172 (2010).
55. Tritsch, N.X., Granger, A.J. & Sabatini, B.L. Mechanisms and functions of GABA co-release. *Nat. Rev. Neurosci.* **17**, 139-145 (2016).

Figures and legends

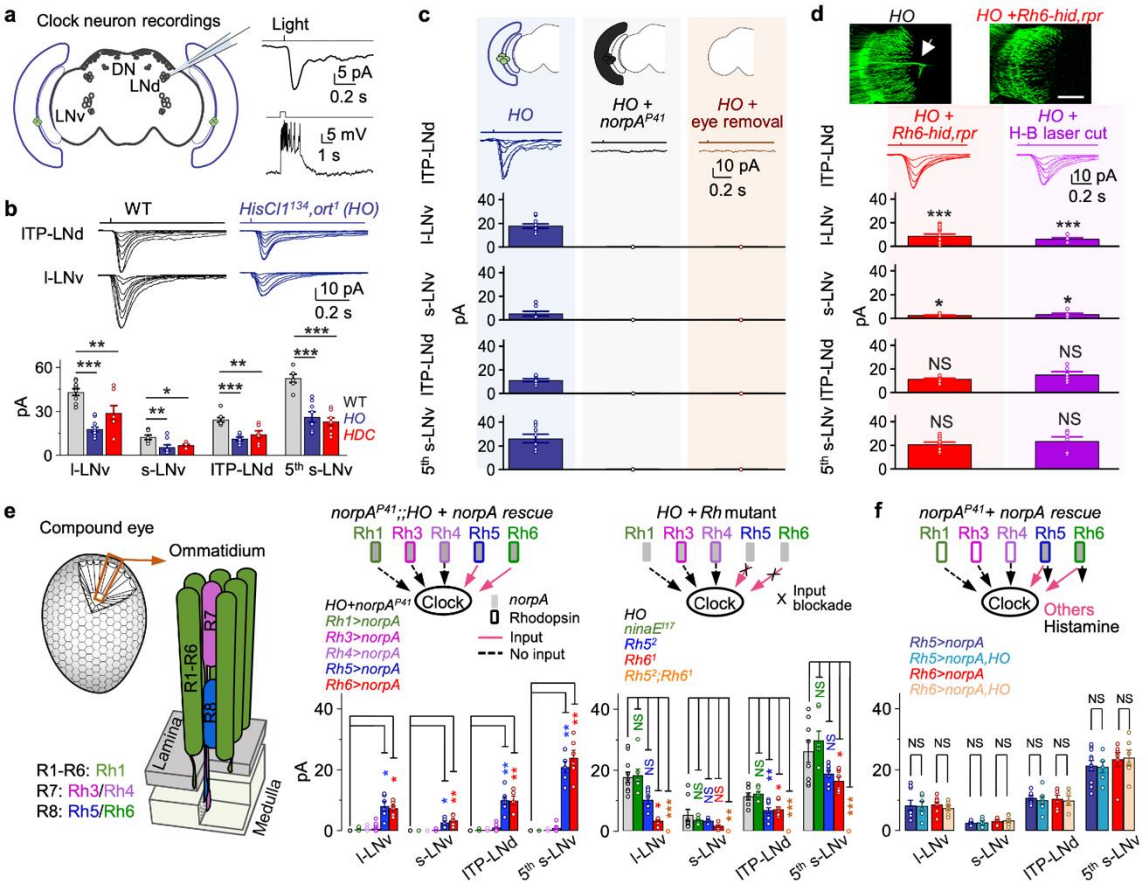

Fig. 1 | Histamine-independent irradiance signals. a, Left, schematic of patch-clamp recording from a clock neuron (ITP-LNd); **right**, representative current (top, voltage-clamp) and voltage (bottom, current-clamp) responses to a pulse of light (470 nm, 2.51×10^7 photons/μm^2/s, top panel: 2 ms, bottom panel: 500 ms). The timing of light stimulation is indicated on the top of the response traces. Genotypes are listed in Extended Data Table 1. **b,** Histamine-independent responses of clock neurons. **Top**, representative responses of ITP-LNd and l-LNv to light stimuli (470 nm, 2 ms) of intensities from 0.025, 0.042, 0.083, 0.20, 0.41, 0.81, 1.93, to 2.80×10^7 photons/μm^2/s; **bottom**, pooled saturated response amplitudes. **c,** Histamine-independent inputs require PLC signaling in the eyes. **Top**, schematic of eye input manipulation; **middle**, representative responses of ITP-LNd in *HO* double mutant flies, *norpA*^{P41};; *HO* triple mutant flies, and *HO* flies with eyes removed; **bottom**, pooled saturated response amplitudes. Light: 470 nm, 2 ms, intensities from 0.025, 0.042, 0.083, 0.20, 0.41, 0.81, 1.93, to 2.80×10^7 photons/μm^2/s. **d,** Histamine-independent signals from

compound eyes are independent of H-B eyelets. **Top**, representative H-B eyelet axons in the flies with GFP in Rh6-expressing photoreceptors, arrow indicates the GFP-labeled H-B eyelet axons (left), the lack of GFP-labeled H-B eyelet axons indicates H-B eyelet ablation by apoptosis genes (hid and reaper) in *Rh6-hid,rpr* flies (right); **middle**, representative recordings of light-induced ITP-LNd responses in flies with genetic ablation (left, at the age of three days after eclosion) and laser ablation (right) of H-B eyelets; **bottom**, pooled saturated responses. The reduced responses in flies with H-B eyelets ablated (compared with *HO* flies) revealed inputs of H-B eyelets to clock neurons. Light: 470 nm, 2 ms, intensities from 0.042, 0.11, 0.25, 0.41, 0.81, 1.93, to 2.80×10^7 photons/μm^2/s. Scale bar: 50 μm. **e,** Histamine-independent signals from R8s. **Left**, schematics of photoreceptors in compound eyes, each compound eye containing approximately 750 ommatidia and each ommatidium containing 8 photoreceptors (R1- R8) that express different rhodopsins (Rh1-Rh6); **middle**, histamine-independent responses in $norpA^{p41}$;; *HO* triple mutant flies with norpA rescued to different photoreceptors (H-B eyelet axons are laser-ablated); **right**, histamine-independent responses in *HO* flies with mutation of different rhodopsin (H-B eyelet axons are laser-ablated). **f,** R8s do not use histamine to transmit irradiance signals. **Top**, schematic of photoreceptor signaling; **bottom**, pooled saturated response amplitudes of R8s of $norpA^{P41}$ flies with norpA rescued in pR8s or yR8s (with or without *HO* mutants; H-B eyelet axons are laser-ablated). Light in **e** and **f**: 470 nm, 2 ms, 2.80×10^7 photons/μm^2/s. Pooled data: mean ± s.e.m. **P* < 0.05; ***P* < 0.01; ****P* < 0.001; NS, not significant. Statistical analysis is summarized in Extended Data Table 2.

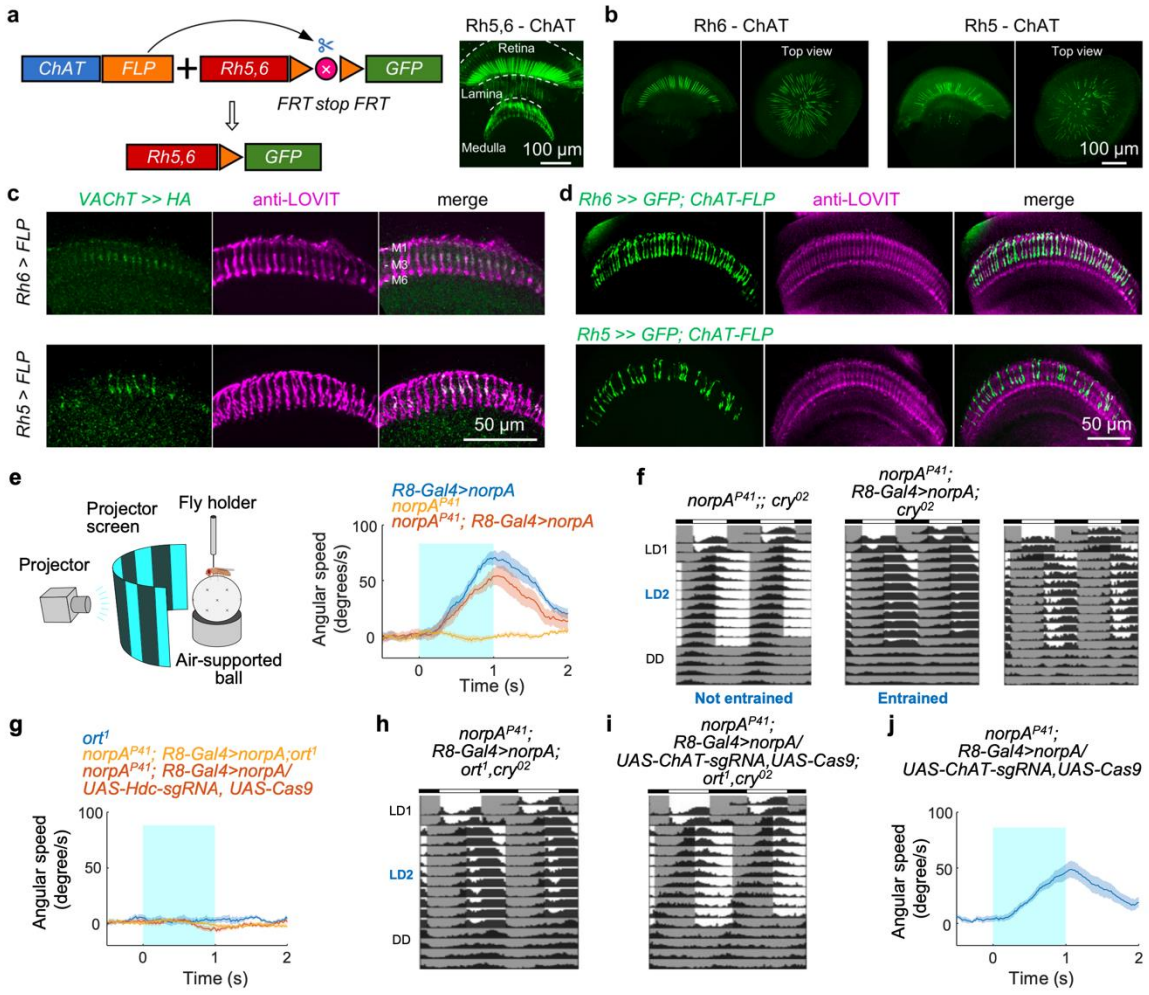

Fig. 2 | R8s use histamine for motion detection and ACh for circadian entrainment. a, R8s contain ACh. **Left**, schematic of genetic intersection; **right**, ChAT in R8s (*Rh5-Gal4+Rh6-Gal4*). **b**, ACh in pR8s (*Rh5-Gal4*) and yR8s (*Rh6-Gal4*). **c,** Single R8s express both VAChT (green, HA tag) and LOVIT (magenta, anti-LOVIT). **d,** Single R8s express both ChAT (green, GFP expression intersected by *ChAT-FLP* and *Rh6/Rh5- Gal4*) and LOVIT (magenta, anti-LOVIT). **e** and **f**, R8s drive both motion detection and circadian entrainment. **e,** Motion detection by R8s. **Left**, schematic of behavioral motion detection; **right**, pooled angular speed in *R8-Gal4>norpA* (n=12), $norpA^{P41}$ (n=18), and $norpA^{P41}$*; R8-Gal4>norpA* (n=13) flies. Data are represented as mean (solid line) and s.e.m. (shading). Visual moving bars: wave width of 30°, angular velocity of 180°/s, contrast of 100%, duration of 1 s. **f,** Circadian entrainment by R8s. Average actograms of the flies of $norpA^{P41}$;; cry^{02} flies (left, n=102), the flies with only R8s and H-B eyelets in dim-light detection (middle, n=93), and the flies with only R8s in dim-light detection (with H-B eyelets ablated

by *Rh6-hid,rpr*) (right, n=73). LD1: 200 lux (white light) together with 25°C/18°C temperature cycles; LD2: 0.05 lux (white light) at 25°C; DD: 25°C. The low light intensity of 0.05 lux in LD2 cycles is used to test specifically the norpA-dependent re-entrainment. **g** and **h**, *ort* is indispensable for R8-mediated motion detection but not circadian entrainment. **g,** Motion detection in *ort* mutants (n=13), *ort* mutants with functional R8s (n=11), or *Hdc*-knockout in R8s (n=11). **h,** Average actograms following genetic ablation of *ort* in $norpA^{P41}$;; cry^{02} flies with norpA rescued in R8s (n=91). **i** and **j**, ACh signaling is required for R8-mediated circadian entrainment but not motion detection. **i**, Average actograms following genetic ablation of both *ort* and *ChAT* in $norpA^{P41}$;; cry^{02} flies with norpA rescued in R8s (n=74). **j,** Pooled angular speed for motion detection by R8s after *ChAT* knockout in $norpA^{P41}$ flies with norpA rescued in R8s (n=12).

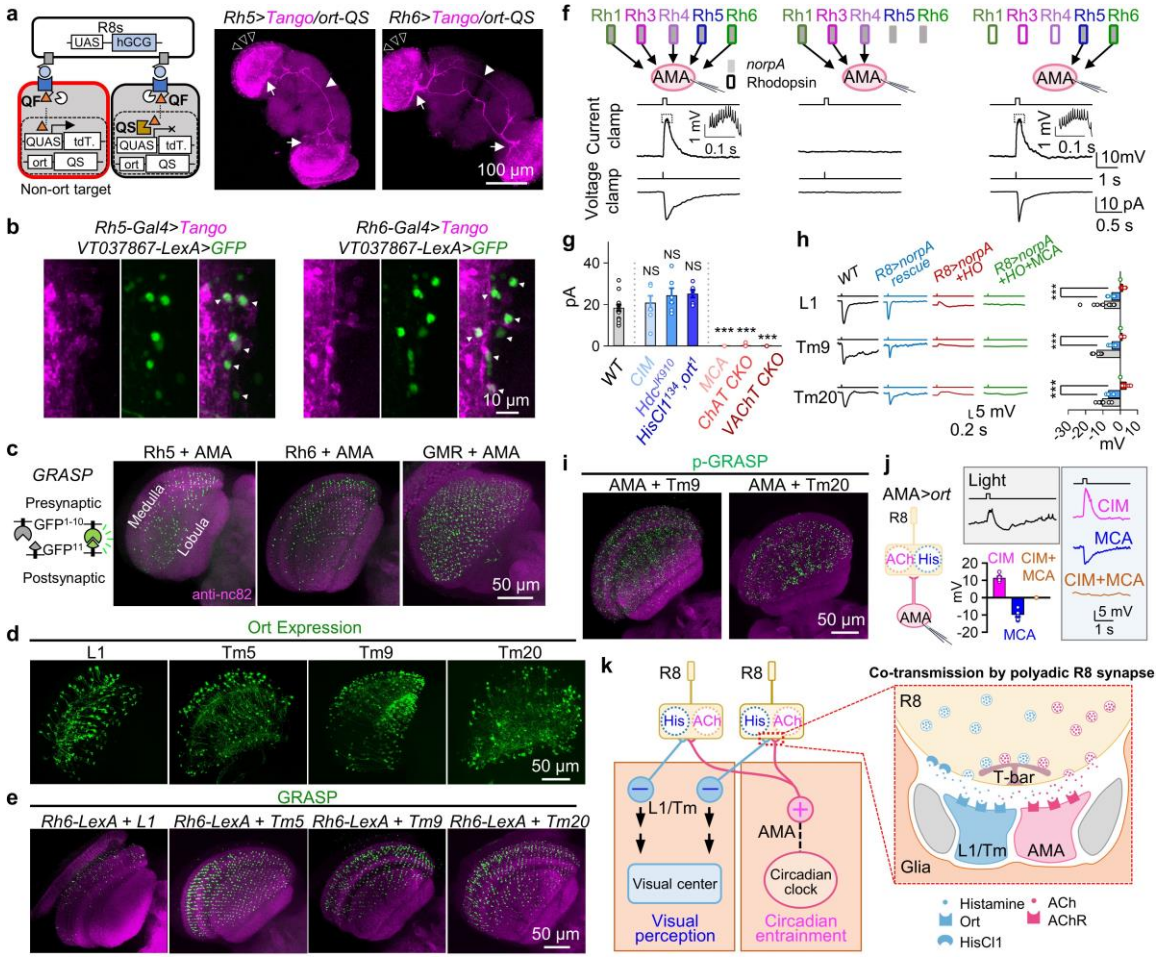

Fig. 3 | ACh and histamine act on distinct neurons. a, *ort*-independent postsynaptic neurons. **Left**, schematic of *trans*-Tango tracing with QS suppression (*ort-QS* excludes QF-driven tdTomato expression in *ort*-expressing neurons); **right**, *ort*-independent postsynaptic neurons of pR8s and yR8s. Unfilled triangles indicate multicolumnar arborization in the medulla, arrows indicate innervation in the aMe; arrowheads indicate the arcuate dorsal commissure. **b,** GFP expression by VT037867-LexA overlaps with *trans*-Tango-labeled *ort*-independent postsynaptic neurons of pR8s (left) and yR8s (right). Arrowheads indicate the co-labeled cells. **c,** Connections between R8s and AMA neurons. **Left**, schematic of GRASP labeling; **right**, GRASP between AMA neurons and pR8s, yR8s, or all photoreceptors (GMR-Gal4). **d,** GFP expression intersected by *ort-LexA>FLP* and *L1, Tm5, Tm9, or Tm20-spGal4*. **e,** GRASP between R8s and L1, Tm5, Tm9, and Tm20. **f,** AMA neurons are excited by R8s. **Top**, schematic of photoreceptor manipulation: wild-type flies (left), $Rh5^{2}$; $Rh6^{1}$ flies (middle), and $norpA^{P41}$ flies with norpA rescued in R8s (right); **middle**, representative light-induced depolarization (current-clamp) of AMA neurons, insets represent spikes in

dashed boxes; **bottom**, representative light-induced inward current (voltage-clamp) of AMA neurons. Light: 470 nm, 5.56×10^7 photons/μm^2/s, 200 ms (current-clamp) and 2 ms (voltage-clamp). **g,** Light-induced saturated responses in AMA neurons of wild-type flies (in the absence or presence of CIM), Hdc^{JK910} flies, *HO* flies, wild-type flies (in the presence of MCA), flies with ChAT conditionally knocked out in R8s, flies with VAChT knocked out in R8s. **h,** Hyperpolarization of ort-expressing postsynaptic neurons. **Left**, representative light-induced hyperpolarization of L1, Tm9, and Tm20 neurons of wild-type flies, $norpA^{P41}$ flies with norpA rescued in R8s, $norpA^{P41}$;; *HO* flies with norpA rescued in R8s, and $norpA^{P41}$;; *HO* flies with norpA rescued in R8s (in MCA); **right**, pooled saturated response amplitudes. Note, a tiny MCA-sensitive depolarization appeared in the absence of histamine signaling. **i,** AMA and Tm9/Tm20 neurons share the same polyadic R8 synapse. p-GRASP between AMA and Tm9 neurons (left) or Tm20 neurons (right). **j,** Histamine-mediated responses in *ort*- expressing AMA neurons. **Left**, schematic of R8 inputs; **right**, representative biphasic light responses in normal saline (top left), depolarization in CIM and hyperpolarization in MCA, no response in CIM and MCA, and pooled data (bottom left). Light in **f-h** and **j**: 470 nm, 5.56×10^7 photons/μm^2/s, duration of 2 ms (**h**) and 200 ms (**f** and **j**). **k,** A model of postsynaptic segregation of co-transmission. Although histamine signaling dominates in transmission from R8s to L1/Tm pathways, very minor ACh signaling also exists in this pathway. Pooled data: mean ± s.e.m. ***$P < 0.001$; NS, not significant. Statistical analysis is summarized in Extended Data Table 2.

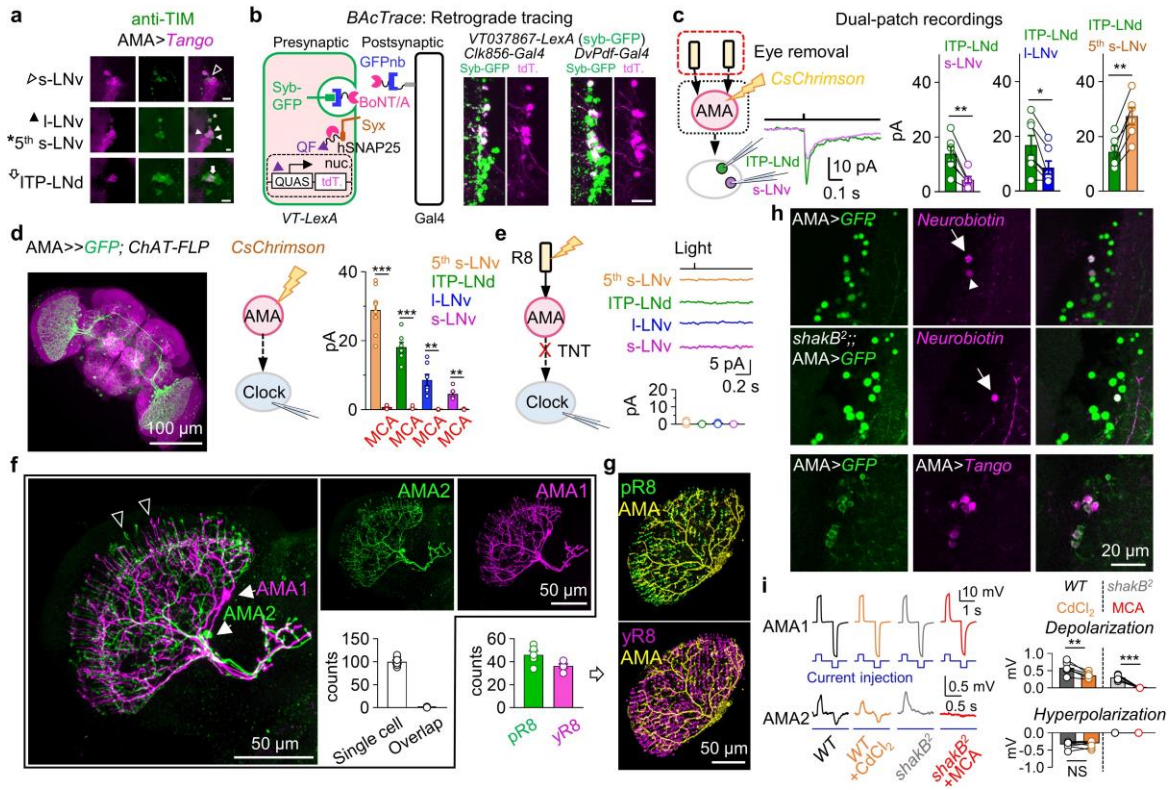

Fig. 4 | A three-node circuit for circadian entrainment. a, *trans*-Tango-labeled postsynaptic neurons of AMA neurons show TIM immunostaining. Scale bar: 20 µm. **b,** Retrograde tracing with BAcTrace shows that AMA neurons are presynaptic to clock neurons. **Left**, schematic of BAcTrace tracing; **right**, AMA neurons (*VT037867-LexA*- syb-GFP) overlap with the BAcTrace-labeled presynaptic neurons of clock neurons. Scale bar: 20 µm. **c,** Varied synaptic strengths between AMA neurons and clock neurons. **Left**, schematic of dual-patch recordings; **middle**, representative responses of a pair of ITP-LNd and s-LNv to optogenetic activation of AMA neurons; **right**, pooled peak responses (lines represent pairs of neurons simultaneously recorded with dual patch-clamp recordings). Light: 617 nm, 2 ms, 2.22×10^9 photons/µm^2/s. **d,** AMA neurons excite clock neurons via ACh. **Left**, GFP expression intersected by *ChAT-FLP* and *VT037867-Gal4*; **middle**, schematic of simultaneous optogenetic activation and patch-clamp recordings; **right**, pooled responses of clock neurons to optogenetic activation of AMA neurons (with or without MCA). Light: 617 nm, 2 ms, 2.22×10^9 photons/µm^2/s. **e,** R8s excite clock neurons via AMA neurons. **Left**, schematic of TNT blockade of AMA transmission; **right**, a complete loss of light responses in clock neurons of *VT037867-Gal4>TNT* flies (top) and pooled data (bottom). Light: 470 nm, 2 ms, 5.56×10^7 photons/µm^2/s. **f,** Spatial irradiance integration by

AMA neurons. **Left**, arborization of two MCFO-labeled AMA neurons, arrows indicate cell bodies, unfilled triangles indicate multicolumnar arborization; **right**, single MCFO-labeled AMA neurons (top) and pooled data for branches of a single AMA neuron and for branch overlap between two AMA neurons (bottom). **g,** Co-labeling pR8s (green) or yR8s (magenta) and AMA neurons (yellow). **h,** Electrical and chemical synapses among AMA neurons. **Top**, neurobiotin injected into a GFP-labeled AMA neuron diffuses to another GFP-labeled AMA neuron; **middle**, loss of neurobiotin coupling to other AMA neurons in *shakB*^{2} flies; **bottom**, AMA neurons are their own *trans*-Tango-labeled postsynaptic neurons. Arrows indicate neurobiotin-injected cells, arrowhead indicates neurobiotin-coupled cells. **i,** Dual recordings of AMA neurons. **Left**, representative dual recordings (with current injection to AMA1) in wild-type flies (with or without 100 µM CdCl2), or *shakB*^{2} mutant flies (with or without 100 µM CdCl2); **right**, pooled peak response amplitudes of the AMA2 neuron. Hyperpolarization current: -30 pA; depolarization current: 30 pA. *P < 0.05; **P < 0.01; ***P < 0.001. Statistical analysis is summarized in Extended Data Table 2.

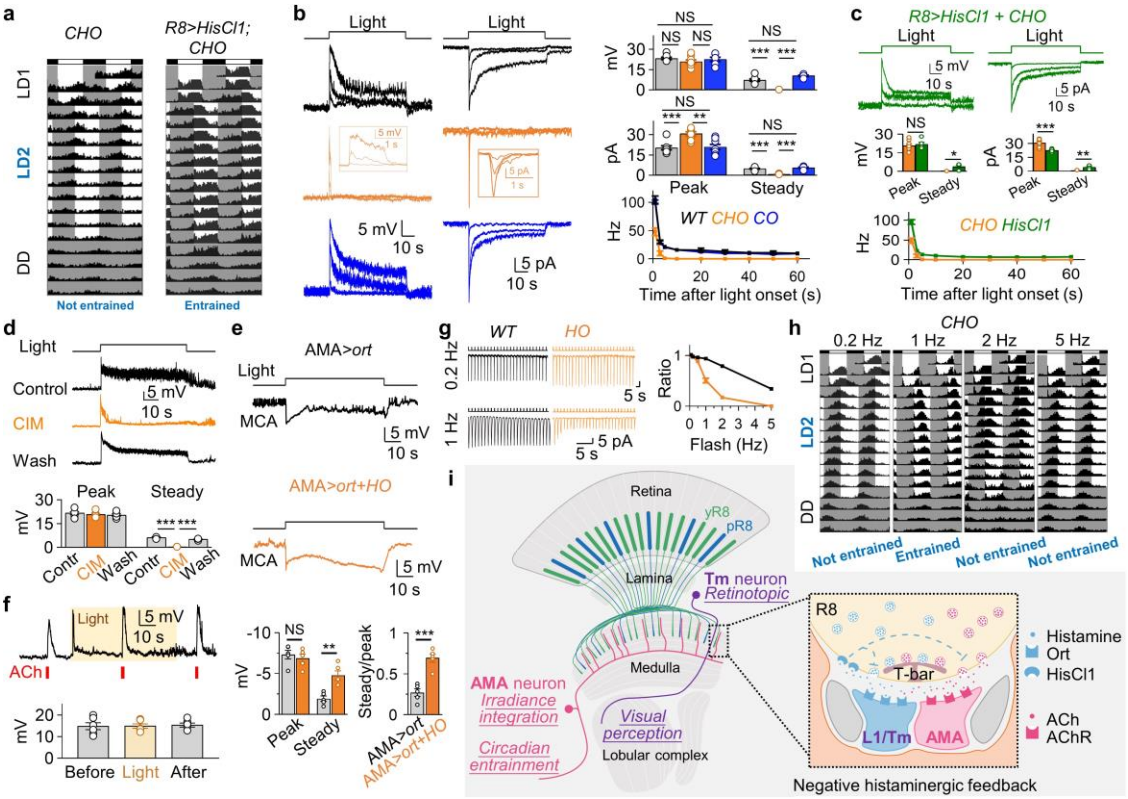

Fig. 5 | Histamine feedback sustains ACh co-release. a, ACh-mediated circadian entrainment requires HisCl1. Average actogram of *CHO* flies (left, n=61) and *CHO* flies with HisCl1 rescued in R8s (right, n=71). **b,** Light step-induced AMA responses in wild-type (black), *CHO* (orange), and *CO* flies (blue). **Left**, representative voltage responses (current-clamp); **middle**, representative current responses (voltage-clamp); **right**, pooled peak and steady current response amplitudes (top), voltage response amplitudes (middle), and firing rates (bottom). Light: 470 nm, 60 s, intensities of 0.0094, 0.19, and 1.88×10^6 photons/μm^2/s. **c,** HisCl1 expression in R8s restored steady depolarization in *CHO* flies. **Top**, representative recordings in *CHO* flies with HisCl1 rescued to R8s; **bottom**, pooled data. Light: 470 nm, 60 s, intensities of 0.0094, 0.19, and 1.88×10^6 photons/μm^2/s. **d,** CIM reduced steady depolarization of AMA neurons. **Top**, representative recordings of the same AMA neuron in normal saline, CIM, and after washout of CIM; **bottom**, pooled peak amplitudes (left) and steady response amplitudes (right). Light: 470 nm, 60 s, 1.88×10^6 photons/μm^2/s. **e,** Histamine- mediated responses of ort-expressing AMA neurons in wild-type (top) and *HO* (middle) flies in the presence of MCA. Pooled steady and peak response amplitudes and their corresponding ratios (bottom). Light: 470 nm, 60 s, 1.88×10^6 photons/μm^2/s. **f,** ACh sensitivity in *CHO* flies. **Top**, representative ACh-induced

depolarization before, during, and after light stimulation; **bottom**, pooled data. Light: 470 nm, 60 s, 1.88×10^6 photons/μm^2/s. **g,** Frequency dependence of light pulse-induced responses in AMA neurons. **Left**, representative responses to light pulses of 0.2 Hz and 1 Hz; **right**, pooled peak response ratios between first and last pulses. Light pulses: 470 nm, duration of 100 ms, 5.65×10^7 photons/μm^2/s. **h,** Circadian entrainment of *CHO* flies to brief light pulses. Average actograms to 100-ms flashes at 0.2 Hz (n=63), 1 Hz (n=65), 2 Hz (n=60), and 5 Hz (n=54). **i,** A model of negative histaminergic feedback in R8s. Pooled data: mean ± s.e.m. **P* < 0.05; ***P* < 0.01; ****P* < 0.001; NS, not significant. Statistical analysis is summarized in Extended Data Table 2.

Methods

Flies

Flies were reared on standard cornmeal medium under a 12-h/12-h light:dark (LD) cycle at a humidity of 60% and temperature of 25 °C, except for *trans*-Tango tracing flies raised at 18 °C. On 1-2 days after eclosion, flies were used for patch-clamp recordings regardless of gender. Recordings from *Rh6-hid, rpr* flies were performed on the third day after eclosion.

DvPdf-Gal4, *norpA^{P41}*, *GMR-Gal4* were from P. Emery. *cry^{02}* and *Clk856-Gal4* were from T. Yoshii. *LexAop-mCD4::spGFP^{11}*, *UAS-mCD4::spGFP$^{1–10}$*, *HisCl^{134}*, *ort^{1}*, *ChAT-FLP*, *TH-FLP*, *Trh-FLP*, *vGlut-FLP*, *vGAT-LexA*, *ort-LexA*, *LexAop2-GFP*, *UAS-mSPA-GFP*, *UAS-ChAT sgRNA*, *UAS-VAChT sgRNA*, *UAS-Hdc sgRNA*, *GMR-RFP*, *LexAop-tdTomato* and *HDC-Gal4* were obtained from Y. Rao. *UAS-RFP,LexAop- GFP* was from C. Liu. *Rh6-LexA* was obtained from T. Suzuki. *shakB^{2}* was obtained from J.M. Blagburn. *UAS-mCD8-GFP* (II and III) and *UAS-FRT-STOP-FRT-mCD8-GFP* (II, III) were provided by C. Potter. *UAS-FRT-STOP-FRT-CsChrimson*, *LexAop- FLP* (II, III) were obtained from C. Zhou. *UAS-post-GFP$^{1-10}$* was from S. Stowers. *Rh5^{2}*, *Rh6^{1}*, *UAS-ort*, *UAS-HisCl1*, and *cry^{02}*, *HisCl1^{134}*, *ort^{1}* triple mutant were provided by F. Rouyer. SS00691, SS00307 and SS00355 were from the Janelia Research Campus. The BAcTrace tool fly was from G. Jefferis. *Rh1-Gal4* (BL8692), *Rh3-Gal4* (BL7457), *Rh4-Gal4* (BL8627), *Rh5-Gal4* (BL7458), *Rh6-Gal4* (II, BL7459), *Rh6-Gal4* (III, BL7464), *UAS-norpA* (II, BL26267), *UAS-norpA* (III, BL26273), *UAS-GCaMP6m* (II, BL42748), *UAS-GCaMP6m* (III, BL42750), *UAS-CsChrimson* (BL55135), *Rh5-eGFP* (BL8600), *Rh6-eGFP* (BL7461), *Hdc^{JK910}* (BL64203), *VACHT-FRT-STOP-FRT-HA (BL76021)*, *UAS-myrGFP,QUAS-mtdTomato-3xHA; trans-Tango* (BL77124), *UAS- FLP* (BL4539), *MCFO-1* (BL64085), *ort-Gal4.C1a.DBD, ET.VP16.AD tou[9A30]* (BL56521), *ort-Gal4.C1a.DBD; dVP16AD[ET18k]* (BL56524), *UAS-Cas9.P2* (BL58985), *GMR27G06-LexA* (BL54779), *GMR24C08-Gal4* (BL48050), *LexAop2- GCaMP6f* (BL44277), *LexAop2-GCaMP6m* (BL44276), *LexAop2-GFP* (BL32209), *LexAop2-GCaMP7s* (BL80913) and *UAS-TNTE* (BL28837) were from the Bloomington Stock Center. *VT037867-Gal4* (v203797) was from the Vienna *Drosophila* Resource Center. *GMR54D11-Hack-LexA* was generated from *GMR54D11- Gal4* (BL41279). *DvPdf-LexA* (II), *DvPdf-LexA* (III), and *VT037867-LexA* (II) were from our own stocks. *Rh6-hid,rpr*, *ort-QS* and *LexAop-post-GFP^{11}*were generated in this study. The details

of fly sources are listed in Extended Data Table 3, and fly genotypes are listed in Extended Data Table 1.

Generation of transgenic flies

To generate the *Rh6-hid,rpr* construct, a 2.9-kb enhancer was amplified from *Rh6- eGFP* flies (BDSC7461) with HindIII (5') and NotI (3') sites added to the primers. Primers sequences: forward: 5′-CACCCGTGGCCAGGGCCGCAAGCTTATGAACATGTTGCC TCATTGAATC-3′; reverse: 5'-TCGATCCCCGGGCGAGCTCGGCGCGCCCACACCCA TTTTGCTCAGTGCATCT-3'. The *head involution defective-2A-reaper (hid,rpr)* sequence was amplified from *UAS-hid,rpr* with NotI (5') and XbaI (3') sites added to the primers. Primer sequences: forward: 5'- ACCAGTACCAGCCATTCGAAGCGGCCGCGCCAC CATGGCCGTGCCCTTT-3'; reverse: 5'-GTTATTTTAAAAACGATTCATTCTAGTC ATTGCGATGGCTTGCGATA-3'. The *Rh6-hid,rpr* fragment was then inserted into the *pUASTattB* vector, and the *p10* sequence was inserted downstream of the *hid,rpr* sequence. To generate transgenic flies, the above constructs were injected and integrated into the *attp5* landing sites through phiC31-mediated gene integration.

To generate the *ort-QS* construct, the ort promoter was amplified from the ort^{C1-3}*-Gal4* fly[39] with HindIII (5') and NotI (3') sites added to the primers. Primer sequences: forward: 5'-ACCCGTGGCCAGGGCCGCAAGCTTGCCAAACACAAGTAAAAAGTTTGC-3'; reverse: 5'-GGGATGGTGTTCATTTTGCGGCCGCTTTAATGTGAGCTCTTTCT GTGTGG-3'. The promoter fragment was then inserted into the *pUASTattB* vector, and the *QS-P10* sequence was inserted downstream of the ort promoter. To generate transgenic flies, the above constructs were injected and integrated into the *VK00005* landing sites through phiC31-mediated gene integration.

To generate the *LexAop2-post-*GFP^{11} construct, the mouse *neuroligin-1 (Nlgn1)* fragment sequence was amplified from *UAS-post-*GFP^{1-10} fly, with NotI (5') sites added to the primers. Primer sequences: forward: 5'- CTTATCCTTTACTTCAGGCG GCCGCAAAATGGCACTTCCTAGATGTATGTGGCCTA-3'; reverse: 5'- CACATAT TCGTGCAGCACCATGTGGTCGCGGGAAGCGTCATCCAGCTTCTGTGAAAG-3'.

Telencephalin (TLN) and the linker sequence were amplified from *UAS- post-GFP*$^{1-10}$ fly, with XbaI (3') sites added to the primers: Primer sequences: forward: 5'-GGTGCTGCACGAATATGTGAACGCTGCTGGCATCACAGGGACGGGCGGATCTG GCGGATCT-3'; reverse: 5'-GTTATTTTAAAAACGATTCATTCTAGATC AGGAAGATGTCAGCTGGATA-3'. *Nlgn1-GFP*^{11}*-TLN* sequence was then amplified using the above two sequences as templates. Primer sequences: forward: 5'-CTTATCCTTTACTTCAGGCGGCCGCAAAATGGCACTTCCTAGATGTATGTGG

CCTA-3'; reverse: 5'-GTTATTTTAAAAACGATTCATTCTAGATCAGGAAGATGTCAG CTGGATA-3'. The above sequence was then inserted into the *LexAop2-IVS-p10* vector (constructed from Addgene, 36431). To generate transgenic flies, the above constructs were then injected and integrated into the *VK00005* landing sites through phiC31-mediated gene integration.

UAS-ChAT-sgRNA and *UAS-VAChT-sgRNA* constructs were designed by inserting single guide RNAs (sgRNAs) into the pMt:sgRNA$^{3\times}$ vectors based on pACU2, with rice transfer RNA (tRNA) used to separate different sgRNAs.

Electrophysiological recordings

Fly dissections were performed as described previously[15,45]. Briefly, flies were dark- adapted over 30 min before experiments. The fly heads were dissected and covered with pre-oxygenized *Drosophila* dissection saline composed of (mM): 124 NaCl, 3 KCl, 4 MgCl2, 1.5 CaCl2, 10 HEPES (pH 7.3), 1 NaH2PO4, 5 *N*-tri-(hydroxymethyl)-methyl- 2-aminoethane-sulfonic acid (TES), 20 D-glucose, 17 sucrose, and 5 trehalose. Under a dissection microscope (M125, Leica) with dim red-light illumination, the cuticle and air sac covering the targeted brain neurons were removed, leaving compound eyes intact. After dissection, the preparation was stabilized in the recording chamber with blue histoacryl (B. Braun, Germany). The chamber was then transferred to the recording platform and continuously perfused with the 95% O2/5% CO2-bubbled *Drosophila* perfusion saline, which contained (mM): 103 NaCl, 3 KCl, 4 MgCl2, 1.5 CaCl2, 26 NaHCO3, 1 NaH2PO4, 5 TES, 20 D-glucose, 17 sucrose, and 5 trehalose. Free calcium concentrations were calculated based on the program provided by https://somapp.ucdmc.ucdavis.edu/pharm

acology/bers/maxchelator/CaMgATPEGTA-NIST.htm.

An upright microscope (A1 MP+, Nikon) equipped with a 60× water-immersion objective (CFI Fluor, Nikon) was used to visualize the preparations. With transmitting infrared (IR) illumination, images from IR-CCD (DAGE-1000, MTI) combined with differential interference contrast optics were displayed on a TV monitor (Sony). Local application of protease XIV (0.33 mg/mL) via a glass pipette with a 3-μm opening was used to expose the cell bodies of target neurons, identified based on their GFP/GCaMP expression. Fluorescence was briefly excited with a 470-nm LED (M470L4, Thorlabs).

Patch-clamp electrodes (~10 MΩ) were made from borosilicate glass (PG10165-4, WPI) using a puller (P-1000, Sutter Instrument). The recording pipette was filled with intracellular solutions composed of (mM): 140 K-gluconate, 6 NaCl, 2 MgCl2, 0.1 CaCl2, 1 EGTA, 10 HEPES (pH 7.3), and 100 μg mL^{-1} amphotericin B (A9528, Sigma- Aldrich), with a final osmolality of 270 mOsm. All chemicals were obtained from Sigma-Aldrich.

Electrical signals were amplified with a MultiClamp 700B amplifier (Axon), digitized with Digidata 1440A, and recorded with Clampex v10.6 (Molecular Devices, https://www.moleculardevices.com/), with a sampling rate of 5 kHz and a low-pass filter at 2 kHz. VT037867 and clock neurons exhibit robust rhythmic bursting activity[45]. To reduce its interference with the analysis of light-induced responses, we selected the voltage recordings with weak rhythmic bursting activity or averaged more than 15 traces for the current recordings by flatting baselines. Data were processed and visualized with: Clampfit v10 (https://www.moleculardevices.com/), Matlab R2020b (https://www.mathworks.com/products/matlab.html), Origin 2018 (https://www.originlab.com/), and GraphPad Prism 9 (https://www.graphpad.com/scientific-software/prism/).

As for the recordings on AMA neurons, we selected the ten pairs of VT037867-expressing neurons in the aMe region for patch-clamp recordings since they have the same morphological features of AMA neurons, based on their single-cell morphology as revealed by MCFO labeling (Extended Data Fig. 5c). Furthermore, we confirmed that this group of neurons are indeed the AMA neurons based on their single-cell morphology that is revealed by neurobiotin injection via the patch-recording electrode after whole-cell recordings (Extended Date Fig. 5d).

Dual patch-clamp recordings

Dual patch-clamp recordings were performed similarly to the single patch-clamp recordings above. The two target neurons were identified based on GFP expression, and their cell bodies were exposed before patch-clamp recordings. After cell body exposure, two patch-recording electrodes were sequentially positioned ~50 μm above each target neuron. The target neurons were then sequentially patched one by one.

Light stimulation

Light stimulation was performed as described previously[15]. The light source was a 470- nm LED (M470L4, Thorlabs) controlled by an LED driver (LED D1B and DC 4100, Thorlabs) and connected to the fluorescence port of an A1 MP+ microscope via a liquid light guide. A light spot (diameter 400 μm) was projected onto the preparations, roughly covering the ipsilateral compound eye. Light intensity was calibrated with a power meter (Model 1936-R, 918D-ST-UV, Newport) before the experiments. In both electrophysiological recordings and calcium imaging, light intensity was reported in the unit of photons/$\square m^2$/s. For example, for the monochromatic 470-nm light spot (with a diameter of 400 μm), 3 mW is equivalent to 5.65×10^7 photons/$\square m^2$/s. Brief or short light pulses were typically used in our electrophysiological recordings and calcium imaging. An identical light condition was challenging to achieve in cellular recordings and behavioral studies.

Neuropharmacology: drug delivery by fast-solution changes

A three-barrel tube (SF77B, Warner Instruments) was positioned ~200 μm from the brain preparation and, controlled by a stepper (SF77B, Warner Instruments). External saline was first perfused through the middle barrel to cover the brain preparation, then the drugs in the side barrels were switched to cover the preparations using a step motor, achieved within milliseconds. The timing and duration of drug application were controlled by Clampex and Digidata 1440A. 100 μM CdCl2 (20899, Fluka Sigma- Aldrich)[56], 50 μM mecamylamine

(M9020, Sigma-Aldrich)[56], 2 mM cimetidine (C4522, Sigma-Aldrich)[57], 1 mM histamine (H7250, Sigma-Aldrich)[57], and 1 mM ACh (A6625, Sigma-Aldrich)[58] were used. Note, Cd^{2+} is a non-specific blocker of voltage-gated calcium channels, in addition to some voltage-gated potassium channels.

Optogenetic manipulation

CsChrimson was expressed in the target neurons with a specific Gal4 driver. All parental flies were raised on food containing 0.4 mM all-trans-Retinal (ATR, R2500, Sigma-Aldrich), with progenies also fed 0.4 mM ATR-food for 3 days after eclosion. Fly vials were kept in darkness to avoid ATR degeneration and CsChrimson activation. Isolated brains (without compound eye) were dissected under dim blue light, and a 625-nm LED (M625L4, Thorlabs) was used for optogenetic stimulation during patch-clamp recordings.

***In vivo* two-photon calcium imaging**

The chamber used for *in vivo* imaging was modified from a published version[56]. The bottom of the chamber was made of a stainless-steel sheet (20-μm thick) with a rectangle hole (800 μm × 1200 μm). Flies were anesthetized on ice for 1 min, then quickly inserted into the chamber hole with the dorsal brain and thorax facing upwards. Legs and thorax were stabilized with low-melting-point paraffin. The head was bent downward to expose the posterior brain, keeping the compound eyes below the chamber. The chamber was filled with *Drosophila* saline, and a small window was opened in the dorsal brain to expose axon terminals of R8s.

Imaging was acquired with a Nikon A1 MP+ microscope that is equipped with a Maitai DeepSee Ti:Sapphire ultrafast laser (Spectra-Physics). Excitation of GCaMP6f was achieved by a two-photon laser of 920 nm, and images (256 × 128-pixel resolution) was acquired with a DU4 PMT detector at 8 Hz. Full-field light stimulation (460 nm) was projected to the compound eyes through a condenser, whose duration and timing were controlled by a D1B LED driver via the NIS Element (https://www.microscope.healthcare.nikon.com/) and Clampex (Molecular Device). Relative change in fluorescence (ΔF/F)

of manually-selected regions of interest (ROIs) was analyzed using NIS-Element.

Mapping the receptive field of AMA neurons

The recording chamber was similar to the *in vivo* imaging chamber except for a smaller chamber hole (500 × 500 μm), which is slightly larger than a compound eye. Fly brains with intact compound eyes were dissected, and one compound eye was inserted into the chamber hole and exposed to the air. The other compound eye was stabilized to the chamber with vacuum grease (Dow Corning). A hemispherical screen (a diameter of 40 mm) was placed under the chamber, with the exposed compound eye facing the center of the screen. Light spots were projected to the screen from a back projector via a reflecting mirror. The duration and timing of visual stimuli were controlled by Matlab. Light stimulation of 460 nm was used to avoid interference with the fluorescence-imaging detector. Calcium responses reported by GCaMP6m were acquired with a Nikon A1 MP+ microscope equipped with 25× water-immersion objective and fluorescence excitation by a two-photon laser of 920 nm.

Neuronal tracing with photoactivatable GFP

VT037867-Gal4,UAS-tdTomato/UAS-mSPA-GFP was used for PA-GFP labeling the AMA neurons. Ex vivo brain preparations were stabilized in the chamber with the posterior brain facing upwards to expose the td-Tomato-marked dorsal commissural track of AMA neurons. Photoactivation of PA-GFP was achieved with a Nikon A1 MP+ multiphoton laser scanning microscope and a two-photon laser of 720 nm. One cycle of photoactivation of the commissure track contained 30 times of photoexcitation, each with a dwell time of 4.8 μs per pixel at an interval of 8 s. The cycle was repeated 10 times at 30-s intervals for a complete photoactivation episode. After a 10-min wait for GFP diffusion, the brain preparations were repositioned with the anterior side facing up, and images of the photoactivated cell bodies were acquired with a two-photon laser of 920 nm.

Immunostaining

Flies were first dissected in phosphate-buffered saline (PBS) and fixed in 4% (w/v)

paraformaldehyde (PFA, 157-8, Electron Microscopy Science) for 1 h on ice. Brains and compound eyes were then washed three times (15 min/time) in PBST (0.5% v/v Triton X-100 in PBS). The fixed samples were incubated with penetration/blocking buffer (10% normal goat serum and 2% Triton X-100 in PBS) for 2 h at room temperature, followed by incubation with primary antibodies (rat anti-LOVIT, 1:100, a gift from T. Wang; rabbit anti-HA, 1:200, 3724, Cell Signaling Technology; mouse anti- nc82, 1:100, DSHB; mouse anti-PDF, 1:4000, PDF C7, DSHB; mouse anti-V5 DyLight 549, 1:100, MCA2894D549GA, Bio-Rad; mouse anti-V5 DyLight 647, 1:10, MCA1360A647, Bio-Rad) at 4 ℃ for 24 h. After being washed in PBST three times, the samples were incubated with secondary antibodies (goat anti-rat Alexa Fluor 568, 1:200, ab175710, Abcam; goat anti-rabbit Alexa Fluor 488, 1:200, A27034, Thermo Fisher; goat anti-mouse Alexa Fluor 647, 1:200, A21235, Thermo Fisher; goat anti-mouse Alexa Fluor 568, 1:200, A11004, Thermo Fisher) at 4 ℃ overnight. The antibodies were diluted in antibody dilution buffer (1% normal goat serum and 0.25% Triton X-100 in PBS). The samples were washed three times before mounting in FocusClear (FC101, Cedarlane Labs).

Neurobiotin-labeling

Neurobiotin was injected into VT037867 neurons to reveal their coupling through electrical synapses. To balance the osmolality of high-concentration neurobiotin, 2% (w/w) neurobiotin (Vector Laboratories, SP-1120) was diluted in a modified internal solution composed of (mM): 70 K-gluconate, 6 NaCl, 2 MgCl2, 0.1 CaCl2, 1 EGTA, 4 Mg-ATP, 0.5 GTP-Tris, and 10 HEPES, pH adjusted to 7.3. A positive current (20-50 pA, 250 ms, 2 Hz) was injected into the target cell under whole-cell current clamp mode for 20-30 min. The pipette was then gently detached without damaging the neuronal structure. After another 20 min for neurobiotin diffusion, the sample was transferred to 4% PFA for 2-4 h on ice. The fixed brains were washed three times with PBST, then blocked for 2 h in bovine serum albumin (BSA) blocking buffer (5% w/v BSA, A3059, Sigma-Aldrich, and 1% Triton X-100 in PBS) and incubated with streptavidin-568 (1:600, S-11226, Thermo Fisher, diluted in BSA blocking buffer) at 4 ℃ overnight. After washing three times with PBST, the brains were mounted in FocusClear.

MultiColor FlpOut (MCFO)

For single- and two-cell labeling of VT037867 neurons, *VT037867-Gal4* flies were crossed with *MCFO-1* flies. The flies were raised at 25 ℃, and 1-day-old adult progenies were placed in empty vials and incubated in a 37 ℃ water bath for 3 min to induce flippase expression. On the third day after heat shock, the flies were fixed for immunostaining. The fly brains were dissected in PBS and fixed in 4% PFA for 1 h on ice. Brains were then washed three times in PBST. The fixed brains were incubated with penetration/blocking buffer for 2 h at room temperature.

For single-cell labeling, brains were incubated with DyLight549-conjugated mouse anti-V5 (1:100, MCA2894D549GA, Bio-Rad) at 4 ℃ overnight. For co-labeling VT037867 neurons with pR8/yR8 photoreceptors, brains were incubated with DyLight647-conjugated mouse anti-V5 (1:10, MCA1360A647, Bio-Rad) at 4 ℃ overnight. For two-cell labeling, brains were first incubated with rabbit anti-HA primary antibody (1:100, 3724, Cell Signaling Technology) at 4 ℃ overnight. After washed three times with PBST at room temperature, the brains were then incubated with goat anti-rabbit IgG-conjugated Alexa Fluor 488 (1:200, A-27034, Thermo Fisher) and DyLight549-conjugated mouse anti-V5 (1:100) for 24 h. The brains were then washed three times in PBST and mounted in FocusClear.

Chemoconnectomics intersection

We used an intersection strategy to identify the neurotransmitter used by R8s and VT037867 neurons. FLP knock-in flies (*ChAT-FLP*, *vGlut-FLP*, *Trh-FLP*, *TH-FLP*, *GAD1-LexA*, *LexAop-FLP*, *vGAT-LexA*, and *LexAop-FLP*) were crossed with *Rh5-Gal4*, *Rh6-Gal4; UAS-FRT-STOP-FRT-GFP* flies. *ChAT-FLP* flies were crossed with *UAS- FRT-STOP-FRT-GFP; VT037867-Gal4* flies. The flies were raised at 25 ℃ and dissected at 2-3 days after eclosion. The fixed samples were washed three times with PBST and then mounted in FocusClear without immunostaining.

trans-Tango

We used *UAS-myrGFP, QUAS-mtdTomato (3×HA); trans-Tango* fly for anterograde tracing of R8s and VT037867 neurons. Progeny flies were maintained in 12-h LD cycles at 18 ℃ after eclosion and dissected at 10 or more days after eclosion. We used *ort-QS* for labeling the non-ort target of R8s. The brains were then fixed in 4% PFA for 1 h on ice. For direct observation of fluorescence, the samples were mounted in FocusClear after washing three times with PBST.

For co-labeling with clock neurons, whole flies were fixed at ZT20 with 4% PFA and 0.1% Triton X-100 in PBS for 2.5 h at room temperature. The flies were then washed with PBST and dissected in PBST. Subsequently, the brains were incubated with 10% normal goat serum and 0.1% Triton-X in PBS for 4 h at room temperature, then with rabbit anti-TIM (1:250) at 4 ℃ overnight, or together with mouse anti-PDF (1:4000, PDF C7, DSHB). After washing three times with PBST (20 min/time), the brains were incubated with goat anti-rabbit IgG conjugated with Alexa Fluor 488 (1:200, A27034, Thermo Fisher), or together with goat anti-mouse IgG conjugated with Alexa Fluor 647 (1: 200 A21235, Thermo Fisher) for 7 h at room temperature. Brains were then rinsed three times with PBST (20 min/time) and mounted in FocusClear.

BAcTrace

BAcTrace retrograde tracing was used to identify connections between clock neurons and VT037867 neurons. *VT037867-LexA, Clk856-Gal4* and *VT037867-LexA, DvPdf- Gal4* flies were crossed with *LexAop2-Syb::GFP-P10 (VK37) LexAop-QF2::SNAP25::HIVNES::Syntaxin (VK18); UAS-B3Recombinase (attP2) UAS<B3STOP<BoNT/A (VK5) UAS<B3STOP<BoNT/A(VK27) QUAS-mtdTomato::HA* flies. The flies were raised at 25 ℃, and progenies were dissected and fixed at 2-3 days after eclosion. After washing three times with PBST, the samples were mounted in FocusClear without immunostaining.

GRASP

GFP reconstitution across synaptic partners (GRASP) was used to examine the monosynaptic connections between photoreceptors and L1, Tm5, Tm9, Tm20, and VT037867 neurons. *LexAop-mCD4::spGFP*^{11} and *UAS-mCD4::spGFP*$^{1–10}$ were driven by specific LexA and Gal4 drivers. The flies were dissected 1 week after eclosion. Fly brains were dissected in PBS and fixed in 4% PFA for 1 h on ice. Brains were then washed three times in PBST. The fixed brains were incubated with penetration/blocking buffer for 2 h at room temperature. The brains were then incubated with mouse anti- nc82 primary antibody (1:100, DSH-B) at 4 ℃ overnight. After being washed three times with PBST at room temperature, the brains were then incubated with goat anti-mouse IgG conjugated to Alexa Fluor 568 (1:200, A11004, Thermo Fisher) overnight. The brains were then washed three times in PBST, and mounted in FocusClear for imaging.

Genetic and laser ablation of H-B eyelets

Apoptosis genes *hid* and *rpr* were used to ablate H-B eyelets. We first generated transgenic flies with *hid* and *rpr* expression using the Rh6 promotor. We found that *Rh6-hid,rpr* flies lost H-B eyelets on the third day after eclosion. However, pR8s that also express Rh6 remained partially functional up to two weeks after eclosion. Therefore, our recordings from *Rh6-hid,rpr* flies were performed on the third day after eclosion when H-B eyelets were lost, but most yR8s remained functional.

For laser ablation, the H-B eyelet axons were identified by GFP expression with *Rh6-eGFP* or *Rh6-Gal4,UAS-GFP*. Light responses of the targeted neurons were recorded before ablation. The H-B eyelet axons were selected as an ROI using Nikon Nis-Element software. A Maitai DeepSee Ti:Sapphire ultrafast laser (Spectra-physics) tuned to 800 nm was used to ablate the ROI for 1 s with a dwell time of 2.4 μs per pixel. The laser power at the back of the 60× objective was 50-70 mW at 800 nm. The size of the ROI, duration, and power of the laser were optimized for different preparations to achieve a visible cavitation bubble and destruction of the H-B eyelet axons. The perforated patch-clamp recordings were maintained during ablation.

Removal of compound eyes and H-B eyelets

Flies (1-day after eclosion) were dark-adapted over 30 min before the experiments. The fly head was dissected in pre-oxygenized *Drosophila* dissection saline. The compound eye and lamina were carefully removed under a dissection microscope (M125, Leica) with dim red-light illumination, which also removed the H-B eyelets as they are physically located between the compound eye retina and lamina.

Image acquirement and processing

Images were acquired sequentially in 1-µm sections using the Nikon A1 MP+ microscope equipped with 25× water-immersion objective (CFI75 Apochromat 25×C W, Nikon) at a resolution of 1024 × 1024. For co-labeling of single VT037867 neurons, pR8 and yR8 photoreceptors and co-labeling of VT037867 driven *trans*-Tango, anti- TIM and anti-PDF, images were acquired in 1-µm sections on a Dragonfly Spinning Disk Confocal Microscope equipped with 40× oil-immersion objective. Images were processed and rendered using NIS-Element (Nikon) and ImageJ (Fiji, https://fiji.sc/).

Motion detection assay

We used flies 2-4 days after eclosion for motion detection assays. After anesthetization on ice for 20 s, the flies were tethered to a fine platinum wire with histoacryl (B. Braun Medical Inc.). Flies that recovered from anesthesia within a few seconds were used for further experiments. The platinum wire was then fixed to a three-axis linear micromanipulator to help place the fly on an air-supported plastic ball[59]. Using a calibration camera, each fly was positioned at the center and 0.4 mm above the ball, allowing it to walk freely. Ball movement was tracked by two cameras with ADNS-6090 chips, with real-time data recorded using MATLAB and saved on a PC. Recordings were synchronized using TTL signals.

Visual stimuli were presented through a DMD projector (DLP4710EVM-LC, Texas

Instruments) controlled by Psychtoolbox3. The cylindrical screen covered the front 180° azimuth angle of the fly. The green and blue channels of the projector were used as visual stimuli, with a refresh rate of 120 Hz. For motion detection stimuli, the spatial wavelength was 30° and angular velocity was 180°/s or 60°/s. Each trial lasted 5 s and randomly included clockwise and counter-clockwise rotation stimuli. The stimulus was presented for 1 s. Trials were abandoned if the fly moved less than 50% of the total trial time, and the fly was removed if it failed in more than half of the trials. Each fly was tested for 30 min in total.

Circadian entrainment assay

Locomotor activity was measured using the DAM2 system (TriKinetics). Individual male flies were placed in a glass tube at 25 ℃ and 60% humidity. Flies were first subjected to three 12-h/12-h LD cycles (200 lux, white light) combined with 25 ℃/18 ℃ temperature cycles, then subjected to 10 LD2 cycles (0.05 lux, white light) with 8-h phase delay at 25 ℃, followed by constant darkness at 25 ℃. The light intensity of 0.05 lux in LD2 cycles was used to study the norpA-dependent photoentrainment by eye photoreceptors.

For pulse light synchronization, the flies were first subjected to three 12-h/12-h LD1 cycles (200 lux, white light) combined with 25 ℃/18 ℃ temperature cycles, followed by nine LD2 cycles with 8-h phase delay at 25 ℃ (with light phase composed of 0.2, 1, 2, or 5 Hz light pulses of 100-ms duration, 0.05 lux, white light), and then subjected to constant darkness at 25 ℃. Light pulses were generated and controlled by microcontrollers (UNO, Arduino). Data were analyzed and visualized with the ImageJ plugin Actogram J69.

Statistical analysis

All experimental data are reported as mean ± s.e.m. The Shapiro-Wilk normality test was used to determine the normal distribution of samples. Comparisons between two groups were performed using two-tailed paired or unpaired Student's t-tests (normal distribution) or Mann-Whitney U-tests (non-normal distribution). Comparisons across multiple groups were assessed using one-way ANOVA followed by Tukey's post hoc test (non-normal distribution), or Kruskal-Wallis test (non-normal distribution) followed by Dunn's test. The

statistical analysis is detailed in Extended Data Table 2.

Data availability

Behavioral, electrophysiological, morphological raw data and additional information required to reanalyze the data reported in this paper are available from the corresponding upon request.

References

56. Yaksi, E. & Wilson, R.I. Electrical coupling between olfactory glomeruli. *Neuron* **67**, 1034-1047 (2010).

57. Gisselmann, G., Pusch, H., Hovemann, B.T. & Hatt, H. Two cDNAs coding for histamine-gated ion channels in D. *melanogaster*. *Nat. Neurosci.* **5**, 11-12 (2002).

58. Wegener, C., Hamasaka, Y. & Nässel, D.R. Acetylcholine Increases Intracellular Ca^{2+} Via Nicotinic Receptors in Cultured PDF-Containing Clock Neurons of *Drosophila*. *J. Neurophysiol.* **91**, 912-923 (2004).

59. Seelig, J.D. et al. Two-photon calcium imaging from head-fixed *Drosophila* during optomotor walking behavior. *Nat. Methods.* **7**, 535-540 (2010).

Acknowledgments

We thank P. Emery, A. Sehgal, Y. Rao, T. Suzuki, J.M. Blagburn, C. Potter, S. Stowers, G. Jefferis, Bloomington Stock Center, and Janelia Research Campus for sharing fly stocks; and T. Wang for sharing the anti-LOVIT antibody. We thank the Core Facilities in the School of Life Sciences, Peking University, for using Dragonfly High Speed Spinning Disk Confocal Microscope and S.Y. Qin for technical assistance. We are grateful to J. Yang, M.M. Luo, W.W.S. Yue, Y. Naya, F. Liu, X. Yu, Y. Lin, H. Zhao, C.R. Ren, J. Ding, Y.L. Li, X.K. Chen, J. Bao, L.Y. Zhang, C. Liu, M. Cho, R.G. Foster, and C. Helfrich-Forster for discussion. This work was supported by National Natural Science Foundation of China grants 31930043 (D.G.L), 31871058 (D.G.L), 32271046 (L.H.C), and 62088102; Collaborative Research Fund of Chinese Institute for Brain Research, Beijing (2021-NKX-XM01); STI2030-Major Projects, grant number 2021ZD0203303; State Key Laboratory of Membrane Biology, Peking University; and Peking-Tsinghua Joint Center for Life Sciences.

Author contributions

D.G.L. and L.H.C. conceived the study. N.X., L.H.C, and D.G.L. designed the experiments. N.X. performed electrophysiological recordings and neurobiotin labeling. N.X., S.X., and T.Y. performed immunostaining and circadian entrainment experiments. Z.K.L. and P.H.W. designed and constructed motion detection devices; Z.K.L. performed motion detection experiments. R.M. generated *UAS-sgRNA* flies. S.X., N.X., and S.X. performed calcium imaging experiments. M.T. help to screen and identify the *VT037867-Gal4* line. M.T.L. developed the ex vivo fly brain preparation; S.X. developed the fly preparation for mapping visual field. Z.K.L. programmed the stimuli for mapping the visual field. A.S. and F.R. generated *CHO* flies. N.X., L.H.C., and D.G.L. analyzed and visualized the data. L.H.C., N.X., F.R., S.X., and D.G.L. wrote and revised the manuscript.

Competing interests

The authors declare no competing interests.

Extended Data Figures and Legends

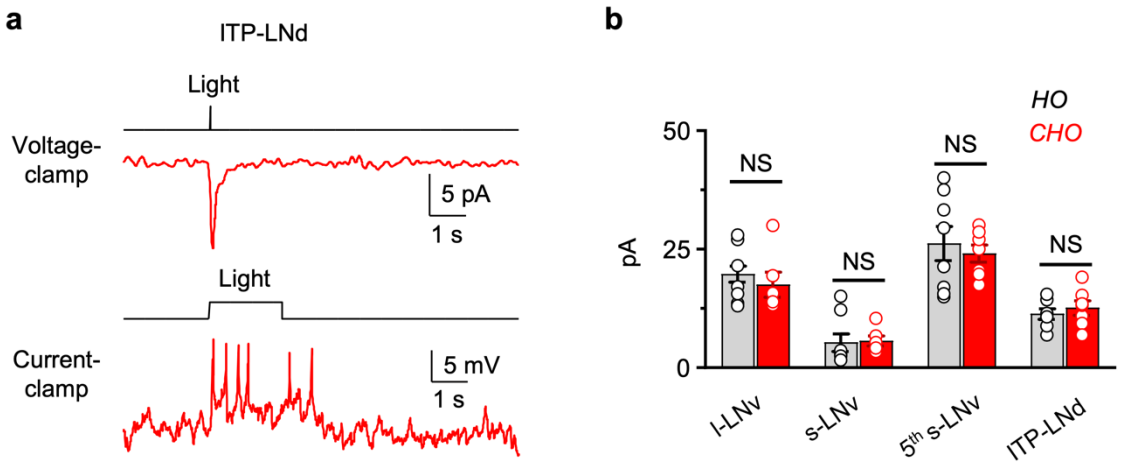

Extended Data Fig. 1 | Histamine-independent irradiance signals. a, Histamine-independent responses in clock neurons. Representative light-triggered inward currents (top, voltage-clamp) and depolarization (bottom, current-clamp) in an ITP-LNd of *CHO* flies. Light: 470 nm, 5.65×10^7 photons/μm^2/s, duration of 2 ms (top) and 2 s (bottom). **b,** Pooled data of different clock neurons. NS, not significant. Statistical analysis is summarized in Extended Data Table 2

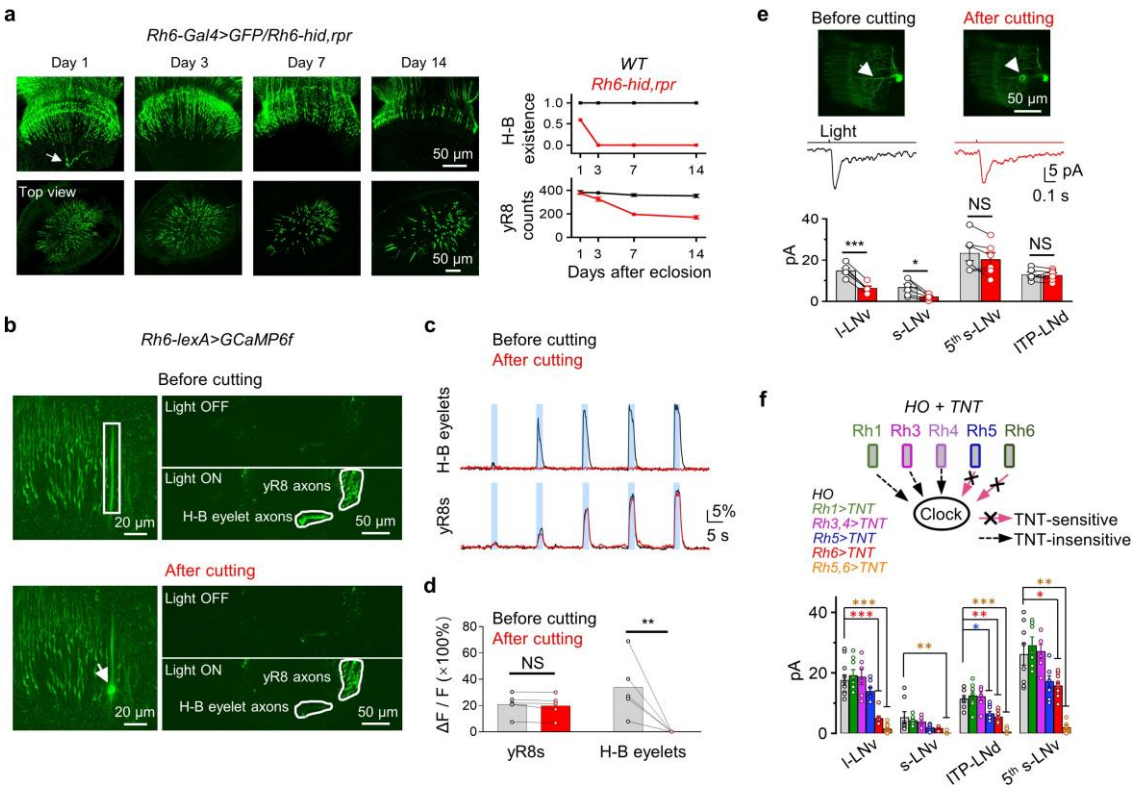

Extended Data Fig. 2 | R8-mediated histamine-independent irradiance signals. a, Impact of *Rh6-hid,rpr* on H-B eyelets in *Rh6-Gal4*>GFP flies. **Left**, H-B eyelet axons (top) and yR8s (bottom) on different days after eclosion; **right**, probability of H-B eyelet existence (top), and pooled data of yR8 counts (bottom). Arrow indicates the GFP-labeled H-B eyelet axon. **b-d**, Specificity and completeness of laser cutting H-B eyelet axons. **b, Top**, representative H-B eyelets and yR8s labeled by *Rh6- LexA>GCaMP6f* (left), and representative calcium response of H-B eyelet and yR8s to light stimulation (right); **bottom**, cutting H-B eyelet axons by a two-photon laser of 800 nm (left), and representative calcium responses of H-B eyelets and yR8s to light stimulation after laser cutting. Light stimulation: 460 nm, 2 s, 1.18×10^6 photons/μm^2/s. The white rectangle indicates the axon bundle of H-B eyelets; the arrow indicates the cutting site with a cavity that appears as a bright spot in the fluorescence image. **c,** Representative calcium responses of H-B eyelets (top) and yR8s (bottom) before (black) and after (red) laser cutting H-B eyelet axons. Light stimulation: 460 nm, 2 s, intensities of 0.032, 0.30, 0.97, 1.18, and 2.36×10^6 photons/μm^2/s. Blue bars show the timing of light stimulation. **d,** Pooled data of calcium responses of yR8s (n=5 flies) and H-B eyelets (n=5 flies) to light stimulation of 460 nm, 2 s, 1.18×10^6 photons/μm^2/s. **e,** Histamine-independent responses in *HO* flies with H-B eyelet axons laser-ablated. **Top**,

schematic of laser cutting H-B eyelet axons, **middle**, representative ITP-LNd responses before and after laser cutting; **bottom**, pooled data. Arrow indicates the intact H-B eyelet axon with GFP expression by *Rh6-Gal4* before laser cutting, arrowhead indicates the laser-ablated H- B eyelet axon with a cavitation bubble. Light stimulation: 470 nm, 2 ms, 5.65×10^7 photons/μm^2/s. **f**, Histamine-independent responses by TNT silencing photoreceptors. Pooled data: mean ± s.e.m. **P* < 0.05; ***P* < 0.01; ****P* < 0.001; NS, not significant. Statistical analysis is summarized in Extended Data Table 2.

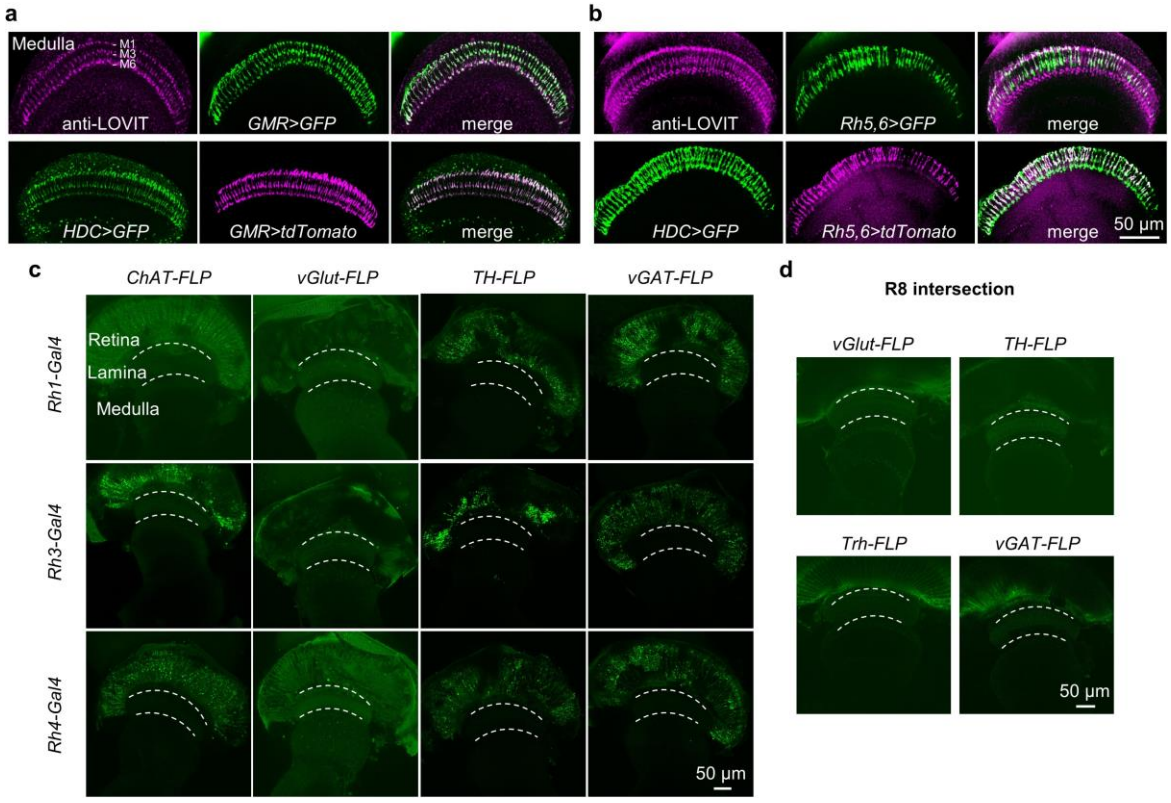

Extended Data Fig. 3 | Single R8 photoreceptor contains both histamine and ACh. a, Histamine in compound-eye photoreceptors. **Top**, anti-LOVIT staining in the medulla; **bottom**, GFP expression by *HDC-Gal4* in the medulla. R8s terminate in the layers of M1-M3, and R7s in M1-M6. *GMR-LexA* labeled all eye photoreceptors. **b,** R8s contain histamine. **Top**, anti-LOVIT staining; **bottom**, HDC expression. **c,** No ACh, glutamate, dopamine, and GABA in R1-R7 photoreceptors. **d,** No glutamate, dopamine, serotonin, and GABA in R8s.

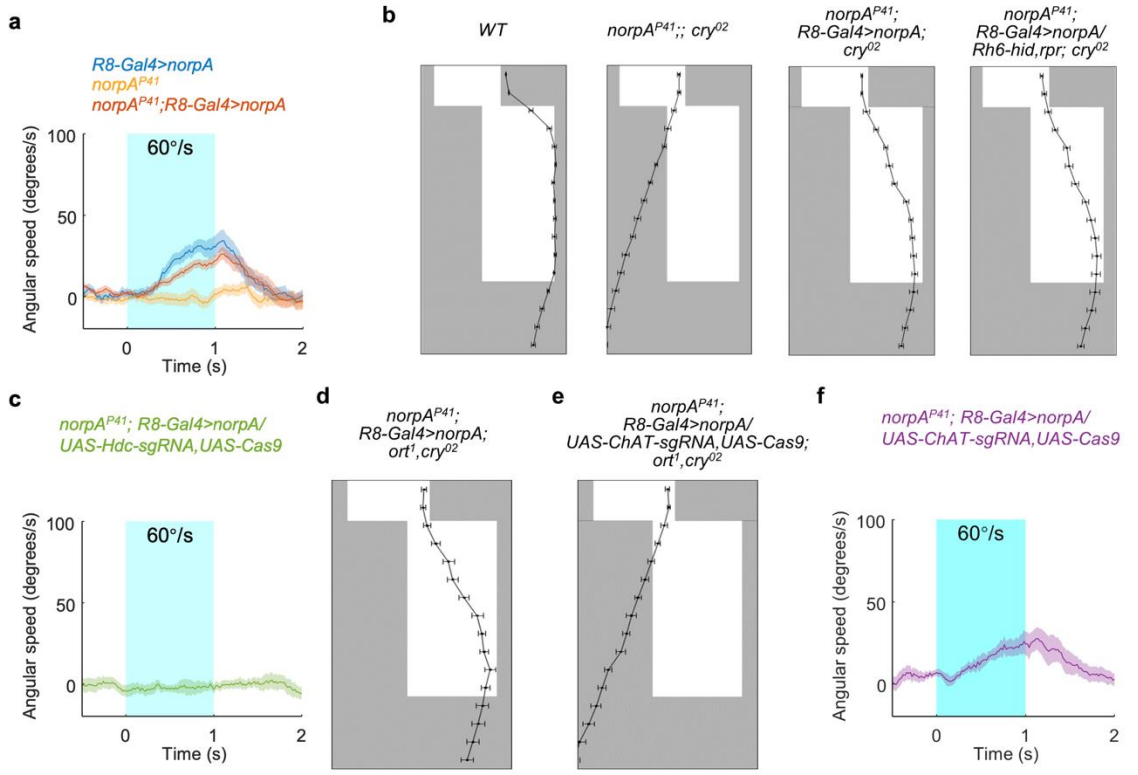

Extended Data Fig. 4 | R8s use histamine for motion detection and ACh for circadian entrainment. a, Motion detection by R8s. Pooled angular speed in *norpA*^{P41} (n=10), *R8-Gal4>norpA* (n=12), and *norpA*^{P41}*; R8-Gal4>norpA* (n=11) flies. Data are represented as mean (solid line) and s.e.m. (shading). **b,** Circadian photoentrainment by R8s. Phase plots of evening peaks of wild-type flies (left, n=33), *norpA*^{P41};; *cry*^{02} mutant flies (second panel from left, n=102), the flies with only R8s and H-B eyelets in dim-light detection (third panel from left, n=93), and the flies with only R8s in dim-light detection (H-B eyelets are genetically ablated) (right, n=73). **c,** Histamine-dependent motion detection by R8s. Pooled angular speed of flies with *Hdc*-knockout in R8s (n=11). **d** and **e,** Phase plots of evening peaks following genetic ablation of *ort* (**d,** n=91), or ablation of both *ort* and *ChAT* (**e,** n=74) in *norpA*^{P41};; *cry*^{02} flies with norpA rescued in R8s. **f,** Pooled angular speed for motion detection by R8s after *ChAT* knockout in *norpA*^{P41} flies with norpA rescued in R8s (n=9). Visual moving bars in **a, c,** and **f**: wave width of 30°, angular velocity of 60°/s, contrast of 100%, duration of 1 s. Pooled data: mean ± s.e.m.

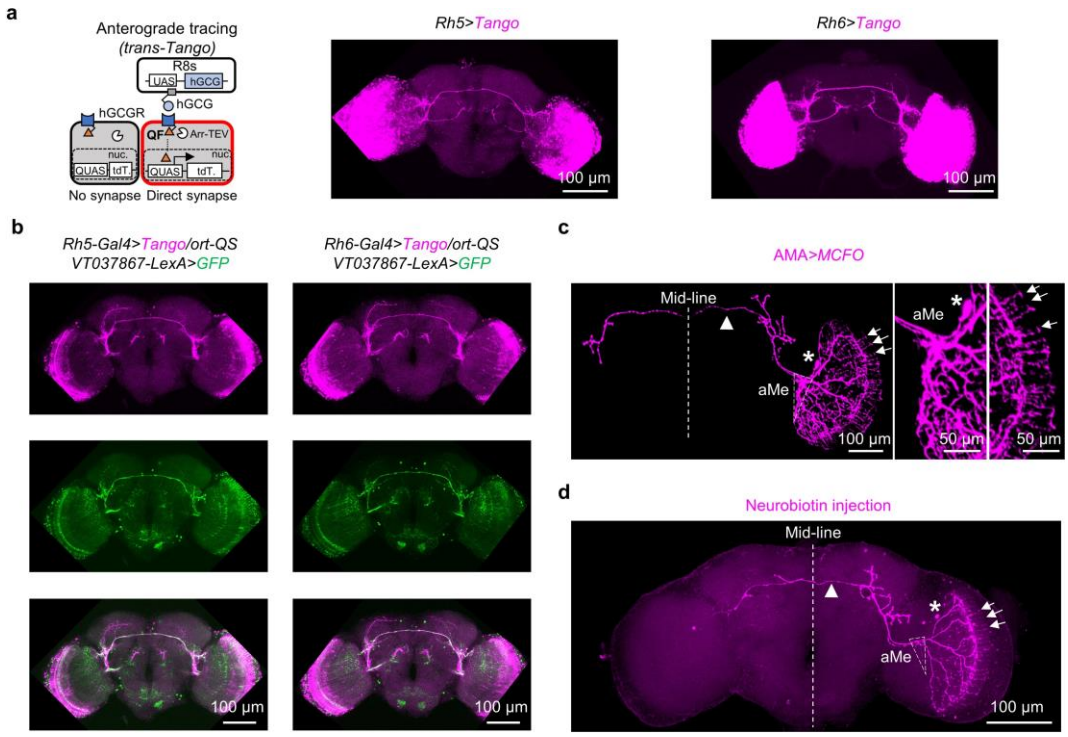

Extended Data Fig. 5 | Morphology of R8-targeted AMA neurons. a, Postsynaptic candidates of R8s labeled by *trans*-Tango. **Left**, schematic of *trans*-Tango labeling; **right**, postsynaptic neurons of pR8s (*Rh5-Gal4*) and yR8s (*Rh6-Gal4*). **b,** GFP expression by *VT037867-LexA* overlaps with *trans*-Tango-driven tdTomato in *ort*- independent postsynaptic neurons of pR8s (left) and yR8s (right). **c,** Single MCFO-labeled AMA neuron innervates the aMe, arborizes in multiple visual columns of the medulla, and exhibits an arcuate dorsal commissure with contralateral projections. **Left**, an overview of the entire brain; **middle**, an expanded view of the aMe region; **right**, an expanded view of columnar arborization. Asterisk indicates the cell body; dashed triangle indicates the aMe; arrows indicate arborization in medulla columns, arrowhead indicates the arcuate dorsal commissure. **d,** Morphology of the recorded AMA neurons. Single-cell morphology of a patch-clamp recorded AMA neuron, revealed by neurobiotin injection via the recording pipette after whole-cell recordings. Asterisk indicates the cell body that is injected with neurobiotin, dashed triangle indicates the aMe, arrows indicate multicolumnar arborization in the medulla columns, arrowhead indicates the arcuate dorsal commissure.

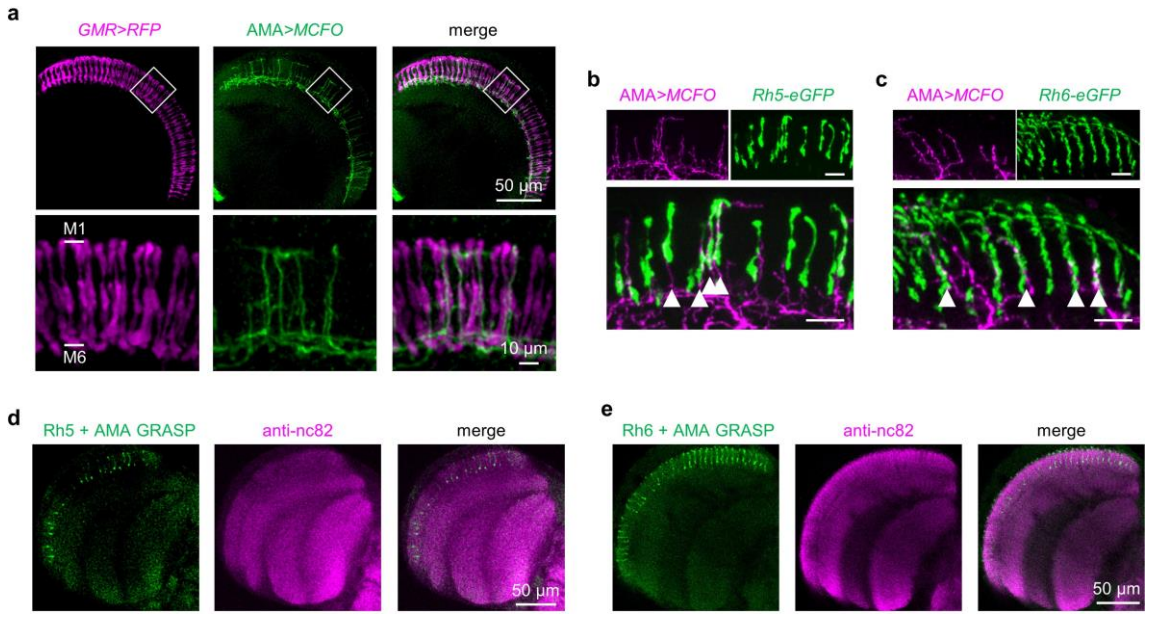

Extended Data Fig. 6 | AMA neurons are postsynaptic to both pR8s and yR8s. a, Single MCFO-labeled AMA neuron innervates many medulla columns. **Top**, RFP- labeled photoreceptors and a MCFO-labeled AMA neuron; **bottom**, an expanded view of the dashed boxes in top panels. **b,** AMA neurons innervate pR8 columns (Rh5-eGFP). **Top**, single MCFO-labeled AMA neuron (left) and pR8s (right); **bottom**, overlap image. Arrowheads indicate overlap between an AMA neuron and many pR8s. Scale bar: 10 µm. **c,** AMA neuron innervates yR8 column (Rh6-eGFP). **Top**, single MCFO-labeled AMA neuron (left) and yR8s (right); **bottom**, overlap image. Arrowheads indicate overlap between an AMA neuron and many yR8s. Scale bar: 10 µm. **d and e**, Connections between R8s and AMA neurons. Single-section image of GRASP signals between AMA neurons and pR8s (**d**) and yR8s (**e**).

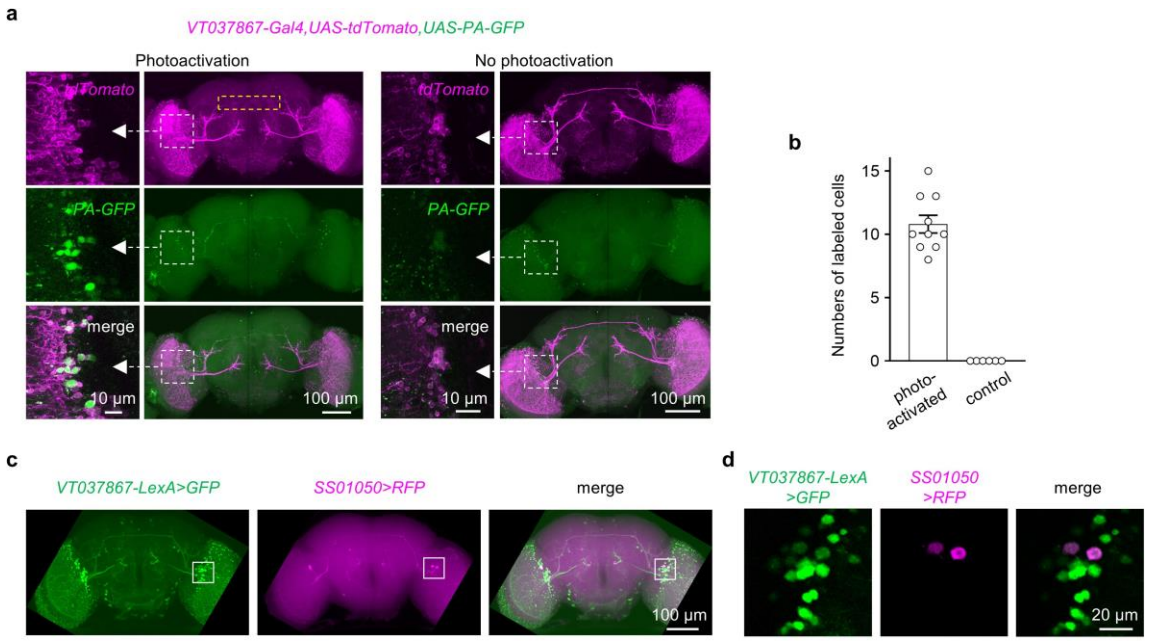

Extended Data Fig. 7 | Estimation of the number of AMA neurons. a, PA-GFP labeling of AMA neurons. **Left**, tdTomato is used to identify the dorsal commissure track in *VT037867-Gal4,UAS-tdTomato,UAS-PA-GFP* flies for photoactivation (top), PA-GFP-labeled cell bodies and commissure track of AMA neurons (middle), merged image (bottom); **right,** negative control of PA-GFP labeling: tdTomato-labeled dorsal commissure track in *VT037867-Gal4,UAS-tdTomato,UAS-PA-GFP* flies (top), no PA- GFP-labeling without photoactivation (middle), merged image (bottom). Left, an expanded view of the dashed boxes in the right panels. **b,** pooled total number of PA-GFP- labeled AMA neurons. Pooled data: mean ± s.e.m. **c,** Co-labeling of aMe 12 neurons (*SS01050>RFP*) and AMA neurons (*VT037867-LexA>GFP*). **d,** An expanded view of the dashed boxes in **c**.

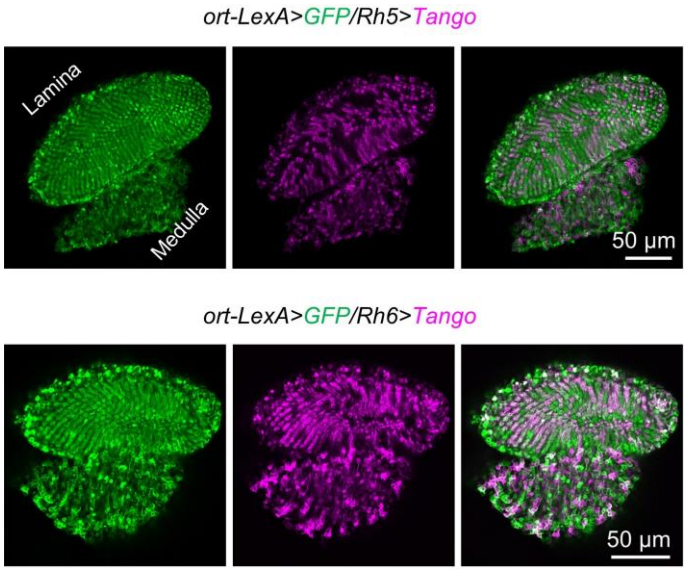

Extended Data Fig. 8 | ort-expressing postsynaptic neurons of R8s. Overlap of anterograde tdTomato labeling with *trans*-Tango and *ort-LexA>GFP* revealed ort-expressing postsynaptic neurons downstream of pR8s (top) and yR8s (bottom).

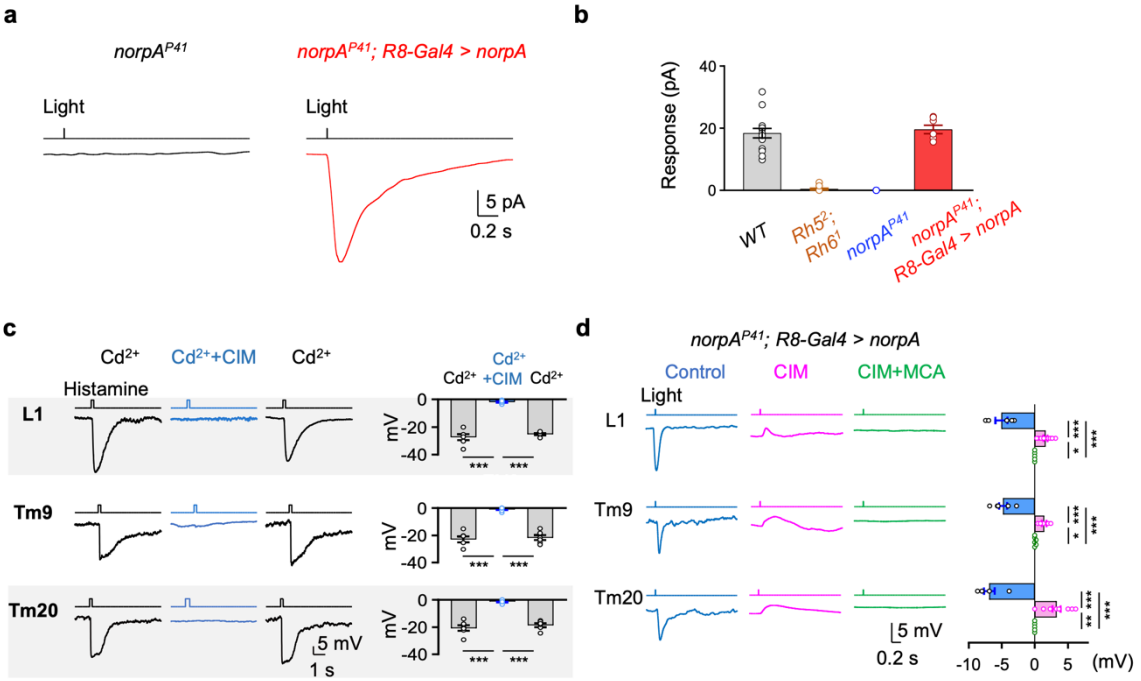

Extended Data Fig. 9 | Light responses of postsynaptic neurons of R8s. a, Representative response of AMA neurons in *norpA*^{P41} flies with norpA-rescued in R8s. **b,** Pooled data of light response of AMA in wild-type, *Rh5*^{2}*; Rh6*^{1} double mutant, *norpA*^{P41} flies with norpA rescued in R8s. Light stimulation in **a** and **b**: 470 nm, 2 ms, 5.56×10^{7} photons/μm^2/s. **c,** Histamine directly hyperpolarizes L1, Tm9 and Tm20 neurons (in the presence of cadmium). **Left**, representative hyperpolarization in L1, Tm9 and Tm20 (first column), which is blocked by 2 mM CIM (second column) and recovered after wash out (third column). **Right**, pooled data. Histamine: 1 mM, duration of 200 ms. **d,** R8-driven responses in L1, Tm9, and Tm20 neurons require histamine transmission. **Left**, representative R8-driven responses in L1, Tm9, and Tm20; **right**, pooled data. Light: 470 nm, 2 ms, 5.65×10^{7} photons/μm^2/s. Pooled data are mean ± s.e.m. **P* < 0.05; ***P* < 0.01; ****P* < 0.001. Note a tiny light-triggered depolarization of L1, Tm9, and Tm20 in the absence of histamine signaling. Statistical analysis is summarized in Extended Data Table

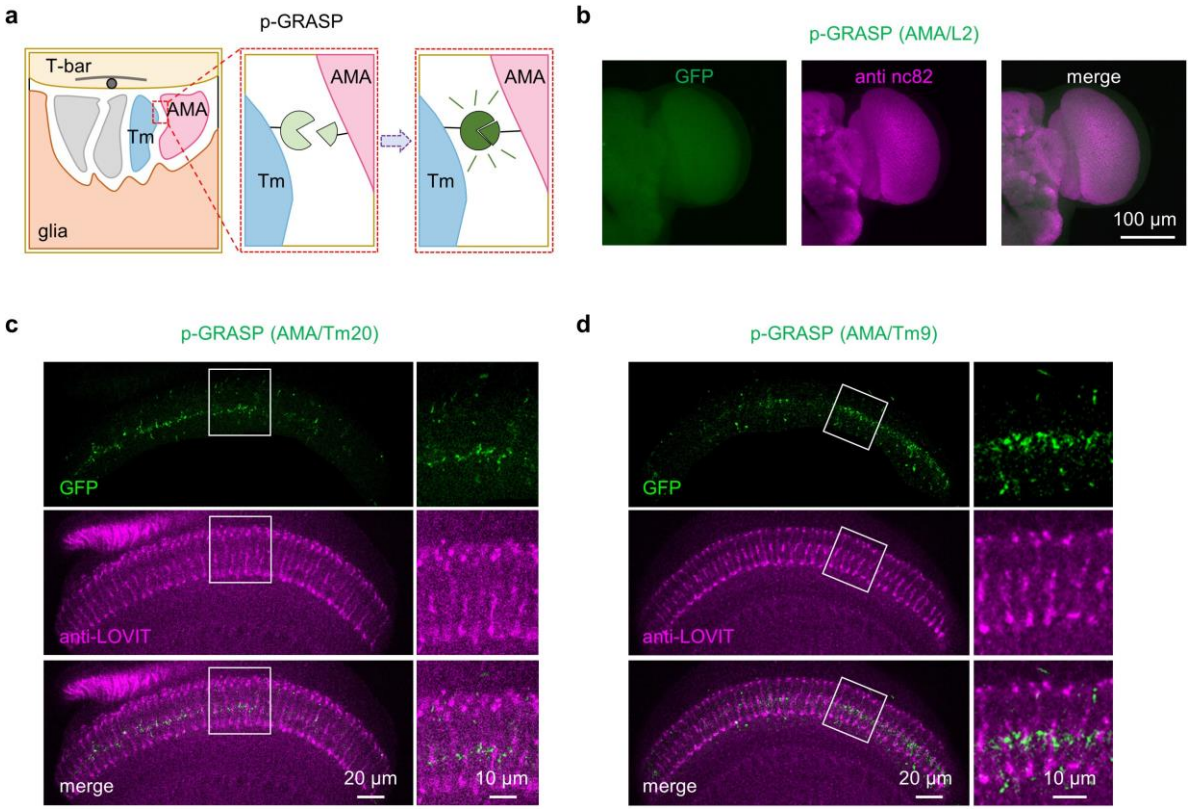

Extended Data Fig. 10 | p-GRASP method. a, A working model of p-GRASP method. Two complementary split-GFP segments are expressed in postsynaptic sites of two different neurons. GFP signals appear when these two neurons share the same presynaptic site. **b,** Negative control of p-GRASP. No recombined GFP is detected between AMA neurons (*VT037867-LexA*) and L2 neurons (*SS00690-spGal4*) in the medulla. **c,** AMA neurons share the same polyadic R8 synapse with Tm9. **Left**, p- GRASP between AMA neurons (*VT037867-LexA*) and *Tm9* neurons (*SS00307-spGal4*) (top), anti-LOVIT labels R8 axons in the medulla (middle), and overlap image (bottom); **right**, an expanded view of the white boxes in left panels. **d,** AMA neurons share the same polyadic R8 synapse with Tm20. **Left**, p-GRASP between AMA neurons (*VT037867-LexA*) and *Tm20* neurons (*SS00355-spGal4*) (top), anti-LOVIT labels R8 axons in the medulla (middle), and overlap image (bottom); **right**, an expanded view of the white boxes in left panels.

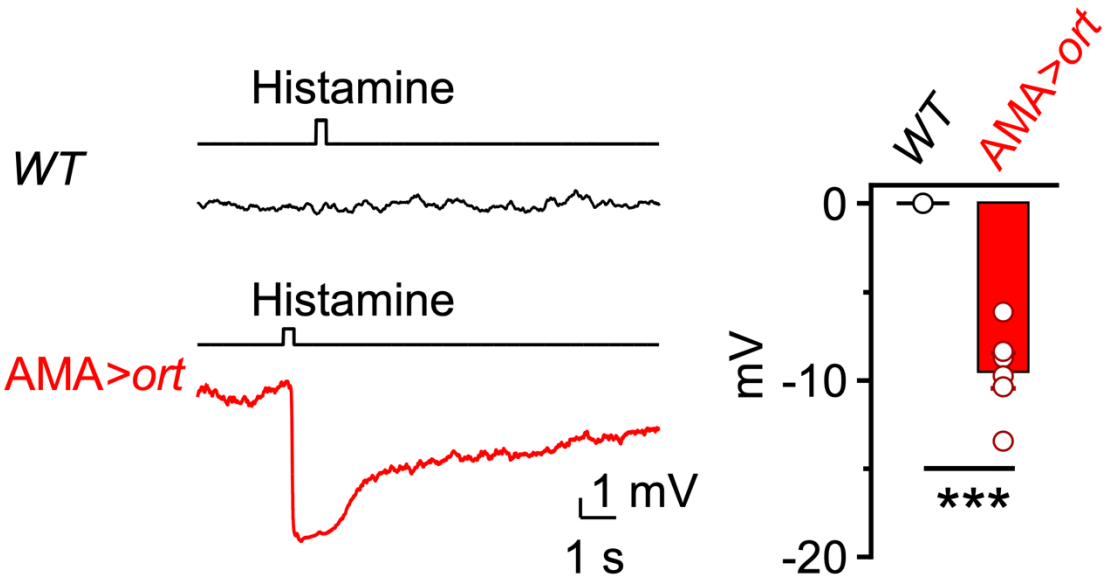

Extended Data Fig. 11 | Ectopic ort expression in AMA neurons. Left, representative histamine-induced responses in AMA neurons of wild-type flies (top), and transgenic flies with ort expressed ectopically in AMA neurons; **right**, pooled data of peak response amplitudes (n=6). Histamine stimulation: 1 mM, duration of 250 ms. Pooled data are mean ± s.e.m. ***$P < 0.001$. Statistical analysis is summarized in Extended Data Table 2.

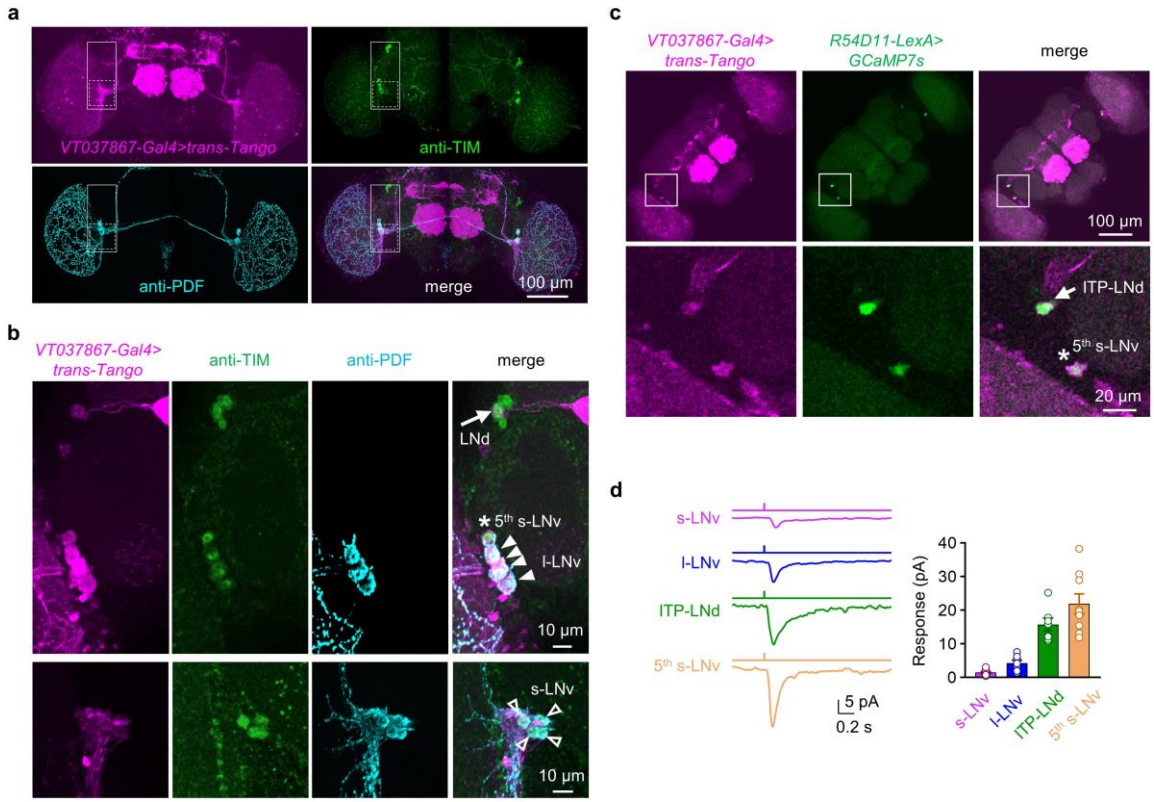

Extended Data Fig. 12 | Clock neurons are postsynaptic to AMA neurons. a, Co-labeling clock neurons (with anti-TIM and anti-PDF) together with the labeling of postsynaptic neurons of AMA neurons (*VT037867-Gal4>trans-Tango*). **b,** An expanded view of the white rectangles (top) and the dashed boxes (bottom) in **a**. Arrow indicates LNds, asterisk indicates 5th s-LNv, arrowhead indicates l-LNv, and unfilled arrowhead indicates s-LNv. **c**, **Top**, Co-labeling ITP-LNd and 5th s-LNv (*R54D11- LexA>GCaMP7s*) and postsynaptic neurons of AMA neurons (*VT037867-Gal4>trans- Tango*); **bottom**, an expanded view of the white boxes in top panels. **d,** R8s differentially excite different clock neurons. **Left**, representative R8-driven responses of different clock neurons; **right,** pooled peak response amplitudes (mean ± s.e.m.). Light: 470 nm, 2 ms, 5.65×10^7 photons/µm^2/s. Statistical analysis is summarized in Extended Data Table 2.

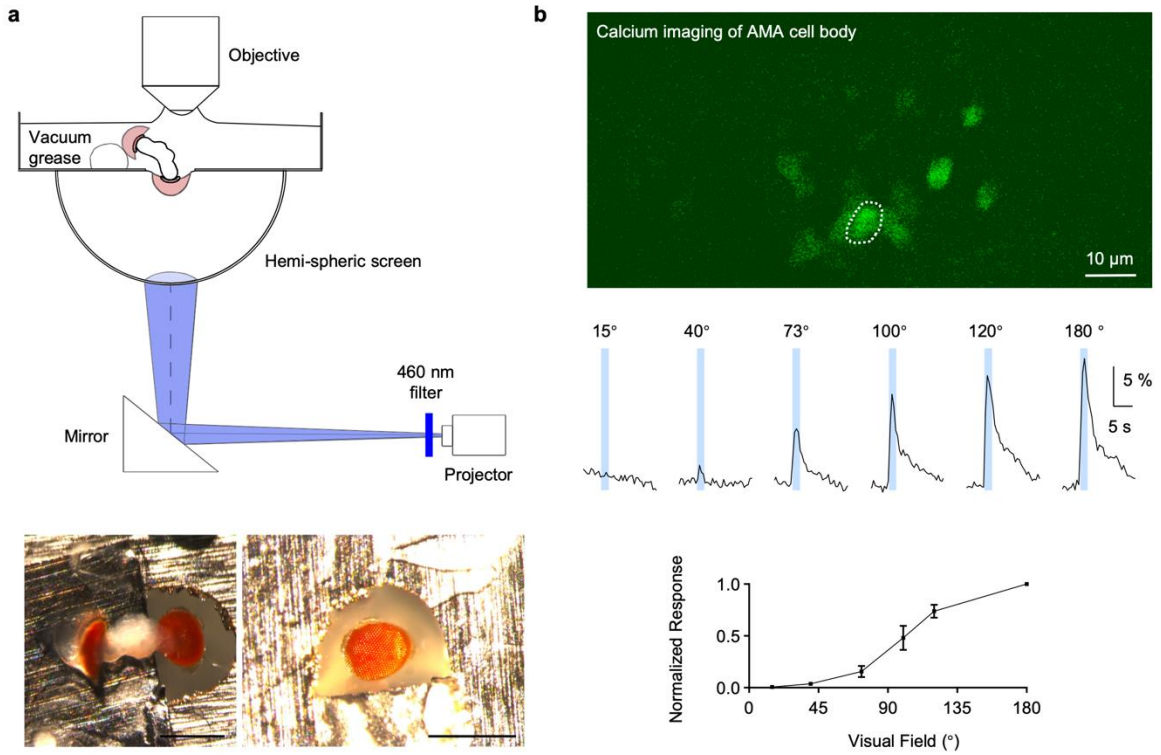

Extended Data Fig. 13 | Receptive field of AMA neurons. a, Top, Schematic of ex vivo preparations for mapping the receptive field of AMA neurons. The recording chamber was made of a thin sheet of stainless steel (20 µm thick), with a rectangle hole slightly larger than a compound eye. Fly brains with intact compound eyes were dissected, and one compound eye was inserted into the chamber hole to expose it to the air. The other compound eye was stabilized in the chamber with vacuum grease. A hemispherical screen (a diameter of 40 mm) was placed under the chamber, with the exposed compound eye facing the center of the screen. Light spots were projected to the screen from a back projector via a reflecting mirror. Light simulation of 460 nm was used to avoid interference with the fluorescence-imaging detector. Calcium responses reported by GCaMP6m were acquired with a two-photon microscopy and fluorescence excitation by a two-photon laser of 920 nm. **Bottom**, a representative top view of the brain preparation (left) and a representative bottom view of the exposed compound eye (right). Scale bar: 500 µm. **b, Top,** representative calcium imaging of AMA neurons; **middle**, representative response traces of AMA neurons to visual stimuli of varying spot sizes; **bottom,** pooled normalized peak response amplitudes against the spot size. Light stimulation: 460 nm, 2.5 s, 3 µW, spot size: 15, 40, 73, 100, 120, and 180°. Blue bars show the timing of light stimulation. Pooled data are mean ± s.e.m. Statistical analysis is summarized in Extended Data Table 2.

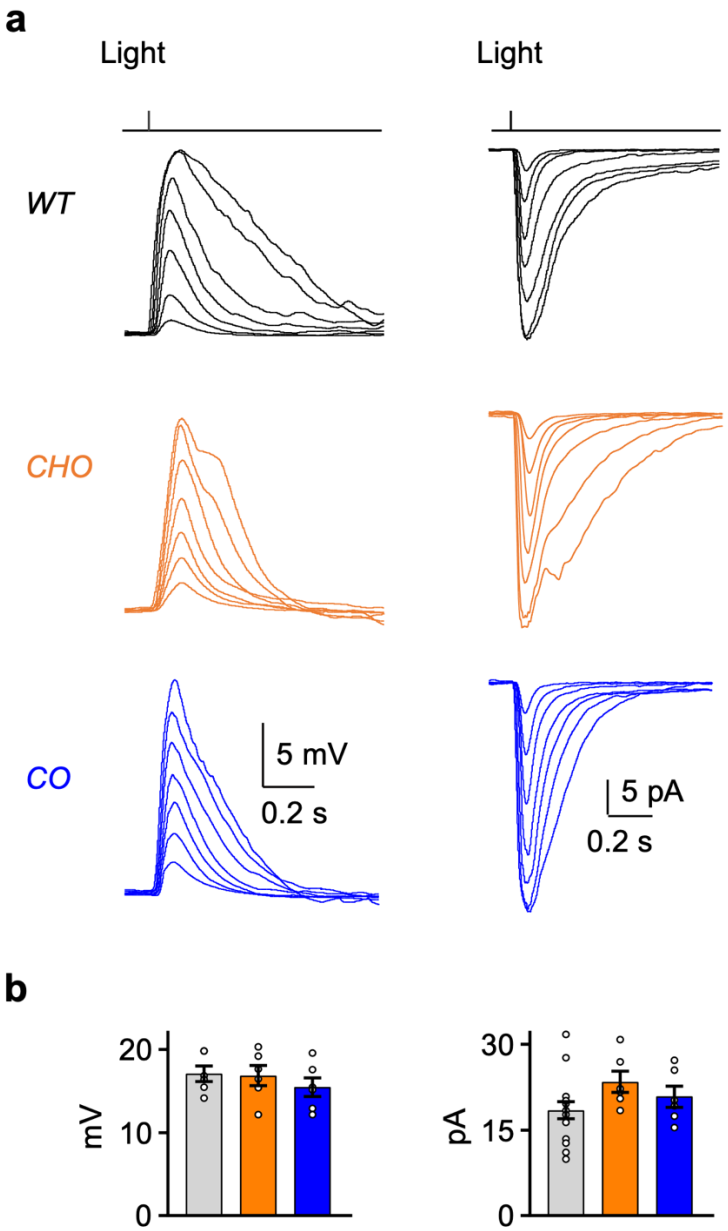

Extended Data Fig. 14 | Light pulse-triggered responses are intact in *CHO* flies. a, Left, representative voltage responses (current-clamp); **right**, representative current responses (voltage-clamp) of AMA neurons. Light stimulation: 470 nm, 2 ms, intensities of 0.51, 0.94, 1.51, 1.88, 2.82, 4.52, and 6.59×10^7 photons/μm^2/s. **b**, pooled data for depolarization (left), and inward current (right) induced by 470 nm, 2 ms, and 5.65×10^7 photons/μm^2/s. Pooled data are mean ± s.e.m. Statistical analysis is summarized in Extended Data Table 2.

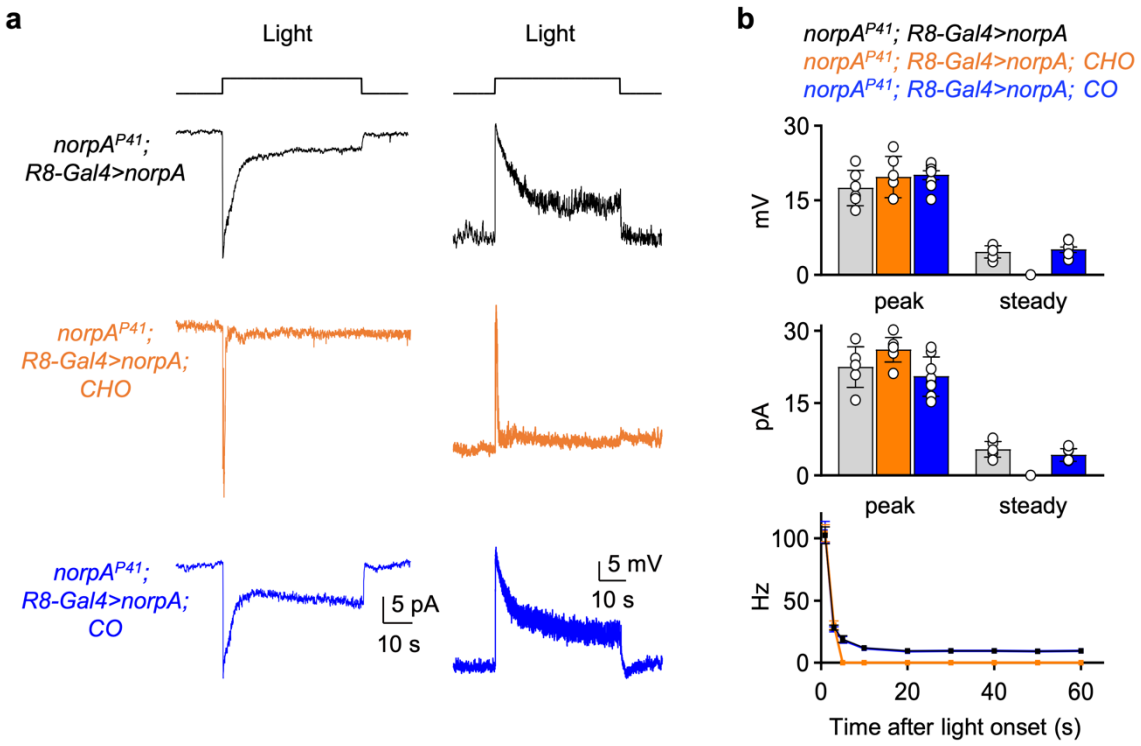

Extended Data Fig. 15 | Cell-autonomous feedback in R8s maintains steady responses in AMA neurons. a, Representative light step-triggered steady inward currents (left, voltage-clamp) and membrane depolarization and spike firing (right, current-clamp) of AMA neurons in *norpA*^{P41} flies with norpA rescued in R8s (top), *norpA*^{P41}*;; CHO* flies with norpA rescued in R8s (middle), and *norpA*^{P41}*;;CO* flies with norpA rescued in R8s (bottom). **b**, Pooled peak and steady inward currents (top), membrane depolarization (middle), and firing rates (bottom). Light stimuli: 470 nm, 60 s, 1.88×10^6 photons/μm^2/s. Pooled data are mean ± s.e.m. Statistical analysis is summarized in Extended Data Table 2.

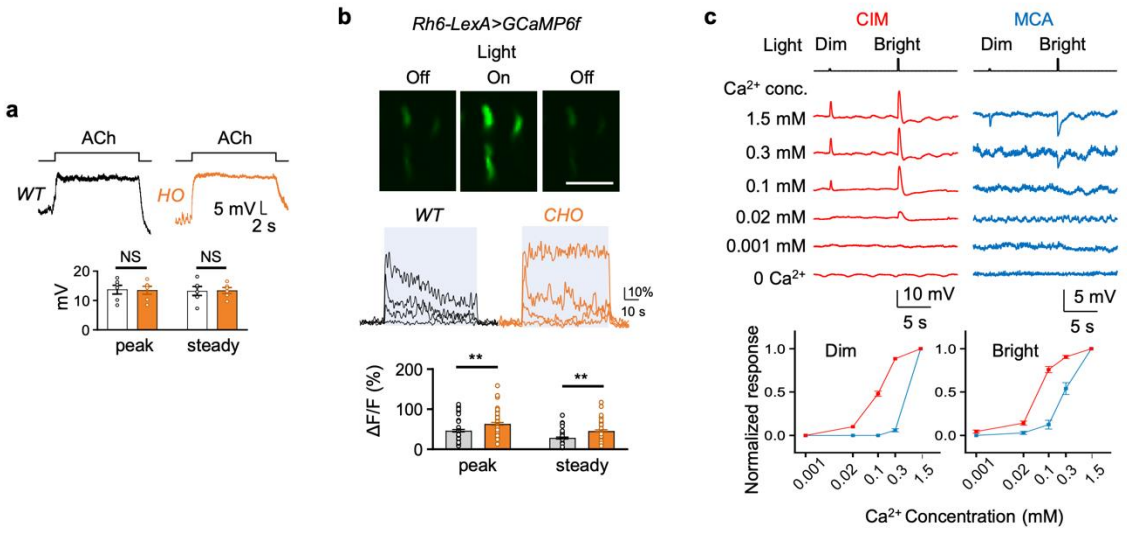

Extended Data Fig. 16 | Presynaptic mechanism supports continuous ACh release. a, AChRs function normally in *HO* flies. **Top**, representative response of AMA neurons to 1 mM ACh in WT and *HO* flies; **bottom**, pooled data. Note, there is a hyperpolarization after washing out ACh (top, left). **b,** Enhanced light-triggered calcium influx in R8 axon terminals of *CHO* flies. **Top**, representative light-triggered calcium response in R8 axons; **middle**, representative calcium response families of yR8 axons in *WT* and *CHO* flies; **bottom**, pooled peak and steady response amplitudes. Light: 470 nm, 60 s, intensities of 0.33, 1.81, 4.22, and 9.64×10^5 photons/μm^2/s. The timing of light stimulation is indicated by grey bars. Scale bar: 10 µm. **c,** Distinct calcium sensitivity in the release of histamine and ACh. **Top**, representative flash- triggered responses of ort-expressing AMA neurons in the presence of CIM (left) or MCA (right) at different calcium concentrations, as indicated on the left; **bottom**, pooled data. Light stimulation: 470 nm, 2 ms, 9.41×10^6 photons/μm^2/s (dim) and 6.78×10^7 photons/μm^2/s (bright). Pooled data are mean ± s.e.m. Statistical analysis is summarized in Extended Data Table 2.

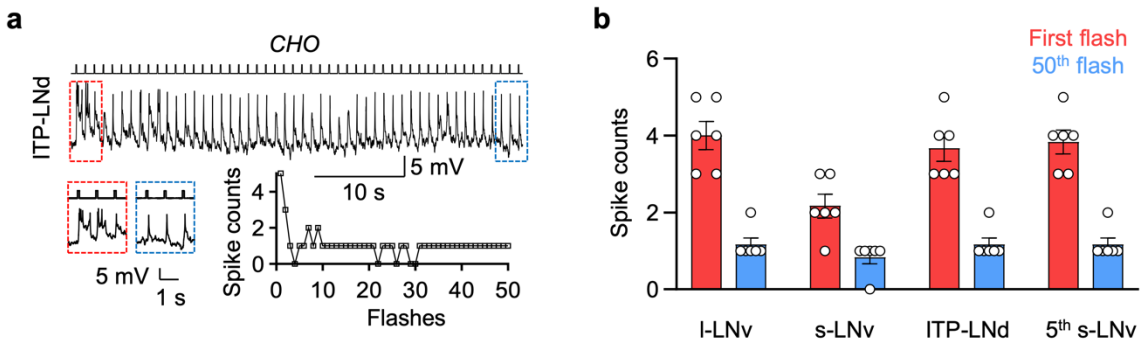

Extended Data Fig. 17 | Frequency-dependent flash-triggered responses in clock neurons of *CHO* flies. a, Top, representative response to 1 Hz flashes of ITP-LNd in *CHO* flies; **bottom**, an expanded view of the first three (red box) and last three (blue box) responses (left), and spike counts (right). **b,** Pooled data of the first and the 50th flash-induced spikes in different clock neurons of *CHO* flies. Light: 470 nm, 100 ms, 4.71×10^{7} photons/μm^{2}/s. Pooled data are mean ± s.e.m. Statistical analysis is summarized in Extended Data Table 2.

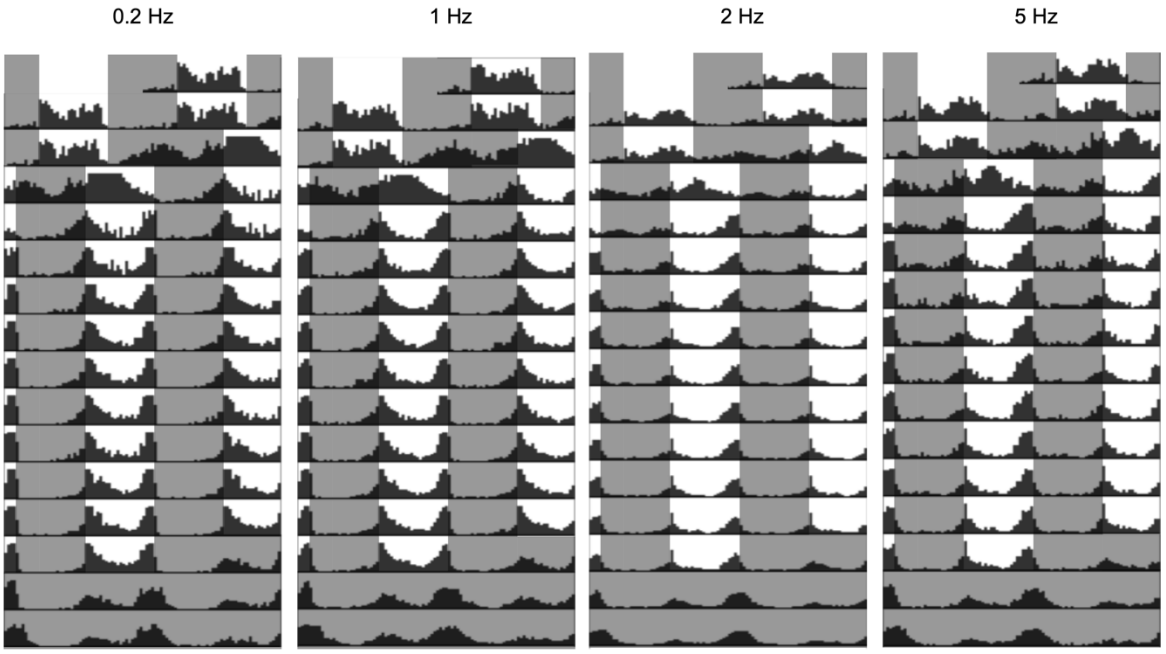

Extended Data Fig. 18 | Circadian entrainment to brief light pulses in wild-type flies. Average actograms to light flashes (duration of 100 ms) at 0.2 Hz (n=15), 1 Hz (n=20), 2 (n=23), and 5 Hz (n=21). LD1: 200 lux (white light) together with 25°C/18°C temperature cycles; LD2: 0.5 lux (white light) at 25°C; DD: 25°C.

Extended Data Tables

Extended Data Table. 1 | Fly genotypes

Figure	Genotypes	Purpose
Fig. 1a	*DvPdf-Gal4,UAS-GFP*	Labeling clock neurons (l-LNv, s-LNv, 5th s-LNv, ITP-LNd, and cry-negative LNd)
Fig. 1b	*DvPdf-Gal4,UAS-GFP* *Hdc^{JK910}; DvPdf-LexA,LexAop-GFP* *DvPdf-Gal4,UAS-GFP; HisCl1^{134},ort^{1}*	Labeling clock neurons in WT, *Hdc^{JK910}*, or *HO* flies
Fig. 1c	*DvPdf-Gal4,UAS-GFP; HisCl1^{134},ort^{1}* *norpA^{P41}/y; DvPdf-Gal4,UAS-GFP; HisCl1^{134},ort^{1}*	Labeling clock neurons in *HO*, or *norpA^{P41}* and *HO* flies
Fig. 1d	*Rh6-Gal4,UAS-GFP; HisCl1^{134},ort^{1}* *Rh6-Gal4,UAS-GFP/Rh6-hid,rpr; HisCl1^{134},ort^{1}* *DvPdf-Gal4,UAS-GFP/Rh6-hid,rpr; HisCl1^{134},ort^{1}* *DvPdf-Gal4,UAS-GFP/Rh6-Gal4,UAS-GFP; HisCl1^{134},ort^{1}*	Labeling clock neurons in *HO* flies (with HB eyelets genetically ablated or laser-ablated)
Fig. 1e	*DvPdf-Gal4,UAS-GFP; HisCl1^{134},ort^{1}* *DvPdf-Gal4,UAS-GFP; ninaE^{I17},HisCl1^{134},ort^{1}* *Rh5^{2},DvPdf-Gal4,UAS-GFP; HisCl1^{134},ort^{1}* *DvPdf-Gal4,UAS-GFP; Rh6^{1},HisCl1^{134},ort^{1}* *Rh5^{2},DvPdf-Gal4,UAS-GFP; Rh6^{1},HisCl1^{134},ort^{1}*	Labeling clock neurons in *HO* flies with loss of Rh1, Rh5, or Rh6 (with HB eyelets laser-ablated)
	norpA^{P41}/y; UAS-norpA/DvPdf-LexA,LexAop-GFP; HisCl1^{134},ort^{1} *norpA^{P41}/y; Rh1-Gal4,UAS-norpA/DvPdf-LexA,LexAop-GFP; HisCl1^{134},ort^{1}* *norpA^{P41}/y; Rh3-Gal4,UAS-norpA/DvPdf-LexA,LexAop-GFP; HisCl1^{134},ort^{1}* *norpA^{P41}/y; Rh4-Gal4,UAS-norpA/DvPdf-LexA,LexAop-GFP; HisCl1^{134},ort^{1}* *norpA^{P41}/y; Rh5-Gal4,UAS-norpA/DvPdf-LexA,LexAop-GFP; HisCl1^{134},ort^{1}* *norpA^{P41}/y; Rh6-Gal4,UAS-norpA/DvPdf-LexA,LexAop-GFP; HisCl1^{134},ort^{1}*	Labeling clock neurons in *norpA^{P41}* and *HO* triple mutant flies with norpA rescued in different photoreceptors (with HB eyelets laser-ablated)
Fig. 1f	*norpA^{P41}/y; Rh5-Gal4,UAS-norpA/DvPdf-LexA,LexAop-GFP* *norpA^{P41}/y; Rh5-Gal4,UAS-norpA/DvPdf-LexA,LexAop-GFP; HisCl1^{134},ort^{1}* *norpA^{P41}/y; Rh6-Gal4,UAS-norpA/DvPdf-LexA,LexAop-GFP* *norpA^{P41}/y; Rh6-Gal4,UAS-norpA/DvPdf-LexA,LexAop-GFP; HisCl1^{134},ort^{1}*	Labeling clock neurons in *norpA^{P41}* or *norpA^{P41}* and *HO* triple mutant flies with norpA rescued in different photoreceptors (with HB eyelets laser-ablated)
Fig. 2a	*Rh5-Gal4,Rh6-Gal4/UAS-FRT-STOP-FRT-GFP; ChAT-FLP/+*	Labeling ChAT-expressing R8s
Fig. 2b	*Rh5-Gal4/UAS-FRT-STOP-FRT-GFP; ChAT-FLP/+* *Rh6-Gal4/UAS-FRT-STOP-FRT-GFP; ChAT-FLP/+*	Labeling ChAT-expressing R8s
Fig. 2c	*Rh5-Gal4/UAS-FLP; VAChT-FRT-STOP-FRT-HA/+* *Rh6-Gal4/UAS-FLP; VAChT-FRT-STOP-FRT-HA/+*	HA labeling in ChAT-expressing R8s
Fig. 2d	*Rh5-Gal4; UAS-FRT-STOP-FRT-GFP,ChAT-FLP/+* *Rh6-Gal4; UAS-FRT-STOP-FRT-GFP,ChAT-FLP/+*	HA labeling in ChAT-expressing R8s
Fig. 2e	*Rh5-Gal4,Rh6-Gal4; UAS-norpA* *norpA^{P41}/y* *norpA^{P41}/y; Rh5-Gal4,Rh6-Gal4; UAS-norpA*	norpA rescue in R8s of *norpA^{p41}* flies

Fig. 2f	*norpA^{P41}; cry^{02}* *norpA^{P41}/y; Rh5-Gal4,Rh6-Gal4,UAS-norpA; cry^{02}*	norpA rescue in R8s of *norpA^{P41}* and *cry^{02}* double mutant flies
	norpA^{P41}/y; Rh5-Gal4,Rh6-Gal4,UAS-norpA/Rh6-hid,rpr; cry^{02}	norpA rescue in R8s of *norpA^{P41}* and *cry^{02}*double mutant flies (with HB eyelets ablated genetically)
Fig. 2g	*ort^{1}*	*ort^{1}*mutant flies
	norpA^{P41}/y; Rh5-Gal4,Rh6-Gal4,UAS-norpA; ort^{1}	norpA rescue in R8s of *norpA^{P41}* and *ort^{1}* double mutant flies
	norpA^{P41}/y; Rh5-Gal4,Rh6-Gal4,UAS-norpA/UAS-Hdc-sgRNA,UAS-Cas9.P2	Hdc knockout in R8s of flies with norpA rescued in R8s of *norpA^{P41}* flies
Fig. 2h	*norpA^{p41}/y; Rh5-Gal4,Rh6-Gal4,UAS-norpA; cry^{02},ort^{1}*	norpA rescue in R8s of *norpA^{P41}*, *ort^{1}*, and *cry^{02}* triple mutant flies
Fig. 2i	*norpA^{P41}/y; Rh5-Gal4,Rh6-Gal4,UAS-norpA/UAS-ChAT-sgRNA,UAS-Cas9.P2; ort^{1},cry^{02}*	ChAT knockout in R8s with norpA rescued in *norpA^{P41}*, *ort^{1}*, and *cry^{02}* triple mutant flies
Fig. 2j	*norpA^{P41}/y; Rh5-Gal4,Rh6-Gal4,UAS-norpA/UAS-Cas9.P2,UAS-ChAT-sgRNA*	ChAT knockout in R8s with norpA rescued in *norpA^{P41}* flies
Fig. 3a	*UAS-GFP,QUAS-tdTomato/+; Rh5-Gal4/trans-Tango; ort-QS/+*	Exclusion of QUAS-tdTomato expression in ort-expressing postsynaptic neurons of pR8s by ort-QS
	UAS-GFP,QUAS-tdTomato/+; Rh6-Gal4/trans-Tango; ort-QS/+	Exclusion of QUAS-tdTomato expression in ort-expressing postsynaptic neurons of yR8s by ort-QS
Fig. 3b	*UAS-GFP,QUAS-tdTomato/+; VT037867-LexA,LexAop-GFP,Rh5-Gal4/ trans-Tango; ort-QS/+*	AMA neurons overlap with postsynaptic neurons of pR8s
	UAS-GFP,QUAS-tdTomato/+; VT037867-LexA,LexAop-GFP/trans-Tango; Rh6-Gal4/ort-QS	AMA neurons overlap with postsynaptic neurons of yR8s
Fig. 3c	*Rh5-Gal4/VT037867-LexA; UAS-GFP$^{1-10}$,LexAop-GFP^{11}/+* *Rh6-LexA/+; UAS-GFP$^{1-10}$,LexAop-GFP^{11}/VT037867-Gal4* *GMR-LexA/+; UAS-GFP$^{1-10}$,LexAop-GFP^{11}/VT037867-Gal4*	GRASP between AMA neurons and pR8s, yR8s, or eye photoreceptors
Fig. 3d	*UAS-FRT-STOP-FRT-CsChrimson,LexAop-FLP/SS00691-AD; ort-LexA/SS00691-DBD* *UAS-FRT-STOP-FRT-CsChrimson,LexAop-FLP/ort-Gal4.C1a.DBD; ort-LexA/dVP16AD[ET18k]* *UAS-FRT-STOP-FRT-CsChrimson,LexAop-FLP/SS00307-AD; ort-LexA/SS00307-DBD* *UAS-FRT-STOP-FRT-CsChrimson,LexAop-FLP/SS00355-AD; ort-LexA/SS00355-DBD*	Labeling ort-expressing L1, Tm5, Tm9, or Tm20, respectively
Fig. 3e	*Rh6-LexA/SS00691-AD; UAS-GFP$^{1-10}$,LexAop-GFP^{11}/SS00691-DBD* *Rh6-LexA/ort-Gal4.C1a.DBD; UAS-GFP$^{1-10}$,LexAop-GFP^{11}/dVP16AD[ET18k]* *Rh6-LexA/SS00307-AD; UAS-GFP$^{1-10}$,LexAop-GFP^{11}/SS00307-DBD* *Rh6-LexA/SS00355-AD; UAS-GFP$^{1-10}$,LexAop-GFP^{11}/ SS00355-DBD*	GRASP between yR8s and L1, Tm5, Tm9, or Tm20, respectively

Fig. 3f	*VT037867-Gal4,UAS-GCaMP6m* *$Rh5^{2}$; VT037867-Gal4,UAS-GCaMP6m,$Rh6^{1}$* *$norpA^{P41}$/y; Rh5-Gal4,Rh6-Gal4/+; VT037867-Gal4,UAS-GCaMP6m/UAS-norpA*	Labeling AMA neurons in WT, or *$Rh5^{2}$;$Rh6^{1}$* mutant flies, or *$norpA^{P41}$* flies with norpA rescued in R8s
Fig. 3g	*VT037867-Gal4,UAS-GCaMP6m* *Hdc^{JK910}; VT037867-Gal4,UAS-GCaMP6m* *VT037867-Gal4,UAS-GCaMP6m,$HisCl^{134}$,ort^{1}* *Rh5-Gal4,Rh6-Gal4,UAS-Cas9.P2/UAS-ChAT sgRNA; VT037867-Gal4,UAS-GCaMP6m* *Rh5-Gal4,Rh6-Gal4,UAS-Cas9.P2/UAS-VAChT sgRNA; VT037867-Gal4,UAS-GCaMP6m*	Labeling AMA neurons in WT, or *hdc*^{JK910}, or *ort^{1}* flies, or flies with ChAT knocked out in R8s
Fig. 3h	*27G06-LexA,LexAop-GFP* *24C08-Gal4,UAS-GCaMP6m* *ort-Gal4.C1a.DBD, ET.VP16.AD [tou9A30],UAS-GFP*	Labeling L1, Tm9, Tm20, respectively
	$norpA^{P41}$/y; 27G06-LexA,LexAop-GFP/Rh5-Gal4,Rh6-Gal4,UAS-norpA *$norpA^{P41}$/y; Rh5-Gal4,Rh6-Gal4,UAS-norpA; 24C08-Gal4,UAS-GCaMP6m* *$norpA^{P41}$/y; ort-Gal4.C1a.DBD, ET.VP16.AD [tou9A30],UAS-GFP/Rh5-Gal4,Rh6-Gal4,UAS-norpA*	Labeling L1, Tm9, or Tm20 in *$norpA^{P41}$* flies with norpA rescued in R8s
	$norpA^{P41}$/y; 27G06-LexA,LexAop-GFP/Rh5-Gal4,Rh6-Gal4,UAS-norpA; $HisCl^{134}$,ort^{1} *$norpA^{P41}$/y; Rh5-Gal4,Rh6-Gal4,UAS-norpA; 24C08-Gal4,UAS-G6M,$HisCl^{134}$,ort^{1}* *$norpA^{P41}$/y; ort-Gal4.C1a.DBD, ET.VP16.AD [tou9A30],UAS-GFP/Rh5-Gal4,Rh6-Gal4,UAS-NorpA; $HisCl^{134}$,ort^{1}*	Labeling L1, Tm9, or Tm20 in *HO* and *$norpA^{P41}$* flies with norpA rescued in R8s
Fig. 3i	*VT037867-LexA/SS00307-AD; UAS-post-GFP^{1-10},LexAop-post-GFP^{11}/SS00307-DBD* *VT037867-LexA/SS00355-AD; UAS-post-GFP^{1-10},LexAop-post-GFP^{11}/SS00355-DBD*	p-GRASP between AMA neurons and Tm9 or Tm20
Fig. 3j	*UAS-ort/+; VT037867-Gal4,UAS-GCaMP6m,cry^{02},$HisCl1^{134}$,ort^{1}*	Ectopic ort expression in AMA neurons of *CHO* flies
Fig. 4a	*UAS-GFP,UAS-tdTomato/; trans-Tango; VT037867-Gal4/+*	Labeling postsynaptic neurons of AMA neurons
Fig. 4b	*VT037867-LexA,Clk856-Gal4/LexAop2-Syb::GFP-P10,LexAop-QF2::SNAP25::HIVNES::Syntaxin; UAS-B3Recombinase,UAS<B3STOP<BoNT/A,UAS<B3STOP<BoNT/A,Q UAS-mtdTomato::HA/+* *VT037867-LexA,DvPdf-Gal4/LexAop2-Syb::GFP-P10,LexAop-QF2::SNAP25::HIVNES::Syntaxin; UAS-B3Recombinase,UAS<B3STOP<BoNT/A,UAS<B3STOP<BoNT/A,Q UAS-mtdTomato::HA/+*	Labeling presynaptic AMA neurons of clock neurons
Fig. 4c	*UAS-CsChrimson/+; DvPdf-LexA,LexAop-GCaMP6m/VT037867-Gal4*	Expression of CsChrimson and GCaMP in AMA and clock neurons, respectively
Fig. 4d	*UAS-FRT-STOP-FRT-GFP/+; VT037867-Gal4/ChAT-FLP*	Labeling ChAT-expressing AMA neurons
	UAS-CsChrimson/+; DvPdf-LexA,LexAop-GCaMP6m/VT037867-Gal4	Expression of CsChrimson and GCaMP in AMA and clock neurons, respectively

Fig. 4e	*norpA^{P41}/y; Rh6-LexA,LexAop-norpA/UAS-TNTE;DvPdf-LexA,LexAop-GCaMP6m/VT037867-Gal4*	Labeling clock neurons in *norpA^{P41}* flies with norpA rescued in R8s and with AMA neurons silenced by TNT
Fig. 4f	*pBPhsFlp2::PEST/+;; UAS-FRT>STOP>FRT-myr::smGFP-HA,UAS-FRT>STOP>FRT-myr::smGFP-V5-THS-10XUAS-FRT>STOP>FRT-myr::smGFP-FLAG/VT037867-Gal4*	Single-cell labeling of AMA neurons by MCFO
Fig. 4g	*pBPhsFlp2::PEST/+;Rh5-eGFP/Rh6-LexA,LexAop-tdTomato; UAS-FRT>STOP>FRT-myr::smGFP-HA,UAS-FRT>STOP>FRT-myr::smGFP-V5-THS-10XUAS-FRT>STOP>FRT-myr::smGFP-FLAG/VT037867-Gal4*	Simultaneous labeling of pR8s, yR8s, and AMA neurons
Fig. 4h	*VT037867-Gal4,UAS-GFP* *shakB^{2}/y;; VT037867-Gal4,UAS-GFP/+* *UAS-GFP,QUAS-tdTomato/+; trans-Tango/+; VT037867-Gal4/+*	Labeling AMA neuron in *shakB^{2}* flies
Fig. 4i	*VT037867-Gal4,UAS-GCaMP6m* *shakB^{2}/y;; VT037867-Gal4,UAS-GCaMP6m*	Labeling AMA neuron in *shakB^{2}* flies
Fig. 5a	*cry^{02},HisCl1^{134},ort^{1}* *Rh6-Gal4/UAS-HisCl1; cry^{02},HisCl1^{134},ort^{1}*	HisCl1 expression in R8s of *CHO* flies
Fig. 5b	*VT037867-Gal4,UAS-GCaMP6m* *VT037867-LexA,LexAop2-GFP; cry^{02},ort^{1}* *VT037867-LexA,LexAop2-GFP; cry^{02},HisCl1^{134},ort^{1}*	Labeling AMA neurons in *CO* or *CHO* flies
Fig. 5c	*Rh6-Gal4,UAS-HisCl1/VT037867-LexA,LexAop2-GFP*; *cry^{02},HisCl1^{134},ort^{1}*	HisCl1 expression in yR8s of *CHO* flies
Fig. 5d	*VT037867-Gal4,UAS-GCaMP6m*	Labeling AMA neurons
Fig. 5e	*VT037867-Gal4,UAS-GCaMP6m,cry^{02},HisCl1^{134},ort^{1}*	Labeling AMA neurons in *CHO* flies
Fig. 5f	*UAS-ort; VT037867-Gal4,UAS-GCaMP6m* *UAS-ort; VT037867-Gal4,UAS-G6M,HisCl1^{134},ort^{1}*	Ectopic ort expressing in AMA neurons of WT or *HO* flies
Fig. 5g	*VT037867-Gal4,UAS-GCaMP6m* *VT037867-Gal4,UAS-GCaMP6m,HisCl1^{134},ort^{1}*	Labeling AMA neurons in WT or *CHO* flies
Fig. 5h	*cry^{02},HisCl1^{134},ort^{1}*	*CHO* flies
Extended Data Fig. 1a	*DvPdf-Gal4,UAS-GFP; cry^{02},HisCl1^{134},ort^{1}*	Labeling clock neurons in *CHO* flies
Extended Data Fig. 1b	*DvPdf-Gal4,UAS-GFP; HisCl1^{134},ort^{1}* *DvPdf-Gal4,UAS-GFP; cry^{02},HisCl1^{134},ort^{1}*	Labeling clock neurons in *HO* or *CHO* flies
Extended Data Fig. 2a	*Rh6-Gal4,UAS-GFP* *Rh6-hid,rpr/+; Rh6-Gal4,UAS-GFP*	Labeling yR8s in WT or flies with HB eyelets genetically ablated
Extended Data Fig. 2b,c,d	*Rh6-LexA,LexAop2-GCaMP6f*	Labeling yR8s and H-B eyelets before and after laser cutting
Extended Data Fig. 2e	*DvPdf-Gal4,UAS-GFP/Rh6-eGFP; HisCl1^{134},ort^{1}*	Labeling clock neurons and yR8s in *HO* flies
Extended Data Fig. 2f	*DvPdf-Gal4,UAS-GFP; HisCl1^{134},ort^{1}* *DvPdf-Gal4,UAS-GFP/Rh1-Gal4,UAS-TNTE; HisCl1^{134},ort^{1}* *DvPdf-Gal4,UAS-GFP/Rh3+4-Gal4,UAS-TNTE; HisCl1^{134},ort^{1}* *DvPdf-Gal4,UAS-GFP/Rh5-Gal4,UAS-TNTE; HisCl1^{134},ort^{1}* *DvPdf-Gal4,UAS-GFP/Rh6-Gal4,UAS-TNTE; HisCl1^{134},ort^{1}* *DvPdf-Gal4,UAS-GFP/Rh5-Gal4,Rh6-Gal4,UAS-TNTE; HisCl1^{134},ort^{1}*	Labeling clock neurons in *HO* flies with different photoreceptors silenced by TNT
Extended Data Fig. 3a	*GMR-LexA,LexAop2-GFP*	Labeling eye photoreceptors
Extended Data Fig. 3a Extended Data Fig. 3b	*HDC-Gal4,UAS-GFP/GMR-LexA,LexAop2-tdTomato*	Co-labeling histaminergic cells and eye photoreceptors
	Rh5-Gal4/+; Rh6-Gal4,UAS-GFP/+	Labeling R8s

Extended Data Fig. 3b Extended Data Fig. 3c	*HDC-Gal4,UAS-GFP/Rh5-LexA,Rh6-LexA,LexAop2-tdTomato*	Co-labeling histaminergic cells and R8s
	Rh1-Gal4/UAS-FRT-STOP-FRT-GFP; ChAT-FLP/+ *Rh3-Gal4/UAS-FRT-STOP-FRT-GFP; ChAT-FLP/+* *Rh4-Gal4/UAS-FRT-STOP-FRT-GFP; ChAT-FLP/+*	Labeling cholinergic cells that express Rh1, Rh3, or Rh4
Extended Data Fig. 3c Extended Data Fig. 3d	*vGlut-FLP/ Rh1-Gal4; UAS-FRT-STOP-FRT-GFP/+* *vGlut-FLP/ Rh3-Gal4; UAS-FRT-STOP-FRT-GFP/+* *vGlut-FLP/ Rh4-Gal4; UAS-FRT-STOP-FRT-GFP/+*	Labeling glutamatergic cells that express Rh1, Rh3, or Rh4
	Rh1-Gal4/UAS-FRT-STOP-FRT-GFP; TH-FLP/+ *Rh3-Gal4/UAS-FRT-STOP-FRT-GFP; TH-FLP/+* *Rh4-Gal4/UAS-FRT-STOP-FRT-GFP; TH-FLP/+*	Labeling dopaminergic cells that express Rh1, Rh3, or Rh4
	Rh1-Gal4/vGAT-LexA; UAS-FRT-STOP-FRT-CsChrimson,LexAop-FLP *Rh3-Gal4/vGAT-LexA; UAS-FRT-STOP-FRT-CsChrimson,LexAop-FLP* *Rh4-Gal4/vGAT-LexA; UAS-FRT-STOP-FRT-CsChrimson,LexAop-FLP*	Labeling GABAergic cells that express Rh1, Rh3, or Rh4
	vGlut-FLP/ Rh5-Gal4,Rh6-Gal4; UAS-FRT-STOP-FRT-GFP/+ *Rh5-Gal4,Rh6-Gal4/UAS-FRT-STOP-FRT-GFP; TH-FLP/+* *Rh5-Gal4,Rh6-Gal4/vGAT-LexA; UAS-FRT-STOP-FRT-CsChrimson,LexAop-FLP/+* *Rh5-Gal4,Rh6-Gal4/UAS-FRT-STOP-FRT-GFP; Trh-FLP/+*	Labeling R8s that contain glutamate, dopamine, GABA, or serotonin
Extended Data Fig. 4a	*Rh5-Gal4,Rh6-Gal4; UAS-norpA* *norpA^{P41}/y* *norpA^{P41}/y; Rh5-Gal4,Rh6-Gal4/+; UAS-norpA/+*	norpA rescue in R8s of *norpA^{P41}* flies
Extended Data Fig. 4b	*norpA^{P41}; cry^{02}* *norpA^{P41}/y; Rh5-Gal4,Rh6-Gal4,UAS-norpA; cry^{02}*	norpA rescue in R8s of *norpA^{P41}*;;*cry^{02}* double mutant flies
Extended Data Fig. 4b Extended Data Fig. 4c	*norpA^{P41}/y; Rh5-Gal4,Rh6-Gal4,UAS-norpA/Rh6-hid,rpr; cry^{02}*	norpA rescue in R8s of *norpA^{P41}*;;*cry^{02}*double mutant flies (with HB eyelets ablated genetically)
	norpA^{P41}/y; Rh5-Gal4,Rh6-Gal4,UAS-norpA/UAS-Hdc-sgRNA,UAS-Cas9.P2	Knocking out *hdc* in R8s with norpA rescued in *norpA^{P41}* flies
Extended Data Fig. 4d	*norpA^{P41}; R8-Gal4>norpA; ort^{1},cry^{02}*	
Extended Data Fig. 4e	*norpA^{P41}/y; Rh5-Gal4,Rh6-Gal4,UAS-norpA/UAS-ChAT-sgRNA,UAS-Cas9.P2; ort^{1},cry^{02}*	ChAT knockout in norpA-rescued R8s of *norpA^{P41}*;*ort^{1}*, *cry^{02}* flies
Extended Data Fig. 4f	*norpA^{P41}/y; Rh5-Gal4,Rh6-Gal4,UAS-norpA/UAS-Cas9.P2,UAS-ChAT-sgRNA*	ChAT knockout in norpA-rescued R8s of *norpA^{P41}* flies
Extended Data Fig. 5a	*UAS-GFP,QUAS-tdTomato/+; Rh5-Gal4/trans-Tango* *UAS-GFP,QUAS-tdTomato/+; Rh6-Gal4/trans-Tango*	Labeling postsynaptic neurons of pR8s and yR8s
Extended Data Fig. 5b	*UAS-GFP,QUAS-tdTomato/+; Rh5-Gal4,VT037867-LexA, LexAop-GFP/trans-Tango; ort-QS/+* *UAS-GFP,QUAS-tdTomato/+; VT037867-LexA,LexAop-GFP/trans-Tango;Rh6-Gal4/ort-QS*	Co-labeling of AMA neurons and non-*ort* target of R8s
Extended Data Fig. 5c	*pBPhsFlp2::PEST/+; ; UAS-FRT>STOP>FRT-myr::smGFP-HA,UAS-FRT>STOP>FRT-myr::smGFP-V5-THS-10XUAS-FRT>STOP>FRT-myr::smGFP-FLAG/VT037867-Gal4*	Single-cell labeling of AMA neurons with MCFO
Extended Data Fig. 5d	*VT037867-Gal4, UAS-GCaMP6m*	Single-cell labeling of AMA neurons by neurobiotin injection

Extended Data Fig. 6a	*pBPhsFlp2::PEST/+; GMR-RFP/+; UAS-FRT>STOP>FRT-myr::smGFP-HA,UAS-FRT>STOP>FRT-myr::smGFP-V5-THS-10XUAS-FRT>STOP>FRT-myr::smGFP-FLAG/VT037867-Gal4*	Co-labeling of photoreceptors and single AMA neuron
Extended Data Fig. 6b	*pBPhsFlp2::PEST/+; Rh5-eGFP /+; UAS-FRT>STOP>FRT-myr::smGFP-HA,UAS-FRT>STOP>FRT-myr::smGFP-V5-THS-10XUAS-FRT>STOP>FRT-myr::smGFP-FLAG/VT037867-Gal4*	Co-labeling of pR8s and single AMA neuron
Extended Data Fig. 6c	*pBPhsFlp2::PEST/+; Rh6-eGFP /+; UAS-FRT>STOP>FRT-myr::smGFP-HA,UAS-FRT>STOP>FRT-myr::smGFP-V5-THS-10XUAS-FRT>STOP>FRT-myr::smGFP-FLAG/VT037867-Gal4*	Co-labeling of yR8s and single AMA neuron
Extended Data Fig. 6d	*VT037867-LexA/SS00307-AD; UAS-GFP$^{1-10}$,LexAop-GFP^{11}/SS00307-DBD*	GRASP between AMA neuron and Tm9
Extended Data Fig. 6e	*VT037867-LexA/SS00355-AD; UAS-GFP$^{1-10}$,LexAop-GFP^{11}/SS00355-DBD*	GRASP between AMA neuron and Tm20
Extended Data Fig. 7a	*UAS-sPA-GFP/+; UAS-tdTomato/VT037867-Gal4*	Labeling AMA neurons with photoactivable GFP
Extended Data Fig. 7b	*UAS-RFP,LexAop-GFP/+; SS01050-AD/VT037867-LexA; SS01050-DBD/+*	Co-labeling AMA neurons (*VT037867-LexA*) and aMe12 neurons.
Extended Data Fig. 8	*UAS-GFP,QUAS-tdTomato/+; Rh5-Gal4/trans-Tango; ort-LexA,LexAop-GFP/+* *UAS-GFP,QUAS-tdTomato/+; Rh6-Gal4/trans-Tango; ort-LexA,LexAop-GFP/+*	Co-labeling ort-expressing cells and postsynaptic neurons of pR8s or yR8s
Extended Data Fig. 9a	*norpA^{P41}/y;; VT037867-Gal4,UAS-GCaMP6m/+* *norpA^{P41}/y; Rh5-Gal4,Rh6-Gal4/+; VT037867-Gal4,UAS-GCaMP6m/UAS-norpA*	Labeling AMA neurons in *norpA^{P41}* flies or *norpA^{P41}* flies with norpA rescued in R8s
Extended Data Fig. 9b	*VT037867-Gal4,UAS-GCaMP6m* *Rh5^{2}; VT037867-Gal4,UAS-GCaMP6m,Rh6^{1}* *norpA^{P41}/y;; VT037867-Gal4,UAS-GCaMP6m/+* *norpA^{P41}/y; Rh5-Gal4,Rh6-Gal4/+; VT037867-Gal4,UAS-GCaMP6m/UAS-norpA*	Labeling AMA neurons in WT, *Rh5^{2}*; *Rh6^{1}* mutant flies, *norpA^{P41}* flies, or *norpA^{P41}* flies with norpA rescued in R8s
Extended Data Fig. 9c	*27G06-LexA,LexAop-GFP* *24C08-Gal4,UAS-GCaMP6m* *ort-Gal4.C1a.DBD, ET.VP16.AD [tou9A30],UAS-GFP*	Labeling L1, Tm9, or Tm20
Extended Data Fig. 9d	*norpA^{P41}/y; 27G06-LexA,LexAop-GFP/Rh5-Gal4,Rh6-Gal4,UAS-norpA* *norpA^{P41}/y; Rh5-Gal4,Rh6-Gal4,UAS-norpA; 24C08-Gal4,UAS-GCaMP6m* *norpA^{P41}/y; ort-Gal4.C1a.DBD, ET.VP16.AD [tou9A30],UAS-GFP/Rh5-Gal4,Rh6-Gal4,UAS-norpA*	Labeling L1, Tm9, or Tm20 in *norpA^{P41}* flies with norpA rescued in R8s
Extended Data Fig. 10b	*VT037867-LexA/SS00690-AD; UAS-post-GFP$^{1-10}$,LexAop-post-GFP^{11}/SS00690-DBD*	p-GRASP between AMA neurons and L2 neurons
Extended Data Fig. 10c	*VT037867-LexA/SS00307-AD; UAS-post-GFP$^{1-10}$,LexAop-post-GFP^{11}/SS00307-DBD*	p-GRASP between AMA neurons and Tm9 neurons
Extended Data Fig. 10d	*VT037867-LexA/SS00355-AD; UAS-post-GFP$^{1-10}$,LexAop-post-GFP^{11}/SS00355-DBD*	p-GRASP between AMA neurons and Tm20 neurons
Extended Data Fig. 11	*VT037867-Gal4,UAS-GCaMP6m*	Labeling AMA neurons

Extended Data Fig. 11	*VT037867-Gal4,UAS-GCaMP6m*	Labeling AMA neurons.
	UAS-ort/+; VT037867-Gal4,UAS-GCaMP6m	Labeling AMA neurons that ectopically express *ort*
Extended Data Fig. 12a, b	*trans-Tango/+; VT03867-Gal4,QUAS-tdTomato/+*	Labeling postsynaptic neurons of AMA neurons
Extended Data Fig. 12c	*trans-Tango/+; VT03867-Gal4,QUAS-tdTomato/R54D11-LexA, LexAop-GCaMP7s*	Co-labeling ITP-LNd/5th s-LNv and postsynaptic neurons of AMA neurons
Extended Data Fig. 12d	*norpA^{P41}/y; Rh5-Gal4,Rh6-Gal4,UAS-NorpA/Rh6-eGFP; DvPdf-LexA,LexAop-GCaMP6m/+*	Labeling clock neurons in *norpA^{P41}* flies with norpA rescued in R8s of (with HB eyelets laser-ablated)
Extended Data Fig. 13a,b	*UAS-GCaMP6m; VT037867-Gal4,UAS-GCaMP6m/+*	Labeling AMA neurons
Extended Data Fig. 14	*VT037867-Gal4,UAS-GCaMP6m* *VT037867-LexA,LexAop2-GFP; cry^{02},ort^{1}* *VT037867-LexA,LexAop2-GFP; cry^{02},HisCl1^{134},ort^{1}*	Labeling AMA neurons in *CO* or *CHO* flies
Extended Data Fig. 15	*norpA^{P41}/y; Rh5-Gal4,Rh6-Gal4/+; VT037867-Gal4,UAS-GCaMP6m/UAS-norpA* *norpA^{P41}/y; Rh5-Gal4,Rh6-Gal4,UAS-norpA/VT037867-LexA,LexAop-GFP ; cry^{02},HisCl1^{134}, ort^{1}*	Labeling AMA neurons in *norpA^{P41}*;*CHO* (or *CO*) flies with norpA rescued in R8s
Extended Data Fig. 16a	*VT037867-Gal4,UAS-GCaMP6m* *VT037867-Gal4,UAS-GCaMP6m,HisCl1^{134},ort^{1}*	Labeling AMA neurons in WT or *HO* flies
Extended Data Fig. 16b	*Rh6-LexA,LexAop2-GCaMP6f* *Rh6-LexA,LexAop2-GCaMP6f; cry^{02},HisCl1^{134},ort^{1}*	Labeling yR8s in WT or *CHO* flies
Extended Data Fig. 16c	*UAS-ort; VT037867-Gal4,UAS-GCaMP6m*	Ectopic *ort* expression in AMA neurons
Extended Data Fig. 17	*DvPdf-Gal4,UAS-GFP; cry^{02},HisCl1^{134},ort^{1}*	Labeling clock neurons in *CHO* flies
Extended Data Fig. 18	*w1118*	Photoentrainment

Extended Data Table. 2 | Statistical details

Figure		Cell type	P value
Fig. 1b	one-way ANOVA followed by Tukey's post hoc test	l-LNv	WT (n = 9 from 5 flies) vs. HO (n = 11 from 7 flies), P = 2.06904E-6 WT (n = 9 from 5 flies) vs. HDC (n = 11 from 7 flies), P = 0.00782 HO (n = 11 from 7 flies) vs. HDC (n = 11 from 7 flies), P = 0.03169
		s-LNv	WT (n = 8 from 5 flies) vs. HO (n = 8 from 5 flies), P = 0.00489 WT (n = 8 from 5 flies) vs. HDC (n = 6 from 6 flies), P = 0.02149 HO (n = 8 from 7 flies) vs. HDC (n = 8 from 8 flies), P = 0.85111
		ITP-LNd	WT (n = 8 from 6 flies) vs. HO (n = 7 from 6 flies), P = 1.45641E-4 WT (n = 8 from 6 flies) vs. HDC (n = 6 from 5 flies), P = 0.00264 HO (n = 7 from 6 flies) vs. HDC (n = 6 from 5 flies), P = 0.53599
		5^{th} s-LNv	WT (n = 6 from 6 flies) vs. HO (n = 8 from 7 flies), P = 4.30265E-5 WT (n = 6 from 6 flies) vs. HDC (n = 8 from 8 flies), P = 1.00666E-5 HO (n = 8 from 7 flies) vs. HDC (n = 8 from 8 flies), P = 0.74038
Fig. 1c		l-LNv	HO (n = 11 from 7 flies) HO+norpA^{P41} (n = 5 from 5 flies) HO+eye removal (n = 5 from 5 flies)
		s-LNv	HO (n = 8 from 5 flies) HO+norpA^{P41} (n = 6 from 5 flies) HO+eye removal (n = 6 from 5 flies)
		ITP-LNd	HO (n = 7 from 6 flies) HO+norpA^{P41} (n = 5 from 5 flies) HO+eye removal (n = 5 from 5 flies)
		5^{th} s-LNv	HO (n = 8 from 7 flies) HO+norpA^{P41} (n = 5 from 5 flies) HO+eye removal (n = 5 from 5 flies)
Fig. 1d	one-way ANOVA followed by Tukey's post hoc test	l-LNv	HO (n = 11 from 7 flies) vs. HO+Rh6-hid,rpr (n = 16 from 10 flies), P = 5.71922E-4 HO (n = 11 from 7 flies) vs. HO+H-B ablation (n = 6 from 6 flies), P = 4.91934E-4 HO+Rh6-hid,rpr (n = 16 from 10 flies) vs. HO+H-B ablation (n = 6 from 6 flies), P = 0.53211
		s-LNv	HO (n = 8 from 5 flies) vs. HO+Rh6-hid,rpr (n = 10 from 6 flies), P = 0.02069 HO (n = 8 from 5 flies) vs. HO+H-B ablation (n = 9 from 6 flies), P = 0.03849 HO+Rh6-hid,rpr (n = 10 from 6 flies) vs. HO+H-B ablation (n = 9 from 6 flies), P = 0.98553
		ITP-LNd	HO (n = 7 from 6 flies) vs. HO+Rh6-hid,rpr (n = 11 from 9 flies), P = 0.99677 HO (n = 7 from 6 flies) vs. HO+H-B ablation (n = 6 from 6 flies), P = 0.17636 HO+Rh6-hid,rpr (n = 11 from 9 flies) vs. HO+H-B ablation (n = 6 from 6 flies), P = 0.14665
		5^{th} s-LNv	HO (n = 8 from 7 flies) vs. HO+Rh6-hid,rpr (n = 10 from 10 flies), P = 0.38375 HO (n = 8 from 7 flies) vs. HO+H-B ablation (n = 6 from 6 flies), P = 0.83488 HO+Rh6-hid,rpr (n = 10 from 10 flies) vs. HO+H-B ablation (n = 6 from 6 flies), P = 0.79993
Fig. 1e-middle	Kruskal-Wallis followed by Dunn's tests	l-LNv	HO (n = 11 from 7 flies) vs. HO+ninaE^{I17} (n = 7 from 5 flies), P = 1 HO (n = 11 from 7 flies) vs. HO+Rh5^{2} (n = 7 from 5 flies), P = 0.8486 HO (n = 11 from 7 flies) vs. HO+Rh6^{1} (n = 7 from 6 flies), P = 0.01172 HO (n = 11 from 7 flies) vs. HO+ Rh5^{2} + Rh6^{1} (n = 8 from 7 flies), P = 1.90416E-5
		s-LNv	HO (n = 8 from 5 flies) vs. HO+ninaE^{I17} (n = 8 from 5 flies), P = 1 HO (n = 8 from 5 flies) vs. HO+Rh5^{2} (n = 7 from 5 flies), P = 1 HO (n = 8 from 5 flies) vs. HO+Rh6^{1} (n = 6 from 5 flies), P = 1 HO (n = 8 from 5 flies) vs. HO+ Rh5^{2} + Rh6^{1} (n = 7 from 7 flies), P = 0.00749

		ITP-LNd	HO (n = 7 from 6 flies) vs. HO+ninaE^{I17} (n = 6 from 6 flies), P = 0.96653
			HO (n = 7 from 6 flies) vs. HO+Rh5^{2} (n = 8 from 7 flies), P = 0.00642 HO (n = 7 from 6 flies) vs. HO+Rh6^{1} (n = 8 from 6 flies), P = 0.013 HO (n = 7 from 6 flies) vs. HO+ Rh5^{2} + Rh6^{1} (n = 7 from 7 flies), P = 2.51138E-4
		5th s-LNv	HO (n = 8 from 7 flies) vs. HO+ninaE^{I17} (n = 7 from 6 flies), P = 0.8332 HO (n = 8 from 7 flies) vs. HO+Rh5^{2} (n = 8 from 8 flies), P = 0.20614 HO (n = 8 from 7 flies) vs. HO+Rh6^{1} (n = 8 from 8 flies), P = 0.03637 HO (n = 8 from 7 flies) vs. HO+ Rh5^{2} + Rh6^{1} (n = 7 from 7 flies), P = 3.90852E-8
Fig. 1e-right	Kruskal-Wallis followed by Dunn's tests	l-LNv	HO+norpA^{P41} (n = 5 from 5 flies) vs. HO+norpA^{P41}+Rh1>norpA rescue (n = 7 from 5 flies), P = 1 HO+norpA^{P41} (n = 5 from 5 flies) vs. HO+norpA^{P41}+Rh3>norpA rescue (n = 9 from 5 flies), P = 1 HO+norpA^{P41} (n = 5 from 5 flies) vs. HO+norpA^{P41}+Rh4>norpA rescue (n = 8 from 6 flies), P = 1 HO+norpA^{P41} (n = 5 from 5 flies) vs. HO+norpA^{P41}+Rh5>norpA rescue (n = 6 from 6 flies), P = 0.01114 HO+norpA^{P41} (n = 5 from 5 flies) vs. HO+norpA^{P41}+Rh6>norpA rescue (n = 6 from 6 flies), P = 0.01649
		s-LNv	HO+norpA^{P41} (n = 6 from 5 flies) vs. HO+norpA^{P41}+Rh1>norpA rescue (n = 6 from 5 flies), P = 1 HO+norpA^{P41} (n = 6 from 5 flies) vs. HO+norpA^{P41}+Rh3>norpA rescue (n = 8 from 6 flies), P = 1 HO+norpA^{P41} (n = 6 from 5 flies) vs. HO+norpA^{P41}+Rh4>norpA rescue (n = 7 from 6 flies), P = 1 HO+norpA^{P41} (n = 6 from 5 flies) vs. HO+norpA^{P41}+Rh5>norpA rescue (n = 5 from 5 flies), P = 0.0251 HO+norpA^{P41} (n = 6 from 5 flies) vs. HO+norpA^{P41}+Rh6>norpA rescue (n = 6 from 6 flies), P = 0.00585
		ITP-LNd	HO+norpA^{P41} (n = 5 from 5 flies) vs. HO+norpA^{P41}+Rh1>norpA rescue (n = 6 from 6 flies), P = 1 HO+norpA^{P41} (n = 5 from 5 flies) vs. HO+norpA^{P41}+Rh3>norpA rescue (n = 9 from 7 flies), P = 1 HO+norpA^{P41} (n = 5 from 5 flies) vs. HO+norpA^{P41}+Rh4>norpA rescue (n = 8 from 6 flies), P = 1 HO+norpA^{P41} (n = 5 from 5 flies) vs. HO+norpA^{P41}+Rh5>norpA rescue (n = 7 from 6 flies), P = 0.0028 HO+norpA^{P41} (n = 5 from 5 flies) vs. HO+norpA^{P41}+Rh6>norpA rescue, P = 0.00341
		5th s-LNv	HO+norpA^{P41} (n = 5 from 5 flies) vs. HO+norpA^{P41} +Rh1>norpA rescue (n = 6 from 6 flies), P = 1 HO+norpA^{P41} (n = 5 from 5 flies) vs. HO+norpA^{P41}+Rh3>norpA rescue (n = 8 from 7 flies), P = 1 HO+norpA^{P41} (n = 5 from 5 flies) vs. HO+norpA^{P41}+Rh4>norpA rescue (n = 6 from 6 flies), P = 1 HO+norpA^{P41} (n = 5 from 5 flies) vs. HO+norpA^{P41}+Rh5>norpA rescue (n = 6 from 6 flies), P = 0.00802 HO+norpA^{P41} (n = 5 from 5 flies) vs. HO+norpA^{P41}+Rh6>norpA rescue (n = 6 from 6 flies), P = 0.00275
Fig. 1f	Mann-Whitney test	l-LNv	Rh5>norpA rescue (n = 9 from 6 flies) vs. Rh5>norpA rescue+HO (n = 6 from 6 flies), P = 0.75285
			Rh6>norpA rescue (n = 9 from 6 flies) vs. Rh6>norpA rescue+HO (n = 6 from 6 flies), P = 0.08748
		s-LNv	Rh5>norpA rescue (n = 6 from 6 flies) vs. Rh5>norpA rescue+HO (n = 5 from 5 flies), P = 0.89225
			Rh6>norpA rescue (n = 6 from 6 flies) vs. Rh6>norpA rescue+HO (n = 6 from 6 flies), P = 0.29795
		ITP-LNd	Rh5>norpA rescue (n = 6 from 6 flies) vs. Rh5>norpA rescue+HO (n = 7 from 6 flies), P = 0.72098

			Rh6>norpA rescue (n = 6 from 6 flies) vs. Rh6>norpA rescue+HO (n = 6 from 6 flies), P = 0.9383
		5^{th} s-LNv	Rh5>norpA rescue (n = 11 from 8 flies) vs. Rh5>norpA rescue+HO (n = 8 from 6 flies), P = 0.83645
			Rh6>norpA rescue (n = 7 from 6 flies) vs. Rh6>norpA rescue+HO (n = 6 from 6 flies), P = 0.75938
Fig. 3g	one-way ANOVA followed by Tukey's post hoc test	VT037867 neurons	WT (n = 15 from 10 flies) vs. CIM (n = 7 from 7 flies), P = 0.94499 WT (n = 15 from 10 flies) vs. Hdc^{JK910} (n = 6 from 5 flies), P = 0.20252 WT (n = 15 from 10 flies) vs. $HisCl1^{134}$,ort^{1} (n = 6 from 5 flies), P = 0.10153 WT (n = 15 from 10 flies) vs. MCA (n = 11 from 10 flies), P = 3.09078E-8 WT (n = 15 from 10 flies) vs. ChAT CKO (n = 11 from 6 flies), P = 4.356E-8 WT (n = 15 from 10 flies) vs. VAChT CKO (n = 7 from 6 flies), P = 3.09078E-8
Fig. 3h	one-way ANOVA followed by Tukey's post hoc test	Tm20	WT (n = 10 from 9 flies) vs. R8>norpA rescue (n = 5 from 5 flies), P = 0.01628 WT (n = 10 from 9 flies) vs. R8>norpA rescue+HO (n = 10 from 8 flies), P = 0 WT (n = 10 from 9 flies) vs. R8>norpA rescue+HO+MCA (n = 5 from 5 flies), P = 7.73041E-7 R8>norpA rescue (n = 5 from 5 flies) vs. R8>norpA rescue+HO (n = 10 from 8 flies), P = 2.85563E-7 R8>norpA rescue (n = 5 from 5 flies) vs. R8>norpA rescue+HO+MCA (n = 5 from 5 flies), P = 2.23279E-5 R8>norpA+HO rescue (n = 10 from 8 flies) vs. R8>norpA rescue+HO+MCA (n = 5 from 5 flies), P = 0.00583
		L1	WT (n = 9 from 8 flies) vs. R8>norpA rescue (n = 5 from 5 flies), P = 1.84451E-4 WT (n = 9 from 8 flies) vs. R8>norpA rescue+HO (n = 10 from 9 flies), P = 1.98078E-7 WT (n = 9 from 8 flies) vs. R8>norpA rescue+HO+MCA (n = 5 from 5 flies), P = 4.3755E-8 R8>norpA rescue (n = 5 from 5 flies) vs. R8>norpA rescue+HO (n = 10 from 9 flies), P = 2.95241E-4 R8>norpA rescue (n = 5 from 5 flies) vs. R8>norpA rescue+HO+MCA (n = 5 from 5 flies), P = 0.0126 R8>norpA+HO rescue (n = 10 from 9 flies) vs. R8>norpA rescue+HO+MCA (n = 5 from 5 flies), P = 0.71298
		Tm9	WT (n = 6 from 6 flies) vs. R8>norpA rescue (n = 6 from 6 flies), P = 1.78706E-8 WT (n = 6 from 6 flies) vs. R8>norpA rescue+HO (n = 6 from 6 flies), P = 0 WT (n = 6 from 6 flies) vs. R8>norpA rescue+HO+MCA (n = 6 from 6 flies), P = 0 R8>norpA rescue (n = 6 from 6 flies) vs. R8>norpA rescue+HO (n = 6 from 6 flies), P = 8.06056E-6 R8>norpA rescue (n = 6 from 6 flies) vs. R8>norpA rescue+HO+MCA (n = 6 from 6 flies), P = 1.22448E-4 R8>norpA+HO rescue (n = 6 from 6 flies) vs. R8>norpA rescue+HO+MCA (n = 6 from 6 flies), P = 0.42015
Fig. 3j		AMA neurons	Depolarization after application of CIM (n = 6 from 6 flies) hyperpolarization after application of MCA (n = 6 from 6 flies)
Fig. 4c	two-tailed paired Student's t-tests	Pairs of clock neurons	ITP-LNd vs. 5^{th} s-LNv (n = 6 from 6 flies), P = 0.00165 ITP-LNd vs. l-LNv (n = 7 from 7 flies), P = 0.01039 ITP-LNd vs. s-LNv (n = 6 from 6 flies), P = 0.00306

Fig. 4d	two-tailed paired Student's t-tests	Light response of clock neurons before and after MCA application	5^{th} s-LNv, before vs. after (n = 9 from 9 flies), P = 9.5115E-7 ITP-LNd, before vs. after (n = 7 from 7 flies), P = 1.26965E-5 l-LNv, before vs. after (n = 7 from 7 flies), P = 0.00244 s-LNv, before vs. after (n = 6 from 6 flies), P = 0.00115
Fig. 4e			5^{th} s-LNv (n = 7 from 7 flies)
			ITP-LNd (n = 7 from 7 flies) l-LNv (n = 7 from 5 flies) s-LNv (n = 7 from 6 flies)
Fig. 4f			Single cell (n = 7 from 6 flies) Overlay (n = 7 from 7 flies)
Fig. 4g	two-tailed paired Student's t-tests	Number of columns innervated by pR8s and yR8s	pR8 vs. yR8 (n = 6 from 6 flies), P = 0.01059
Fig. 4i	two-tailed paired Student's t-tests	Pairs of VT037867 neurons	WT, depolarization, before vs. after $CdCl_2$ application (n = 7 from 7 flies), P = 0.0024 WT, hyperpolarization, before vs. after $CdCl_2$ application (n = 7 from 7 flies), P = 0.89874 $shakB^2$, depolarization, before vs. after MCA application (n = 7 from 7 flies), P = 2.64773E-5
	two-tailed unpaired Student's t-tests	Pairs of VT037867 neurons	WT (n = 7 from 7 flies) vs. $shakB^2$ (n = 7 from 7 flies),depolarization, P = 0.00313
Fig. 5b	one-way ANOVA followed by Tukey's post hoc test	VT037867 neurons	Peak response under current clamp: WT (n = 8 from 8 flies) vs. CO (n = 7 from 7 flies), P = 0.93762 WT (n = 8 from 8 flies) vs. CHO (n = 10 from 10 flies), P = 0.35698 CO (n = 7 from 7 flies) vs. CHO (n = 10 from 10 flies), P = 0.59055 Steady response under current clamp: WT (n = 8 from 8 flies) vs. CO (n = 7 from 7 flies), P = 0.09709 WT (n = 8 from 8 flies) vs. CHO (n = 10 from 10 flies), P = 0 CO (n = 7 from 7 flies) vs. CHO (n = 10 from 10 flies), P = 0 Spike firing rate under current clamp: WT (n = 8 from 8 flies) CO (n = 7 from 7 flies) CHO (n = 10 from 10 flies) Peak response under voltage clamp: WT (n = 8 from 8 flies) vs. CO (n = 8 from 8 flies), P = 0.94866 WT (n = 8 from 8 flies) vs. CHO (n = 8 from 8 flies), P = 8.12053E-4 CO (n = 8 from 8 flies) vs. CHO (n = 8 from 8 flies), P = 0.00169 Steady response under voltage clamp: WT (n = 8 from 8 flies) vs. CO (n = 8 from 8 flies), P = 0.33803 WT (n = 8 from 8 flies) vs. CHO (n = 8 from 8 flies), P = 0 CO (n = 8 from 8 flies) vs. CHO (n = 8 from 8 flies), P = 0

ig. 5c	two-tailed unpaired Student's t-tests	VT037867 neurons	Peak response under current clamp: CHO (n = 5 from 5 flies) vs. R8>HisCl1 rescue+CHO (n = 5 from 5 flies), P = 0.55634 Steady response under current clamp: CHO (n = 5 from 5 flies) vs. R8>HisCl1 rescue (n = 6 from 6 flies), P = 0.01869 Peak response under voltage clamp: CHO (n = 8 from 8 flies) vs. R8>HisCl1 rescue (n = 5 from 5 flies), P = 9.6694E-4 Steady response under voltage clamp: CHO (n = 8 from 8 flies) vs. R8>HisCl1 rescue (n = 5 from 5 flies), P = 0.00437 Spike firing rate: CHO (n = 10 from 10 flies) R8>HisCl1 rescue (n = 5 from 5 flies)
Fig. 5d	one-way ANOVA followed	VT037867 neurons	Peak response before, during and after CIM application (n = 6 from 6 flies): Before vs. during: P = 0.76616
	by Tukey's post hoc test		During vs. after, P = 0.92695 Before vs. after, P = 0.54416 Steady response before, during and after CIM application (n = 6 from 6 flies): Before vs. during: P = 0 During vs. after, P = 0 Before vs. after, P = 0.0974
Fig. 5e	one-way ANOVA followed by Tukey's post hoc test	VT037867 neurons	ACh response before, during and after light stimuli (n = 6 from 6 flies): Before vs. during, P = 0.99858 During vs. after, P = 0.95843 Before vs. after, P = 0.97199
Fig. 5f	two-tailed unpaired Student's t-tests	VT037867 neurons	Peak response: AMA>ort (n = 5 from 5 flies) vs. AMA>ort+HO (n = 5 from 5 flies), P = 0.55519 Steady response: AMA>ort (n = 5 from 5 flies) vs. AMA>ort+HO (n = 5 from 5 flies), P = 0.00443 Steady/Peak Ratio: AMA>ort (n = 5 from 5 flies) vs. AMA>ort+HO (n = 5 from 5 flies), P = 3.28833E-4
Fig. 5g			Spike firing rate: WT (n = 5 from 5 flies) HO (n = 5 from 5 flies)
Extended Fig. 1b	Mann-Whitney tests	lLNv	HO (n = 11 from 7 flies) vs. CHO (n = 6 from 4 flies), P = 0.24631
		sLNv	HO (n = 8 from 5 flies) vs. CHO (n = 6 from 5 flies), P = 0.17524
	two-tailed unpaired Student's t-tests	5^{th} s-LNv	HO (n = 8 from 7 flies) vs. CHO (n = 7 from 7 flies), P = 0.61563
		ITP-LNd	HO (n = 7 from 6 flies) vs. CHO (n = 7 from 7 flies), P = 0.51562

Extended Fig. 2a		probability of H-B existence	WT: Day1 (n = 12 from 7 flies) Day 3 (n = 10 from 6 flies) Day 7 (n = 13 from 7 flies) Day 14 (n = 11 from 7 flies) Rh6-hid,rpr: Day 1 (n = 12 from 10 flies) Day 3 (n = 11 from 8 flies) Day 7 (n = 12 from 8 flies) Day 14 (n = 10 from 6 flies)
		Counts or yR8s	WT: Day 1 (n = 9 from 9 flies) Day 3 (n = 9 from 9 flies) Day 7 (n = 10 from 9 flies) Day 14 (n = 7 from 7 flies) Rh6-hid,rpr: Day 1 (n = 9 from 8 flies) Day 3 (n = 7 from 7 flies) Day 7 (n = 10 from 8 flies) Day 14 (n = 6 from 6 flies)
Extended Fig. 2d	two-tailed paired Student's t-tests	Light response of H-B eyelets and yR8s	Calcium response of H-B eyelets and yR8s before and after laser cutting of H-B eyelets. yR8s (n=5 from 5flies). H-B eyelets (n=5 from 5flies).
Extended Fig. 2e	two-tailed paired Student's t-tests	Pairs of clock neurons before and	lLNv, before vs. after (n = 6 from 6 flies), P = 9.35694E-6 sLNv, before vs. after (n = 6 from 6 flies), P = 0.01255 5th s-LNv, before vs. after (n = 6 from 6 flies), P = 0.09306 ITP-LNd, before vs. after (n = 6 from 6 flies), P = 0.72356
		after H-B ablation	
Extended Fig. 2f	Kruskal-Wallis followed by Dunn's tests	l-LNv	HO (n = 11 from 7 flies) vs. HO+Rh1>TNT (n = 8 from 4 flies), P = 0.97838 HO (n = 11 from 7 flies) vs. HO+Rh34>TNT (n = 6 from 6 flies), P = 0.99738 HO (n = 11 from 7 flies) vs. HO+Rh5>TNT (n = 7 from 4 flies), P = 0.51785 HO (n = 11 from 7 flies) vs. HO+Rh6>TNT (n = 8 from 5 flies), P = 4.3338E-6 HO (n = 11 from 7 flies) vs. HO+Rh56>TNT (n = 8 from 5 flies), P = 1.98684E-8
		s-LNv	HO (n = 8 from 5 flies) vs. HO+Rh1>TNT (n = 8 from 6 flies), P = 0.9997 HO (n = 8 from 5 flies) vs. HO+Rh34>TNT (n = 6 from 6 flies), P = 0.9947 HO (n = 8 from 5 flies) vs. HO+Rh5>TNT (n = 7 from 6 flies), P = 0.20973 HO (n = 8 from 5 flies) vs. HO+Rh6>TNT (n = 6 from 5 flies), P = 0.17621 HO (n = 8 from 5 flies) vs. HO+Rh56>TNT (n = 7 from 6 flies), P = 0.00498
		ITP-LNd	HO (n = 7 from 6 flies) vs. HO+Rh1>TNT (n = 7 from 6 flies), P = 0.97012 HO (n = 8 from 5 flies) vs. HO+Rh34>TNT (n = 6 from 6 flies), P = 0.99113 HO (n = 8 from 5 flies) vs. HO+Rh5>TNT (n = 9 from 7 flies), P = 0.02382 HO (n = 8 from 5 flies) vs. HO+Rh6>TNT (n = 10 from 8 flies), P = 0.00178 HO (n = 8 from 5 flies) vs. HO+Rh56>TNT (n = 6 from 6 flies), P = 5.8113E-7

		5^{th} s-LNv	HO (n = 8 from 7 flies) vs. HO+Rh1>TNT (n = 7 from 6 flies), P = 0.93984 HO (n = 8 from 7 flies) vs. HO+Rh34>TNT (n = 6 from 6 flies), P = 0.9998 HO (n = 8 from 7 flies) vs. HO+Rh5>TNT (n = 8 from 7 flies), P = 0.06453 HO (n = 8 from 7 flies) vs. HO+Rh6>TNT (n = 10 from 9 flies), P = 0.01368 HO (n = 8 from 7 flies) vs. HO+Rh56>TNT (n = 6 from 6 flies), P = 2.16701E-7
Extended Fig. 7a			Photo-activated: n = 10 from 10 flies Control: n=7 from 7 flies
Extended Fig. 9b	one-way ANOVA followed by Tukey's post hoc test	Light response of AMA neurons	WT (n = 15 from 10 flies) vs. $Rh5^2$; $Rh6^1$ (n = 10 from 7 flies), P = 8.42641E-9 WT (n = 15 from 10 flies) vs. $norpA^{P41}$ (n=7 from 7 flies), P = 8.94939E-8 $norpA^{P41}$ (n=7 from 7 flies) vs. $Rh5^2$; $Rh6^1$ (n = 10 from 7 flies), P = 0.99604 WT (n = 15 from 10 flies) vs. R8>norpA rescue (n = 7 from 7 flies), P = 0.9122 $norpA^{P41}$ (n=7 from 7 flies) vs. R8>norpA rescue (n = 7 from 7 flies), P = 8.6929E-8 $Rh5^2$; $Rh6^1$ (n = 10 from 7 flies) vs. R8>norpA rescue (n = 7 from 7 flies), P = 9.24593E-9
Extended Fig. 9c	one-way ANOVA followed by Tukey's post hoc test	L1	n = 6 from 6 flies Before vs. during CIM, P = 0 Before vs. after CIM, P = 0.46348 During vs. after CIM, P = 0
		Tm9	n = 6 from 6 flies Before vs. during CIM, P = 2.55079E-7 Before vs. after CIM, P = 0.87004 During vs. after CIM, P = 5.75476E-7
		Tm20	n = 6 from 6 flies Before vs. during CIM, P = 2.36777E-7
			Before vs. after CIM, P = 0.56326 During vs. after CIM, P = 1.23604E-6
Extended Fig. 9d	one-way ANOVA followed by Tukey's post hoc test	L1	R8>norpA rescue (n = 5 from 5 flies) vs. CIM (n = 10 from 8 flies), P = 0 R8>norpA rescue (n = 6 from 6 flies) vs. CIM+MCA (n = 5 from 5 flies), P = 2.91405E-6 CIM (n = 10 from 8 flies) vs. CIM+MCA (n = 5 from 5 flies), P = 0.03611
		Tm9	R8>norpA rescue (n = 6 from 6 flies) vs. CIM (n = 5 from 5 flies), P = 0 R8>norpA rescue (n = 6 from 6 flies) vs. CIM+MCA (n = 6 from 6 flies), P = 0 CIM (n = 5 from 5 flies) vs. CIM+MCA (n = 6 from 6 flies), P = 0.03108
		Tm20	R8>norpA rescue (n = 5 from 5 flies) vs. CIM (n = 10 from 7 flies), P = 0 R8>norpA rescue (n = 5 from 5 flies) vs. CIM+MCA (n = 5 from 5 flies), P = 1.52303E-5 CIM (n = 10 from 7 flies) vs. CIM+MCA (n = 5 from 5 flies), P = 0.00621
Extended Fig. 11	Mann-Whitney tests	VT037867 neurons	WT (n = 6 from 4 flies) vs. VT>ort (n = 6 from 5 flies), P = 0.00278
Extended Fig. 12d			l-LNv: n = 7 from 5 flies s-LNv: n = 7 from 5 flies ITP-LNd: n = 7 from 6 flies 5th s-LNv: n = 9 from 9 flies
Extended Fig. 13b		Calcium response of VT037867 neurons	n = 6 from 5 flies

Extended Fig. 14	one-way ANOVA followed by Tukey's post hoc test	Light response of VT037867 neurons	Depolarization under current clamp WT (n = 6 from 6 flies) vs. CHO (n = 6 from 6 flies), P = 0.15126. WT (n = 6 from 6 flies) vs. CO (n = 6 from 6 flies), P = 0.63188. CO (n = 6 from 6 flies) vs. CHO (n = 6 from 6 flies), P = 0.67885. Inward current under voltage clamp WT (n = 15 from 6 flies) vs. CHO (n = 6 from 6 flies), P = 0.99094. WT (n = 15 from 6 flies) vs. CO (n = 6 from 6 flies), P = 0.56875. CO (n = 6 from 6 flies) vs. CHO (n = 6 from 6 flies), P = 0.64628.
Extended Fig. 15	one-way ANOVA followed by Tukey's post hoc test	Light response of VT037867 neurons	Peak response under current clamp: R8>norpA rescue (n = 6 from 6 flies) vs. R8>norpA rescue; CO (n = 6 from 6 flies), P = 0.35378. R8>norpA rescue (n = 6 from 6 flies) vs. R8>norpA rescue; CHO (n = 8 from 6 flies), P = 0.5171. R8>norpA rescue;CO (n = 6 from 6 flies) vs. R8>norpA rescue; CHO (n = 8 from 6 flies), P = 0.97255. Steady response under current clamp: R8>norpA rescue (n = 6 from 6 flies) vs. R8>norpA rescue; CO (n = 6 from 6 flies), P = 0.75518. R8>norpA rescue (n = 6 from 6 flies) vs. R8>norpA rescue; CHO (n = 8 from 6 flies), P = 1.2233E-5. R8>norpA rescue;CO (n = 6 from 6 flies) vs. R8>norpA rescue; CHO (n = 8 from 6 flies), P = 1.40482E-6. Peak response under voltage clamp: R8>norpA rescue (n = 6 from 6 flies) vs. R8>norpA rescue; CO (n = 8 from 6 flies), P = 0.57735. R8>norpA rescue (n = 6 from 6 flies) vs. R8>norpA rescue; CHO (n = 8 from 6 flies), P = 0.18575. R8>norpA rescue;CO (n = 6 from 6 flies) vs. R8>norpA rescue; CHO (n = 8 from 6 flies), P = 0.01636. Steady response under voltage clamp: R8>norpA rescue (n = 6 from 6 flies) vs. R8>norpA rescue; CO (n = 8 from 6 flies), P = 0.16982.
			R8>norpA rescue (n = 6 from 6 flies) vs. R8>norpA rescue; CHO (n = 8 from 6 flies), P = 6.02925E-8. R8>norpA rescue;CO (n = 6 from 6 flies) vs. R8>norpA rescue; CHO (n = 8 from 6 flies), P = 1.29424E-6. Spike firing rate: R8>norpA rescue (n = 5 from 5 flies) R8>norpA rescue; CO (n = 5 from 5 flies) R8>norpA rescue; CHO (n = 6 from 5 flies)
Extended Fig. 16a	two-tailed unpaired Student's t-tests	ACh response of VT037867 neurons	Peak response, WT (n = 6 from 6 flies) vs. HO (n = 6 from 6 flies), P = 0.9121 Steady response, WT (n = 6 from 6 flies) vs. HO (n = 6 from 6 flies), P = 0.93939
Extended Fig. 16b	Mann-Whitney tests	Calcium response of R8 terminal	Peak response, WT (n = 59 from 6 flies) vs. CHO (n = 58 from 5 flies), P = 1.63472E-4 Steady response, WT (n = 59 from 6 flies) vs. CHO (n = 58 from 5 flies), P = 6.28698E-6
Extended Fig. 16c			Depolarization induced by dim and bright light under different calcium concentration, in the presence of CIM or MCA, n = 6
Extended Fig. 17b			l-LNv (n = 6 from 5 flies) s-LNv (n = 6 from 6 flies) ITP-LNd (n = 6 from 6 flies) 5th s-LNv (n = 6 from 6 flies)

Extended Data Table. 3 | Fly Strains used in this paper

Fly Strains	Source	Identifier
Gal4		
DvPdf-Gal4 (II)	From P. Emery	N/A
Clk856-Gal4 (II)	From T. Yoshii	N/A
GMR-Gal4 (II)	From P. Emery	N/A
GMR24C08-Gal4 (attp2)	Bloomington Stock Center	#48050
L1 spGal4: SS00691	From Janelia Research Campus	N/A
Tm5 spGal4: ort-Gal4.C1a.DBD; dVP16AD[ET18k]	Bloomington Stock Center	#56524
Tm9 spGal4: SS00307	From Janelia Research Campus	N/A
Tm20 spGal4: ort-Gal4.C1a.DBD, ET.VP16.AD [tou9A30]	Bloomington Stock Center	#56521
Tm20 spGal4: SS00355	From Janelia Research Campus	N/A
aMe12 spGal4: SS01050	From Janelia Research Campus	N/A
HDC-Gal4 (II)	From Y. Rao	N/A
Rh1-Gal4 (II)	Bloomington Stock Center	#8692
Rh3-Gal4 (II)	Bloomington Stock Center	#7457
Rh4-Gal4 (II)	Bloomington Stock Center	#8627
Rh5-Gal4 (II)	Bloomington Stock Center	#7458
Rh6-Gal4 (II)	Bloomington Stock Center	#7459
Rh6-Gal4 (III)	Bloomington Stock Center	#7464
VT037867-Gal4 (attp2)	Vienna *Drosophila* Resource Center	#v203797
LexA		
DvPdf-LexA (attp2)	our own lab	N/A
DvPdf-LexA (attp40)	our own lab	N/A
GMR27G06-LexA (attp40)	Bloomington Stock Center	#54779
GMR54D11-LexA (attp2)	This study	
GMR-LexA (II)	From Y. Rao	N/A
ort-LexA (III)	From Y. Rao	N/A
Rh5-LexA (II)	From Y. Rao	N/A
Rh6-LexA (attp40)	From T. Suzuki	N/A
vGAT-LexA (II)	From Y. Rao	N/A
VT037867-LexA (attp40)	our own lab	N/A
QS		
ort-QS (VK00005)	This paper	N/A
FLP		

ChAT-FLP (III)	From Y. Rao	N/A
TH-FLP (III)	From Y. Rao	N/A
Trh-FLP (III)	From Y. Rao	N/A
vGlut-FLP (II)	From Y. Rao	N/A
UAS		
UAS-Cas9.P2 (attp40)	Bloomington Stock Center	#58985
UAS-ChAT sgRNA (attp5)	From Y. Rao	N/A
UAS-Hdc sgRNA (attp5)	From Y. Rao	N/A
UAS-VAChT sgRNA (attp5)	From Y. Rao	N/A
UAS-mSPA-GFP (III)	From Y. Rao	N/A
UAS-CsChrimson (attp40)	Bloomington Stock Center	#55135
UAS-FRT-STOP-FRT-mCD8-GFP (II)	From C. Potter	N/A
UAS-FRT-STOP-FRT-mCD8-GFP (III)	From C. Potter	N/A
UAS-GCaMP6m (attp40)	Bloomington Stock Center	#42748
UAS-GCaMP6m (VK00005)	Bloomington Stock Center	#42750
UAS-FLP(II)	Bloomington Stock Center	#4539
UAS-mCD8-GFP (II)	From C. Potter	N/A
UAS-mCD8-GFP (III)	From C. Potter	N/A
UAS-norpA.K (II)	Bloomington Stock Center	#26267
UAS-norpA.K (III)	Bloomington Stock Center	#26273
UAS-HisCl1(II)	From F. Rouyer	N/A
UAS-ort (II)	From F. Rouyer	N/A
UAS-post-GFP$^{1-10}$ (attp2)	From S. Stowers	N/A
UAS-TNTE (II)	Bloomington Stock Center	#28837
LexAop		
LexAop2-GCaMP6f (attp5)	Bloomington Stock Center	#44277
LexAop2-jGCaMP7s	Bloomington Stock Center	#80913
LexAop2-GCaMP6m (VK00005)	Bloomington Stock Center	#44276
LexAop-tdTomato (attp5)	From Y. Rao	N/A
LexAop-norpA (attp5)	From Y. Rao	N/A
LexAop-post-GFP^{11} (VK00005)	This paper	N/A
LexAop2-GFP (attp5)	From Y. Rao	N/A
LexAop2-GFP (attp2)	Bloomington Stock Center	#32209
Mutant		
cry^{02}	From T. Yoshii	N/A
cry^{02}, HisCl1^{134}, ort^{1}	From F. Rouyer	N/A
Hdc^{JK910}	Bloomington Stock Center	#64203

ort^{1}	From Y. Rao	N/A
HisCl^{134}, *ort*^{1}	From Y. Rao	N/A
norpA^{P41}	From P. Emery	N/A
Rh5^{2}	From F. Rouyer	N/A
ninaE^{I17}	Kyoto stock center	#109599
Rh6^{1}	Kyoto stock center	#109600
Rh6^{1}, *HisCl*^{134}, *ort*^{1}	From F. Rouyer	N/A
shakB^{2}	From J.M. Blagburn	N/A
Others		
MCFO-1: pBPhsFlp2::PEST (attP3); pJFRC201-10XUAS-FRT-STOP-FRT-myr::smGFP-HA (VK0005), pJFRC240-10XUAS-FRT-STOP-FRT-myr::smGFP-V5-THS-10XUAS-FRT-STOP-FRT-myr::smGFP-FLAG (su(Hw)attP1)hsFLP(attP3);; HA_V5_FLAG	Bloomington Stock Center	#64085
BAcTrace: LexAop2-Syb::GFP-P10 (VK37) LexAop-QF2::SNAP25::HIVNES::Syntaxin (VK18); UAS-B3Recombinase (attP2) UAS<B3STOP<BoNT/A (VK5) UAS<B3STOP<BoNT/A(VK27) QUAS-mtdTomato::HA	From G. Jefferis	N/A
GRASP: UAS-GFP$^{1-10}$, *LexAop-GFP*^{11}	From Y. Rao	N/A
trans-Tango: UAS-myrGFP.QUAS-mtdTomato-3×HA (attp8);trans-Tango (attp40)	Bloomington Stock Center	#77124
UAS-FRT-STOP-FRT-CsChrimson, LexAop-FLP (II)	From C. Zhou	N/A
UAS-FRT-STOP-FRT-CsChrimson, LexAop-FLP (III)	From C. Zhou	N/A
VAChT-FRT-STOP-FRT-HA (III)	Bloomington Stock Center	#76021
GMR-RFP (II)	From Y. Rao	N/A
Rh5-eGFP (II)	Bloomington Stock Center	#8600
Rh6-eGFP (II)	Bloomington Stock Center	#7461
LexAop-GFP, UAS-RFP (I)	From C. Liu	N/A
Rh6-hid,rpr (attp5)	This paper	N/A

Discussion

Virtually all living organisms possess an intrinsic timekeeping mechanism called the circadian clock to anticipate daily environmental changes and to temporally coordinate physiology and behavior in a rhythmic daily fashion. Observations of circadian rhythms in living organisms date back centuries, but our understanding of this phenomenon's genetic and molecular basis started to emerge with *Drosophila* research in the 1960s. Mammals rely on the hypothalamic Suprachiasmatic Nucleus (SCN), composed of approximately 20,000 neurons, as their central circadian pacemaker. In contrast, the brain clock of the *Drosophila melanogaster* (fruit fly) consists of a smaller network of 150 clock neurons. Despite this difference, the underlying molecular mechanisms that generate circadian rhythms are evolutionarily conserved between mammals and *Drosophila*. Due to its relatively more straightforward neural composition and the availability of powerful genetic tools, *Drosophila* serves as an excellent model organism for investigating the fundamental molecular and neural principles of circadian timekeeping. Additionally, *Drosophila* research has significantly contributed to our comprehension of sensory input mechanisms and the intricate interplay between these inputs and circadian regulation, leveraging the advantages offered by *Drosophila*.

The initial discovery of most genes involved in regulating circadian rhythms occurred in *Drosophila*. Since then, several homologous circadian genes have been identified in various organisms, ranging from cyanobacteria to humans. The insights gained from *Drosophila* research extend beyond the realm of fruit flies and hold broader significance in understanding the regulation of circadian clocks in other organisms, including mammals such as mice and humans. This knowledge deepens our understanding of the fundamental principles that govern biological timekeeping and has wide-ranging applications in fields such as chronobiology, sleep medicine, and the development of strategies to mitigate the adverse effects of circadian disruptions caused by modern lifestyles and shift work.

Circadian clocks have evolved to adapt to the cyclic nature of Earth's environmental conditions, which have prevailed since the planet's inception. However, the survival value of a circadian clock is contingent upon its ability to adjust to external environmental cycles through a process known as entrainment. To function as an accurate timekeeper, the circadian system in any organism must coordinate the timing of biological events with the phase of the surrounding environment. Furthermore, since the inherent period of the circadian clock is not precisely 24 hours, circadian rhythms must be entrained on a daily basis through signals known as zeitgebers to maintain synchronization with the environment. Organisms gain a fitness

advantage through this inherent flexibility of circadian clocks, as they efficiently modify their behavior and physiology in response to different times of the day.

To achieve entrainment, biological clocks rely on dedicated sensory input pathways that can detect and integrate reliable environmental time cues into the clock machinery. These zeitgebers convey crucial information about the current time of day, enabling the biological clock to synchronize with the external environment. Among these zeitgebers, the most reliable and significant factor that serves as a surrogate for local time is the daily light-dark cycle resulting from the Earth's 24-hour rotation. Consequently, most organisms utilize variations in the quantity and quality of light over the 24-hour day as their primary zeitgeber for entrainment, a phenomenon commonly referred to as "photoentrainment." Photoperiod, or the duration of daylight in a 24-hour day, exhibits dramatic variations with the changing seasons in many locations worldwide. Shorter days in winter and longer days in summer necessitate adaptations in an organism's physiological and behavioral processes to cope with the corresponding environmental shifts. In addition to perceiving the local time information, such seasonal adjustment is facilitated by photoentrainment, allowing their internal biological clocks to anticipate and prepare for seasonal changes. The ability of circadian clocks to integrate these seasonal changes is vital for survival, reproduction, and overall fitness.

Light entrainment of the *Drosophila* circadian system has been studied for years, and the complexity by which the brain clock integrates multiple light inputs is gradually being revealed. The circadian clock in *Drosophila* evaluates environmental light signals through multiple distinct pathways that work in parallel. Like most animals, *Drosophila* also utilizes multiple photoreceptors to fine-tune clock synchronization. In a broader sense, the photoentrainment of the *Drosophila* circadian clock occurs through two pathways. The first pathway relies on a photoreceptor molecule called Cryptochrome (CRY), which is present in the clock neurons. The second pathway depends on the visual photopigments named rhodopsins located in the photoreceptive organs of *Drosophila*, including the compound eyes, Hofbauer-Buchner (HB) eyelets, and ocelli. Only the elimination of CRY and all these eye structures leads to activity rhythms that are desynchronized to light-dark cycles. The presence of multiple photoreceptors offers organisms an adaptive advantage when it comes to responding to different wavelengths of light. This advantage becomes particularly valuable due to the daily and seasonal changes in spectral composition, light intensity, and day length. Organisms can efficiently detect and react to these variations by utilizing diverse

photoreceptors, which enables them to synchronize their biological rhythms with the natural fluctuations in light conditions.

The primary objective of the current thesis was to advance our understanding of the remarkable complexity involved in circadian entrainment, with a specific emphasis on the circadian light input system that synchronizes the network of neuronal clocks. Throughout my Ph.D. research, I have been involved in three different projects where I employed *Drosophila melanogaster* to investigate the different photoentrainment pathways, including both CRY and visual system-mediated light input. We explored various light input pathways, including previously unidentified pathways crucial for finely adjusting the *Drosophila* brain clock. Taken together, this thesis ultimately strives to contribute to a more comprehensive understanding of how clock neurons extract relevant light information from multiplexed light inputs.

I. Ocelli-dependent photoentrainment pathway

The *Drosophila* visual system-mediated circadian input pathway can be again subdivided into the compound eye and HB-eyelet pathways, where the light information is transmitted to the clock neurons via compound eyes and HB-eyelets, respectively. Seven different rhodopsins (Rhs) have been characterized in the *Drosophila* visual organs, and they are known to cover a wide range of wavelengths from 300 nm to 600 nm, with each rhodopsin having a unique absorption spectrum. The compound eyes express Rh1, Rh3, Rh4, Rh5 and Rh6, whereas HB-eyelets contain Rh6 only. The ocelli, instead, expresses Rh2 only, which is neither present in compound eyes nor in the HB eyelets. The seventh rhodopsin, Rh7, is the most recently discovered photopigment and has been detected in some clock neurons. Several studies have shed light on the role of different visual organs and the photosensitive rhodopsins they express in refining locomotor activity patterns in response to varying light conditions. Even in this context, no particular study has ever concluded the involvement of Rh2-expressing ocelli in providing light inputs to any clock neurons. This highlights the relevance of our first project, where we conducted a detailed investigation to identify whether ocelli can facilitate photoentrainment of the circadian clock and subsequently synchronize activity rhythms with light-dark cycles. While a study published in 2003 (Reiger et al., 2003) suggested a minor contribution of ocelli in photoentrainment, our research aims to delve deeper into characterizing the behavioral functions of the ocelli-mediated photoentrainment pathway and

elucidating the neuronal circuits that connect the ocelli to the clock neurons.

Initially, we generated a *Drosophila* mutant with all other circadian photoreceptors absent except Rh2 and Rh7 in a cry^{02} background. We conducted light shift experiments to assess the entrainment capability of this mutant (genotype was named Rh2+) to light-dark cycles and compared it with another mutant generated by us, which lacks CRY and all rhodopsins except Rh7 (genotype was named Rh7+). The obtained results conclusively revealed that Rh2+ flies resynchronized their rest-activity rhythms when they were shifted to the new LD regime, which was 8 hours advanced from the previous one. In contrast, Rh7+ did not synchronize to the new LD cycle. These findings provide compelling evidence for the involvement of Rh2 in the entrainment of rest-activity rhythms in *Drosophila*. We further revealed that Rh2-expressing ocelli could resynchronize rest-activity rhythms to high-intensity light conditions (~2000 lux) but not low-intensity light conditions (<5 lux). Furthermore, we observed that the ability of Rh2+ flies to re-entrain their activity rhythms was disrupted when subjected to phase-delayed LD cycles, regardless of the light intensity (high or low), indicating a loss of entrainment capability in such conditions.

Previous results published from our lab demonstrated that the Rh2-mediated photoentrainment pathway is insufficient to contribute to synchronizing the clock under low light conditions where *norpA*-dependent signaling mechanisms are employed. Our findings align with this previous study, showing that Rh2+ flies fail to synchronize under low light conditions, confirming that Rh2 alone is insufficient for photoentrainment in LD cycles with dim light. However, we observed that Rh2+ flies successfully synchronize in advanced high-light LD cycles, suggesting the utilization of NorpA-dependent, NorpA-independent, or both signaling pathways to transmit light information to clock cells. Interestingly, another study (Ogueta et al., 2018) has refuted the notion that the Rh2-mediated photoentrainment pathway exclusively relies on a NorpA-independent pathway, which is limited to high-light conditions. Considering these findings, it is plausible that Rh2-mediated photoentrainment involves both NorpA-dependent and NorpA-independent pathways or solely relies on the NorpA-dependent pathway to transmit high-intensity light signals to clock neurons. Conflicting data were obtained in the laboratory with flies having only Rh2 and Rh7 in the absence of NorpA, but they appear to not entrain in most experiments (not shown). This suggests that the Rh2-expressing photoreceptors of the ocelli do not possess the NorpA-independent pathway and would thus rely on NorpA to allow synchronization in high-light conditions.

After establishing the role of Rh2 photoreceptors in light-mediated circadian responses, our focus shifted towards identifying the neural circuitry involved in this light input pathway. First, we employed the in-situ hybridization technique to examine which histamine receptors were expressed in the first-order downstream neurons of ocelli as Rh2 photoreceptor cells were already known to be histaminergic. Our findings revealed that the ORT is the only histamine receptor expressed in the post-synaptic neurons of ocelli. In contrast, the HisCl1 histamine receptor, the only other receptor of its kind, was not detected in these neurons. Thus, we could conclude that light signals transmitted by ocelli depend on ORT only. Thus, unlike compound eyes, which use Ort and HisCl1, histamine receptors in the ocelli-mediated light input pathway were identified as Ort exclusively. We then investigated the downstream circuit. To accomplish this, we employed advanced circuit mapping techniques and the recently published EM hemibrain dataset of the *Drosophila* adult brain. We successfully traced the neural connections connecting ocelli to different clock neurons through these methods. We discovered that the 5^{th} s-LNv and three CRY+ve LNds, clock neurons responsible for regulating evening peaks in LD cycles, were the primary recipients of ocelli inputs since these neurons employed a relatively minimum number of interneurons to receive such input. Two types of interneurons were found to be involved in relaying ocelli inputs to this specific clock neuron cluster. OCG04 neurons were identified as the first-order downstream neurons of ocelli, while aMe8 neurons were identified as the second-order downstream neurons in this circuit. These data appear to be validated by the GRASP experiments. Thus, we propose that the ocelli-mediated circadian light input to evening cells involve the sequential flow of light information from Rh2 photoreceptors to OCG04 neurons to aMe8 neurons and, finally, 5^{th} s-LNv and 3 CRY+ve LNds. We also explored the neural connections between ocelli and s-LNvs. Our findings indicate that s-LNvs, which are crucial for the morning peak, indirectly receive input from OCG04, which are the first-order downstream neurons of ocelli, through a minimum of two interneurons. Overall, our research suggests that OCG04 neurons serve as the primary first-order downstream partners of Rh2-expressing cells for transmitting light inputs from the ocelli to the clock network, employing different types and quantities of interneurons depending on the specific clock cluster they are destined for. Finally, a series of physiological studies were started to validate the proposed circuit in vivo. Preliminary data with the P2X2/ATP system for targeted neuronal activation of the Rh2 photoreceptors suggest that the activation of photoreceptors induces a calcium increase in different LN and DN subsets (J. Carcaud).

Besides their role in synchronizing sleep-wake cycles to LD cycles, we discovered that

the ocellary pathway is essential in adapting flies' bimodal activity to summer-like days. Specifically, we observed that flies lacking functional Rh2 and, consequently, lacking ocelli input exhibited improper phase delay of their evening peak under long-day conditions compared to wild-type flies. Previous studies have emphasized the crucial involvement of the visual system pathway, particularly R8 photoreceptor cells in the compound eyes, in shaping bimodal activity patterns under different photoperiod conditions. However, our discovery reveals that Rh2 also plays a vital role in providing necessary light signals to clock neurons for optimal adaptation of *Drosophila* locomotor activity patterns to varying photoperiods. It is intriguing that removing only Rh2 contribution significantly affects the proper positioning of evening activity in long days. This indicates that different rhodopsins have non-redundant roles in this behavioral adaptation. The results of our experiments pronounce some novel insights into the entrainment of rest-activity rhythms in *Drosophila* through ocelli. Hence, this study uncovers a previously unknown circadian light input pathway and its associated circuitry, shedding light on the fine-tuning of circadian rhythms.

II. Non-cell autonomous CRY action

The molecular basis of circadian rhythms involves a feedback loop at the transcriptional and translational levels, resulting in oscillations of clock gene expression. In *Drosophila*, this feedback loop is present in around 150 brain neurons, known as clock neurons. These interconnected clock neurons coordinate their molecular clocks via inter-neuronal communication to generate robust circadian locomotor activity. The significance of these cross-talks has been demonstrated in establishing a unified clock network and sustaining the molecular rhythmicity of individual clock neurons. Recent studies have affirmed the pivotal role of such network interactions in comprehending pertinent light cues from the external environment. The *Drosophila* brain clock consists of neuron clusters that form a variably coupled network with high circadian plasticity. It's established that visual light information, as well as multifaceted PDF information, utilize this network. Although the predominant mechanism of photoentrainment via CRY signaling operates autonomously by inducing TIM degradation, there are signs suggesting that CRY-dependent photoreception might also operate in a non-cell autonomous manner.

Not all clock neurons can detect light autonomously. Most of the clock neurons in the

Drosophila brain clock do not express CRY, necessitating their dependence on non-autonomous mechanisms for photoreception. This aspect might explain the rationale behind clock neurons functioning collaboratively within an intact circadian circuit, enabling them to achieve precise and consistent perception of information regarding external light conditions. This study tried to address some relevant inquiries concerning the underlying neural and molecular mechanisms, as well as the behavioral implications of the discussed pathway. Our objectives encompass uncovering the intricate circuitry and clock network arrangement that regulates the transmission of CRY signals within the *Drosophila* clock circuit. Moreover, we investigated the possibility of CRY^+ neurons serving as enablers and receivers of these signals. Additionally, our aim was to pinpoint the pivotal clock neuron subgroups utilizing the non-autonomous CRY pathway and to delve deeper into the molecular and neural mechanisms underpinning this intricate pathway.

Our primary approach for addressing these inquiries involved rescuing CRY expression within distinct clusters of clock neurons in circadian blind flies (lacking visual and CRY input) and subsequently analyzing their molecular and behavioral responses. While previous studies have concentrated mainly on the behavioral and molecular consequences of the non-autonomous CRY pathway triggered by brief light exposure, our investigation pivoted towards assessing the importance of this input under more extended light conditions, such as regular day-night cycles.

Our study's findings furnish compelling evidence for a multi-oscillator system that is intricately coupled to propagate CRY signals within the circuit. Even the CRY+ neurons actively exchange their CRY status, culminating in network-wide synchronized molecular and behavioral outputs. These interactions again underscore the notion of the brain clock as a unified network, where their mutual influence on photosensitivity amplifies this concept. Our findings unveil that the function of CRY solely within PDF^+ neurons is sufficient to achieve effective LD entrainment of molecular oscillations in other essential groups, including CRY+ LNds, 5^{th} s-LNv, and DN1ps. When CRY expression is confined to LN^{EO} (CRY+ LNds + 5^{th} s-LNv), it results in the export of CRY signals to s-LNvs and DN1ps while not extending to CRY- LNds and l-LNvs. Under LD cycles, the DN1p cluster exhibited a lack of capacity to induce molecular synchronization in other subgroups, indicating their inability to export their CRY-transduced light signals to other oscillators. Thus, DN1ps (containing both DN^{MO} and DN^{EO}) could be considered a confined group positioned as recipients during the exchange of

CRY-related photic signals within the circadian circuit. Notably, our observations reveal that the sharing of CRY signals across the circadian neural network follows a distributed pattern with diverse coupling.

Following these observations, we then studied more about the behavioral relevance of this photoentrainment pathway by examining its effect in synchronizing the daily locomotor behavior under LD cycles. Notably, in the case of flies where the CRY was present only in PDF cells (LN^{MO}), we found that those flies could generate a definite evening peak in addition to the morning peak. This suggests that non-cell autonomous CRY information was transferred from M to E cells to elicit an entrained evening peak in 12:12 LD cycles. Even when the only light input to E-cells was non-cell autonomous CRY signals from LN^{MO}, E-cells were able to drive adequately phased evening behavior. Unexpectedly, confining CRY expression to LN^{EO} failed to elicit M peaks through non-autonomous mechanisms. This outcome was particularly intriguing in light of our earlier discoveries, which demonstrated the ability of s-LNvs and DN1ps to synchronize their molecular oscillations via non-autonomous CRY signals from LN^{EO}. Hence, the daily activity patterns of flies could be exclusively orchestrated by the non-autonomous CRY action originating from PDF^{+} cells, efficiently synchronizing E oscillators alongside M cells. Conversely, the CRY actions arising from LN^{EO} are incapable of inducing entrained output from M oscillators like LN^{MO} and DN^{MO} despite their capacity to photoentrain LN^{MO} and DN^{MO}'s clockwork.

In the latter phase of our study, our emphasis shifted towards investigating the export of CRY signals from PDF neurons, aiming to gain more profound insights into the fundamental mechanism involved in this neural communication. We found that PDF/PDFR signaling, the crucial signaling pathway that facilitates the coupling between PDF^{+} and PDF^{-} neurons, was also found to be involved in this circadian photoreception pathway. The expression of PDF neuropeptide and its receptor PDFR was indispensable in transferring CRY information from the LN^{MO} to the E-oscillator, which confers the hierarchical power to M-cells in the entrainment of diurnal behavior via non-autonomous CRY input. Subsequent experiments revealed that such export of CRY signals to the E oscillator requires a functional molecular clock in LN^{MO} cells. Hence, the clock-dependent role of PDF serves to distribute CRY-related light-responsive inputs to other oscillators, in contrast to the scenario observed with inputs mediated by the visual system, where PDF operates independently of the clock. Therefore, the signaling pathway of PDF can be regarded as a vital conduit within the circadian network for

light-based inputs, aiding in the distribution of both CRY-related and visual information, potentially via distinct mechanisms.

Finally, to decipher the ubiquitin ligase component involved in this clock resetting mechanism, we examined the role of various candidate proteins. Our findings suggest that the canonical CRY-JET pathway essential for cell-autonomous CRY input might not be implicated in the non-cell-autonomous effects of CRY in LD entrainment. The non-cell-autonomous pathway remained unaffected even with a significant loss of function of JET (*jet*^{set}), which essentially abolishes intra-oscillator CRY function. This discovery is surprising as a JET-independent pathway for conveying CRY-mediated light signals to clock neurons has not been previously identified. However, our analysis of the entrainment of *Drosophila* diurnal behavior under LD cycles suggests the presence of an unknown JET-independent mechanism involved in the light entrainment of circadian rhythms by CRY.

This outcome came as a surprise, given that previous research has implied that JET functions cell-autonomously to promote TIM degradation in LN^{MO}- and LN^{EO}, and non-autonomously in LN^{EO} when expressed in LN^{MO}. Additionally, the non-autonomous JET pathway from M cells to E cells was insufficient to induce behavioral phase shifts as JET expression was required in both groups of neurons to phase-shift locomotor rhythms in response to a short light pulse. However, our investigation diverged from previous work by focusing on the non-autonomous CRY pathway's involvement in entraining diurnal behavior instead of examining light pulse-induced TIM degradation and behavioral phase shifts. Additionally, in contrast to the aforementioned study, we conducted CRY rescue in a *GMR-hid jet*^{set} *cry*^{02} triple mutant background, rather than performing JET rescue within a *jet*^{set} mutant background.

It's worth noting that our ability to definitively conclude the presence of a JET-independent pathway is limited, as the nature of the *jet*^{set} mutant remains unclear—it's uncertain whether it's a complete null mutant of JET. Earlier findings indicated that under LD conditions, TIM cycling was not completely eliminated but rather exhibited reduced amplitude in *jet*^{set} mutants. The authors attributed this to the retention of residual activity of JET in *jet*^{set} mutants, which could possibly be detectable with prolonged light exposure (Lamba et al., 2014). In our experiments, we also employed extended exposure to light in the form of LD cycles. Thus, it's plausible that the unaffected entrainment of diurnal behavior via the non-autonomous CRY pathway in a *jet*^{set} mutant background could be attributed to the residual JET activity present

in *jet*^{set} mutants. An alternative scenario could involve the existence of a JET-independent pathway in both autonomous and non-autonomous CRY photoreception, with its functions becoming discernible only when subjected to prolonged light exposure. Additional experiments are required involving a comprehensive null mutant of JET in order to arrive at a definitive conclusion regarding this potential scenario.

III. Light entrainment pathway mediated by retinal photoreceptor cells

Despite numerous studies in *Drosophila* aimed at unraveling the astonishing complexity of light entrainment through compound eye input, the complete neural circuitry connecting the retina to clock neurons still needs to be discovered. In the absence of CRY, the entrainment of rest-activity rhythms via the visual system relies on histaminergic signaling, as flies depleted for both histidine carboxylase and CRY lack the ability to entrain. Furthermore, flies lacking ORT and HisCl1, the two histamine receptors in *Drosophila,* also fail to synchronize their rest-activity rhythms with LD cycles. However, each of these receptors can independently mediate entrainment and has recently been found to utilize distinct neural pathways for relaying eye input to clock neurons. ORT, which is not expressed in any photoreceptor cells, plays a role in entrainment through its expression in the interneurons of the optic lobe. Thus, ORT-positive optic lobe neurons receive light-dependent histaminergic signals from photoreceptor cells and transmit them to clock neurons for photic resetting. On the other hand, HisCl1 mediates circadian entrainment through its expression in Rh6-positive cells. Rescuing HisCl1 expression in Rh6-expressing photoreceptors successfully restores entrainment, whereas the same rescue in other photoreceptors does facilitate entrainment. Consequently, this leads to the conclusion that Rh6-expressing R8 photoreceptor cells fulfill a dual role as both photoreceptors and interneurons in the HisCl1-dependent pathway.

The HisCl1-dependent photoentrainment involves multiple histaminergic inputs to Rh6-expressing cells originating from other photoreceptors. This enables them to combine and integrate the light signals received from the other receptor cells within the compound eye. The present study focused on investigating histaminergic pathways, specifically the HisCl1-dependent histaminergic input to Rh6-positive R8 cells and the subsequent neural pathway responsible for transmitting these signals to clock neurons. During a significant portion of my Ph.D. research, I performed multiple experiments to address the aforementioned inquiry and

uncovered several noteworthy findings. Later, we became aware that a separate research group led by Donggen Luo at Peking University in China was working on a similar project. Their extensive efforts included conducting numerous additional electrophysiological and circuit tracing experiments, which enabled them to elucidate the complete circuitry connecting RH6-expressing cells to clock neurons, which we failed to do. Notably, their findings aligned with and supported our own. Considering this, we made the decision to share multiple rhodopsin mutants and other genotypes that we had made and integrate our findings into the manuscript that they were preparing for submission, enabling the comprehensive work to be published as a whole.

Restoring HisCl1 exclusively in Rh6-expressing receptor cells of flies depleted for CRY and histamine receptors (CHO) allowed entrainment. This intriguing result indicated that Rh6-expressing photoreceptors establish communication with their downstream neurons through histamine-independent neurotransmission to achieve synchronization of rest-activity rhythms to LD cycles. Furthermore, in addition to histaminergic transmission, a recently published transcriptomics study revealed the involvement of cholinergic transmission in inner photoreceptors R7 and R8. Given this information, we aimed to investigate whether cholinergic transmission from Rh6-expressing cells plays a role in the HisCl1-dependent light input to clock neurons. In addition to this, we also sought to decipher the neural circuit underlying different histaminergic inputs to Rh6-expressing cells, particularly inter-ommatidial-based communications and subsequent pathways connecting R8 cells to clock neurons.

Results from electrophysiological experiments demonstrated that clock neurons, including ventral and dorsal lateral neurons, exhibited light-induced depolarization even in the absence of histamine synthesizing enzyme histidine decarboxylase (HDC). Furthermore, the response of clock neurons remained unaffected by genetic or laser ablation of H-B eyelets, suggesting that clock neurons receive non-histaminergic inputs from compound eyes. Finally, it was also shown that such Histamine-independent responses of clock neurons were abolished when synaptic transmission of R8 cells was blocked. Notably, the R8-mediated responses to brief pulses of light were similar regardless of the presence or absence of histamine receptors. Thus, it could be inferred that R8 cells utilize histamine-independent transmission to send irradiance information to clock neurons.

As acetylcholine was the primary candidate to be the neurotransmitter employed by R8 cells to talk to clock neurons, we assessed the role of cholinergic transmission in R8 cells for

circadian entrainment. Results obtained from our lab show that ChAT knock-out in R8 cells of flies lacking CRY, ORT, and Rh1 failed to synchronize locomotor rhythms to red light LD cycles (RD cycles). Since circadian entrainment to RD cycles requires either Rh1 or Rh6, we used a shifted RD cycle protocol to isolate these two rhodopsins functionally. Thus, in the triple mutant cry^{02} ort^{1} $ninaE^{17}$, the only functional photoreceptor cell is Rh6-expressing R8 cells, and disrupting the cholinergic transmission in those cells abolished photoentrainment, indicating that R8 cells employ acetylcholine for circadian entrainment.

In a significant finding, Dongen's laboratory made an intriguing discovery that R8 photoreceptors possess the ability to divide the responsibilities of visual perception and circadian entrainment through the simultaneous release of two distinct neurotransmitters. By monitoring fly behavioral responses to motion stimuli, they demonstrated that disabling the histamine synthesizing enzyme HDC in R8s or the histamine receptor *ort* abolished R8-mediated motion detection but not circadian entrainment. In contrast, when ChAT in R8 cells was suppressed using CRISPR-mediated knockdown, circadian entrainment was impaired while motion detection remained intact. Furthermore, they show another segregation in the transmission of retinotopic (visual) and irradiance (circadian) in the postsynaptic circuitry in the medulla. When exposed to light stimulation, R8 photoreceptors undergo depolarization and release both histamine and ACh from the same axonal terminals. However, the postsynaptic neurons, which express different receptors for these neurotransmitters, effectively segregate and differentiate these signals. This circuitry ensures that each unicolumnar neuron predominantly receives histaminergic inputs from a single R8 photoreceptor, thereby transmitting the retinotopic signal. On the other hand, each multicolumnar neuron that innervates aMe integrates cholinergic inputs from numerous R8 photoreceptor cells, allowing for the integration of the irradiance signal. These aMe innervating multiclumnar neurons, which were named AMA (***a***Me- innervating, ***m***ulticolumnar, and ***a***rcuate neurons), were found to be postsynaptic partners of R8 cells, and upon light input, R8 depolarize AMA neurons via acetylcholine. By utilizing anterograde *trans*-Tango tracing, it was also found that AMA neurons were presynaptically connected to most of the clock neurons. Thus, it was proposed that a three-node circuit consisting of R8s, AMA, and clock neurons facilitates circadian entrainment through cholinergic transmission.

Even though the ACh-mediated relay of light signals facilitates photoentrainment, flies devoid of histaminergic signaling alone failed to entrain the locomotor activity rhythms via

CRY-independent mechanisms, as shown by the entrainment incapability of CHO (Alejevski et al., 2019). However, HisCl1 rescue in Rh6-expressing cells restored entrainment, indicating the essential role of HisCl1 expression in R8 cells for the ACh-mediated communication of these photoreceptor cells with their downstream targets. The histaminergic feedback in R8 cells diminishes their depolarization, potentially preventing local ACh release depletion and facilitating continuous ACh release throughout the light phase. Consequently, When HisCl1 was absent, the ability of R8 photoreceptors to transmit ACh alongside other signals was impaired under prolonged exposure to light. However, this impairment was reversed when HisCl1 was reintroduced in R8 photoreceptors. Conversely, the transmission of histamine continued uninterrupted in the absence of HisCl1 during long light exposures. These findings suggest that ACh and histamine are released independently from R8 photoreceptors, which is reinforced by the observation that ACh release is more susceptible to calcium levels compared to histamine release.

Altogether, this study uncovers a neural mechanism within the early visual system where a single photoreceptor can achieve distinct photosensory tasks such as visual perception and circadian light responses at the first visual synapse. *Drosophila* R8 photoreceptors achieve this dichotomy of visual and circadian photoreception through the process of co-transmission. In addition to their role in driving visual perception through histaminergic transmission, R8 photoreceptors also contribute to the timing of circadian photoentrainment by co-transmitting ACh. Distinct neurotransmitter receptors in postsynaptic neurons segregate this dual transmitter signaling. Multicolumnar neurons expressing ACh receptors integrate irradiance signals, while unicolumnar neurons expressing Ort receptors receive retinotopic signals specifically from R8 photoreceptors. Loss of ACh signaling from R8 photoreceptors results in the elimination of R8-mediated circadian photoentrainment, while disruption of histamine signaling impairs R8-driven visual perception. Additionally, histaminergic feedback onto R8 cells was discovered to be a crucial mechanism that prevents ACh depletion in R8 photoreceptors during prolonged illumination, thereby supporting circadian photoentrainment.

Bibliography

Abruzzi, Katharine C., Abigail Zadina, Weifei Luo, Evelyn Wiyanto, Reazur Rahman, Fang Guo, Orie Shafer, and Michael Rosbash. 2017. “RNA-Seq Analysis of Drosophila Clock and Non-Clock Neurons Reveals Neuron-Specific Cycling and Novel Candidate Neuropeptides.” *PLOS Genetics* 13(2):e1006613. doi: 10.1371/journal.pgen.1006613.

Agrawal, Parul, Jerry H. Houl, Kushan L. Gunawardhana, Tianxin Liu, Jian Zhou, Mark J. Zoran, and Paul E. Hardin. 2017. “Drosophila CRY Entrains Clocks in Body Tissues to Light and Maintains Passive Membrane Properties in a Non-Clock Body Tissue Independent of Light.” *Current Biology* 27(16):2431-2441.e3. doi: 10.1016/j.cub.2017.06.064.

Ahmad, Margaret, and Anthony R. Cashmore. 1993. “HY4 Gene of A. Thaliana Encodes a Protein with Characteristics of a Blue-Light Photoreceptor.” *Nature* 366(6451):162–66. doi: 10.1038/366162a0.

Ahmad, Myra, Wanhe Li, and Deniz Top. 2021. “Integration of Circadian Clock Information in the Drosophila Circadian Neuronal Network.” *Journal of Biological Rhythms* 36(3):203–20. doi: 10.1177/0748730421993953.

Akten, Bikem, Eike Jauch, Ginka K. Genova, Eun Young Kim, Isaac Edery, Thomas Raabe, and F. Rob Jackson. 2003. “A Role for CK2 in the Drosophila Circadian Oscillator.” *Nature Neuroscience* 6(3):251–57. doi: 10.1038/nn1007.

Alejevski, Faredin, Alexandra Saint-Charles, Christine Michard-Vanhée, Béatrice Martin, Sonya Galant, Daniel Vasiliauskas, and François Rouyer. 2019. “The HisCl1 Histamine Receptor Acts in Photoreceptors to Synchronize Drosophila Behavioral Rhythms with Light-Dark Cycles.” *Nature Communications* 10(1):252. doi: 10.1038/s41467-018-08116-7.

Allada, Ravi. 2003. “Circadian Clocks: A Tale of Two Feedback Loops.” *Cell* 112(3):284–86. doi: 10.1016/S0092-8674(03)00076-X.

Allada, Ravi, Neal E. White, W. Venus So, Jeffrey C. Hall, and Michael Rosbash. 1998. “A Mutant Drosophila Homolog of Mammalian Clock Disrupts Circadian Rhythms and Transcription of Period and Timeless.” *Cell* 93(5):791–804. doi: 10.1016/S0092-8674(00)81440-3.

Andreani, Tomas S., Taichi Q. Itoh, Evrim Yildirim, Dae-Sung Hwangbo, and Ravi Allada. 2015. “Genetics of Circadian Rhythms.” *Sleep Medicine Clinics* 10(4):413–21. doi: 10.1016/j.jsmc.2015.08.007.

Antoch, Marina P., Eun-Joo Song, Anne-Marie Chang, Martha Hotz Vitaterna, Yaliang Zhao, Lisa D. Wilsbacher, Ashvin M. Sangoram, David P. King, Lawrence H. Pinto, and Joseph S. Takahashi. 1997. “Functional Identification of the Mouse Circadian Clock Gene by Transgenic BAC Rescue.” *Cell* 89(4):655–67. doi: 10.1016/S0092-8674(00)80246-9.

Aschoff, J. 1947. “Regulating the Range of physical Temperature regulation.” *Pflugers Archiv Fur Die Gesamte Physiologie Des Menschen Und Der Tiere* 249(2–3):137–47.

Aschoff, J. 1965. “CIRCADIAN RHYTHMS IN MAN.” *Science (New York, N.Y.)* 148(3676):1427–32. doi: 10.1126/science.148.3676.1427.

Aschoff, J. 1967. “Human Circadian Rhythms in Activity, Body Temperature and Other Functions.” *Life Sciences and Space Research* 5:159–73.

Aschoff, J. 1979. “Circadian Rhythms: Influences of Internal and External Factors on the Period Measured in Constant Conditions.” *Zeitschrift Fur Tierpsychologie* 49(3):225–49. doi: 10.1111/j.1439-0310.1979.tb00290.x.

Aschoff, J., S. Daan, J. Figala, and K. Müller. 1972. “Precision of Entrained Circadian Activity Rhythms under Natural Photoperiodic Conditions.” *Naturwissenschaften* 59(6):276–77. doi: 10.1007/BF00610214.

Aschoff, J., U. Gerecke, and R. Wever. 1967. “Desynchronization of Human Circadian Rhythms.” *The Japanese Journal of Physiology* 17(4):450–57. doi: 10.2170/jjphysiol.17.450.

Aschoff, J., and H. Pohl. 1978. “Phase Relations between a Circadian Rhythm and Its Zeitgeber within the Range of Entrainment.” *Die Naturwissenschaften* 65(2):80–84. doi: 10.1007/BF00440545.

Aschoff, Jürgen. 1960. “Exogenous and Endogenous Components in Circadian Rhythms.” *Cold Spring Harbor Symposia on Quantitative Biology* 25:11–28. doi: 10.1101/SQB.1960.025.01.004.

Aschoff, Jurgen, Jaroslav Figala, and Ernst Poppel. 1973. “Circadian Rhythms of Locomotor Activity in the Golden Hamster (Mesocricetus Auratus) Measured with Two Different Techniques.” *Journal of Comparative and Physiological Psychology* 85:20–28. doi: 10.1037/h0034849.

Aschoff, Jürgen, and Rütger Wever. 1962. “Spontanperiodik des Menschen bei Ausschluß aller Zeitgeber.” *Naturwissenschaften* 49(15):337–42. doi: 10.1007/BF01185109.

Bae, K., X. Jin, E. S. Maywood, M. H. Hastings, S. M. Reppert, and D. R. Weaver. 2001. “Differential Functions of MPer1, MPer2, and MPer3 in the SCN Circadian Clock.” *Neuron* 30(2):525–36. doi: 10.1016/s0896-6273(01)00302-6.

Bae, Kiho, Choogon Lee, Paul E. Hardin, and Isaac Edery. 2000. “DCLOCK Is Present in Limiting Amounts and Likely Mediates Daily Interactions between the DCLOCK–CYC Transcription Factor and the PER–TIM Complex.” *Journal of Neuroscience* 20(5):1746–53. doi: 10.1523/JNEUROSCI.20-05-01746.2000.

Bae, Kiho, Choogon Lee, David Sidote, Keng-yu Chuang, and Isaac Edery. 1998. “Circadian Regulation of a *Drosophila* Homolog of the Mammalian *Clock* Gene: PER and TIM Function as Positive Regulators.” *Molecular and Cellular Biology* 18(10):6142–51. doi: 10.1128/MCB.18.10.6142.

Baik, Lisa S., David D. Au, Ceazar Nave, Alexander J. Foden, Wendy K. Enrriquez-Villalva, and Todd C. Holmes. 2019. “Distinct Mechanisms of Drosophila CRYPTOCHROME-Mediated Light-Evoked Membrane Depolarization and in Vivo Clock Resetting.” *Proceedings of the National Academy of Sciences* 116(46):23339–44. doi: 10.1073/pnas.1905023116.

Bargiello, T. A., F. R. Jackson, and M. W. Young. 1984. “Restoration of Circadian Behavioural Rhythms by Gene Transfer in Drosophila.” *Nature* 312(5996):752–54. doi: 10.1038/312752a0.

Beckwith, Esteban J., and M. Fernanda Ceriani. 2015a. “Communication between Circadian Clusters: The Key to a Plastic Network.” *FEBS Letters* 589(22):3336–42. doi: 10.1016/j.febslet.2015.08.017.

Beckwith, Esteban J., and M. Fernanda Ceriani. 2015b. “Experimental Assessment of the

Network Properties of the Drosophila Circadian Clock." *Journal of Comparative Neurology* 523(6):982–96. doi: 10.1002/cne.23728.

Behnia, Rudy, and Claude Desplan. 2015. "Visual Circuits in Flies: Beginning to See the Whole Picture." *Current Opinion in Neurobiology* 34:125–32. doi: 10.1016/j.conb.2015.03.010.

Bell-Pedersen, Deborah, Vincent M. Cassone, David J. Earnest, Susan S. Golden, Paul E. Hardin, Terry L. Thomas, and Mark J. Zoran. 2005. "Circadian Rhythms from Multiple Oscillators: Lessons from Diverse Organisms." *Nature Reviews Genetics* 6(7):544–56. doi: 10.1038/nrg1633.

Benito, Juliana, Jerry H. Houl, Gregg W. Roman, and Paul E. Hardin. 2008. "The Blue-Light Photoreceptor CRYPTOCHROME Is Expressed in a Subset of Circadian Oscillator Neurons in the Drosophila CNS." *Journal of Biological Rhythms* 23(4):296–307. doi: 10.1177/0748730408318588.

Benito, Juliana, Hao Zheng, Fanny S. Ng, and Paul E. Hardin. 2007. "Transcriptional Feedback Loop Regulation, Function and Ontogeny in Drosophila." *Cold Spring Harbor Symposia on Quantitative Biology* 72:437–44. doi: 10.1101/sqb.2007.72.009.

Bergmann, Andreas, Julie Agapite, Kimberly McCall, and Hermann Steller. 1998. "The Drosophila Gene Hid Is a Direct Molecular Target of Ras-Dependent Survival Signaling." *Cell* 95(3):331–41. doi: 10.1016/S0092-8674(00)81765-1.

Berndt, Alex, Tilman Kottke, Helena Breitkreuz, Radovan Dvorsky, Sven Hennig, Michael Alexander, and Eva Wolf. 2007. "A Novel Photoreaction Mechanism for the Circadian Blue Light Photoreceptor Drosophila Cryptochrome *." *Journal of Biological Chemistry* 282(17):13011–21. doi: 10.1074/jbc.M608872200.

Blau, Justin, and Michael W. Young. 1999. "Cycling Vrille Expression Is Required for a Functional Drosophila Clock." *Cell* 99(6):661–71. doi: 10.1016/S0092-8674(00)81554-8.

Bloomquist, B. T., R. D. Shortridge, S. Schneuwly, M. Perdew, C. Montell, H. Steller, G. Rubin, and W. L. Pak. 1988. "Isolation of a Putative Phospholipase c Gene of Drosophila, NorpA, and Its Role in Phototransduction." *Cell* 54(5):723–33. doi: 10.1016/S0092-8674(88)80017-5.

Blume, Christine, Corrado Garbazza, and Manuel Spitschan. 2019. “Effects of Light on Human Circadian Rhythms, Sleep and Mood.” *Somnologie* 23(3):147–56. doi: 10.1007/s11818-019-00215-x.

Borst, Alexander, Michael Drews, and Matthias Meier. 2020. “The Neural Network behind the Eyes of a Fly.” *Current Opinion in Physiology* 16:33–42. doi: 10.1016/j.cophys.2020.05.004.

Borst, Alexander, and Moritz Helmstaedter. 2015. “Common Circuit Design in Fly and Mammalian Motion Vision.” *Nature Neuroscience* 18(8):1067–76. doi: 10.1038/nn.4050.

Bouly, Jean-Pierre, Erik Schleicher, Maribel Dionisio-Sese, Filip Vandenbussche, Dominique Van Der Straeten, Nadia Bakrim, Stefan Meier, Alfred Batschauer, Paul Galland, Robert Bittl, and Margaret Ahmad. 2007. “Cryptochrome Blue Light Photoreceptors Are Activated through Interconversion of Flavin Redox States *.” *Journal of Biological Chemistry* 282(13):9383–91. doi: 10.1074/jbc.M609842200.

Buchner, Erich, Sigrid Buchner, Martin G. Burg, Alois Hofbauer, William L. Pak, and Inken Pollack. 1993. “Histamine Is a Major Mechanosensory Neurotransmitter Candidate in Drosophila Melanogaster.” *Cell and Tissue Research* 273(1):119–25. doi: 10.1007/BF00304618.

Bulthuis, Nicholas, Katrina R. Spontak, Benjamin Kleeman, and Daniel J. Cavanaugh. 2019. “Neuronal Activity in Non-LNv Clock Cells Is Required to Produce Free-Running Rest:Activity Rhythms in Drosophila.” *Journal of Biological Rhythms* 34(3):249–71. doi: 10.1177/0748730419841468.

Bünning, Erwin. 1930. “Über die Erregungsvorgänge bei Seismonastischen Bewegungen.” *Planta* 12(3):545–74. doi: 10.1007/BF01948817.

Bünning, Erwin. 1932. “Die Erblichkeit der Tagesperiodizität bei Pflanzen.” *Naturwissenschaften* 20(20):340–45. doi: 10.1007/BF01504731.

Bünning, Erwin. 1933. “Refraktärstadium, Ermüdung und Narkose bei der Seismonastie.” *Planta* 21(2):324–52. doi: 10.1007/BF01909334.

Busino, Luca, Florian Bassermann, Alessio Maiolica, Choogon Lee, Patrick M. Nolan, Sofia

I. H. Godinho, Giulio F. Draetta, and Michele Pagano. 2007. “SCFFbxl3 Controls the Oscillation of the Circadian Clock by Directing the Degradation of Cryptochrome Proteins.” *Science (New York, N.Y.)* 316(5826):900–904. doi: 10.1126/science.1141194.

Busza, Ania, Myai Emery-Le, Michael Rosbash, and Patrick Emery. 2004. “Roles of the Two Drosophila CRYPTOCHROME Structural Domains in Circadian Photoreception.” *Science* 304(5676):1503–6. doi: 10.1126/science.1096973.

Candolle, Augustin Pyramus de (1778-1841) Auteur du texte. 1832. *Physiologie Végétale, Ou Exposition Des Forces et Des Fonctions Vitales Des Végétaux.... Tome 1 / Par M. Aug.-Pyr. de Candolle...*

Cao, Guan, and Michael N. Nitabach. 2008. “Circadian Control of Membrane Excitability in Drosophila Melanogaster Lateral Ventral Clock Neurons.” *Journal of Neuroscience* 28(25):6493–6501. doi: 10.1523/JNEUROSCI.1503-08.2008.

Ceriani, M. Fernanda, Thomas K. Darlington, David Staknis, Paloma Más, Allegra A. Petti, Charles J. Weitz, and Steve A. Kay. 1999. “Light-Dependent Sequestration of TIMELESS by CRYPTOCHROME.” *Science* 285(5427):553–56. doi: 10.1126/science.285.5427.553.

Ceriani, M. Fernanda, John B. Hogenesch, Marcelo Yanovsky, Satchidananda Panda, Martin Straume, and Steve A. Kay. 2002. “Genome-Wide Expression Analysis in Drosophila Reveals Genes Controlling Circadian Behavior.” *The Journal of Neuroscience: The Official Journal of the Society for Neuroscience* 22(21):9305–19. doi: 10.1523/JNEUROSCI.22-21-09305.2002.

Chaix, Amandine, Amir Zarrinpar, and Satchidananda Panda. 2016. “The Circadian Coordination of Cell Biology.” *Journal of Cell Biology* 215(1):15–25. doi: 10.1083/jcb.201603076.

Chandrashekaran, M. K. 1998. “Biological Rhythms Research: A Personal Account.” *Journal of Biosciences* 23(5):545–55. doi: 10.1007/BF02709165.

Chang, Dennis C., and Steven M. Reppert. 2003. “A Novel C-Terminal Domain of Drosophila PERIOD Inhibits DCLOCK: CYCLE-Mediated Transcription.” *Current Biology: CB* 13(9):758–62. doi: 10.1016/s0960-9822(03)00286-0.

Chatterjee, Abhishek, Angélique Lamaze, Joydeep De, Wilson Mena, Elisabeth Chélot, Béatrice Martin, Paul Hardin, Sebastian Kadener, Patrick Emery, and François Rouyer. 2018. "Reconfiguration of a Multi-Oscillator Network by Light in the Drosophila Circadian Clock." *Current Biology* 28(13):2007-2017.e4. doi: 10.1016/j.cub.2018.04.064.

Chatterjee, Abhishek, and François Rouyer. 2016. "Control of Sleep-Wake Cycles in Drosophila." in *A Time for Metabolism and Hormones*, edited by P. Sassone-Corsi and Y. Christen. Cham (CH): Springer.

Chaves, Inês, Richard Pokorny, Martin Byrdin, Nathalie Hoang, Thorsten Ritz, Klaus Brettel, Lars-Oliver Essen, Gijsbertus T. J. Van Der Horst, Alfred Batschauer, and Margaret Ahmad. 2011. "The Cryptochromes: Blue Light Photoreceptors in Plants and Animals." *Annual Review of Plant Biology* 62(1):335–64. doi: 10.1146/annurev-arplant-042110-103759.

Chen, Chenghao, Edgar Buhl, Min Xu, Vincent Croset, Johanna S. Rees, Kathryn S. Lilley, Richard Benton, James J. L. Hodge, and Ralf Stanewsky. 2015. "Drosophila Ionotropic Receptor 25a Mediates Circadian Clock Resetting by Temperature." *Nature* 527(7579):516–20. doi: 10.1038/nature16148.

Cheng, Hai-Ying M., Matias Alvarez-Saavedra, Heather Dziema, Yun Sik Choi, Aiqing Li, and Karl Obrietan. 2009. "Segregation of Expression of MPeriod Gene Homologs in Neurons and Glia: Possible Divergent Roles of MPeriod1 and MPeriod2 in the Brain." *Human Molecular Genetics* 18(16):3110–24. doi: 10.1093/hmg/ddp252.

Chiu, Joanna C., Jens T. Vanselow, Achim Kramer, and Isaac Edery. 2008. "The Phospho-Occupancy of an Atypical SLIMB-Binding Site on PERIOD That Is Phosphorylated by DOUBLETIME Controls the Pace of the Clock." *Genes & Development* 22(13):1758–72. doi: 10.1101/gad.1682708.

Choi, Charles, Guan Cao, Anne K. Tanenhaus, Ellena V. McCarthy, Misun Jung, William Schleyer, Yuhua Shang, Michael Rosbash, Jerry C. P. Yin, and Michael N. Nitabach. 2012. "Autoreceptor Control of Peptide/Neurotransmitter Corelease from PDF Neurons Determines Allocation of Circadian Activity in Drosophila." *Cell Reports* 2(2):332–44. doi: 10.1016/j.celrep.2012.06.021.

Claridge-Chang, A., H. Wijnen, F. Naef, C. Boothroyd, N. Rajewsky, and M. W. Young. 2001. "Circadian Regulation of Gene Expression Systems in the Drosophila Head." *Neuron* 32(4):657–71. doi: 10.1016/s0896-6273(01)00515-3.

Cockcroft, S., and B. D. Gomperts. 1985. "Role of Guanine Nucleotide Binding Protein in the Activation of Polyphosphoinositide Phosphodiesterase." *Nature* 314(6011):534–36. doi: 10.1038/314534a0.

Collins, Ben, Elizabeth A. Kane, David C. Reeves, Myles H. Akabas, and Justin Blau. 2012. "Balance of Activity between LNvs and Glutamatergic Dorsal Clock Neurons Promotes Robust Circadian Rhythms in Drosophila." *Neuron* 74(4):706–18. doi: 10.1016/j.neuron.2012.02.034.

Crespo-Flores, Sergio L., and Annika F. Barber. 2022. "The Drosophila Circadian Clock Circuit Is a Nonhierarchical Network of Peptidergic Oscillators." *Current Opinion in Insect Science* 52:100944. doi: 10.1016/j.cois.2022.100944.

Curtin, K. D., Z. J. Huang, and M. Rosbash. 1995. "Temporally Regulated Nuclear Entry of the Drosophila Period Protein Contributes to the Circadian Clock." *Neuron* 14(2):365–72. doi: 10.1016/0896-6273(95)90292-9.

Cusumano, Paola, André Klarsfeld, Elisabeth Chélot, Marie Picot, Benjamin Richier, and François Rouyer. 2009. "PDF-Modulated Visual Inputs and Cryptochrome Define Diurnal Behavior in Drosophila." *Nature Neuroscience* 12(11):1431–37. doi: 10.1038/nn.2429.

Cyran, Shawn A., Anna M. Buchsbaum, Karen L. Reddy, Meng-Chi Lin, Nicholas R. J. Glossop, Paul E. Hardin, Michael W. Young, Robert V. Storti, and Justin Blau. 2003. "Vrille, Pdp1, and DClock Form a Second Feedback Loop in the Drosophila Circadian Clock." *Cell* 112(3):329–41. doi: 10.1016/S0092-8674(03)00074-6.

Cyran, Shawn A., Georgia Yiannoulos, Anna M. Buchsbaum, Lino Saez, Michael W. Young, and Justin Blau. 2005. "The Double-Time Protein Kinase Regulates the Subcellular Localization of the Drosophila Clock Protein Period." *Journal of Neuroscience* 25(22):5430–37. doi: 10.1523/JNEUROSCI.0263-05.2005.

Czeisler, C. A., J. F. Duffy, T. L. Shanahan, E. N. Brown, J. F. Mitchell, D. W. Rimmer, J. M. Ronda, E. J. Silva, J. S. Allan, J. S. Emens, D. J. Dijk, and R. E. Kronauer. 1999. "Stability,

Precision, and near-24-Hour Period of the Human Circadian Pacemaker." *Science (New York, N.Y.)* 284(5423):2177–81. doi: 10.1126/science.284.5423.2177.

Daan, S. 2000. "The Colin S. Pittendrigh Lecture. Colin Pittendrigh, Jürgen Aschoff, and the Natural Entrainment of Circadian Systems." *Journal of Biological Rhythms* 15(3):195–207. doi: 10.1177/074873040001500301.

Daan, Serge. 1977. "Tonic and Phasic Effects of Light in the Entrainment of Circadian Rhythms." *Annals of the New York Academy of Sciences* 290(1):51–59. doi: 10.1111/j.1749-6632.1977.tb39716.x.

Dannerfjord, Adam A., Laurence A. Brown, Russell G. Foster, and Stuart N. Peirson. 2021. "Light Input to the Mammalian Circadian Clock." *Methods in Molecular Biology (Clifton, N.J.)* 2130:233–47. doi: 10.1007/978-1-0716-0381-9_18.

Darlington, T. K., K. Wager-Smith, M. F. Ceriani, D. Staknis, N. Gekakis, T. D. Steeves, C. J. Weitz, J. S. Takahashi, and S. A. Kay. 1998. "Closing the Circadian Loop: CLOCK-Induced Transcription of Its Own Inhibitors per and Tim." *Science (New York, N.Y.)* 280(5369):1599–1603. doi: 10.1126/science.280.5369.1599.

Davis, Fred P., Aljoscha Nern, Serge Picard, Michael B. Reiser, Gerald M. Rubin, Sean R. Eddy, and Gilbert L. Henry. 2020. "A Genetic, Genomic, and Computational Resource for Exploring Neural Circuit Function" edited by H. J. Bellen and K. VijayRaghavan. *ELife* 9:e50901. doi: 10.7554/eLife.50901.

DeCoursey, Patricia J. 2004. "The Behavioral Ecology and Evolution of Biological Timing Systems." Pp. 27–65 in *Chronobiology: Biological timekeeping*. Sunderland, MA, US: Sinauer Associates.

Delventhal, Rebecca, Reed M. O'Connor, Meghan M. Pantalia, Matthew Ulgherait, Han X. Kim, Maylis K. Basturk, Julie C. Canman, and Mimi Shirasu-Hiza. 2019. "Dissection of Central Clock Function in Drosophila through Cell-Specific CRISPR-Mediated Clock Gene Disruption." *ELife* 8:e48308. doi: 10.7554/eLife.48308.

Depetris-Chauvin, Ana, Jimena Berni, Ezequiel J. Aranovich, Nara I. Muraro, Esteban J. Beckwith, and María Fernanda Ceriani. 2011. "Adult-Specific Electrical Silencing of Pacemaker Neurons Uncouples Molecular Clock from Circadian Outputs." *Current*

Biology 21(21):1783–93. doi: 10.1016/j.cub.2011.09.027.

Desplan, Claude. n.d. "Color and Polarized Light Vision: The Drosophila Retinal Mosaic."

Devary, O., O. Heichal, A. Blumenfeld, D. Cassel, E. Suss, S. Barash, C. T. Rubinstein, B. Minke, and Z. Selinger. 1987. "Coupling of Photoexcited Rhodopsin to Inositol Phospholipid Hydrolysis in Fly Photoreceptors." *Proceedings of the National Academy of Sciences of the United States of America* 84(19):6939–43. doi: 10.1073/pnas.84.19.6939.

Díaz, Madelen M., Matthias Schlichting, Katharine C. Abruzzi, Xi Long, and Michael Rosbash. 2019. "Allatostatin-C/AstC-R2 Is a Novel Pathway to Modulate the Circadian Activity Pattern in Drosophila." *Current Biology* 29(1):13-22.e3. doi: 10.1016/j.cub.2018.11.005.

Dibner, Charna, Ueli Schibler, and Urs Albrecht. 2010. "The Mammalian Circadian Timing System: Organization and Coordination of Central and Peripheral Clocks." *Annual Review of Physiology* 72:517–49. doi: 10.1146/annurev-physiol-021909-135821.

Dissel, Stephane, Veryan Codd, Robert Fedic, Karen J. Garner, Rodolfo Costa, Charalambos P. Kyriacou, and Ezio Rosato. 2004. "A Constitutively Active Cryptochrome in Drosophila Melanogaster." *Nature Neuroscience* 7(8):834–40. doi: 10.1038/nn1285.

Dissel, Stephane, Celia N. Hansen, Özge Özkaya, Matthew Hemsley, Charalambos P. Kyriacou, and Ezio Rosato. 2014. "The Logic of Circadian Organization in Drosophila." *Current Biology* 24(19):2257–66. doi: 10.1016/j.cub.2014.08.023.

Dolezelova, Eva, David Dolezel, and Jeffrey C. Hall. 2007. "Rhythm Defects Caused by Newly Engineered Null Mutations in Drosophila's Cryptochrome Gene." *Genetics* 177(1):329–45. doi: 10.1534/genetics.107.076513.

Dubowy, Christine, and Amita Sehgal. 2017. "Circadian Rhythms and Sleep in Drosophila Melanogaster." *Genetics* 205(4):1373–97. doi: 10.1534/genetics.115.185157.

Duhart, José M., Anastasia Herrero, Gabriel de la Cruz, Juan I. Ispizua, Nicolás Pírez, and M. Fernanda Ceriani. 2020. "Circadian Structural Plasticity Drives Remodeling of E Cell Output." *Current Biology* 30(24):5040-5048.e5. doi: 10.1016/j.cub.2020.09.057.

Dunlap, Jay C. 1999. "Molecular Bases for Circadian Clocks." *Cell* 96(2):271–90. doi:

10.1016/S0092-8674(00)80566-8.

Dunlap, Jay C., Jennifer J. Loros, and Patricia J. DeCoursey. 2004. *Chronobiology: Biological Timekeeping*. Sunderland, Mass.: Sinauer Associates.

Dusik, Verena, Pingkalai R. Senthilan, Benjamin Mentzel, Heiko Hartlieb, Corinna Wülbeck, Taishi Yoshii, Thomas Raabe, and Charlotte Helfrich-Förster. 2014. "The MAP Kinase P38 Is Part of Drosophila Melanogaster's Circadian Clock." *PLOS Genetics* 10(8):e1004565. doi: 10.1371/journal.pgen.1004565.

Duvall, Laura B., and Paul H. Taghert. 2012. "The Circadian Neuropeptide PDF Signals Preferentially through a Specific Adenylate Cyclase Isoform AC3 in M Pacemakers of Drosophila." *PLoS Biology* 10(6):e1001337. doi: 10.1371/journal.pbio.1001337.

Duvall, Laura B., and Paul H. Taghert. 2013. "E and M Circadian Pacemaker Neurons Use Different PDF Receptor Signalosome Components in Drosophila." *Journal of Biological Rhythms* 28(4):239–48. doi: 10.1177/0748730413497179.

Edery, I., L. J. Zwiebel, M. E. Dembinska, and M. Rosbash. 1994. "Temporal Phosphorylation of the Drosophila Period Protein." *Proceedings of the National Academy of Sciences* 91(6):2260–64. doi: 10.1073/pnas.91.6.2260.

Eide, Erik J., Margaret F. Woolf, Heeseog Kang, Peter Woolf, William Hurst, Fernando Camacho, Erica L. Vielhaber, Andrew Giovanni, and David M. Virshup. 2005. "Control of Mammalian Circadian Rhythm by CKIε-Regulated Proteasome-Mediated PER2 Degradation." *Molecular and Cellular Biology* 25(7):2795–2807. doi: 10.1128/MCB.25.7.2795-2807.2005.

Emery, P., W. V. So, M. Kaneko, J. C. Hall, and M. Rosbash. 1998. "CRY, a Drosophila Clock and Light-Regulated Cryptochrome, Is a Major Contributor to Circadian Rhythm Resetting and Photosensitivity." *Cell* 95(5):669–79. doi: 10.1016/s0092-8674(00)81637-2.

Emery, Patrick, Ralf Stanewsky, Charlotte Helfrich-Förster, Myai Emery-Le, Jeffrey C. Hall, and Michael Rosbash. 2000. "Drosophila CRY Is a Deep Brain Circadian Photoreceptor." *Neuron* 26(2):493–504. doi: 10.1016/S0896-6273(00)81181-2.

Fang, Yanshan, Sriram Sathyanarayanan, and Amita Sehgal. 2007. “Post-Translational Regulation of the Drosophila Circadian Clock Requires Protein Phosphatase 1 (PP1).” *Genes & Development* 21(12):1506–18. doi: 10.1101/gad.1541607.

Feiler, R., R. Bjornson, K. Kirschfeld, D. Mismer, G. M. Rubin, D. P. Smith, M. Socolich, and C. S. Zuker. 1992. “Ectopic Expression of Ultraviolet-Rhodopsins in the Blue Photoreceptor Cells of Drosophila: Visual Physiology and Photochemistry of Transgenic Animals.” *The Journal of Neuroscience: The Official Journal of the Society for Neuroscience* 12(10):3862–68. doi: 10.1523/JNEUROSCI.12-10-03862.1992.

Fernandez, Maria P., Hannah L. Pettibone, Joseph T. Bogart, Casey J. Roell, Charles E. Davey, Ausra Pranevicius, Khang V. Huynh, Sara M. Lennox, Boyan S. Kostadinov, and Orie T. Shafer. 2020. “Sites of Circadian Clock Neuron Plasticity Mediate Sensory Integration and Entrainment.” *Current Biology : CB* 30(12):2225-2237.e5. doi: 10.1016/j.cub.2020.04.025.

Fernández, María Paz, Jimena Berni, and María Fernanda Ceriani. 2008. “Circadian Remodeling of Neuronal Circuits Involved in Rhythmic Behavior.” *PLoS Biology* 6(3):e69. doi: 10.1371/journal.pbio.0060069.

Finger, Anna-Marie, and Achim Kramer. 2021. “Mammalian Circadian Systems: Organization and Modern Life Challenges.” *Acta Physiologica* 231(3):e13548. doi: 10.1111/apha.13548.

Flourakis, Matthieu, Elzbieta Kula-Eversole, Alan L. Hutchison, Tae Hee Han, Kimberly Aranda, Devon L. Moose, Kevin P. White, Aaron R. Dinner, Bridget C. Lear, Dejian Ren, Casey O. Diekman, Indira M. Raman, and Ravi Allada. 2015. “A Conserved Bicycle Model for Circadian Clock Control of Membrane Excitability.” *Cell* 162(4):836–48. doi: 10.1016/j.cell.2015.07.036.

Fogle, Keri J., Lisa S. Baik, Jerry H. Houl, Tri T. Tran, Logan Roberts, Nicole A. Dahm, Yu Cao, Ming Zhou, and Todd C. Holmes. 2015. “CRYPTOCHROME-Mediated Phototransduction by Modulation of the Potassium Ion Channel β-Subunit Redox Sensor.” *Proceedings of the National Academy of Sciences of the United States of America* 112(7):2245–50. doi: 10.1073/pnas.1416586112.

Fogle, Keri J., Kelly G. Parson, Nicole A. Dahm, and Todd C. Holmes. 2011. "CRYPTOCHROME Is a Blue-Light Sensor That Regulates Neuronal Firing Rate." *Science* 331(6023):1409–13. doi: 10.1126/science.1199702.

Foley, Lauren E., and Patrick Emery. 2020. "Drosophila Cryptochrome: Variations in Blue." *Journal of Biological Rhythms* 35(1):16–27. doi: 10.1177/0748730419878290.

Foster, Russell G., and Charlotte Helfrich-Forster. 2001. "The Regulation of Circadian Clocks by Light in Fruitflies and Mice." *Philosophical Transactions of the Royal Society of London. Series B: Biological Sciences* 356(1415):1779–89. doi: 10.1098/rstb.2001.0962.

Frenkel, Lia, Nara I. Muraro, Andrea N. Beltrán González, María S. Marcora, Guillermo Bernabó, Christiane Hermann-Luibl, Juan I. Romero, Charlotte Helfrich-Förster, Eduardo M. Castaño, Cristina Marino-Busjle, Daniel J. Calvo, and M. Fernanda Ceriani. 2017. "Organization of Circadian Behavior Relies on Glycinergic Transmission." *Cell Reports* 19(1):72–85. doi: 10.1016/j.celrep.2017.03.034.

Fujiwara, Yuri, Christiane Hermann-Luibl, Maki Katsura, Manabu Sekiguchi, Takanori Ida, Charlotte Helfrich-Förster, and Taishi Yoshii. 2018. "The CCHamide1 Neuropeptide Expressed in the Anterior Dorsal Neuron 1 Conveys a Circadian Signal to the Ventral Lateral Neurons in Drosophila Melanogaster." *Frontiers in Physiology* 9.

Ganguly, Abir, Craig C. Manahan, Deniz Top, Estella F. Yee, Changfan Lin, Michael W. Young, Walter Thiel, and Brian R. Crane. 2016. "Changes in Active Site Histidine Hydrogen Bonding Trigger Cryptochrome Activation." *Proceedings of the National Academy of Sciences* 113(36):10073–78. doi: 10.1073/pnas.1606610113.

Gekakis, N., D. Staknis, H. B. Nguyen, F. C. Davis, L. D. Wilsbacher, D. P. King, J. S. Takahashi, and C. J. Weitz. 1998. "Role of the CLOCK Protein in the Mammalian Circadian Mechanism." *Science (New York, N.Y.)* 280(5369):1564–69. doi: 10.1126/science.280.5369.1564.

Gekakis, Nicholas, Lino Saez, Anne-Marie Delahaye-Brown, Michael P. Myers, Amita Sehgal, Michael W. Young, and Charles J. Weitz. 1995. "Isolation of Timeless by PER Protein Interaction: Defective Interaction Between Timeless Protein and Long-Period Mutant PERL." *Science* 270(5237):811–15. doi: 10.1126/science.270.5237.811.

Gengs, Chaoxian, Hung-Tat Leung, David R. Skingsley, Mladen I. Iovchev, Zhan Yin, Eugene P. Semenov, Martin G. Burg, Roger C. Hardie, and William L. Pak. 2002. "The Target of Drosophila Photoreceptor Synaptic Transmission Is a Histamine-Gated Chloride Channel Encoded Byort (HclA)*." *Journal of Biological Chemistry* 277(44):42113–20. doi: 10.1074/jbc.M207133200.

Gisselmann, Günter, Hermann Pusch, Bernd T. Hovemann, and Hanns Hatt. 2002. "Two CDNAs Coding for Histamine-Gated Ion Channels in D. Melanogaster." *Nature Neuroscience* 5(1):11–12. doi: 10.1038/nn787.

Glaser, F. T., and R. Stanewsky. 2007. "Synchronization of the Drosophila Circadian Clock by Temperature Cycles." *Cold Spring Harbor Symposia on Quantitative Biology* 72:233–42. doi: 10.1101/sqb.2007.72.046.

Glossop, Nicholas R. J., Jerry H. Houl, Hao Zheng, Fanny S. Ng, Scott M. Dudek, and Paul E. Hardin. 2003. "VRILLE Feeds Back to Control Circadian Transcription of Clock in the Drosophila Circadian Oscillator." *Neuron* 37(2):249–61. doi: 10.1016/S0896-6273(03)00002-3.

Glossop, Nick R. J., Lisa C. Lyons, and Paul E. Hardin. 1999. "Interlocked Feedback Loops Within the Drosophila Circadian Oscillator." *Science* 286(5440):766–68. doi: 10.1126/science.286.5440.766.

Goda, Tadahiro, Xin Tang, Yujiro Umezaki, Michelle L. Chu, Michael Kunst, Michael N. Nitabach, and Fumika N. Hamada. 2016. "Drosophila DH31 Neuropeptide and PDF Receptor Regulate Night-Onset Temperature Preference." *Journal of Neuroscience* 36(46):11739–54. doi: 10.1523/JNEUROSCI.0964-16.2016.

Golombek, Diego A., and Ruth E. Rosenstein. 2010. "Physiology of Circadian Entrainment." *Physiological Reviews* 90(3):1063–1102. doi: 10.1152/physrev.00009.2009.

Gorostiza, E. Axel, Ana Depetris-Chauvin, Lia Frenkel, Nicolás Pírez, and María Fernanda Ceriani. 2014. "Circadian Pacemaker Neurons Change Synaptic Contacts across the Day." *Current Biology: CB* 24(18):2161–67. doi: 10.1016/j.cub.2014.07.063.

Griffin, Edmund A., David Staknis, and Charles J. Weitz. 1999. "Light-Independent Role of CRY1 and CRY2 in the Mammalian Circadian Clock." *Science* 286(5440):768–71. doi:

10.1126/science.286.5440.768.

Grima, Brigitte, Elisabeth Chélot, Ruohan Xia, and François Rouyer. 2004. “Morning and Evening Peaks of Activity Rely on Different Clock Neurons of the Drosophila Brain.” *Nature* 431(7010):869–73. doi: 10.1038/nature02935.

Grima, Brigitte, Annie Lamouroux, Elisabeth Chélot, Christian Papin, Bernadette Limbourg-Bouchon, and François Rouyer. 2002. “The F-Box Protein Slimb Controls the Levels of Clock Proteins Period and Timeless.” *Nature* 420(6912):178–82. doi: 10.1038/nature01122.

Guo, Fang, Isadora Cerullo, Xiao Chen, and Michael Rosbash. 2014. “PDF Neuron Firing Phase-Shifts Key Circadian Activity Neurons in Drosophila” edited by L. Ptáček. *ELife* 3:e02780. doi: 10.7554/eLife.02780.

Guo, Fang, Junwei Yu, Hyung Jae Jung, Katharine C. Abruzzi, Weifei Luo, Leslie C. Griffith, and Michael Rosbash. 2016. “Circadian Neuron Feedback Controls the Drosophila Sleep--Activity Profile.” *Nature* 536(7616):292–97. doi: 10.1038/nature19097.

Gustafson, Chelsea L., and Carrie L. Partch. 2015. “Emerging Models for the Molecular Basis of Mammalian Circadian Timing.” *Biochemistry* 54(2):134–49. doi: 10.1021/bi500731f.

Hamasaka, Yasutaka, Dirk Rieger, Marie-Laure Parmentier, Yves Grau, Charlotte Helfrich-Förster, and Dick R. Nässel. 2007. “Glutamate and Its Metabotropic Receptor in Drosophila Clock Neuron Circuits.” *Journal of Comparative Neurology* 505(1):32–45. doi: 10.1002/cne.21471.

Hamasaka, Yasutaka, Takahiro Suzuki, Shuji Hanai, and Norio Ishida. 2010. “Evening Circadian Oscillator as the Primary Determinant of Rhythmic Motivation for Drosophila Courtship Behavior.” *Genes to Cells* 15(12):1240–48. doi: 10.1111/j.1365-2443.2010.01456.x.

Hanai, Shuji, Yasutaka Hamasaka, and Norio Ishida. 2008. “Circadian Entrainment to Red Light in Drosophila: Requirement of Rhodopsin 1 and Rhodopsin 6.” *Neuroreport* 19(14):1441–44. doi: 10.1097/WNR.0b013e32830e4961.

Hanai, Shuji, and Norio Ishida. 2009. “Entrainment of Drosophila Circadian Clock to Green

and Yellow Light by Rh1, Rh5, Rh6 and CRY." *Neuroreport* 20(8):755–58. doi: 10.1097/WNR.0b013e32832a7c4e.

Hao, H., D. L. Allen, and P. E. Hardin. 1997. "A Circadian Enhancer Mediates PER-Dependent MRNA Cycling in Drosophila Melanogaster." *Molecular and Cellular Biology* 17(7):3687–93. doi: 10.1128/MCB.17.7.3687.

Hardcastle, Ben J., Jaison J. Omoto, Pratyush Kandimalla, Bao-Chau M. Nguyen, Mehmet F. Keleş, Natalie K. Boyd, Volker Hartenstein, and Mark A. Frye. 2021. "A Visual Pathway for Skylight Polarization Processing in Drosophila" edited by C. Desplan, R. L. Calabrese, S. Heinze, and R. Franconville. *ELife* 10:e63225. doi: 10.7554/eLife.63225.

Hardie, R. C., and B. Minke. 1992. "The Trp Gene Is Essential for a Light-Activated Ca2+ Channel in Drosophila Photoreceptors." *Neuron* 8(4):643–51. doi: 10.1016/0896-6273(92)90086-s.

Hardie, Roger C., and Padinjat Raghu. 2001. "Visual Transduction in Drosophila." *Nature* 413(6852):186–93. doi: 10.1038/35093002.

Hardin, P. E., J. C. Hall, and M. Rosbash. 1992. "Circadian Oscillations in Period Gene MRNA Levels Are Transcriptionally Regulated." *Proceedings of the National Academy of Sciences of the United States of America* 89(24):11711–15.

Hardin, Paul E. 2005. "The Circadian Timekeeping System of Drosophila." *Current Biology* 15(17):R714–22. doi: 10.1016/j.cub.2005.08.019.

Hardin, Paul E. 2006. "Essential and Expendable Features of the Circadian Timekeeping Mechanism." *Current Opinion in Neurobiology* 16(6):686–92. doi: 10.1016/j.conb.2006.09.001.

Hardin, Paul E. 2011. "Molecular Genetic Analysis of Circadian Timekeeping in Drosophila." *Advances in Genetics* 74:141–73. doi: 10.1016/B978-0-12-387690-4.00005-2.

Hardin, Paul E., Jeffrey C. Hall, and Michael Rosbash. 1990. "Feedback of the Drosophila Period Gene Product on Circadian Cycling of Its Messenger RNA Levels." *Nature* 343(6258):536–40. doi: 10.1038/343536a0.

Hardin, Paul E., and Satchidananda Panda. 2013. "Circadian Timekeeping and Output

Mechanisms in Animals." *Current Opinion in Neurobiology* 23(5):724–31. doi: 10.1016/j.conb.2013.02.018.

He, C., X. Cong, R. Zhang, D. Wu, C. An, and Z. Zhao. 2013. "Regulation of Circadian Locomotor Rhythm by Neuropeptide Y-like System in Drosophila Melanogaster." *Insect Molecular Biology* 22(4):376–88. doi: 10.1111/imb.12027.

Heisenberg, Martin, and Erich Buchner. 1977. "The Rôle of Retinula Cell Types in Visual Behavior OfDrosophila Melanogaster." *Journal of Comparative Physiology* 117(2):127–62. doi: 10.1007/BF00612784.

Helfrich-Förster, C. 1995. "The Period Clock Gene Is Expressed in Central Nervous System Neurons Which Also Produce a Neuropeptide That Reveals the Projections of Circadian Pacemaker Cells within the Brain of Drosophila Melanogaster." *Proceedings of the National Academy of Sciences of the United States of America* 92(2):612–16. doi: 10.1073/pnas.92.2.612.

Helfrich-Förster, C., T. Yoshii, C. Wülbeck, E. Grieshaber, D. Rieger, W. Bachleitner, P. Cusumano, and F. Rouyer. 2007. "The Lateral and Dorsal Neurons of Drosophila Melanogaster: New Insights about Their Morphology and Function." *Cold Spring Harbor Symposia on Quantitative Biology* 72:517–25. doi: 10.1101/sqb.2007.72.063.

Helfrich-Förster, Charlotte. 2003. "The Neuroarchitecture of the Circadian Clock in the Brain of Drosophila Melanogaster." *Microscopy Research and Technique* 62(2):94–102. doi: 10.1002/jemt.10357.

Helfrich-Förster, Charlotte. 2017. "The Drosophila Clock System." Pp. 133–76 in *Biological Timekeeping: Clocks, Rhythms and Behaviour*, edited by V. Kumar. New Delhi: Springer India.

Helfrich-Förster, Charlotte. 2019. "Polarization Vision: Targets of Polarization-Sensitive Photoreceptors in the Drosophila Visual System." *Current Biology* 29(17):R839–42. doi: 10.1016/j.cub.2019.07.032.

Helfrich-Förster, Charlotte. 2020. "Light Input Pathways to the Circadian Clock of Insects with an Emphasis on the Fruit Fly Drosophila Melanogaster." *Journal of Comparative Physiology. A, Neuroethology, Sensory, Neural, and Behavioral Physiology* 206(2):259–

72. doi: 10.1007/s00359-019-01379-5.

Helfrich-Förster, Charlotte, Tara Edwards, Kouji Yasuyama, Barbara Wisotzki, Stephan Schneuwly, Ralf Stanewsky, Ian A. Meinertzhagen, and Alois Hofbauer. 2002. "The Extraretinal Eyelet of Drosophila: Development, Ultrastructure, and Putative Circadian Function." *The Journal of Neuroscience: The Official Journal of the Society for Neuroscience* 22(21):9255–66. doi: 10.1523/JNEUROSCI.22-21-09255.2002.

Helfrich-Förster, Charlotte, Orie T. Shafer, Corinna Wülbeck, Eva Grieshaber, Dirk Rieger, and Paul Taghert. 2007. "Development and Morphology of the Clock-Gene-Expressing Lateral Neurons of Drosophila Melanogaster." *Journal of Comparative Neurology* 500(1):47–70. doi: 10.1002/cne.21146.

Helfrich-Förster, Charlotte, Christine Winter, Alois Hofbauer, Jeffrey C. Hall, and Ralf Stanewsky. 2001. "The Circadian Clock of Fruit Flies Is Blind after Elimination of All Known Photoreceptors." *Neuron* 30(1):249–61. doi: 10.1016/S0896-6273(01)00277-X.

Hemsley, Matthew J., Gabriella M. Mazzotta, Moyra Mason, Stephane Dissel, Stefano Toppo, Mario A. Pagano, Federica Sandrelli, Flavio Meggio, Ezio Rosato, Rodolfo Costa, and Silvio C. E. Tosatto. 2007. "Linear Motifs in the C-Terminus of D. Melanogaster Cryptochrome." *Biochemical and Biophysical Research Communications* 355(2):531–37. doi: 10.1016/j.bbrc.2007.01.189.

Hermann, Christiane, Taishi Yoshii, Verena Dusik, and Charlotte Helfrich-Förster. 2012. "Neuropeptide F Immunoreactive Clock Neurons Modify Evening Locomotor Activity and Free-Running Period in Drosophila Melanogaster." *Journal of Comparative Neurology* 520(5):970–87. doi: 10.1002/cne.22742.

Hermann-Luibl, Christiane, and Charlotte Helfrich-Förster. 2015. "Clock Network in Drosophila." *Current Opinion in Insect Science* 7:65–70. doi: 10.1016/j.cois.2014.11.003.

Hermann-Luibl, Christiane, Taishi Yoshii, Pingkalai R. Senthilan, Heinrich Dircksen, and Charlotte Helfrich-Förster. 2014. "The Ion Transport Peptide Is a New Functional Clock Neuropeptide in the Fruit Fly Drosophila Melanogaster." *Journal of Neuroscience* 34(29):9522–36. doi: 10.1523/JNEUROSCI.0111-14.2014.

Hirano, Arisa, Kanae Yumimoto, Ryosuke Tsunematsu, Masaki Matsumoto, Masaaki Oyama,

Hiroko Kozuka-Hata, Tomoki Nakagawa, Darin Lanjakornsiripan, Keiichi I. Nakayama, and Yoshitaka Fukada. 2013. “FBXL21 Regulates Oscillation of the Circadian Clock through Ubiquitination and Stabilization of Cryptochromes.” *Cell* 152(5):1106–18. doi: 10.1016/j.cell.2013.01.054.

Hoang, Nathalie, Erik Schleicher, Sylwia Kacprzak, Jean-Pierre Bouly, Marie Picot, William Wu, Albrecht Berndt, Eva Wolf, Robert Bittl, and Margaret Ahmad. 2008. “Human and Drosophila Cryptochromes Are Light Activated by Flavin Photoreduction in Living Cells.” *PLOS Biology* 6(7):e160. doi: 10.1371/journal.pbio.0060160.

Hofbauer, A., and E. Buchner. 1989. “Does Drosophila Have Seven Eyes?” *Naturwissenschaften* 76(7):335–36. doi: 10.1007/BF00368438.

Horst, Gijsbertus T. J. van der, Manja Muijtjens, Kumiko Kobayashi, Riya Takano, Shin-ichiro Kanno, Masashi Takao, Jan de Wit, Anton Verkerk, Andre P. M. Eker, Dik van Leenen, Ruud Buijs, Dirk Bootsma, Jan H. J. Hoeijmakers, and Akira Yasui. 1999. “Mammalian Cry1 and Cry2 Are Essential for Maintenance of Circadian Rhythms.” *Nature* 398(6728):627–30. doi: 10.1038/19323.

Huang, Zuoshi Josh, Isaac Edery, and Michael Rosbash. 1993. “PAS Is a Dimerization Domain Common to Drosophila Period and Several Transcription Factors.” *Nature* 364(6434):259–62. doi: 10.1038/364259a0.

Hunter-Ensor, Melissa, Andrea Ousley, and Amita Sehgal. 1996. “Regulation of the Drosophila Protein Timeless Suggests a Mechanism for Resetting the Circadian Clock by Light.” *Cell* 84(5):677–85. doi: 10.1016/S0092-8674(00)81046-6.

Hut, R. A., and D. G. M. Beersma. 2011. “Evolution of Time-Keeping Mechanisms: Early Emergence and Adaptation to Photoperiod.” *Philosophical Transactions of the Royal Society B: Biological Sciences* 366(1574):2141–54. doi: 10.1098/rstb.2010.0409.

Hut, Roelof A., Bob E. H. van Oort, and Serge Daan. 1999. “Natural Entrainment without Dawn and Dusk: The Case of the European Ground Squirrel (Spermophilus Citellus).” *Journal of Biological Rhythms* 14:290–99. doi: 10.1177/074873099129000704.

Hyun, Seogang, Youngseok Lee, Sung-Tae Hong, Sunhoe Bang, Donggi Paik, Jongkyun Kang, Jinwhan Shin, Jaejung Lee, Keunhye Jeon, Seungyoon Hwang, Eunkyung Bae, and

Jaeseob Kim. 2005. “Drosophila GPCR Han Is a Receptor for the Circadian Clock Neuropeptide PDF.” *Neuron* 48(2):267–78. doi: 10.1016/j.neuron.2005.08.025.

Im, Seol Hee, Weihua Li, and Paul H. Taghert. 2011. “PDFR and CRY Signaling Converge in a Subset of Clock Neurons to Modulate the Amplitude and Phase of Circadian Behavior in Drosophila.” *PLOS ONE* 6(4):e18974. doi: 10.1371/journal.pone.0018974.

Im, Seol Hee, and Paul H. Taghert. 2010. “PDF Receptor Expression Reveals Direct Interactions between Circadian Oscillators in Drosophila.” *The Journal of Comparative Neurology* 518(11):1925–45. doi: 10.1002/cne.22311.

Ito, Chihiro, and Kenji Tomioka. 2016. “Heterogeneity of the Peripheral Circadian Systems in Drosophila Melanogaster: A Review.” *Frontiers in Physiology* 7:8. doi: 10.3389/fphys.2016.00008.

Jackson, F. Rob, Fanny S. Ng, Sukanya Sengupta, Samantha You, and Yanmei Huang. 2015. “Glial Cell Regulation of Rhythmic Behavior.” *Methods in Enzymology* 552:45–73. doi: 10.1016/bs.mie.2014.10.016.

Jang, A. Reum, Katarina Moravcevic, Lino Saez, Michael W. Young, and Amita Sehgal. 2015. “Drosophila TIM Binds Importin A1, and Acts as an Adapter to Transport PER to the Nucleus.” *PLOS Genetics* 11(2):e1004974. doi: 10.1371/journal.pgen.1004974.

Jean-Guillaume, Claude Bernard, and Justin P. Kumar. 2022. “Development of the Ocellar Visual System in Drosophila Melanogaster.” *The FEBS Journal* 289(23):7411–27. doi: 10.1111/febs.16468.

Johard, Helena A. D., Taishi Yoishii, Heinrich Dircksen, Paola Cusumano, Francois Rouyer, Charlotte Helfrich-Förster, and Dick R. Nässel. 2009. “Peptidergic Clock Neurons in Drosophila: Ion Transport Peptide and Short Neuropeptide F in Subsets of Dorsal and Ventral Lateral Neurons.” *The Journal of Comparative Neurology* 516(1):59–73. doi: 10.1002/cne.22099.

Johnson, C. H. 1999. “Forty Years of PRCs--What Have We Learned?” *Chronobiology International* 16(6):711–43. doi: 10.3109/07420529909016940.

Jung, Sung-Hwan, Jae-Hyuk Lee, Hyo-Seok Chae, Jae Young Seong, Yoonseong Park, Zee-

Yong Park, and Young-Joon Kim. 2014. “Identification of a Novel Insect Neuropeptide, CNMa and Its Receptor.” *FEBS Letters* 588(12):2037–41. doi: 10.1016/j.febslet.2014.04.028.

Kadener, Sebastian, Dan Stoleru, Michael McDonald, Pipat Nawathean, and Michael Rosbash. 2007. “Clockwork Orange Is a Transcriptional Repressor and a New Drosophila Circadian Pacemaker Component.” *Genes & Development* 21(13):1675–86. doi: 10.1101/gad.1552607.

Kaneko, M., and J. C. Hall. 2000. “Neuroanatomy of Cells Expressing Clock Genes in Drosophila: Transgenic Manipulation of the Period and Timeless Genes to Mark the Perikarya of Circadian Pacemaker Neurons and Their Projections.” *The Journal of Comparative Neurology* 422(1):66–94. doi: 10.1002/(sici)1096-9861(20000619)422:1<66::aid-cne5>3.0.co;2-2.

Kaneko, Maki, Charlotte Helfrich-Förster, and Jeffrey C. Hall. 1997. “Spatial and Temporal Expression of the *Period* and *Timeless* Genes in the Developing Nervous System of *Drosophila* : Newly Identified Pacemaker Candidates and Novel Features of Clock Gene Product Cycling.” *The Journal of Neuroscience* 17(17):6745–60. doi: 10.1523/JNEUROSCI.17-17-06745.1997.

Keegan, Kevin P., Suraj Pradhan, Ji-Ping Wang, and Ravi Allada. 2007. “Meta-Analysis of Drosophila Circadian Microarray Studies Identifies a Novel Set of Rhythmically Expressed Genes.” *PLoS Computational Biology* 3(11):e208. doi: 10.1371/journal.pcbi.0030208.

Kelber, Almut, and Miriam J. Henze. 2013. “Colour Vision: Parallel Pathways Intersect in Drosophila.” *Current Biology: CB* 23(23):R1043-1045. doi: 10.1016/j.cub.2013.10.025.

Khalsa, Sat Bir S., Megan E. Jewett, Christian Cajochen, and Charles A. Czeisler. 2003. “A Phase Response Curve to Single Bright Light Pulses in Human Subjects.” *The Journal of Physiology* 549(Pt 3):945–52. doi: 10.1113/jphysiol.2003.040477.

Kibelbek, J., D. C. Mitchell, J. M. Beach, and B. J. Litman. 1991. “Functional Equivalence of Metarhodopsin II and the Gt-Activating Form of Photolyzed Bovine Rhodopsin.” *Biochemistry* 30(27):6761–68. doi: 10.1021/bi00241a019.

Kim, Eun Young, Kiho Bae, Fanny S. Ng, Nick R. J. Glossop, Paul E. Hardin, and Isaac Edery. 2002. “Drosophila CLOCK Protein Is under Posttranscriptional Control and Influences Light-Induced Activity.” *Neuron* 34(1):69–81. doi: 10.1016/s0896-6273(02)00639-6.

Kim, Eun Young, and Isaac Edery. 2006. “Balance between DBT/CKIε Kinase and Protein Phosphatase Activities Regulate Phosphorylation and Stability of Drosophila CLOCK Protein.” *Proceedings of the National Academy of Sciences* 103(16):6178–83. doi: 10.1073/pnas.0511215103.

Kim, Woo Jae, Lily Yeh Jan, and Yuh Nung Jan. 2013. “A PDF/NPF Neuropeptide Signaling Circuitry of Male Drosophila Melanogaster Controls Rival-Induced Prolonged Mating.” *Neuron* 80(5):10.1016/j.neuron.2013.09.034. doi: 10.1016/j.neuron.2013.09.034.

King, Anna N., and Amita Sehgal. 2020. “Molecular and Circuit Mechanisms Mediating Circadian Clock Output in the Drosophila Brain.” *European Journal of Neuroscience* 51(1):268–81. doi: 10.1111/ejn.14092.

King, David P., Yaliang Zhao, Ashvin M. Sangoram, Lisa D. Wilsbacher, Minoru Tanaka, Marina P. Antoch, Thomas D. L. Steeves, Martha Hotz Vitaterna, Jon M. Kornhauser, Phillip L. Lowrey, Fred W. Turek, and Joseph S. Takahashi. 1997. “Positional Cloning of the Mouse Circadian Clock Gene.” *Cell* 89(4):641–53. doi: 10.1016/S0092-8674(00)80245-7.

Kiselev, A., and S. Subramaniam. 1994. “Activation and Regeneration of Rhodopsin in the Insect Visual Cycle.” *Science (New York, N.Y.)* 266(5189):1369–73. doi: 10.1126/science.7973725.

Kistenpfennig, Christa, Rudi Grebler, Maite Ogueta, Christiane Hermann-Luibl, Matthias Schlichting, Ralf Stanewsky, Pingkalai R. Senthilan, and Charlotte Helfrich-Förster. 2017. “A New Rhodopsin Influences Light-Dependent Daily Activity Patterns of Fruit Flies.” *Journal of Biological Rhythms* 32(5):406–22. doi: 10.1177/0748730417721826.

Kivimäe, Saul, Lino Saez, and Michael W. Young. 2008. “Activating PER Repressor through a DBT-Directed Phosphorylation Switch.” *PLOS Biology* 6(7):e183. doi: 10.1371/journal.pbio.0060183.

Klarsfeld, André, Sébastien Malpel, Christine Michard-Vanhée, Marie Picot, Elisabeth Chélot,

and François Rouyer. 2004. “Novel Features of Cryptochrome-Mediated Photoreception in the Brain Circadian Clock of Drosophila.” *Journal of Neuroscience* 24(6):1468–77. doi: 10.1523/JNEUROSCI.3661-03.2004.

Klose, Markus, Laura Duvall, Weihua Li, Xitong Liang, Chi Ren, Joe Henry Steinbach, and Paul H. Taghert. 2016. “Functional PDF Signaling in the Drosophila Circadian Neural Circuit Is Gated by Ral A-Dependent Modulation.” *Neuron* 90(4):781–94. doi: 10.1016/j.neuron.2016.04.002.

Kloss, Brian, Jeffrey L. Price, Lino Saez, Justin Blau, Adrian Rothenfluh, Cedric S. Wesley, and Michael W. Young. 1998. “The Drosophila Clock Gene Double-Time Encodes a Protein Closely Related to Human Casein Kinase Iε.” *Cell* 94(1):97–107. doi: 10.1016/S0092-8674(00)81225-8.

Kloss, Brian, Adrian Rothenfluh, Michael W. Young, and Lino Saez. 2001. “Phosphorylation of PERIOD Is Influenced by Cycling Physical Associations of DOUBLE-TIME, PERIOD, and TIMELESS in the Drosophila Clock.” *Neuron* 30(3):699–706. doi: 10.1016/S0896-6273(01)00320-8.

Ko, Gladys Y. P. 2020. “Circadian Regulation in the Retina: From Molecules to Network.” *European Journal of Neuroscience* 51(1):194–216. doi: 10.1111/ejn.14185.

Ko, Hyuk Wan, Jin Jiang, and Isaac Edery. 2002. “Role for Slimb in the Degradation of Drosophila Period Protein Phosphorylated by Doubletime.” *Nature* 420(6916):673–78. doi: 10.1038/nature01272.

Ko, Hyuk Wan, Eun Young Kim, Joanna Chiu, Jens T. Vanselow, Achim Kramer, and Isaac Edery. 2010. “A Hierarchical Phosphorylation Cascade That Regulates the Timing of PERIOD Nuclear Entry Reveals Novel Roles for Proline-Directed Kinases and GSK-3β/SGG in Circadian Clocks.” *Journal of Neuroscience* 30(38):12664–75. doi: 10.1523/JNEUROSCI.1586-10.2010.

Koh, Kyunghee, Xiangzhong Zheng, and Amita Sehgal. 2006. “JETLAG Resets the Drosophila Circadian Clock by Promoting Light-Induced Degradation of TIMELESS.” *Science* 312(5781):1809–12. doi: 10.1126/science.1124951.

Konopka, R. J., C. Pittendrigh, and D. Orr. 1989. “Reciprocal Behaviour Associated with

Altered Homeostasis and Photosensitivity of Drosophila Clock Mutants." *Journal of Neurogenetics* 6(1):1–10. doi: 10.3109/01677068909107096.

Konopka, Ronald J., and Seymour Benzer. 1971. "Clock Mutants of Drosophila Melanogaster." *Proceedings of the National Academy of Sciences of the United States of America* 68(9):2112–16.

Kumar, Vinod, ed. 2017. *Biological Timekeeping: Clocks, Rhythms and Behaviour*. New Delhi: Springer India.

Kume, Kazuhiko, Mark J. Zylka, Sathyanarayanan Sriram, Lauren P. Shearman, David R. Weaver, Xiaowei Jin, Elizabeth S. Maywood, Michael H. Hastings, and Steven M. Reppert. 1999. "MCRY1 and MCRY2 Are Essential Components of the Negative Limb of the Circadian Clock Feedback Loop." *Cell* 98(2):193–205. doi: 10.1016/S0092-8674(00)81014-4.

Kunst, Michael, Michael E. Hughes, Davide Raccuglia, Mario Felix, Michael Li, Gregory Barnett, Janelle Duah, and Michael N. Nitabach. 2014. "Calcitonin Gene-Related Peptide Neurons Mediate Sleep-Specific Circadian Output in Drosophila." *Current Biology: CB* 24(22):2652–64. doi: 10.1016/j.cub.2014.09.077.

Lamaze, Angélique, and Ralf Stanewsky. 2020. "DN1p or the 'Fluffy' Cerberus of Clock Outputs." *Frontiers in Physiology* 10:1540. doi: 10.3389/fphys.2019.01540.

Lamba, Pallavi, Diana Bilodeau-Wentworth, Patrick Emery, and Yong Zhang. 2014. "Morning and Evening Oscillators Cooperate to Reset Circadian Behavior in Response to Light Input." *Cell Reports* 7(3):601–8. doi: 10.1016/j.celrep.2014.03.044.

Lamba, Pallavi, Lauren E. Foley, and Patrick Emery. 2018. "Neural Network Interactions Modulate CRY-Dependent Photoresponses in *Drosophila*." *The Journal of Neuroscience* 38(27):6161–71. doi: 10.1523/JNEUROSCI.2259-17.2018.

Lear, Bridget C., C. Elaine Merrill, Jui-Ming Lin, Analyne Schroeder, Luoying Zhang, and Ravi Allada. 2005. "A G Protein-Coupled Receptor, Groom-of-PDF, Is Required for PDF Neuron Action in Circadian Behavior." *Neuron* 48(2):221–27. doi: 10.1016/j.neuron.2005.09.008.

Lear, Bridget C., Luoying Zhang, and Ravi Allada. 2009. “The Neuropeptide PDF Acts Directly on Evening Pacemaker Neurons to Regulate Multiple Features of Circadian Behavior” edited by E. Mignot. *PLoS Biology* 7(7):e1000154. doi: 10.1371/journal.pbio.1000154.

Lee, C., K. Bae, and I. Edery. 1999. “PER and TIM Inhibit the DNA Binding Activity of a Drosophila CLOCK-CYC/DBMAL1 Heterodimer without Disrupting Formation of the Heterodimer: A Basis for Circadian Transcription.” *Molecular and Cellular Biology* 19(8):5316–25. doi: 10.1128/MCB.19.8.5316.

Lee, Choogon, Kiho Bae, and Isaac Edery. 1998. “The Drosophila CLOCK Protein Undergoes Daily Rhythms in Abundance, Phosphorylation, and Interactions with the PER–TIM Complex.” *Neuron* 21(4):857–67. doi: 10.1016/S0896-6273(00)80601-7.

Lee, Choogon, Vaishali Parikh, Tomoko Itsukaichi, Kiho Bae, and Isaac Edery. 1996. “Resetting the Drosophila Clock by Photic Regulation of PER and a PER-TIM Complex.” *Science* 271(5256):1740–44. doi: 10.1126/science.271.5256.1740.

Lee, Gyunghee, Jae Hoon Bahn, and Jae H. Park. 2006. “Sex- and Clock-Controlled Expression of the Neuropeptide F Gene in Drosophila.” *Proceedings of the National Academy of Sciences* 103(33):12580–85. doi: 10.1073/pnas.0601171103.

Li, Meng-Tong, Li-Hui Cao, Na Xiao, Min Tang, Bowen Deng, Tian Yang, Taishi Yoshii, and Dong-Gen Luo. 2018. “Hub-Organized Parallel Circuits of Central Circadian Pacemaker Neurons for Visual Photoentrainment in Drosophila.” *Nature Communications* 9(1):4247. doi: 10.1038/s41467-018-06506-5.

Li, Yue, Fang Guo, James Shen, and Michael Rosbash. 2014. “PDF and CAMP Enhance PER Stability in Drosophila Clock Neurons.” *Proceedings of the National Academy of Sciences of the United States of America* 111(13):E1284-1290. doi: 10.1073/pnas.1402562111.

Liang, Xitong, Margaret C. W. Ho, Yajun Zhang, Yulong Li, Mark N. Wu, Timothy E. Holy, and Paul H. Taghert. 2019. “Morning and Evening Circadian Pacemakers Independently Drive Premotor Centers via a Specific Dopamine Relay.” *Neuron* 102(4):843-857.e4. doi: 10.1016/j.neuron.2019.03.028.

Liang, Xitong, Timothy E. Holy, and Paul H. Taghert. 2016. “Synchronous Drosophila

Circadian Pacemakers Display Nonsynchronous Ca^{2+} Rhythms in Vivo." *Science (New York, N.Y.)* 351(6276):976–81. doi: 10.1126/science.aad3997.

Liang, Xitong, Timothy E. Holy, and Paul H. Taghert. 2017. "A Series of Suppressive Signals within the Drosophila Circadian Neural Circuit Generates Sequential Daily Outputs." *Neuron* 94(6):1173-1189.e4. doi: 10.1016/j.neuron.2017.05.007.

Lim, Chunghun, Brian Y. Chung, Jena L. Pitman, Jermaine J. McGill, Suraj Pradhan, Jongbin Lee, Kevin P. Keegan, Joonho Choe, and Ravi Allada. 2007. "Clockwork Orange Encodes a Transcriptional Repressor Important for Circadian-Clock Amplitude in Drosophila." *Current Biology: CB* 17(12):1082–89. doi: 10.1016/j.cub.2007.05.039.

Lin, Changfan, Deniz Top, Craig C. Manahan, Michael W. Young, and Brian R. Crane. 2018. "Circadian Clock Activity of Cryptochrome Relies on Tryptophan-Mediated Photoreduction." *Proceedings of the National Academy of Sciences* 115(15):3822–27. doi: 10.1073/pnas.1719376115.

Lin, Fang-Ju, Wei Song, Elizabeth Meyer-Bernstein, Nirinjini Naidoo, and Amita Sehgal. 2001. "Photic Signaling by Cryptochrome in the Drosophila Circadian System." *Molecular and Cellular Biology* 21(21):7287–94. doi: 10.1128/MCB.21.21.7287-7294.2001.

Lin, Jui-Ming, Analyne Schroeder, and Ravi Allada. 2005. "In Vivo Circadian Function of Casein Kinase 2 Phosphorylation Sites in Drosophila PERIOD." *Journal of Neuroscience* 25(48):11175–83. doi: 10.1523/JNEUROSCI.2159-05.2005.

Lin, Yiing, Gary D. Stormo, and Paul H. Taghert. 2004. "The Neuropeptide Pigment-Dispersing Factor Coordinates Pacemaker Interactions in the Drosophila Circadian System." *Journal of Neuroscience* 24(36):7951–57. doi: 10.1523/JNEUROSCI.2370-04.2004.

Liu, Bin, Hongtao Liu, Dongping Zhong, and Chentao Lin. 2010. "Searching for a Photocycle of the Cryptochrome Photoreceptors." *Current Opinion in Plant Biology* 13(5):578–86. doi: 10.1016/j.pbi.2010.09.005.

Liu, X., Lj Zwiebel, D. Hinton, S. Benzer, Jc Hall, and M. Rosbash. 1992. "The Period Gene Encodes a Predominantly Nuclear Protein in Adult Drosophila." *The Journal of*

Neuroscience 12(7):2735–44. doi: 10.1523/JNEUROSCI.12-07-02735.1992.

Liu, Y., M. Merrow, J. J. Loros, and J. C. Dunlap. 1998. "How Temperature Changes Reset a Circadian Oscillator." *Science (New York, N.Y.)* 281(5378):825–29. doi: 10.1126/science.281.5378.825.

Lucas, Robert J., Gurprit S. Lall, Annette E. Allen, and Timothy M. Brown. 2012. "Chapter 1 - How Rod, Cone, and Melanopsin Photoreceptors Come Together to Enlighten the Mammalian Circadian Clock." Pp. 1–18 in *Progress in Brain Research*. Vol. 199, *The Neurobiology of Circadian Timing*, edited by A. Kalsbeek, M. Merrow, T. Roenneberg, and R. G. Foster. Elsevier.

Ma, Dingbang, Dariusz Przybylski, Katharine C. Abruzzi, Matthias Schlichting, Qunlong Li, Xi Long, and Michael Rosbash. 2021. "A Transcriptomic Taxonomy of Drosophila Circadian Neurons around the Clock" edited by A. Sehgal and U. Banerjee. *ELife* 10:e63056. doi: 10.7554/eLife.63056.

Malpel, Sébastien, André Klarsfeld, and François Rouyer. 2002. "Larval Optic Nerve and Adult Extra-Retinal Photoreceptors Sequentially Associate with Clock Neurons during Drosophila Brain Development." *Development* 129(6):1443–53. doi: 10.1242/dev.129.6.1443.

Martinek, Sebastian, Susan Inonog, Armen S. Manoukian, and Michael W. Young. 2001. "A Role for the Segment Polarity Gene Shaggy/GSK-3 in the Drosophila Circadian Clock." *Cell* 105(6):769–79. doi: 10.1016/S0092-8674(01)00383-X.

Matsumoto, Akira, Maki Ukai-Tadenuma, Rikuhiro G. Yamada, Jerry Houl, Kenichiro D. Uno, Takeya Kasukawa, Brigitte Dauwalder, Taichi Q. Itoh, Kuniaki Takahashi, Ryu Ueda, Paul E. Hardin, Teiichi Tanimura, and Hiroki R. Ueda. 2007. "A Functional Genomics Strategy Reveals Clockwork Orange as a Transcriptional Regulator in the Drosophila Circadian Clock." *Genes & Development* 21(13):1687–1700. doi: 10.1101/gad.1552207.

Mazzoni, Esteban O., Claude Desplan, and Justin Blau. 2005. "Circadian Pacemaker Neurons Transmit and Modulate Visual Information to Control a Rapid Behavioral Response." *Neuron* 45(2):293–300. doi: 10.1016/j.neuron.2004.12.038.

McDonald, M. J., and M. Rosbash. 2001. "Microarray Analysis and Organization of Circadian

Gene Expression in Drosophila." *Cell* 107(5):567–78. doi: 10.1016/s0092-8674(01)00545-1.

McDonald, Michael J., Michael Rosbash, and Patrick Emery. 2001. "Wild-Type Circadian Rhythmicity Is Dependent on Closely Spaced E Boxes in the Drosophila TimelessPromoter." *Molecular and Cellular Biology* 21(4):1207–17. doi: 10.1128/MCB.21.4.1207-1217.2001.

Meiselman, Matthew R., Michael H. Alpert, Xinyue Cui, Jamien Shea, Ian Gregg, Marco Gallio, and Nilay Yapici. 2022. "Recovery from Cold-Induced Reproductive Dormancy Is Regulated by Temperature-Dependent AstC Signaling." *Current Biology* 32(6):1362-1375.e8. doi: 10.1016/j.cub.2022.01.061.

Meissner, Rose-Anne, Valerie L. Kilman, Jui-Ming Lin, and Ravi Allada. 2008. "TIMELESS Is an Important Mediator of CK2 Effects on Circadian Clock Function In Vivo." *Journal of Neuroscience* 28(39):9732–40. doi: 10.1523/JNEUROSCI.0840-08.2008.

Mendoza, J. 2007. "Circadian Clocks: Setting Time by Food." *Journal of Neuroendocrinology* 19(2):127–37. doi: 10.1111/j.1365-2826.2006.01510.x.

Mertens, Inge, Anick Vandingenen, Erik C. Johnson, Orie T. Shafer, W. Li, J. S. Trigg, Arnold De Loof, Liliane Schoofs, and Paul H. Taghert. 2005. "PDF Receptor Signaling in Drosophila Contributes to Both Circadian and Geotactic Behaviors." *Neuron* 48(2):213–19. doi: 10.1016/j.neuron.2005.09.009.

Meyer, Pablo, Lino Saez, and Michael W. Young. 2006. "PER-TIM Interactions in Living Drosophila Cells: An Interval Timer for the Circadian Clock." *Science (New York, N.Y.)* 311(5758):226–29. doi: 10.1126/science.1118126.

Millar, A. J. 2003. "Input Signals to the Plant Circadian Clock." *Journal of Experimental Botany* 55(395):277–83. doi: 10.1093/jxb/erh034.

Mismer, D., W. M. Michael, T. R. Laverty, and G. M. Rubin. 1988. "Analysis of the Promoter of the Rh2 Opsin Gene in Drosophila Melanogaster." *Genetics* 120(1):173–80. doi: 10.1093/genetics/120.1.173.

Mizrak, Dogukan, Marc Ruben, Gabrielle N. Myers, Kahn Rhrissorrakrai, Kristin C. Gunsalus,

and Justin Blau. 2012. “Electrical Activity Can Impose Time of Day on the Circadian Transcriptome of Pacemaker Neurons.” *Current Biology* 22(20):1871–80. doi: 10.1016/j.cub.2012.07.070.

Mohawk, Jennifer A., Carla B. Green, and Joseph S. Takahashi. 2012. “CENTRAL AND PERIPHERAL CIRCADIAN CLOCKS IN MAMMALS.” *Annual Review of Neuroscience* 35:445–62. doi: 10.1146/annurev-neuro-060909-153128.

Montell, C., K. Jones, E. Hafen, and G. Rubin. 1985. “Rescue of the Drosophila Phototransduction Mutation Trp by Germline Transformation.” *Science (New York, N.Y.)* 230(4729):1040–43. doi: 10.1126/science.3933112.

Montell, C., and G. M. Rubin. 1989. “Molecular Characterization of the Drosophila Trp Locus: A Putative Integral Membrane Protein Required for Phototransduction.” *Neuron* 2(4):1313–23. doi: 10.1016/0896-6273(89)90069-x.

Montell, Craig. 2012. “Drosophila Visual Transduction.” *Trends in Neurosciences* 35(6):356–63. doi: 10.1016/j.tins.2012.03.004.

Moore, Robert Y., and Victor B. Eichler. 1972. “Loss of a Circadian Adrenal Corticosterone Rhythm Following Suprachiasmatic Lesions in the Rat.” *Brain Research* 42(1):201–6. doi: 10.1016/0006-8993(72)90054-6.

Morante, Javier, and Claude Desplan. 2008. “The Color-Vision Circuit in the Medulla of Drosophila.” *Current Biology: CB* 18(8):553–65. doi: 10.1016/j.cub.2008.02.075.

Mrosovsky, N. 1988. “Phase Response Curves for Social Entrainment.” *Journal of Comparative Physiology. A, Sensory, Neural, and Behavioral Physiology* 162(1):35–46. doi: 10.1007/BF01342701.

Muraro, N. I., N. Pírez, and M. F. Ceriani. 2013. “The Circadian System: Plasticity at Many Levels.” *Neuroscience* 247:280–93. doi: 10.1016/j.neuroscience.2013.05.036.

Muraro, Nara I., and M. Fernanda Ceriani. 2015. “Acetylcholine from Visual Circuits Modulates the Activity of Arousal Neurons in Drosophila.” *Journal of Neuroscience* 35(50):16315–27. doi: 10.1523/JNEUROSCI.1571-15.2015.

Myers, M. P., K. Wager-Smith, A. Rothenfluh-Hilfiker, and M. W. Young. 1996. “Light-

Induced Degradation of TIMELESS and Entrainment of the Drosophila Circadian Clock." *Science (New York, N.Y.)* 271(5256):1736–40. doi: 10.1126/science.271.5256.1736.

Myers, Michael P., Karen Wager-Smith, Cedric S. Wesley, Michael W. Young, and Amita Sehgal. 1995. "Positional Cloning and Sequence Analysis of the Drosophila Clock Gene, Timeless." *Science* 270(5237):805–8. doi: 10.1126/science.270.5237.805.

Naidoo, Nirinjini, Wei Song, Melissa Hunter-Ensor, and Amita Sehgal. 1999. "A Role for the Proteasome in the Light Response of the Timeless Clock Protein." *Science* 285(5434):1737–41. doi: 10.1126/science.285.5434.1737.

Nash, Howard A., Robert L. Scott, Bridget C. Lear, and Ravi Allada. 2002. "An Unusual Cation Channel Mediates Photic Control of Locomotion in Drosophila." *Current Biology* 12(24):2152–58. doi: 10.1016/S0960-9822(02)01358-1.

Nériec, Nathalie, and Claude Desplan. 2016. "From The Eye To The Brain: Development Of The Drosophila Visual System." *Current Topics in Developmental Biology* 116:247–71. doi: 10.1016/bs.ctdb.2015.11.032.

Ni, Jinfei D., Lisa S. Baik, Todd C. Holmes, and Craig Montell. 2017. "A Rhodopsin in the Brain Functions in Circadian Photoentrainment in Drosophila." *Nature* 545(7654):340–44. doi: 10.1038/nature22325.

Niemeyer, B. A., E. Suzuki, K. Scott, K. Jalink, and C. S. Zuker. 1996. "The Drosophila Light-Activated Conductance Is Composed of the Two Channels TRP and TRPL." *Cell* 85(5):651–59. doi: 10.1016/s0092-8674(00)81232-5.

Nitabach, Michael N., Justin Blau, and Todd C. Holmes. 2002. "Electrical Silencing of Drosophila Pacemaker Neurons Stops the Free-Running Circadian Clock." *Cell* 109(4):485–95. doi: 10.1016/S0092-8674(02)00737-7.

Ogueta, Maite, Roger C. Hardie, and Ralf Stanewsky. 2018. "Non-Canonical Phototransduction Mediates Synchronization of the Drosophila Melanogaster Circadian Clock and Retinal Light Responses." *Current Biology* 28(11):1725-1735.e3. doi: 10.1016/j.cub.2018.04.016.

Ouyang, Yan, Carol R. Andersson, Takao Kondo, Susan S. Golden, and Carl Hirschie Johnson.

1998. “Resonating Circadian Clocks Enhance Fitness in Cyanobacteria.” *Proceedings of the National Academy of Sciences* 95(15):8660–64. doi: 10.1073/pnas.95.15.8660.

Özkaya, Özge, and Ezio Rosato. 2012. “The Circadian Clock of the Fly: A Neurogenetics Journey Through Time.” Pp. 79–123 in *Advances in Genetics*. Vol. 77, *Gene-Environment Interplay*, edited by M. B. Sokolowski and S. F. Goodwin. Academic Press.

Ozturk, Nuri, Christopher P. Selby, Yunus Annayev, Dongping Zhong, and Aziz Sancar. 2011. “Reaction Mechanism of Drosophila Cryptochrome.” *Proceedings of the National Academy of Sciences* 108(2):516–21. doi: 10.1073/pnas.1017093108.

Ozturk, Nuri, Christopher P. Selby, Dongping Zhong, and Aziz Sancar. 2014. “Mechanism of Photosignaling by Drosophila Cryptochrome: ROLE OF THE REDOX STATUS OF THE FLAVIN CHROMOPHORE *♦.” *Journal of Biological Chemistry* 289(8):4634–42. doi: 10.1074/jbc.M113.542498.

Öztürk, Nuri, Sang-Hun Song, Christopher P. Selby, and Aziz Sancar. 2008. “Animal Type 1 Cryptochromes: ANALYSIS OF THE REDOX STATE OF THE FLAVIN COFACTOR BY SITE-DIRECTED MUTAGENESIS *.” *Journal of Biological Chemistry* 283(6):3256–63. doi: 10.1074/jbc.M708612200.

Pagni, Manuel, Väinö Haikala, Vitus Oberhauser, Patrik B. Meyer, Dierk F. Reiff, and Christopher Schnaitmann. 2021. “Interaction of ‘Chromatic’ and ‘Achromatic’ Circuits in Drosophila Color Opponent Processing.” *Current Biology: CB* 31(8):1687-1698.e4. doi: 10.1016/j.cub.2021.01.105.

Park, Jae H., Charlotte Helfrich-Förster, Gyunghee Lee, Li Liu, Michael Rosbash, and Jeffrey C. Hall. 2000. “Differential Regulation of Circadian Pacemaker Output by Separate Clock Genes in Drosophila.” *Proceedings of the National Academy of Sciences* 97(7):3608–13. doi: 10.1073/pnas.97.7.3608.

Patke, Alina, Michael W. Young, and Sofia Axelrod. 2020. “Molecular Mechanisms and Physiological Importance of Circadian Rhythms.” *Nature Reviews Molecular Cell Biology* 21(2):67–84. doi: 10.1038/s41580-019-0179-2.

Paulk, Angelique, S. Sean Millard, and Bruno Van Swinderen. 2013. “Vision in *Drosophila* : Seeing the World Through a Model’s Eyes.” *Annual Review of Entomology* 58(1):313–32.

doi: 10.1146/annurev-ento-120811-153715.

Peng, Ying, Dan Stoleru, Joel D. Levine, Jeffrey C. Hall, and Michael Rosbash. 2003. "Drosophila Free-Running Rhythms Require Intercellular Communication." *PLOS Biology* 1(1):e13. doi: 10.1371/journal.pbio.0000013.

Peschel, Nicolai, Ko Fan Chen, Gisela Szabo, and Ralf Stanewsky. 2009. "Light-Dependent Interactions between the Drosophila Circadian Clock Factors Cryptochrome, Jetlag, and Timeless." *Current Biology* 19(3):241–47. doi: 10.1016/j.cub.2008.12.042.

Phillips, A. M., A. Bull, and L. E. Kelly. 1992. "Identification of a Drosophila Gene Encoding a Calmodulin-Binding Protein with Homology to the Trp Phototransduction Gene." *Neuron* 8(4):631–42. doi: 10.1016/0896-6273(92)90085-r.

Picot, Marie, Paola Cusumano, André Klarsfeld, Ryu Ueda, and François Rouyer. 2007. "Light Activates Output from Evening Neurons and Inhibits Output from Morning Neurons in the Drosophila Circadian Clock" edited by U. Schibler. *PLoS Biology* 5(11):e315. doi: 10.1371/journal.pbio.0050315.

Pittendrigh, C. S. 1960. "Circadian Rhythms and the Circadian Organization of Living Systems." *Cold Spring Harbor Symposia on Quantitative Biology* 25:159–84. doi: 10.1101/sqb.1960.025.01.015.

Pittendrigh, C. S. 1993. "Temporal Organization: Reflections of a Darwinian Clock-Watcher." *Annual Review of Physiology* 55:16–54. doi: 10.1146/annurev.ph.55.030193.000313.

Pittendrigh, C. S., and D. H. Minis. 1972. "Circadian Systems: Longevity as a Function of Circadian Resonance in Drosophila Melanogaster." *Proceedings of the National Academy of Sciences of the United States of America* 69(6):1537–39. doi: 10.1073/pnas.69.6.1537.

Pittendrigh, Colin S. 1954. "ON TEMPERATURE INDEPENDENCE IN THE CLOCK SYSTEM CONTROLLING EMERGENCE TIME IN DROSOPHILA*." *Proceedings of the National Academy of Sciences of the United States of America* 40(10):1018–29.

Pittendrigh, Colin S. 1981. "Circadian Systems: Entrainment." Pp. 95–124 in *Biological Rhythms*, edited by J. Aschoff. Boston, MA: Springer US.

Pittendrigh, Colin S., and Serge Daan. 1976. "A Functional Analysis of Circadian Pacemakers

in Nocturnal Rodents." *Journal of Comparative Physiology* 106(3):333–55. doi: 10.1007/BF01417860.

Pollack, I., and A. Hofbauer. 1991. "Histamine-like Immunoreactivity in the Visual System and Brain of Drosophila Melanogaster." *Cell and Tissue Research* 266(2):391–98. doi: 10.1007/BF00318195.

Pollock, John A., and Seymour Benzer. 1988. "Transcript Localization of Four Opsin Genes in the Three Visual Organs of Drosophila; RH2 Is Ocellus Specific." *Nature* 333(6175):779–82. doi: 10.1038/333779a0.

Preitner, Nicolas, Francesca Damiola, Luis Lopez-Molina, Joszef Zakany, Denis Duboule, Urs Albrecht, and Ueli Schibler. 2002. "The Orphan Nuclear Receptor REV-ERBalpha Controls Circadian Transcription within the Positive Limb of the Mammalian Circadian Oscillator." *Cell* 110(2):251–60. doi: 10.1016/s0092-8674(02)00825-5.

Price, J. L., M. E. Dembinska, M. W. Young, and M. Rosbash. 1995. "Suppression of PERIOD Protein Abundance and Circadian Cycling by the Drosophila Clock Mutation Timeless." *The EMBO Journal* 14(16):4044–49. doi: 10.1002/j.1460-2075.1995.tb00075.x.

Price, Jeffrey L., Justin Blau, Adrian Rothenfluh, Marla Abodeely, Brian Kloss, and Michael W. Young. 1998. "Double-Time Is a Novel Drosophila Clock Gene That Regulates PERIOD Protein Accumulation." *Cell* 94(1):83–95. doi: 10.1016/S0092-8674(00)81224-6.

Ralph, Martin R., Russell G. Foster, Fred C. Davis, and Michael Menaker. 1990. "Transplanted Suprachiasmatic Nucleus Determines Circadian Period." *Science* 247(4945):975–78. doi: 10.1126/science.2305266.

Reddy, P., W. A. Zehring, D. A. Wheeler, V. Pirrotta, C. Hadfield, J. C. Hall, and M. Rosbash. 1984. "Molecular Analysis of the Period Locus in Drosophila Melanogaster and Identification of a Transcript Involved in Biological Rhythms." *Cell* 38(3):701–10. doi: 10.1016/0092-8674(84)90265-4.

Redlin, U., and N. Mrosovsky. 1999. "Masking by Light in Hamsters with SCN Lesions." *Journal of Comparative Physiology. A, Sensory, Neural, and Behavioral Physiology* 184(4):439–48. doi: 10.1007/s003590050343.

Reinhard, Nils, Enrico Bertolini, Aika Saito, Manabu Sekiguchi, Taishi Yoshii, Dirk Rieger, and Charlotte Helfrich-Förster. 2022. "The Lateral Posterior Clock Neurons of Drosophila Melanogaster Express Three Neuropeptides and Have Multiple Connections within the Circadian Clock Network and Beyond." *Journal of Comparative Neurology* 530(9):1507–29. doi: 10.1002/cne.25294.

Reinhard, Nils, Frank K. Schubert, Enrico Bertolini, Nicolas Hagedorn, Giulia Manoli, Manabu Sekiguchi, Taishi Yoshii, Dirk Rieger, and Charlotte Helfrich-Förster. 2022. "The Neuronal Circuit of the Dorsal Circadian Clock Neurons in Drosophila Melanogaster." *Frontiers in Physiology* 13:886432. doi: 10.3389/fphys.2022.886432.

Renn, S. C., J. H. Park, M. Rosbash, J. C. Hall, and P. H. Taghert. 1999. "A Pdf Neuropeptide Gene Mutation and Ablation of PDF Neurons Each Cause Severe Abnormalities of Behavioral Circadian Rhythms in Drosophila." *Cell* 99(7):791–802. doi: 10.1016/s0092-8674(00)81676-1.

Rensing, Ludger, and Peter Ruoff. 2002. "Temperature Effect on Entrainment, Phase Shifting, and Amplitude of Circadian Clocks and Its Molecular Bases." *Chronobiology International* 19(5):807–64. doi: 10.1081/cbi-120014569.

Reppert, Steven M., and David R. Weaver. 2001. "Molecular Analysis of Mammalian Circadian Rhythms." *Annual Review of Physiology* 63(1):647–76. doi: 10.1146/annurev.physiol.63.1.647.

Reppert, Steven M., and David R. Weaver. 2002. "Coordination of Circadian Timing in Mammals." *Nature* 418(6901):935–41. doi: 10.1038/nature00965.

Rieger, Dirk, Ralf Stanewsky, and Charlotte Helfrich-Förster. 2003. "Cryptochrome, Compound Eyes, Hofbauer-Buchner Eyelets, and Ocelli Play Different Roles in the Entrainment and Masking Pathway of the Locomotor Activity Rhythm in the Fruit Fly Drosophila Melanogaster." *Journal of Biological Rhythms* 18(5):377–91. doi: 10.1177/0748730403256997.

Rieger, Dirk, Corinna Wülbeck, Francois Rouyer, and Charlotte Helfrich-Förster. 2009. "Period Gene Expression in Four Neurons Is Sufficient for Rhythmic Activity of Drosophila Melanogaster under Dim Light Conditions." *Journal of Biological Rhythms*

24(4):271–82. doi: 10.1177/0748730409338508.

Roenneberg, Till, Serge Daan, and Martha Merrow. 2003. “The Art of Entrainment.” *Journal of Biological Rhythms* 18(3):183–94. doi: 10.1177/0748730403018003001.

Roenneberg, Till, and Russell G. Foster. 1997. “Twilight Times: Light and the Circadian System.” *Photochemistry and Photobiology* 66(5):549–61. doi: 10.1111/j.1751-1097.1997.tb03188.x.

Roenneberg, Till, and Martha Merrow. 2016. “The Circadian Clock and Human Health.” *Current Biology: CB* 26(10):R432-443. doi: 10.1016/j.cub.2016.04.011.

Rothenfluh, Adrian, Michael W. Young, and Lino Saez. 2000. “A TIMELESS-Independent Function for PERIOD Proteins in the Drosophila Clock.” *Neuron* 26(2):505–14. doi: 10.1016/S0896-6273(00)81182-4.

Rutila, Joan E., Vipin Suri, Myai Le, W. Venus So, Michael Rosbash, and Jeffrey C. Hall. 1998. “CYCLE Is a Second BHLH-PAS Clock Protein Essential for Circadian Rhythmicity and Transcription of Drosophila Period and Timeless.” *Cell* 93(5):805–14. doi: 10.1016/S0092-8674(00)81441-5.

Sabat, Debabrat, Subhashree Priyadarsini, and Monalisa Mishra. 2017. “Understanding the Structural and Developmental Aspect of Simple Eye of Drosophila: The Ocelli.” *Journal of Cell Signaling* 01(02). doi: 10.4172/2576-1471.1000109.

Saez, L., P. Meyer, and M. W. Young. 2007. “A PER/TIM/DBT Interval Timer for Drosophila’s Circadian Clock.” *Cold Spring Harbor Symposia on Quantitative Biology* 72:69–74. doi: 10.1101/sqb.2007.72.034.

Saez, L., and M. W. Young. 1996. “Regulation of Nuclear Entry of the Drosophila Clock Proteins Period and Timeless.” *Neuron* 17(5):911–20. doi: 10.1016/s0896-6273(00)80222-6.

Saez, Lino, Mary Derasmo, Pablo Meyer, J. Stieglitz, and Michael W. Young. 2011. “A Key Temporal Delay in the Circadian Cycle of Drosophila Is Mediated by a Nuclear Localization Signal in the Timeless Protein.” *Genetics* 188(3):591–600. doi: 10.1534/genetics.111.127225.

Saint-Charles, Alexandra, Christine Michard-Vanhée, Faredin Alejevski, Elisabeth Chélot, Antoine Boivin, and François Rouyer. 2016. "Four of the Six Drosophila Rhodopsin-Expressing Photoreceptors Can Mediate Circadian Entrainment in Low Light: Rhodopsin-Dependent Clock Synchronization." *Journal of Comparative Neurology* 524(14):2828–44. doi: 10.1002/cne.23994.

Salcedo, E., A. Huber, S. Henrich, L. V. Chadwell, W. H. Chou, R. Paulsen, and S. G. Britt. 1999. "Blue- and Green-Absorbing Visual Pigments of Drosophila: Ectopic Expression and Physiological Characterization of the R8 Photoreceptor Cell-Specific Rh5 and Rh6 Rhodopsins." *The Journal of Neuroscience: The Official Journal of the Society for Neuroscience* 19(24):10716–26. doi: 10.1523/JNEUROSCI.19-24-10716.1999.

Sancer, Gizem, and Mathias F. Wernet. 2021. "The Development and Function of Neuronal Subtypes Processing Color and Skylight Polarization in the Optic Lobes of Drosophila Melanogaster." *Arthropod Structure & Development* 61:101012. doi: 10.1016/j.asd.2020.101012.

Sarthy, P. Vijay. 1991. "Histamine: A Neurotransmitter Candidate for Drosophila Photoreceptors." *Journal of Neurochemistry* 57(5):1757–68. doi: 10.1111/j.1471-4159.1991.tb06378.x.

Sathyanarayanan, Sriram, Xiangzhong Zheng, Rui Xiao, and Amita Sehgal. 2004. "Posttranslational Regulation of Drosophila PERIOD Protein by Protein Phosphatase 2A." *Cell* 116(4):603–15. doi: 10.1016/S0092-8674(04)00128-X.

Sato, Trey K., Satchidananda Panda, Loren J. Miraglia, Teresa M. Reyes, Radu D. Rudic, Peter McNamara, Kinnery A. Naik, Garret A. FitzGerald, Steve A. Kay, and John B. Hogenesch. 2004. "A Functional Genomics Strategy Reveals Rora as a Component of the Mammalian Circadian Clock." *Neuron* 43(4):527–37. doi: 10.1016/j.neuron.2004.07.018.

Sato, Trey K., Rikuhiro G. Yamada, Hideki Ukai, Julie E. Baggs, Loren J. Miraglia, Tetsuya J. Kobayashi, David K. Welsh, Steve A. Kay, Hiroki R. Ueda, and John B. Hogenesch. 2006. "Feedback Repression Is Required for Mammalian Circadian Clock Function." *Nature Genetics* 38(3):312–19. doi: 10.1038/ng1745.

Scheffer, Louis K., C. Shan Xu, Michal Januszewski, Zhiyuan Lu, Shin-ya Takemura, Kenneth

J. Hayworth, Gary B. Huang, Kazunori Shinomiya, Jeremy Maitlin-Shepard, Stuart Berg, Jody Clements, Philip M. Hubbard, William T. Katz, Lowell Umayam, Ting Zhao, David Ackerman, Tim Blakely, John Bogovic, Tom Dolafi, Dagmar Kainmueller, Takashi Kawase, Khaled A. Khairy, Laramie Leavitt, Peter H. Li, Larry Lindsey, Nicole Neubarth, Donald J. Olbris, Hideo Otsuna, Eric T. Trautman, Masayoshi Ito, Alexander S. Bates, Jens Goldammer, Tanya Wolff, Robert Svirskas, Philipp Schlegel, Erika Neace, Christopher J. Knecht, Chelsea X. Alvarado, Dennis A. Bailey, Samantha Ballinger, Jolanta A. Borycz, Brandon S. Canino, Natasha Cheatham, Michael Cook, Marisa Dreher, Octave Duclos, Bryon Eubanks, Kelli Fairbanks, Samantha Finley, Nora Forknall, Audrey Francis, Gary Patrick Hopkins, Emily M. Joyce, SungJin Kim, Nicole A. Kirk, Julie Kovalyak, Shirley A. Lauchie, Alanna Lohff, Charli Maldonado, Emily A. Manley, Sari McLin, Caroline Mooney, Miatta Ndama, Omotara Ogundeyi, Nneoma Okeoma, Christopher Ordish, Nicholas Padilla, Christopher M. Patrick, Tyler Paterson, Elliott E. Phillips, Emily M. Phillips, Neha Rampally, Caitlin Ribeiro, Madelaine K. Robertson, Jon Thomson Rymer, Sean M. Ryan, Megan Sammons, Anne K. Scott, Ashley L. Scott, Aya Shinomiya, Claire Smith, Kelsey Smith, Natalie L. Smith, Margaret A. Sobeski, Alia Suleiman, Jackie Swift, Satoko Takemura, Iris Talebi, Dorota Tarnogorska, Emily Tenshaw, Temour Tokhi, John J. Walsh, Tansy Yang, Jane Anne Horne, Feng Li, Ruchi Parekh, Patricia K. Rivlin, Vivek Jayaraman, Marta Costa, Gregory SXE Jefferis, Kei Ito, Stephan Saalfeld, Reed George, Ian A. Meinertzhagen, Gerald M. Rubin, Harald F. Hess, Viren Jain, and Stephen M. Plaza. 2020. “A Connectome and Analysis of the Adult Drosophila Central Brain” edited by E. Marder, M. B. Eisen, J. Pipkin, and C. Q. Doe. *ELife* 9:e57443. doi: 10.7554/eLife.57443.

Schibler, Ueli, and Paolo Sassone-Corsi. 2002. “A Web of Circadian Pacemakers.” *Cell* 111(7):919–22. doi: 10.1016/s0092-8674(02)01225-4.

Schlichting, M., P. Menegazzi, K. R. Lelito, Z. Yao, E. Buhl, E. Dalla Benetta, A. Bahle, J. Denike, J. J. Hodge, C. Helfrich-Forster, and O. T. Shafer. 2016. “A Neural Network Underlying Circadian Entrainment and Photoperiodic Adjustment of Sleep and Activity in Drosophila.” *Journal of Neuroscience* 36(35):9084–96. doi: 10.1523/JNEUROSCI.0992-16.2016.

Schlichting, M., P. Menegazzi, M. Rosbash, and C. Helfrich-Förster. 2019. “A Distinct Visual Pathway Mediates High Light Intensity Adaptation of the Circadian Clock in *Drosophila*.”

The Journal of Neuroscience 1497–18. doi: 10.1523/JNEUROSCI.1497-18.2018.

Schlichting, Matthias. 2020. "Entrainment of the Drosophila Clock by the Visual System." *Neuroscience Insights* 15:2633105520903708. doi: 10.1177/2633105520903708.

Schlichting, Matthias, Madelen M. Díaz, Jason Xin, and Michael Rosbash. 2019. "Neuron-Specific Knockouts Indicate the Importance of Network Communication to Drosophila Rhythmicity" edited by A. Sehgal and C. Dulac. *ELife* 8:e48301. doi: 10.7554/eLife.48301.

Schlichting, Matthias, Rudi Grebler, Pamela Menegazzi, and Charlotte Helfrich-Förster. 2015. "Twilight Dominates Over Moonlight in Adjusting Drosophila's Activity Pattern." *Journal of Biological Rhythms* 30(2):117–28. doi: 10.1177/0748730415575245.

Schlichting, Matthias, Rudi Grebler, Nicolai Peschel, Taishi Yoshii, and Charlotte Helfrich-Förster. 2014. "Moonlight Detection by Drosophila's Endogenous Clock Depends on Multiple Photopigments in the Compound Eyes." *Journal of Biological Rhythms* 29(2):75–86. doi: 10.1177/0748730413520428.

Schlichting, Matthias, Patrick Weidner, Madelen Diaz, Pamela Menegazzi, Elena Dalla Benetta, Charlotte Helfrich-Förster, and Michael Rosbash. 2019. "Light-Mediated Circuit Switching in the Drosophila Neuronal Clock Network." *Current Biology* 29(19):3266-3276.e3. doi: 10.1016/j.cub.2019.08.033.

Schnaitmann, Christopher, Christian Garbers, Thomas Wachtler, and Hiromu Tanimoto. 2013. "Color Discrimination with Broadband Photoreceptors." *Current Biology: CB* 23(23):2375–82. doi: 10.1016/j.cub.2013.10.037.

Schnaitmann, Christopher, Väinö Haikala, Eva Abraham, Vitus Oberhauser, Thomas Thestrup, Oliver Griesbeck, and Dierk F. Reiff. 2018. "Color Processing in the Early Visual System of Drosophila." *Cell* 172(1–2):318-330.e18. doi: 10.1016/j.cell.2017.12.018.

Schnaitmann, Christopher, Manuel Pagni, and Dierk F. Reiff. 2020. "Color Vision in Insects: Insights from Drosophila." *Journal of Comparative Physiology. A, Neuroethology, Sensory, Neural, and Behavioral Physiology* 206(2):183–98. doi: 10.1007/s00359-019-01397-3.

Schubert, Frank K., Nicolas Hagedorn, Taishi Yoshii, Charlotte Helfrich-Förster, and Dirk Rieger. 2018. "Neuroanatomical Details of the Lateral Neurons of Drosophila Melanogaster Support Their Functional Role in the Circadian System." *Journal of Comparative Neurology* 526(7):1209–31. doi: 10.1002/cne.24406.

Scott, K., A. Becker, Y. Sun, R. Hardy, and C. Zuker. 1995. "Gq Alpha Protein Function in Vivo: Genetic Dissection of Its Role in Photoreceptor Cell Physiology." *Neuron* 15(4):919–27. doi: 10.1016/0896-6273(95)90182-5.

Sehadova, Hana, Franz T. Glaser, Carla Gentile, Alekos Simoni, Astrid Giesecke, Joerg T. Albert, and Ralf Stanewsky. 2009. "Temperature Entrainment of Drosophila's Circadian Clock Involves the Gene Nocte and Signaling from Peripheral Sensory Tissues to the Brain." *Neuron* 64(2):251–66. doi: 10.1016/j.neuron.2009.08.026.

Sehgal, A., J. L. Price, B. Man, and M. W. Young. 1994. "Loss of Circadian Behavioral Rhythms and per RNA Oscillations in the Drosophila Mutant Timeless." *Science (New York, N.Y.)* 263(5153):1603–6. doi: 10.1126/science.8128246.

Sehgal, Amita, Adrian Rothenfluh-Hilfiker, Melissa Hunter-Ensor, Yifeng Chen, Michael P. Myers, and Michael W. Young. 1995. "Rhythmic Expression of Timeless: A Basis for Promoting Circadian Cycles in Period Gene Autoregulation." *Science* 270(5237):808–10. doi: 10.1126/science.270.5237.808.

Seluzicki, Adam, Matthieu Flourakis, Elzbieta Kula-Eversole, Luoying Zhang, Valerie Kilman, and Ravi Allada. 2014. "Dual PDF Signaling Pathways Reset Clocks Via TIMELESS and Acutely Excite Target Neurons to Control Circadian Behavior." *PLOS Biology* 12(3):e1001810. doi: 10.1371/journal.pbio.1001810.

Senthilan, Pingkalai R., Rudi Grebler, Nils Reinhard, Dirk Rieger, and Charlotte Helfrich-Förster. 2019. "Role of Rhodopsins as Circadian Photoreceptors in the Drosophila Melanogaster." *Biology* 8(1):6. doi: 10.3390/biology8010006.

Shafer, Orie T., Gabrielle J. Gutierrez, Kimberly Li, Amber Mildenhall, Daphna Spira, Jonathan Marty, Aurel A. Lazar, and Maria de la Paz Fernandez. 2022. "Connectomic Analysis of the Drosophila Lateral Neuron Clock Cells Reveals the Synaptic Basis of Functional Pacemaker Classes." *ELife* 11:e79139. doi: 10.7554/eLife.79139.

Shafer, Orie T., Dong Jo Kim, Richard Dunbar-Yaffe, Viacheslav O. Nikolaev, Martin J. Lohse, and Paul H. Taghert. 2008. "Widespread Receptivity to Neuropeptide PDF throughout the Neuronal Circadian Clock Network of Drosophila Revealed by Real-Time Cyclic AMP Imaging." *Neuron* 58(2):223–37. doi: 10.1016/j.neuron.2008.02.018.

Shafer, Orie T., Michael Rosbash, and James W. Truman. 2002. "Sequential Nuclear Accumulation of the Clock Proteins Period and Timeless in the Pacemaker Neurons of Drosophila Melanogaster." *The Journal of Neuroscience: The Official Journal of the Society for Neuroscience* 22(14):5946–54. doi: 10.1523/JNEUROSCI.22-14-05946.2002.

Shafer, Orie T., and Zepeng Yao. 2014. "Pigment-Dispersing Factor Signaling and Circadian Rhythms in Insect Locomotor Activity." *Current Opinion in Insect Science* 1:73–80. doi: 10.1016/j.cois.2014.05.002.

Shafer, Orie Thomas, Charlotte Helfrich-Förster, Susan Christine Portia Renn, and Paul H. Taghert. 2006. "Reevaluation of Drosophila Melanogaster's Neuronal Circadian Pacemakers Reveals New Neuronal Classes." *Journal of Comparative Neurology* 498(2):180–93. doi: 10.1002/cne.21021.

Shang, Yuhua, Nathan C. Donelson, Christopher G. Vecsey, Fang Guo, Michael Rosbash, and Leslie C. Griffith. 2013. "Short Neuropeptide F Is a Sleep-Promoting Inhibitory Modulator." *Neuron* 80(1):171–83. doi: 10.1016/j.neuron.2013.07.029.

Shang, Yuhua, Leslie C. Griffith, and Michael Rosbash. 2008. "Light-Arousal and Circadian Photoreception Circuits Intersect at the Large PDF Cells of the Drosophila Brain." *Proceedings of the National Academy of Sciences of the United States of America* 105(50):19587–94. doi: 10.1073/pnas.0809577105.

Sharkey, Camilla R., Jorge Blanco, Maya M. Leibowitz, Daniel Pinto-Benito, and Trevor J. Wardill. 2020. "The Spectral Sensitivity of Drosophila Photoreceptors." *Scientific Reports* 10:18242. doi: 10.1038/s41598-020-74742-1.

Sharma, Vijay Kumar. 2003. "Adaptive Significance of Circadian Clocks." *Chronobiology International* 20(6):901–19. doi: 10.1081/cbi-120026099.

Sharma, Vijay Kumar. 2005. "Evolution of Temporal Order in Living Organisms." 3(0):Art. 7. doi: 10.1186/1740-3391-3-7.

Shearman, Lauren P., Mark J. Zylka, David R. Weaver, Lee F. Kolakowski, and Steven M. Reppert. 1997. “Two Period Homologs: Circadian Expression and Photic Regulation in the Suprachiasmatic Nuclei.” *Neuron* 19(6):1261–69. doi: 10.1016/S0896-6273(00)80417-1.

Sheeba, Vasu, Huaiyu Gu, Vijay K. Sharma, Diane K. O’Dowd, and Todd C. Holmes. 2008. “Circadian- and Light-Dependent Regulation of Resting Membrane Potential and Spontaneous Action Potential Firing of Drosophila Circadian Pacemaker Neurons.” *Journal of Neurophysiology* 99(2):976–88. doi: 10.1152/jn.00930.2007.

Siepka, Sandra M., Seung-Hee Yoo, Junghea Park, Weimin Song, Vivek Kumar, Yinin Hu, Choogon Lee, and Joseph S. Takahashi. 2007. “Circadian Mutant Overtime Reveals F-Box Protein FBXL3 Regulation of Cryptochrome and Period Gene Expression.” *Cell* 129(5):1011–23. doi: 10.1016/j.cell.2007.04.030.

Silies, Marion, Daryl M. Gohl, and Thomas R. Clandinin. 2014. “Motion-Detecting Circuits in Flies: Coming into View.” *Annual Review of Neuroscience* 37:307–27. doi: 10.1146/annurev-neuro-071013-013931.

Siwicki, K. K., C. Eastman, G. Petersen, M. Rosbash, and J. C. Hall. 1988. “Antibodies to the Period Gene Product of Drosophila Reveal Diverse Tissue Distribution and Rhythmic Changes in the Visual System.” *Neuron* 1(2):141–50. doi: 10.1016/0896-6273(88)90198-5.

Somyajit, Kumar, Rajat Gupta, Hana Sedlackova, Kai John Neelsen, Fena Ochs, Maj-Britt Rask, Chunaram Choudhary, and Jiri Lukas. 2017. “Redox-Sensitive Alteration of Replisome Architecture Safeguards Genome Integrity.” *Science (New York, N.Y.)* 358(6364):797–802. doi: 10.1126/science.aao3172.

Song, Bryan J., Slater J. Sharp, and Dragana Rogulja. 2021. “Daily Rewiring of a Neural Circuit Generates a Predictive Model of Environmental Light.” *Science Advances* 7(13):eabe4284. doi: 10.1126/sciadv.abe4284.

Stanewsky, Ralf, Maki Kaneko, Patrick Emery, Bonnie Beretta, Karen Wager-Smith, Steve A. Kay, Michael Rosbash, and Jeffrey C. Hall. 1998. “The Cryb Mutation Identifies Cryptochrome as a Circadian Photoreceptor in Drosophila.” *Cell* 95(5):681–92. doi:

10.1016/S0092-8674(00)81638-4.

Starnes, Ashley N., and Jeff R. Jones. 2023. “Inputs and Outputs of the Mammalian Circadian Clock.” *Biology* 12(4):508. doi: 10.3390/biology12040508.

Stephan, Friedrich K., and Irving Zucker. 1972. “Circadian Rhythms in Drinking Behavior and Locomotor Activity of Rats Are Eliminated by Hypothalamic Lesions.” *Proceedings of the National Academy of Sciences* 69(6):1583–86. doi: 10.1073/pnas.69.6.1583.

Stoleru, Dan, Pipat Nawathean, María de la Paz Fernández, Jerome S. Menet, M. Fernanda Ceriani, and Michael Rosbash. 2007. “The Drosophila Circadian Network Is a Seasonal Timer.” *Cell* 129(1):207–19. doi: 10.1016/j.cell.2007.02.038.

Stoleru, Dan, Ying Peng, José Agosto, and Michael Rosbash. 2004. “Coupled Oscillators Control Morning and Evening Locomotor Behaviour of Drosophila.” *Nature* 431(7010):862–68. doi: 10.1038/nature02926.

Stoleru, Dan, Ying Peng, Pipat Nawathean, and Michael Rosbash. 2005. “A Resetting Signal between Drosophila Pacemakers Synchronizes Morning and Evening Activity.” *Nature* 438(7065):238–42. doi: 10.1038/nature04192.

Suri, Vipin, Anne Lanjuin, and Michael Rosbash. 1999. “TIMELESS-Dependent Positive and Negative Autoregulation in the Drosophila Circadian Clock.” *The EMBO Journal* 18(3):675–86. doi: 10.1093/emboj/18.3.675.

Szular, Joanna, Hana Sehadova, Carla Gentile, Gisela Szabo, Wen-Hai Chou, Steven G. Britt, and Ralf Stanewsky. 2012. “Rhodopsin 5– and Rhodopsin 6–Mediated Clock Synchronization in Drosophila Melanogaster Is Independent of Retinal Phospholipase C-β Signaling.” *Journal of Biological Rhythms* 27(1):25–36. doi: 10.1177/0748730411431673.

Tang, Chih-Hang Anthony, Erica Hinteregger, Yuhua Shang, and Michael Rosbash. 2010. “Light-Mediated TIM Degradation within Drosophila Pacemaker Neurons (s-LNvs) Is Neither Necessary nor Sufficient for Delay Zone Phase Shifts.” *Neuron* 66(3):378–85. doi: 10.1016/j.neuron.2010.04.015.

Tataroglu, Ozgur, and Patrick Emery. 2015. “The Molecular Ticks of the Drosophila Circadian

Clock." *Current Opinion in Insect Science* 7:51–57. doi: 10.1016/j.cois.2015.01.002.

Top, Deniz, Emily Harms, Sheyum Syed, Eliza L. Adams, and Lino Saez. 2016. "GSK-3 and CK2 Kinases Converge on Timeless to Regulate the Master Clock." *Cell Reports* 16(2):357–67. doi: 10.1016/j.celrep.2016.06.005.

Top, Deniz, and Michael W. Young. 2018. "Coordination between Differentially Regulated Circadian Clocks Generates Rhythmic Behavior." *Cold Spring Harbor Perspectives in Biology* 10(7):a033589. doi: 10.1101/cshperspect.a033589.

Ueda, Hiroki R., Akira Matsumoto, Miho Kawamura, Masamitsu Iino, Teiichi Tanimura, and Seiichi Hashimoto. 2002. "Genome-Wide Transcriptional Orchestration of Circadian Rhythms in Drosophila." *The Journal of Biological Chemistry* 277(16):14048–52. doi: 10.1074/jbc.C100765200.

Vaidya, Anand T., Deniz Top, Craig C. Manahan, Joshua M. Tokuda, Sheng Zhang, Lois Pollack, Michael W. Young, and Brian R. Crane. 2013. "Flavin Reduction Activates Drosophila Cryptochrome." *Proceedings of the National Academy of Sciences* 110(51):20455–60. doi: 10.1073/pnas.1313336110.

VanVickle-Chavez, Sarah J., and Russell N. Van Gelder. 2007. "Action Spectrum of Drosophila Cryptochrome *." *Journal of Biological Chemistry* 282(14):10561–66. doi: 10.1074/jbc.M609314200.

Vaze, Koustubh M., and Vijay Kumar Sharma. 2013. "On the Adaptive Significance of Circadian Clocks for Their Owners." *Chronobiology International* 30(4):413–33. doi: 10.3109/07420528.2012.754457.

Veleri, Shobi, Dirk Rieger, Charlotte Helfrich-Förster, and Ralf Stanewsky. 2007. "Hofbauer-Buchner Eyelet Affects Circadian Photosensitivity and Coordinates TIM and PER Expression in Drosophila Clock Neurons." *Journal of Biological Rhythms* 22(1):29–42. doi: 10.1177/0748730406295754.

Vitaterna, M. H., C. P. Selby, T. Todo, H. Niwa, C. Thompson, E. M. Fruechte, K. Hitomi, R. J. Thresher, T. Ishikawa, J. Miyazaki, J. S. Takahashi, and A. Sancar. 1999. "Differential Regulation of Mammalian Period Genes and Circadian Rhythmicity by Cryptochromes 1 and 2." *Proceedings of the National Academy of Sciences of the United States of America*

96(21):12114–19. doi: 10.1073/pnas.96.21.12114.

Vitaterna, Martha Hotz, David P. King, Anne-Marie Chang, Jon M. Kornhauser, Phillip L. Lowrey, J. David McDonald, William F. Dove, Lawrence H. Pinto, Fred W. Turek, and Joseph S. Takahashi. 1994. "Mutagenesis and Mapping of a Mouse Gene, Clock, Essential for Circadian Behavior." *Science* 264(5159):719–25. doi: 10.1126/science.8171325.

Vogt, K., and K. Kirschfeld. 1984. "Chemical Identity of the Chromophores of Fly Visual Pigment." *Naturwissenschaften* 71(4):211–13. doi: 10.1007/BF00490436.

Vosshall, Leslie B., Jeffrey L. Price, Amita Sehgal, Lino Saez, and Michael W. Young. 1994. "Block in Nuclear Localization of Period Protein by a Second Clock Mutation, Timeless." *Science* 263(5153):1606–9. doi: 10.1126/science.8128247.

Weber, Frank, Daniela Zorn, Christoph Rademacher, and Hsiu-Cheng Hung. 2011. "Post-Translational Timing Mechanisms of the Drosophila Circadian Clock." *FEBS Letters* 585(10):1443–49. doi: 10.1016/j.febslet.2011.04.008.

Whitmore, D., N. S. Foulkes, and P. Sassone-Corsi. 2000. "Light Acts Directly on Organs and Cells in Culture to Set the Vertebrate Circadian Clock." *Nature* 404(6773):87–91. doi: 10.1038/35003589.

Wijnen, Herman, Felix Naef, Catharine Boothroyd, Adam Claridge-Chang, and Michael W. Young. 2006. "Control of Daily Transcript Oscillations in Drosophila by Light and the Circadian Clock." *PLoS Genetics* 2(3):e39. doi: 10.1371/journal.pgen.0020039.

Witte, Ines, Hans-Juergen Kreienkamp, Michael Gewecke, and Thomas Roeder. 2002. "Putative Histamine-Gated Chloride Channel Subunits of the Insect Visual System and Thoracic Ganglion." *Journal of Neurochemistry* 83(3):504–14. doi: 10.1046/j.1471-4159.2002.01076.x.

Wright, Kenneth P., Andrew W. McHill, Brian R. Birks, Brandon R. Griffin, Thomas Rusterholz, and Evan D. Chinoy. 2013. "Entrainment of the Human Circadian Clock to the Natural Light-Dark Cycle." *Current Biology* 23(16):1554–58. doi: 10.1016/j.cub.2013.06.039.

Yamaguchi, Satoko, Claude Desplan, and Martin Heisenberg. 2010. "Contribution of

Photoreceptor Subtypes to Spectral Wavelength Preference in Drosophila." *Proceedings of the National Academy of Sciences of the United States of America* 107(12):5634–39. doi: 10.1073/pnas.0809398107.

Yamaguchi, Satoko, Reinhard Wolf, Claude Desplan, and Martin Heisenberg. 2008. "Motion Vision Is Independent of Color in Drosophila." *Proceedings of the National Academy of Sciences of the United States of America* 105(12):4910–15. doi: 10.1073/pnas.0711484105.

Yamazaki, Shin, Rika Numano, Michikazu Abe, Akiko Hida, Ri-ichi Takahashi, Masatsugu Ueda, Gene D. Block, Yoshiyuki Sakaki, Michael Menaker, and Hajime Tei. 2000. "Resetting Central and Peripheral Circadian Oscillators in Transgenic Rats." *Science* 288(5466):682–85. doi: 10.1126/science.288.5466.682.

Yang, Zhaohai, and Amita Sehgal. 2001. "Role of Molecular Oscillations in Generating Behavioral Rhythms in Drosophila." *Neuron* 29(2):453–67. doi: 10.1016/S0896-6273(01)00218-5.

Yao, Z., and O. T. Shafer. 2014. "The Drosophila Circadian Clock Is a Variably Coupled Network of Multiple Peptidergic Units." *Science* 343(6178):1516–20. doi: 10.1126/science.1251285.

Yao, Zepeng, Amelia J. Bennett, Jenna L. Clem, and Orie T. Shafer. 2016. "The Drosophila Clock Neuron Network Features Diverse Coupling Modes and Requires Network-Wide Coherence for Robust Circadian Rhythms." *Cell Reports* 17(11):2873–81. doi: 10.1016/j.celrep.2016.11.053.

Yasuyama, Kouji, and Ian A. Meinertzhagen. 2010. "Synaptic Connections of PDF-Immunoreactive Lateral Neurons Projecting to the Dorsal Protocerebrum of Drosophila Melanogaster." *The Journal of Comparative Neurology* 518(3):292–304. doi: 10.1002/cne.22210.

Yoo, Seung-Hee, Caroline H. Ko, Phillip L. Lowrey, Ethan D. Buhr, Eun-joo Song, Suhwan Chang, Ook Joon Yoo, Shin Yamazaki, Choogon Lee, and Joseph S. Takahashi. 2005. "A Noncanonical E-Box Enhancer Drives Mouse Period2 Circadian Oscillations in Vivo." *Proceedings of the National Academy of Sciences* 102(7):2608–13. doi:

10.1073/pnas.0409763102.

Yoo, Seung-Hee, Shin Yamazaki, Phillip L. Lowrey, Kazuhiro Shimomura, Caroline H. Ko, Ethan D. Buhr, Sandra M. Siepka, Hee-Kyung Hong, Won Jun Oh, Ook Joon Yoo, Michael Menaker, and Joseph S. Takahashi. 2004. "PERIOD2::LUCIFERASE Real-Time Reporting of Circadian Dynamics Reveals Persistent Circadian Oscillations in Mouse Peripheral Tissues." *Proceedings of the National Academy of Sciences of the United States of America* 101(15):5339–46. doi: 10.1073/pnas.0308709101.

Yoshii, Taishi, Christiane Hermann-Luibl, and Charlotte Helfrich-Förster. 2016. "Circadian Light-Input Pathways in Drosophila." *Communicative & Integrative Biology* 9(1):e1102805. doi: 10.1080/19420889.2015.1102805.

Yoshii, Taishi, Takeshi Todo, Corinna Wülbeck, Ralf Stanewsky, and Charlotte Helfrich-Förster. 2008. "Cryptochrome Is Present in the Compound Eyes and a Subset of Drosophila's Clock Neurons." *The Journal of Comparative Neurology* 508(6):952–66. doi: 10.1002/cne.21702.

Yoshii, Taishi, Corinna Wülbeck, Hana Sehadova, Shobi Veleri, Dominik Bichler, Ralf Stanewsky, and Charlotte Helfrich-Förster. 2009. "The Neuropeptide Pigment-Dispersing Factor Adjusts Period and Phase of Drosophila's Clock." *Journal of Neuroscience* 29(8):2597–2610. doi: 10.1523/JNEUROSCI.5439-08.2009.

Young, Michael W., and Steve A. Kay. 2001. "Time Zones: A Comparative Genetics of Circadian Clocks." *Nature Reviews Genetics* 2(9):702–15. doi: 10.1038/35088576.

Yu, Wangjie, Hao Zheng, Jerry H. Houl, Brigitte Dauwalder, and Paul E. Hardin. 2006. "PER-Dependent Rhythms in CLK Phosphorylation and E-Box Binding Regulate Circadian Transcription." *Genes & Development* 20(6):723–33. doi: 10.1101/gad.1404406.

Yu, Wangjie, Hao Zheng, Jeffrey L. Price, and Paul E. Hardin. 2009. "DOUBLETIME Plays a Noncatalytic Role To Mediate CLOCK Phosphorylation and Repress CLOCK-Dependent Transcription within the Drosophila Circadian Clock." *Molecular and Cellular Biology* 29(6):1452–58. doi: 10.1128/MCB.01777-08.

Zehring, W. A., D. A. Wheeler, P. Reddy, R. J. Konopka, C. P. Kyriacou, M. Rosbash, and J. C. Hall. 1984. "P-Element Transformation with Period Locus DNA Restores Rhythmicity

to Mutant, Arrhythmic Drosophila Melanogaster." *Cell* 39(2 Pt 1):369–76. doi: 10.1016/0092-8674(84)90015-1.

Zeng, H., P. E. Hardin, and M. Rosbash. 1994. "Constitutive Overexpression of the Drosophila Period Protein Inhibits Period MRNA Cycling." *The EMBO Journal* 13(15):3590–98. doi: 10.1002/j.1460-2075.1994.tb06666.x.

Zeng, Hongkui, Zuwei Qian, Michael P. Myers, and Michael Rosbash. 1996. "A Light-Entrainment Mechanism for the Drosophila Circadian Clock." *Nature* 380(6570):129–35. doi: 10.1038/380129a0.

Zhang, Chen, Ivana Daubnerova, Yong-Hoon Jang, Shu Kondo, Dušan Žitňan, and Young-Joon Kim. 2021. "The Neuropeptide Allatostatin C from Clock-Associated DN1p Neurons Generates the Circadian Rhythm for Oogenesis." *Proceedings of the National Academy of Sciences* 118(4):e2016878118. doi: 10.1073/pnas.2016878118.

Zhang, Luoying, Brian Y. Chung, Bridget C. Lear, Valerie L. Kilman, Yixiao Liu, Guruswamy Mahesh, Rose-Anne Meissner, Paul E. Hardin, and Ravi Allada. 2010. "DN1p Circadian Neurons Coordinate Acute Light and PDF Inputs to Produce Robust Daily Behavior in Drosophila." *Current Biology* 20(7):591–99. doi: 10.1016/j.cub.2010.02.056.

Zhang, Yong, Yixiao Liu, Diana Bilodeau-Wentworth, Paul E. Hardin, and Patrick Emery. 2010. "Light and Temperature Control the Contribution of Specific DN1 Neurons to Drosophila Circadian Behavior." *Current Biology* 20(7):600–605. doi: 10.1016/j.cub.2010.02.044.

Zheng, Binhai, Urs Albrecht, Krista Kaasik, Marijke Sage, Weiqin Lu, Sukeshi Vaishnav, Qiu Li, Zhong Sheng Sun, Gregor Eichele, Allan Bradley, and Cheng Chi Lee. 2001. "Nonredundant Roles of the MPer1 and MPer2 Genes in the Mammalian Circadian Clock." *Cell* 105(5):683–94. doi: 10.1016/S0092-8674(01)00380-4.

Zheng, Xiangzhong, Kyunghee Koh, Mallory Sowcik, Corinne J. Smith, Dechun Chen, Mark N. Wu, and Amita Sehgal. 2009. "An Isoform-Specific Mutant Reveals a Role of PDP1ε in the Circadian Oscillator." *Journal of Neuroscience* 29(35):10920–27. doi: 10.1523/JNEUROSCI.2133-09.2009.

Zheng, Xiangzhong, and Amita Sehgal. 2012. "Speed Control: Cogs and Gears That Drive the

Circadian Clock." *Trends in Neurosciences* 35(9):574–85. doi: 10.1016/j.tins.2012.05.007.

Zhu, Yan. 2013. "The Drosophila Visual System." *Cell Adhesion & Migration* 7(4):333–44. doi: 10.4161/cam.25521.

Zoltowski, Brian D., Anand T. Vaidya, Deniz Top, Joanne Widom, Michael W. Young, and Brian R. Crane. 2011. "Structure of Full-Length Drosophila Cryptochrome." *Nature* 480(7377):396–99. doi: 10.1038/nature10618.

Zuker, C. S., A. F. Cowman, and G. M. Rubin. 1985. "Isolation and Structure of a Rhodopsin Gene from D. Melanogaster." *Cell* 40(4):851–58. doi: 10.1016/0092-8674(85)90344-7.